UNCLASSIFIED

AD NUMBER

ADB803042

NEW LIMITATION CHANGE

TO

Approved for public release, distribution unlimited

FROM

DISTRIBUTION AUTHORIZED TO DOD ONLY; ADMINISTRATIVE/OPERATIONAL USE; 03 MAR 1999. OTHER REQUESTS SHALL BE REFERRED THROUGH WRIGHT AIR DEVELOPMENT CENTER, FLIGHT TEST DIV., WRIGHT-PATTERSON AFB, OH.

AUTHORITY

WADC [DTIC form 55] 14 Apr 2000

THIS PAGE IS UNCLASSIFIED

UNCLASSIFIED

AD NUMBER

ADB803042

CLASSIFICATION CHANGES

TO

unclassified

FROM

restricted

AUTHORITY

EO 10501 dtd 5 Nov 1953

THIS PAGE IS UNCLASSIFIED

CLASSIFICATION CHANGED TO UNCLASSIFIED

BY AUTHORITY OF ASTIA Classification cancelled in accordance with Executive Order 10501 issued 5 November 1953

R to U Ex Ord

Date 21 February 1957 Signed Richard E. Reedy

OFFICE SECURITY ADVISOR

A.T.I 99299

Reproduced by

DOCUMENT SERVICE CENTER

ARMED SERVICES TECHNICAL INFORMATION AGENCY

KNOTT BUILDING, DAYTON, 2, OHIO

"NOTICE: When Government or other drawings, specifications or other data are used for any purpose other than in connection with a definitely related Government procurement operation, the U.S. Government thereby incurs no responsibility, nor any obligation whatsoever; and the fact that the Government may have formulated, furnished, or in any way supplied the said drawings, specifications or other data is not to be regarded by implication or otherwise as in any manner licensing the holder or any other person or corporation, or conveying any rights or permission to manufacture, use or sell any patented invention that may in any way be related thereto."

UNCLASSIFIED

RESTRICTED

ENGINEERING REPORT NO.

R107-012

SUBJECT

BASIC AERODYNAMIC DATA

LEGIBILITY POOR

MODEL: XC-120

FAIRCHILD AIRCRAFT

Division of

FAIRCHILD ENGINE & AIRPLANE CORPORATION

HAGERSTOWN, MARYLAND

RESTRICTED

Date: July 9, 1948
February 28, 1949 (Revised and Issued)

No. Pages: 340, a, f

Prepared By J. F. Evans - G. T. Gelow
A. Athanasian - A. Grenis

Approved and Checked By E. F. Morton

Approved By A. J. Thieblot
Chief Engineer

REVISIONS

Date	Pages Affected	By	Remarks

Form FA 29

TABLE OF CONTENTS

Page No.

PART I - GENERAL

A. INTRODUCTION 1
B. NOMENCLATURE 3
C. SUMMARY OF PHYSICAL CHARACTERISTICS 5
1. Airplane Three View 6
2. Wing 7
Flap 9
Ailerons 9
Aileron Tabs 10
3. Fuselage 11
3A. Crew Nacelle 12
4. Booms 13
Power Plant 13
Propeller 13
5. Horizontal Tail 14
Elevator 14
Elevator Tabs 15
6. Vertical Tail 16
Rudder 16
Rudder Tabs 16
7. Landing Gear 18

D. SUMMARY OF AERODYNAMIC CHARACTERISTICS - POWER OFF 19
1. Wing Unflapped 20
2. Wing Flapped 25
3. Ailerons 29
4. Aileron Tabs 34
5. Fuselage 38
5A. Crew Nacelle 43
6. Boom 50
7. Horizontal Tail 57
8. Elevator Tabs 64
9. Vertical Tail 67
10. Rudder Tabs 73
11. Landing Gear 76

E. SUMMARY OF AERODYNAMIC CHARACTERISTICS - POWER ON 78
1. Wing Unflapped 79
2. Wing Flapped 84
3. Ailerons 90
4. Aileron Tabs 91
5. Fuselage 92
5A. Crew Nacelle 92

TABLE OF CONTENTS (Cont.)

Page No.

E. SUMMARY OF AERODYNAMIC CHARACTERISTICS - POWER ON (Cont.)

6. Boom 93
7. Power Plant 94
8. Propeller 96
9. Horizontal Tail 101
10. Elevator Tabs 105
11. Vertical Tail 106
12. Rudder Tabs 110
13. Landing Gear 111

PART II - CALCULATION OF AERODYNAMIC CHARACTERISTICS

A. POWER-OFF 112
1. Wing Unflapped 113
a. Wing Drawing 114
b. Mean Aerodynamic Chord 113
c. Airfoil Section Characteristics 113
d. Effective Reynold's Number 113
e. Aerodynamic Twist 116
f. Lift Curve Slope 113
g. Angle of Zero Lift 113
h. Angle of Attack for any Lift Coefficient 113
i. Aerodynamic Center Location 113
j. Pitching Moment About Aerodynamic Center 113
k. Spanwise Lift Distribution 113
Additional Lift Distribution
Basic Lift Distribution
Total Lift Distribution
l. Maximum Lift Coefficients 113
Positive Angle of Attack
Negative Angle of Attack
m. Spanwise Drag Distribution 113
Induced Drag Distribution
Profile Drag Distribution
Total Drag
n. Polar Diagram 113
o. Aerodynamic Force Coefficients 117
p. Characteristics in Yaw 120
2. Wing Flapped 122
a. Flap Drawings 122
b. Flap Section Characteristics 122
c. Lift Curve Slope 122
d. Angle of Zero Lift 122
e. Angle of Attack for any Lift Coefficient 122
f. Aerodynamic Center Location 122

TABLE OF CONTENTS

Page No.

PART II - CALCULATION OF AERODYNAMIC CHARACTERISTICS (Cont.)

2. Wing Flapped (Cont.)
   - g. Pitching Moment About Aerodynamic Center 122
   - h. Spanwise Lift Distribution 122
     - Additional Lift Distribution
     - Basic Lift Distribution
     - Total Lift Distribution
   - i. Maximum Lift Coefficients 122
     - Positive Angle of Attack
   - j. Spanwise Drag Distribution 122
     - Induced Drag Distribution
     - Profile Drag Distribution
     - Total Drag
   - k. Polar Diagram 122
   - l. Aerodynamic Force Coefficients 123
   - m. Characteristics in Yaw 126
3. Ailerons 127
   - a. Aileron Drawing 127
   - b. Lift Analysis 127
   - c. Pitching Moment About Aerodynamic Center 127
   - d. Aileron Hinge Moments 127
4. Aileron Tabs 128
   - a. Aileron Tab Drawing 128
   - b. Trim Tab Analysis 128
     - Lift
     - Hinge Moment
   - c. Balance Tab Analysis 128
     - Lift
     - Helix Angle
     - Hinge Moment
5. Fuselage 129
   - a. Fuselage Drawing 130
   - b. Lift Analysis 132
   - c. Drag Analysis 134
     - Basic Smooth Drag
     - Drag Due to Roughness, Leakage, Preturberances
   - d. Polar Diagram 139
   - e. Aerodynamic Force Coefficients 141
   - f. Pitching Moment about Quarter Length 144
   - g. Yawing Moment about Quarter Length 146
5A. Crew Nacelle 147
   - a. Crew Nacelle Drawing 148
   - b. Lift Analysis 150
   - c. Drag Analysis 152
   - d. Crew Nacelle Polar Diagram 157
   - e. Aerodynamic Force Coefficients 159
   - f. Pitching Moment Analysis 162
   - g. Yawing Moment Analysis 164

TABLE OF CONTENTS (Cont.)

PART II - Cont. Page No.

6. Boom 167
   a. Boom Drawing 168
   b. Lift Analysis 170
   c. Drag Analysis 172
      Basic Smooth Drag
      Drag Due to Roughness, Leakage, Proturberances
   d. Polar Diagram
   e. Aerodynamic Force Coefficients 177
   f. Pitching Moment about Quarter Length 180
   g. Yawing Moment about Quarter Length 182
7. Horizontal Tail 185
   a. Horizontal Tail Drawing 186
   b. Lift Analysis 188
   c. Drag Analysis 193
      Induced Drag
      Profile Drag
      Total Drag
   d. Polar Diagram 206
   e. Aerodynamic Force Coefficients 208
   f. Pitching Moment about Aerodynamic Center 209
   g. Yawing Moment 211
   h. Downwash and Dynamic Pressure 212
   i. Elevator Hinge Moment 217
8. Elevator Tabs 222
   a. Elevator Tab Drawing 222
   b. Trim Tab Analysis 222
      Lift
      Hinge Moment
   c. Spring Tab Analysis 222
      Lift
      Hinge Moment
9. Vertical Tail 223
   a. Vertical Tail Drawing 224
   b. Cross Force Analysis 226
   c. Drag Analysis 231
      Induced Drag
      Profile Drag
      Total Drag
   d. Polar Diagram 236
   e. Aerodynamic Force Coefficients 238
   f. Yawing Moment About Aerodynamic Center 239
   g. Sidewash and Dynamic Pressure 241
   h. Rudder Hinge Moments 245

TABLE OF CONTENTS (Cont.)

	Page No.
PART II - Cont.	
10. Rudder Tabs	246
a. Rudder Tab Drawing	246
b. Trim Tab Analysis	246
Lift	
Hinge Moments	
c. Spring Tab Analysis	246
Lift	
Hinge Moments	
11. Landing Gear	247
a. Landing Gear Drawing	248
b. Drag	250
c. Force Coefficients	254
B. POWER-ON	257
1. Wing Unflapped	258
a. Slipstream Effects on Pitching Moment	259
b. Slipstream Effects on Lift	259
c. Slipstream Effects on Drag	265
Induced Drag	
Profile Drag	
Total Drag	
d. Polar Diagram	271
e. Aerodynamic Force Coefficients	273
f. Characteristics in Yaw	279
2. Wing Flapped	280
a. Slipstream Effects on Pitching Moment	281
b. Slipstream Effects on Lift	285
c. Slipstream Effects on Drag	289
Induced Drag	
Profile Drag	
Total Drag	
d. Polar Diagram	295
e. Aerodynamic Force Coefficients	297
f. Characteristics in Yaw	303
3. Ailerons	304
4. Aileron Tabs	305
5. Fuselage	306
5A. Crew Nacelle	307
6. Booms	308
7. Power Plant	309
a. Data	
b. Power Characteristics	
8. Propeller	310
a. Physical Characteristics	310
b. Thrust Characteristics	310

TABLE OF CONTENTS (Cont.)

Page No.

PART II - (Cont.)

8. Propeller (Cont.)
   c. Side Force Characteristics 310
   d. Aerodynamic Force Coefficients 310
9. Horizontal Tail 311
   a. Aerodynamic Characteristics 312
   b. Downwash and Dynamic Pressure 312
10. Elevator Tabs 325
11. Vertical Tail 326
   a. Aerodynamic Characteristics 327
   b. Sidewash and Dynamic Pressure 327
12. Rudder Tabs 337
13. Landing Gear 338

PART III - REFERENCES 339

PART I-A

A. INTRODUCTION

It is the purpose of this report to determine the aerodynamic characteristics of each of the component parts of the XC-120 airplane. No attempt is made in this report to determine the characteristics of the complete airplane.

For convenience the report is divided into three parts. Part I consists of general information and includes a complete summary of the physical and aerodynamic characteristics of the component parts. Part II presents the calculations and explains in detail the method of calculation of the aerodynamic characteristics, and Part III presents a complete list of all references.

Power on conditions refer to military power only and flaps down condition is for 40° flap deflection only.

The XC-120 airplane is a modified version of the C-119B airplane and features a detachable cargo compartment with both front and rear loading provisions, which is called the "pack". The compartment provided for pilot and crew members is of course not detachable and is designated "crew nacelle". The fuselage consists of the "pack" plus the "crew nacelle". Due to the peculiar configuration required for the detachable "pack", a quadricycle landing gear is required. Wing incidence has been increased from 3° (C-119B) to 7° at the wing root chord.

PART I-A

This report is one of a series of reports in which the characteristics of the component parts are summed and expanded in order to define the operating characteristics of the complete airplane. The complete series of reports are as follows.

Fairchild No.	Model	Title
R107B-001	XC-120	Estimation of Lateral Stability Derivatives.
R107-012	XC-120	Basic Aerodynamic Data
R107-013	XC-120	Maneuvering Horizontal Tail Loads Volume I - Pack On Volume II - Pack Off
R107-014	XC-120	Basic Flight Criteria Volume I - Pack On Volume II - Pack Off
R107-015	XC-120	Air Load Distribution Volume I - Pack On Volume II - Pack Off
R107-016	XC-120	Performance Calculations
R107-017	XC-120	Analysis of Wind Tunnel Data
R107-018	XC-120	Analysis of Stability and Control Volume I - Pack On Volume II - Pack Off

PART I-B

The nomenclature and sign convention used in this report is the same as in Part I-B of reference (1) with the following additions.

SYMBOL	DEFINITION	UNITS
α_n	Angle of attack of crew nacelle with respect to the relative wind.	Degrees
	AREAS	
F_n	Maximum frontal area of crew nacelle	sq. ft.
P_n	Plan area of crew nacelle	sq. ft.
S_n	Side area of crew nacelle	sq. ft.
	COEFFICIENTS	
C_{C_N}	Crew nacelle side force coefficient	
C_{D_N}	Crew nacelle drag coefficient	
C_{L_N}	Crew nacelle lift coefficient	
$C_{M_{N.25\,L_n}}$	Crew nacelle pitching moment coefficient about its quarter length point.	
$C_{N_{N.25L_n}}$	Crew nacelle yawing moment coefficient about its quarter length point.	
C_{X_N}	Crew nacelle force coefficient parallel to the thrust line.	
C_{Z_N}	Crew nacelle force coefficient perpendicular to the thrust line	
K_{X_N}	Crew nacelle engineering drag coefficient = D_N/V^2	

PART I-B

SYMBOL	DEFINITION	UNITS
	DIMENSIONS	
L_n	Overall length of crew nacelle	in. or ft.
	FORCES	
C_N	Crew nacelle cross force (cross wind)	lbs.
D_N	Crew nacelle drag - parallel to relative wind	lbs.
L_N	Crew nacelle lift-perpendicular to relative wind.	lbs.
M_N	Crew nacelle air force pitching moment	lbs.
N_N	Crew nacelle air force yawing moment	lbs.
X_N	Crew nacelle force parallel to the thrust line.	lbs.
Z_N	Crew nacelle force perpendicular to the thrust line.	lbs.

PART I-C

PHYSICAL CHARACTERISTICS

This section summarizes all of the physical characteristics of the component parts of the airplane. These data are tabulated on the following pages and have been used to determine the aerodynamic characteristics of the component parts.

The general angular relationships of the wing, crew nacelle, boom and fuselage are as follows:

$$\alpha_c = \alpha_{TL} + 7^\circ$$

$$\alpha_b = \alpha_f = \alpha_n = \alpha_{TL}$$

Report No. R107-012
Model X0-120

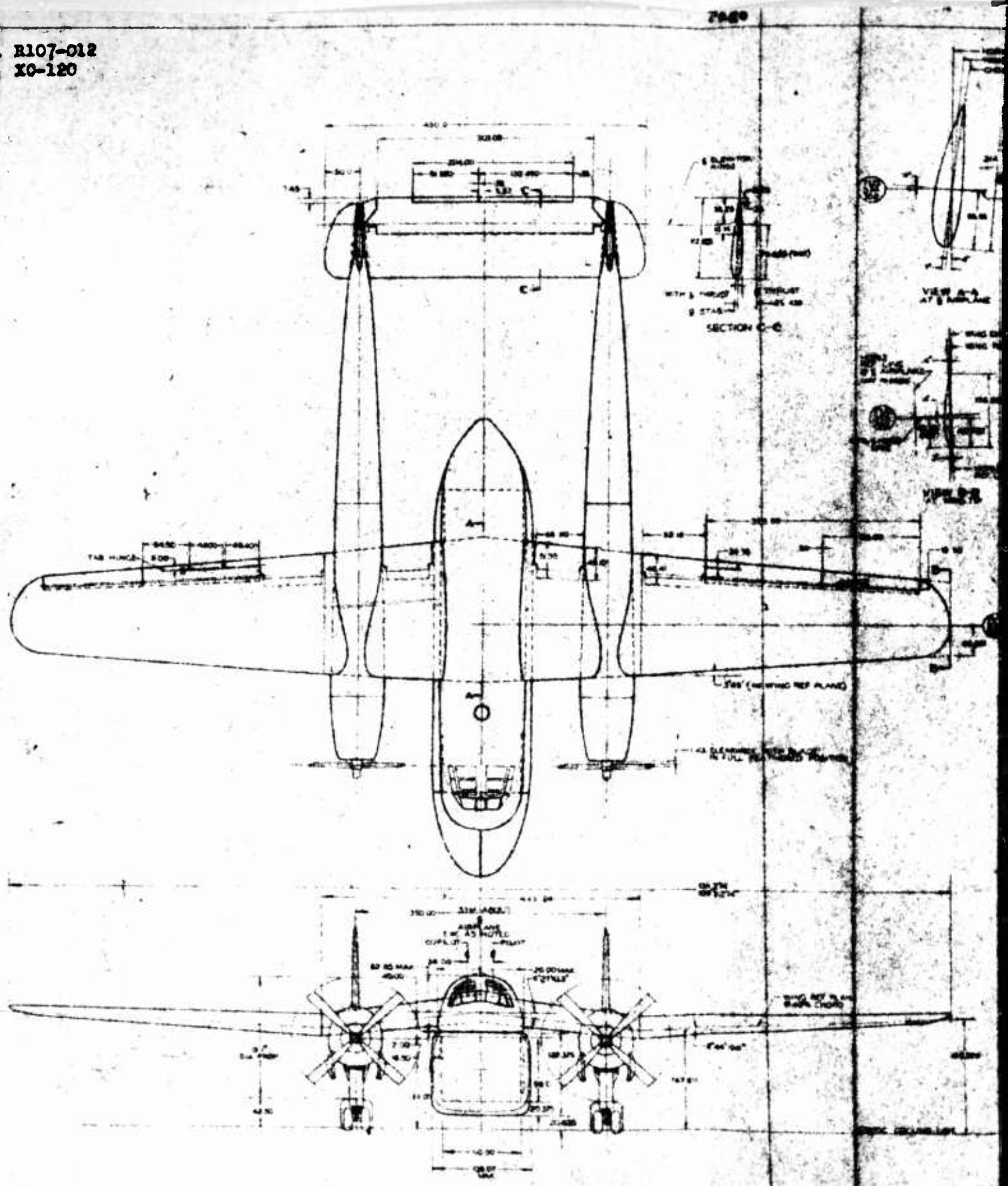

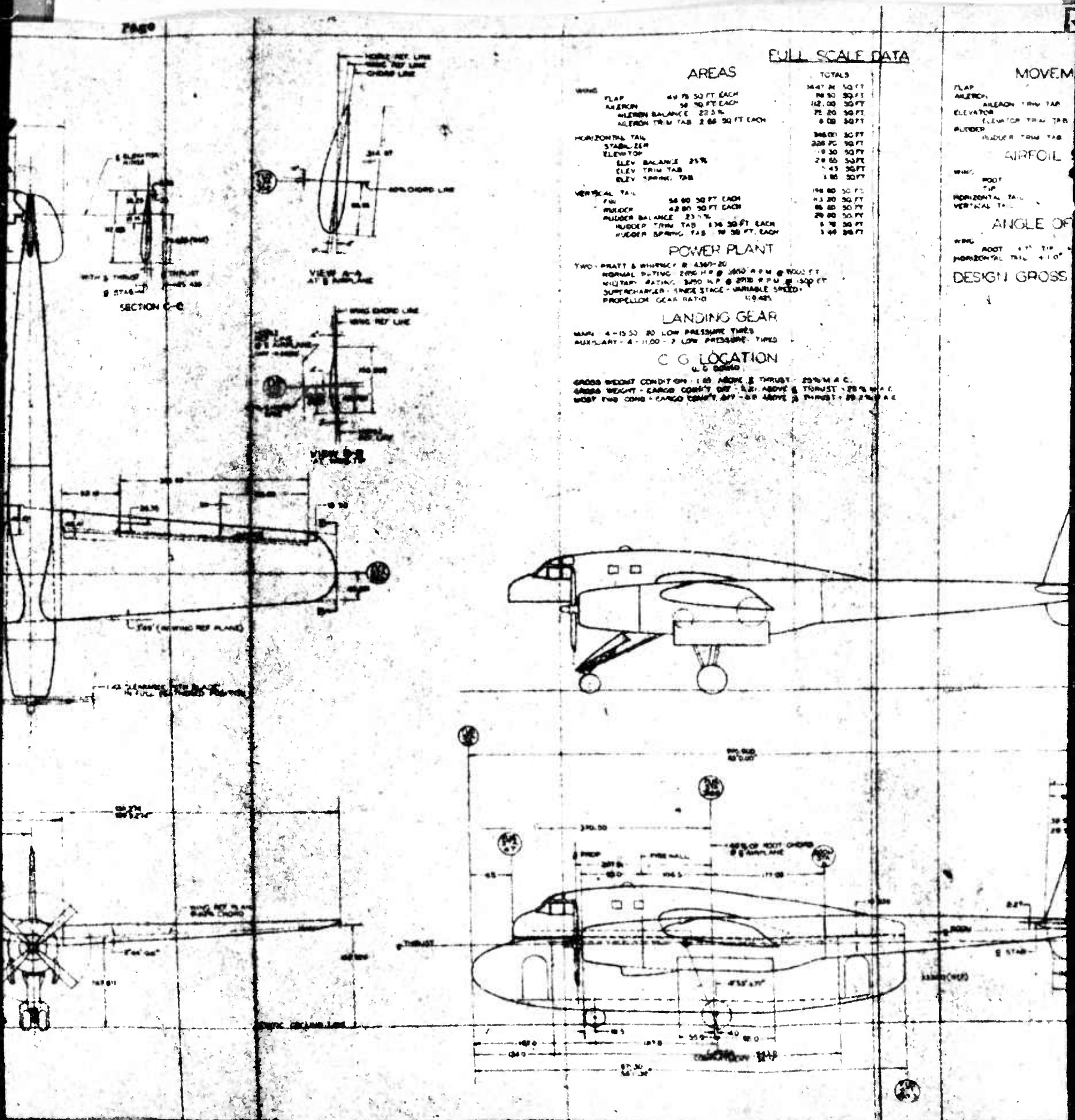
FULL SCALE DATA
AREAS
TOTALS
WING
FLAP
AILERON
AILERON BALANCE
AILERON TRIM TAB
HORIZONTAL TAIL
STABILIZER
ELEVATOR
ELEV. BALANCE
ELEV. TRIM TAB
ELEV. SPRING TAB
VERTICAL TAIL
FIN
RUDDER
RUDDER BALANCE
RUDDER TRIM TAB
RUDDER SPRING TAB
POWER PLANT
LANDING GEAR
C G LOCATION
MOVEM
AIRFOIL
ANGLE OF
DESIGN GROSS
SECTION C-C
VIEW A-A
VIEW B-B

FIG. 1

FULL SCALE DATA

AREAS

		TOTALS
WING		1447.24 SQ FT
FLAP	49.75 SQ FT EACH	99.50 SQ FT
AILERON	56.50 SQ FT EACH	112.00 SQ FT
AILERON BALANCE	22.5%	25.20 SQ FT
AILERON TRIM TAB	2.66 SQ FT EACH	5.32 SQ FT
HORIZONTAL TAIL		346.00 SQ FT
STABILIZER		226.70 SQ FT
ELEVATOR		119.30 SQ FT
ELEV. BALANCE	25%	29.83 SQ FT
ELEV. TRIM TAB		5.43 SQ FT
ELEV. SPRING TAB		3.85 SQ FT
VERTICAL TAIL		196.80 SQ FT
FIN	54.80 SQ FT EACH	113.20 SQ FT
RUDDER	42.80 SQ FT EACH	83.60 SQ FT
RUDDER BALANCE	23.1%	29.80 SQ FT
RUDDER TRIM TAB	1.36 SQ FT EACH	2.72 SQ FT
RUDDER SPRING TAB	1.19 SQ FT EACH	2.44 SQ FT

POWER PLANT

TWO - PRATT & WHITNEY R 4360-20
NORMAL RATING 2000 H.P. @ 2600 R.P.M. @ 1000 FT.
MILITARY RATING 3250 H.P. @ 2700 R.P.M. @ 1500 FT.
SUPERCHARGER - SINGLE STAGE - VARIABLE SPEED
PROPELLOR GEAR RATIO 0.425

LANDING GEAR

MAIN 4 - 15.50 - 20 LOW PRESSURE TIRES
AUXILIARY - 4 - 11.00 - 2 LOW PRESSURE TIRES

C.G. LOCATION

% C.G. BOOM

GROSS WEIGHT CONDITION - 1.65 ABOVE ℄ THRUST - 25.9% M.A.C.
GROSS WEIGHT - CARGO COND'T OFF - 1.20 ABOVE ℄ THRUST - 28.9% M.A.C.
MOST FWD COND - CARGO COND'T OFF - 0.8 ABOVE ℄ THRUST - 29.2% M.A.C.

MOVEMENTS

FLAP	—	40% DOWN
AILERON	24% UP	18% DOWN
AILERON TRIM TAB	5% UP	15% DOWN
ELEVATOR	32% UP	25% DOWN
ELEVATOR TRIM TAB	12% UP	22% DOWN
RUDDER	38% RIGHT	28% LEFT
RUDDER TRIM TAB	18% RIGHT	18% LEFT

AIRFOIL SECTIONS

WING
ROOT N.A.C.A. 2418
TIP N.A.C.A. 4420
HORIZONTAL TAIL N.A.C.A. 0014
VERTICAL TAIL N.A.C.A. 0012

ANGLE OF INCIDENCE

WING
ROOT +1° TIP +3
HORIZONTAL +1° +1.0°

DESIGN GROSS WEIGHT 64,000 LBS.

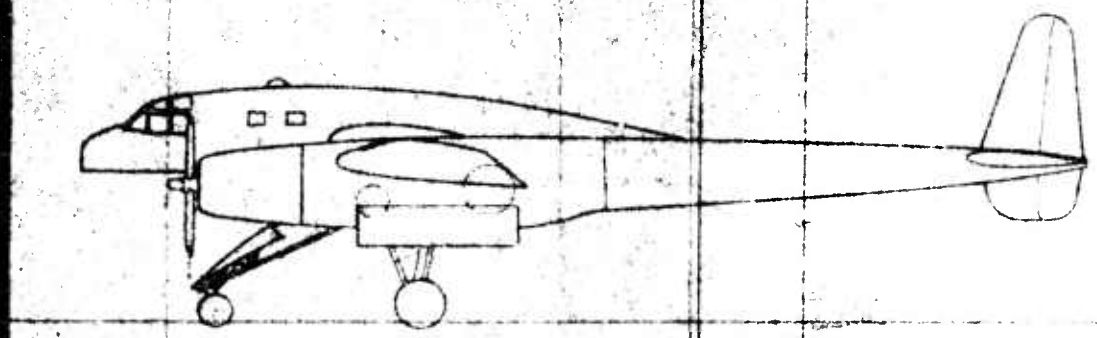

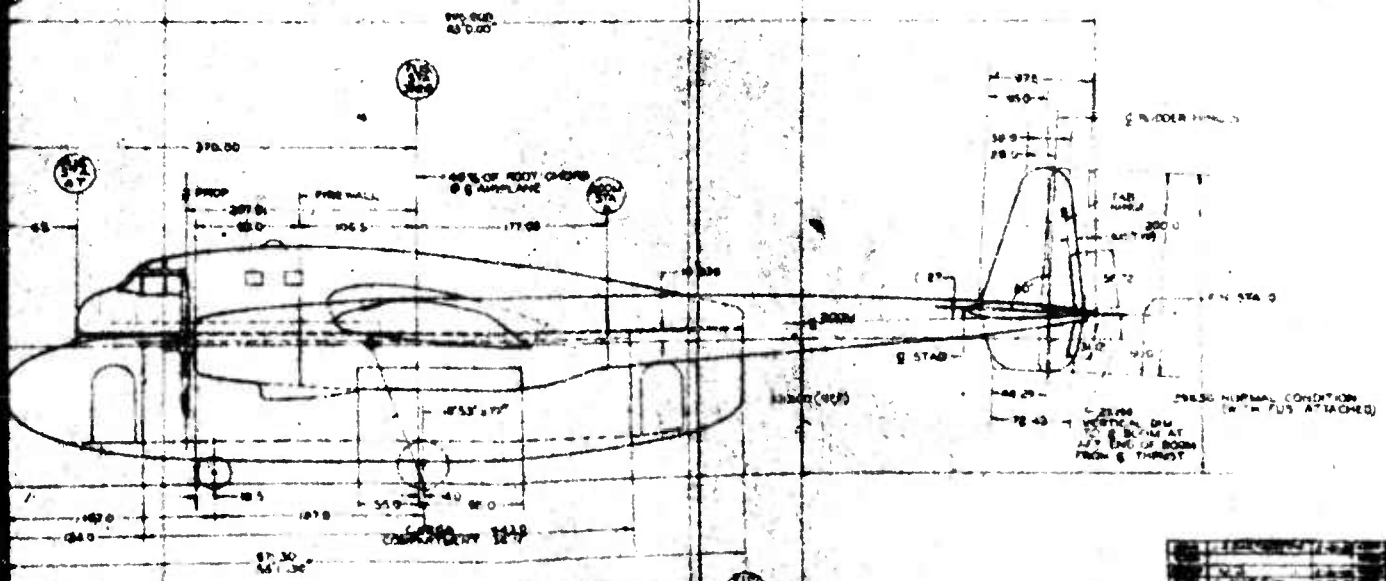

CARGO TRANSPORT
DETACHABLE FUSELAGE
THREE VIEW

107-000000

PART I-C-2

2. WING

The following table summarizes the physical characteristics of the wing, flaps, ailerons and aileron tabs.

ITEM	SYMBOL	VALUE
Area - Total	S_w	1447.25 sq. ft.
One outer panel	S_o	420.267 sq. ft.
One center panel	S_c	303.36 sq. ft.
Span - Total	B_w	109.27 ft.
One outer panel	b_o	433.075 in.
One center panel	b_c	222.562 in.
Chord - Mean Aerodynamic Chord	MAC_w	168.28 in.
Mean Aerodynamic Chord - Outer Panel	mac_o	147.10 in.
Mean Aerodynamic Chord - Center Panel	mac_c	197.62 in.
Root Chord	c_{w_c}	214.87 in.
Theoretical Tip Chord	$c_{w_{tt}}$	106.98 in.
Equivalent Tip Chord	$c_{w_{te}}$	109.25 in.
Chord at intersection of outer and center panels	c_{w_i}	179.29 in.
Location -		
MAC_w - horizontal distance from L.E. of root chord	h_w	18.64 in.
MAC_w - vertical distance from L.E. of root chord	v_w	-14.58 in.
mac_o - horizontal distance from L.E. of root chord	n_o	-16.20 in.
mac_o - vertical distance from L.E. of root chord	h_o	27.11 in.
mac_c - horizontal distance from L.E. of root chord	n_c	-12.34 in.
mac_c - vertical distance from L.E. of root chord	h_c	6.90 in.
Leading edge of intersection chord aft of leading edge of root chord	p_{c_i}	14.23 in.
Leading edge of root chord above leading edge of intersection chord	d_{c_c}	25.45 in.
Leading edge of equivalent tip chord aft of leading edge of intersection	p_{t_e}	28.03 in.
Leading edge of equivalent tip chord above leading edge of intersection	d_{t_e}	20.13 in.
Leading edge of theoretical tip chord aft of leading edge of root chord	b_{tt}	43.16 in.

PART I-C-2 (Cont.)

ITEM	SYMBOL	VALUE
Location -		
Leading edge of theoretical tip chord above leading edge of intersection chord	d_{tt}	20.75 in.
Root chord section a.c. aft of leading edge	$x_{c_{a.c.}}$	52.00 in.
Theoretical tip chord section a.c. aft of L.E.	$x_{tt_{a.c.}}$	69.36 in.
Aerodynamic center of wing, location aft of leading edge of root chord		61.7 in.
Location in percent of MAC_w		25.6%
Miscellaneous		
Airfoil sections Root NACA 2415		
Tip (Theoretical) NACA 4409		
Aspect Ratio	A_w	5.25
Taper Ratio	TR_w	.50
Angles		
Root chord incidence to thrust line	i_c	+7.0°
Theoretical tip chord incidence to thrust line	i_t	+3.0°
Geometric wing twist	ϕ_w	-4.0°
Root chord angle of zero lift	$\alpha_{l_{o_c}}$	-2.0°
Theoretical tip chord angle of zero lift	$\alpha_{l_{o_t}}$	-3.9°
Aerodynamic wing twist	ϵ_w	-2.1°
Sweepback at 40% chord line		0°
Cathedral - 40% chord plane center panel		6° 27' 10.3"
Dihedral - 40% chord plane outer panel		2° 44' 19.6"

PART I-C-2

ITEM	SYMBOL	VALUE
FLAPS		
Type - Slotted		
Area - Total		100 sq. ft.
One inboard flap aft of hinge line	S_{f_i}	14.55 sq. ft.
One outboard flap aft of hinge line	S_{f_o}	15.45 sq. ft.
One inboard flap forward of hinge line	$S_{f_{i_b}}$	8.75 sq. ft.
One outboard flap forward of hinge line	$S_{f_{o_b}}$	11.25 sq. ft.
Span - One inboard flap	b_{f_i}	65.2 in.
One outboard flap	b_{f_o}	85.0 in.
Chords - Inboard flap aft of hinge line (average)	c_{f_i}	30.64 in.
Outboard flap aft of hinge line (average)	c_{f_o}	24.26 in.
Inboard flap forward of hinge line (average)	$c_{f_{i_b}}$	19.74 in.
Outboard flap forward of hinge line (average)	$c_{f_{o_b}}$	19.74 in.
Location - Along semi-span	$\frac{2y_v}{b_v}$	
Inboard end of inboard flap		.1144
Outboard end of inboard flap		.2139
Inboard end of outboard flap		.3469
Outboard end of outboard flap		.4764
Angles - Maximum deflection	δ_f	+ 40°
AILERONS		
Type - Frise		
Area - Total		112.0 sq. ft.
One inboard aileron aft of hinge line	S_{a_i}	26.10 sq. ft.
One outboard aileron aft of hinge line	S_{a_o}	16.85 sq. ft.
One inboard aileron forward of hinge line	$S_{a_{i_b}}$	8.10 sq. ft.
One outboard aileron forward of hinge line	$S_{a_{o_b}}$	4.95 sq. ft.
Span - One inboard aileron	b_{a_i}	163.1 in.
One outboard aileron	b_{a_o}	136.0 in.
Chord - Inboard aileron aft of hinge line (average)	c_{a_i}	23.045 in.
Outboard aileron aft of hinge line (average)	c_{a_o}	17.750 in.
Inboard aileron forward of hinge line (average)	$c_{a_{i_b}}$	6.806 in.
Outboard aileron forward of hinge line (average)	$c_{a_{o_b}}$	5.148 in.

PART I-C-2 (Cont.)

ITEM	SYMBOL	VALUE
AILERONS (Cont.)		
Location - Along semi-span	$\frac{2y_w}{B_w}$	
Inboard end of inboard aileron		.469
Intersection of inboard and outboard ailerons		.725
Outboard end of outboard aileron		.940
Angles - Inboard aileron	δ_a	+12° - 24°
Outboard aileron	δ_a	+12° - 24°
AILERON TRIM TAB		
Area -	$S_{a_{tt}}$	2.72 sq. ft.
Span -	$b_{a_{tt}}$	49 in.
Chord - Aft of hinge line	$c_{a_{tt}}$	8 in.
Location - Along semi-span of right wing	$\frac{2y_w}{B_w}$	
Inboard end of trim tab		.5575
Outboard end of trim tab		.6320
Angles - Maximum deflections	$\delta_{a_{tt}}$	± 15°
AILERON BALANCE TAB		
Area - One balance tab	$S_{a_{bt}}$	2.74 sq. ft.
Span - One balance tab	$b_{a_{bt}}$	49.29 in.
Chord - Aft of hinge line	$c_{a_{bt}}$	8 in.
Location - Along semi-span of each wing	$\frac{2y_w}{B_w}$	
Inboard end of balance tab		.4840
Outboard end of balance tab		.5575
Angles - Maximum deflections	$\delta_{a_{bt}}$	+36° - 16°

PART I-C-3

3. FUSELAGE

The following table summarizes the physical characteristics of the fuselage.

ITEM	SYMBOL	VALUE
FUSELAGE		
Area - Frontal	F_f	175.3 sq. ft.
Planform	P_f	579.0 sq. ft.
Side	S_f	801.0 sq. ft.
Length -	L_f	55.94 ft.
Miscellaneous - Maximum width		11.5 ft.
Maximum depth		17.28 ft.
Location of wing 40% Chord line aft of fuselage nose		370.0 in.

The fuselage consists of the combination of crew nacelle and pack.

PART I-C-3A

3A. Crew Nacelle

The following table summarizes the physical characteristics of the crew nacelle.

ITEM	SYMBOL	VALUE
CREW NACELLE		
Area - Frontal	F_n	58.8 sq. ft.
Planform	P_n	450.0 sq. ft.
Side	S_n	271.0 sq. ft.
Length -	L_n	50.2 ft.
Miscellaneous - Maximum Width		10.0 ft.
Maximum Depth		6.9 ft.
Location of Wing 40% Chord line Aft of Crew Nacelle Nose		301.5 in.

PART I-C-4

4. BOOMS

The following table summarizes the physical characteristics of the booms, power plants and propellers. Note that values as shown here are for one of each item.

ITEM	SYMBOL	VALUE
BOOM		
Area - Frontal	F_b	40.76 sq. ft.
Planform	P_b	312.5 sq. ft.
Side	S_b	363.2 sq. ft.
Length -	L_b	68.2 ft.
Miscellaneous - Maximum width		6.25 ft.
Maximum depth		7.35 ft.
Location of C_L of propeller aft of fuselage nose		162.09 in.
Location of C_L of boom outboard of centerline of fuselage		175.00 in.
POWER PLANT		
Pratt & Whitney - R-4360-20		
PROPELLER		
Type - Hamilton Standard 2H17F3-24		
Area - One propeller disc	F_p	178.2 sq. ft.
Diameter	D_p	15 ft. 1 in.
Number of Blades - 4		

PART I-C-5

5. HORIZONTAL TAIL

The following table summarizes the physical characteristics of the horizontal tail, elevator and elevator tabs.

ITEM	SYMBOL	VALUE
HORIZONTAL TAIL		
Area - Total	S_{ht}	346.2 sq. ft.
Span - Total	B_{ht}	450.0 in.
Between ℄ of fins	b_{ht_f}	350.0 in.
Outboard of ℄ of fins (one tip)	b_{ht_o}	50.0 in.
Chord - Of center section	c_{ht_c}	117.75 in.
At theoretical tips	$c_{ht_{tt}}$	110.25 in.
Miscellaneous - Horizontal tail length from ¼ chord point of wing center section to ¼ chord point horizontal tail	l_{ht}	47.5 ft.
Aspect Ratio	A_{ht}	4.05
Taper Ratio	TR_{ht}	1.0
Airfoil section NACA 0014		
Angles - Angle of incidence of horizontal tail to thrust line.	i_{ht}	1.0°
ELEVATOR		
Area - Aft of hinge line	S_e	83.616 sq. ft.
Forward of hinge line to L.E. of elevator	S_{e_b}	30.245 sq. ft.
Span -	b_e	303.0 in.
Chord - Aft of hinge line	c_e	38.25 in.
Forward of hinge line to L.E. of elevator	c_{e_b}	14.14 in.
Angles - Maximum deflections	δ_e	+ 25° - 35°
ELEVATOR SPRING TAB		
Area -	$S_{e_{st}}$	3.83 sq. ft.

PART I-C-5 (Cont.)

ITEM	SYMBOL	VALUE
ELEVATOR SPRING TAB (Cont.)		
Span -	$b_{e_{st}}$	92.0 in.
Chord -	$c_{e_{st}}$	6.0 in.
Angles - Maximum deflections	$\delta_{e_{st}}$	+22° - 12°
ELEVATOR TRIM TAB		
Area -	$S_{e_{tt}}$	5.44 sq. ft.
Span -	$b_{e_{tt}}$	130.5 in.
Chord-	$c_{e_{tt}}$	6.0 in.
Angles - Maximum deflections	$\delta_{e_{tt}}$	+ 25° - 10°

PART I-C-6

6. VERTICAL TAIL

The following table summarizes the physical characteristics of the vertical tail, rudder, and rudder trim and spring tabs. Note that all data shown are for one item.

ITEM	SYMBOL	VALUE
VERTICAL TAIL		
Area -	S_{vt}	99.6 sq. ft.
Span - Total	B_{vt}	200.0 in.
Above horizontal tail intersection	b_{vt} upper	140.0 in.
Below horizontal tail intersection	b_{vt} lower	60.0 in.
Chord -		
At intersection of horizontal and vertical surfaces	c_{vt_o}	97.5 in.
At upper theoretical tip	$c_{vt_{tt}}$ upper	39.0 in.
At lower theoretical tip	$c_{vt_{tt}}$ lower	72.43 in.
Miscellaneous - Aspect ratio	A_{vt}	2.79
Taper ratio - upper	TR_{vt} upper	.400
Taper ratio - lower	TR_{vt} lower	.764
Airfoil section NACA 0012		
RUDDER		
Area -		
Aft of hinge line	S_r	50.25 sq. ft.
Forward of hinge line to leading edge of rudder	S_{r_b}	17.43 sq. ft.
Span - Above horizontal tail intersection	b_r upper	138.66 in.
Below horizontal tail intersection	b_r lower	60.0 in.
Chord -		
Aft of hinge line	c_r	2.0 ft.
Forward of hinge line	c_{r_b}	.6 ft.
Angles - Maximum deflections	δ_r	$\pm$ 35°
RUDDER TRIM TAB		
Area -	$S_{r_{tt}}$	3.01 sq. ft.
Span - perpendicular to thrust line	$b_{r_{tt}}$	53.635 in.
Chord - parallel to thrust line	$c_{r_{tt}}$	8.077 in.

PART I-C-6 (Cont.)

ITEM	SYMBOL	VALUE
RUDDER TRIM TAB (Cont.)		
Angles - Maximum deflections	$\delta_{r_{tt}}$	$\pm$ 15°
RUDDER SPRING TAB		
Area -	$S_{r_{st}}$	1.66 sq. ft.
Span - perpendicular to thrust line	$b_{r_{st}}$	29.666 in.
Chord - parallel to thrust line	$c_{r_{st}}$	8.077 in.
Angles - Maximum deflections	$\delta_{r_{st}}$	$\pm$ 17.5°

PART I-O-7

7. LANDING GEAR

Due to the special configuration of the XC-120 airplane (with removable pack) a quadricycle type landing gear is used designed to hold the airplane in a level altitude without the aid of a separate nose wheel.

The landing gear consists of two four wheel assemblies, one on the forward portion of each boom. Each assembly consists of a pair of dual rear or main wheels equipped with 15:50 x 20 low pressure tires and dual front or auxiliary wheels equipped with 11:00 x 12 low pressure tires.

PART I-D

SUMMARY OF AERODYNAMIC CHARACTERISTICS

POWER-OFF

This section summarizes all of the power-off aerodynamic characteristics of the component parts of the airplane. These data are tabulated and/or shown graphically on the following pages.

The calculations and basic data used in determining the aerodynamic characteristics summarized in this section may be found in Part II-A.

PART I-D-1

1. WING UNFLAPPED

The following table and figures summarizes the power-off aerodynamic characteristics of the unflapped wing.

MAC_W	168.28 inches
h_W	18.64 inches
v_W	-14.58 inches
$a_W = C_{L_W \alpha_0}$	.0842 per degree
ϵ_W	-2.1°
α_0 ($L_W = 0$)	-1.13°
$A\ C_W$	25.6% of MAC_W
$C_{M_{W_{AC}}}$	-.0630
Positive $C_{L_W\ max}$	1.401
Negative $C_{L_W\ max}$	-0.567
$C_{N_W\ \psi} / \alpha_{co}$	.0000075 per degree

FIG 2

LIFT CURVE OF THE WING
$\delta_f = 0$

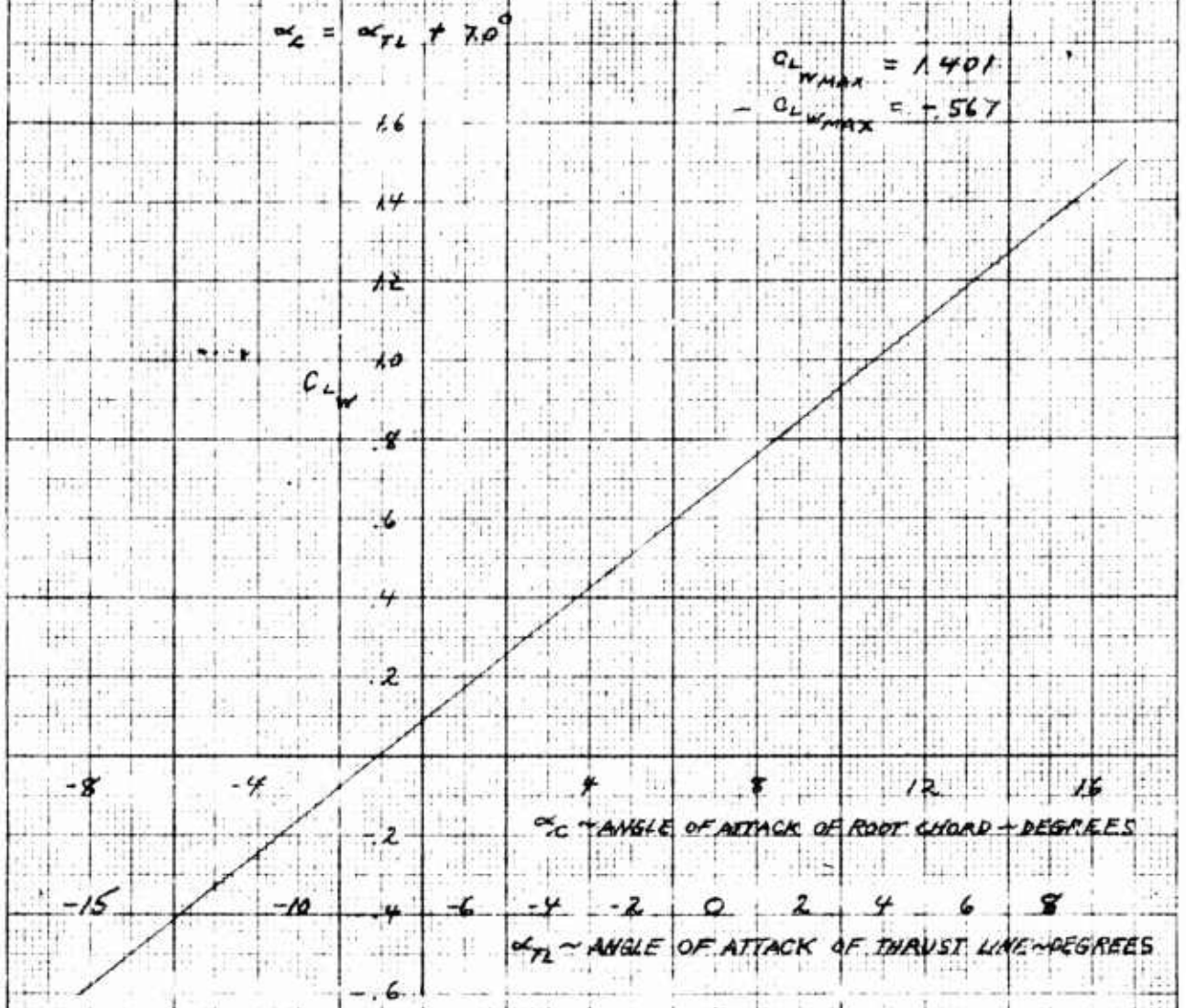

FIG 8

TOTAL WING DRAG COEFFICIENT
AND
INDUCED DRAG COEFFICIENT
FOR
UNFLAPPED WING

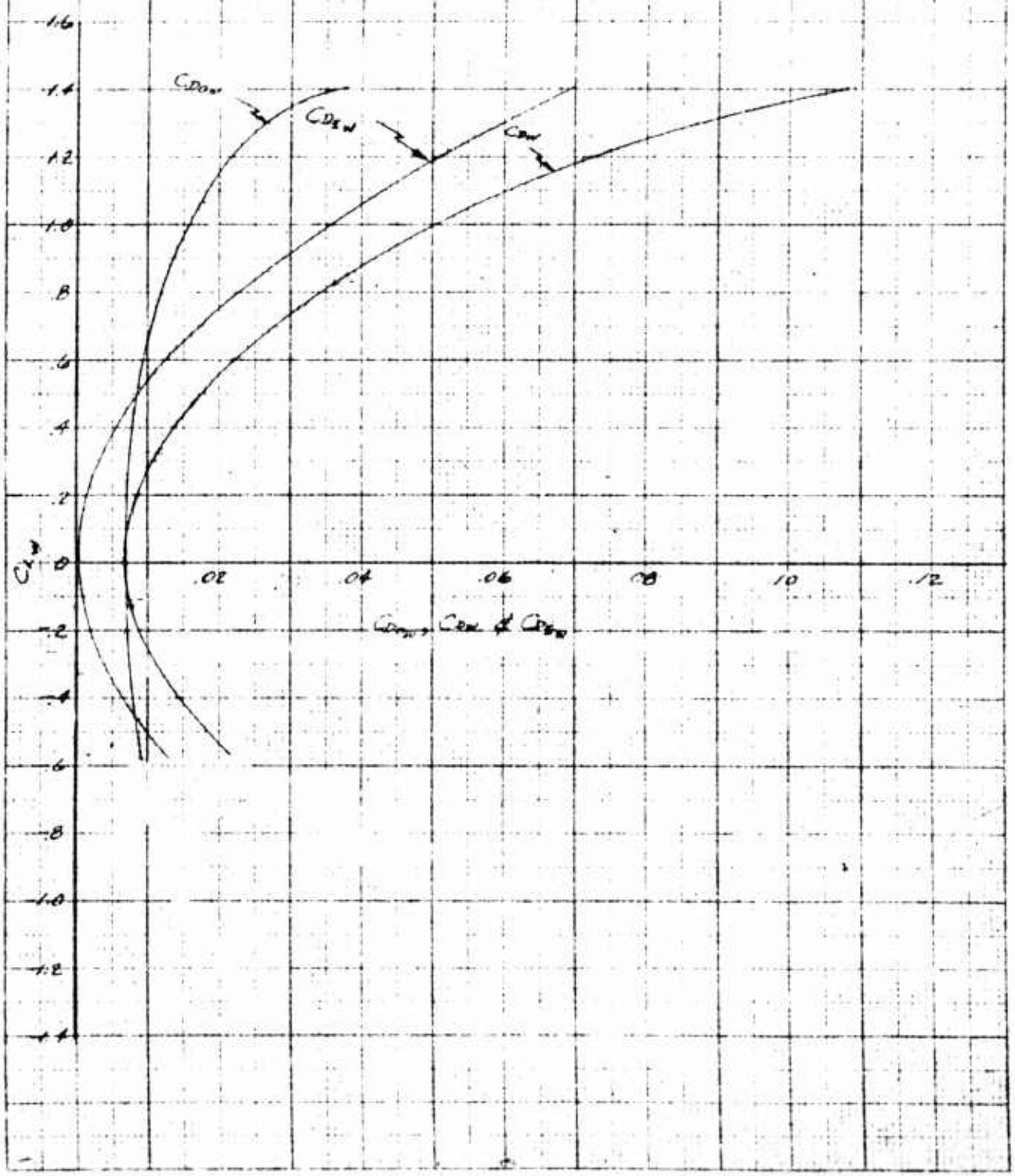

FIG 4
FIG 6A

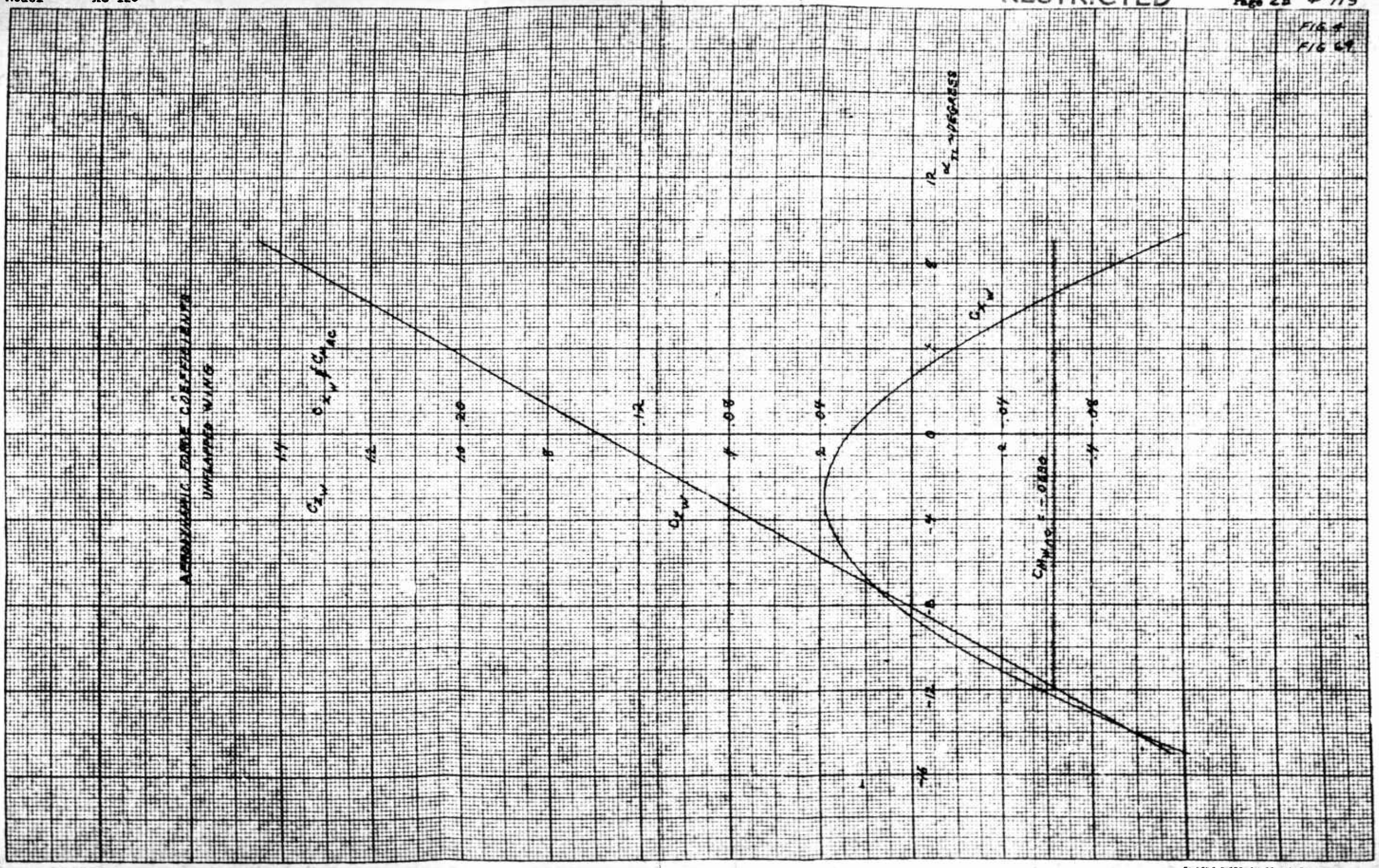
AERODYNAMIC FORCE COEFFICIENTS
UNFLAPPED WING
C_{Z_W}
C_{X_W}
$C_{X_W} \cdot \frac{S}{S_W} C_{M_{AC}}$
C_{L_W}
$C_{M_{W.A.C.}} = 0.000$
α_{TL} ~ DEGREES

FIG. 8
F16 70

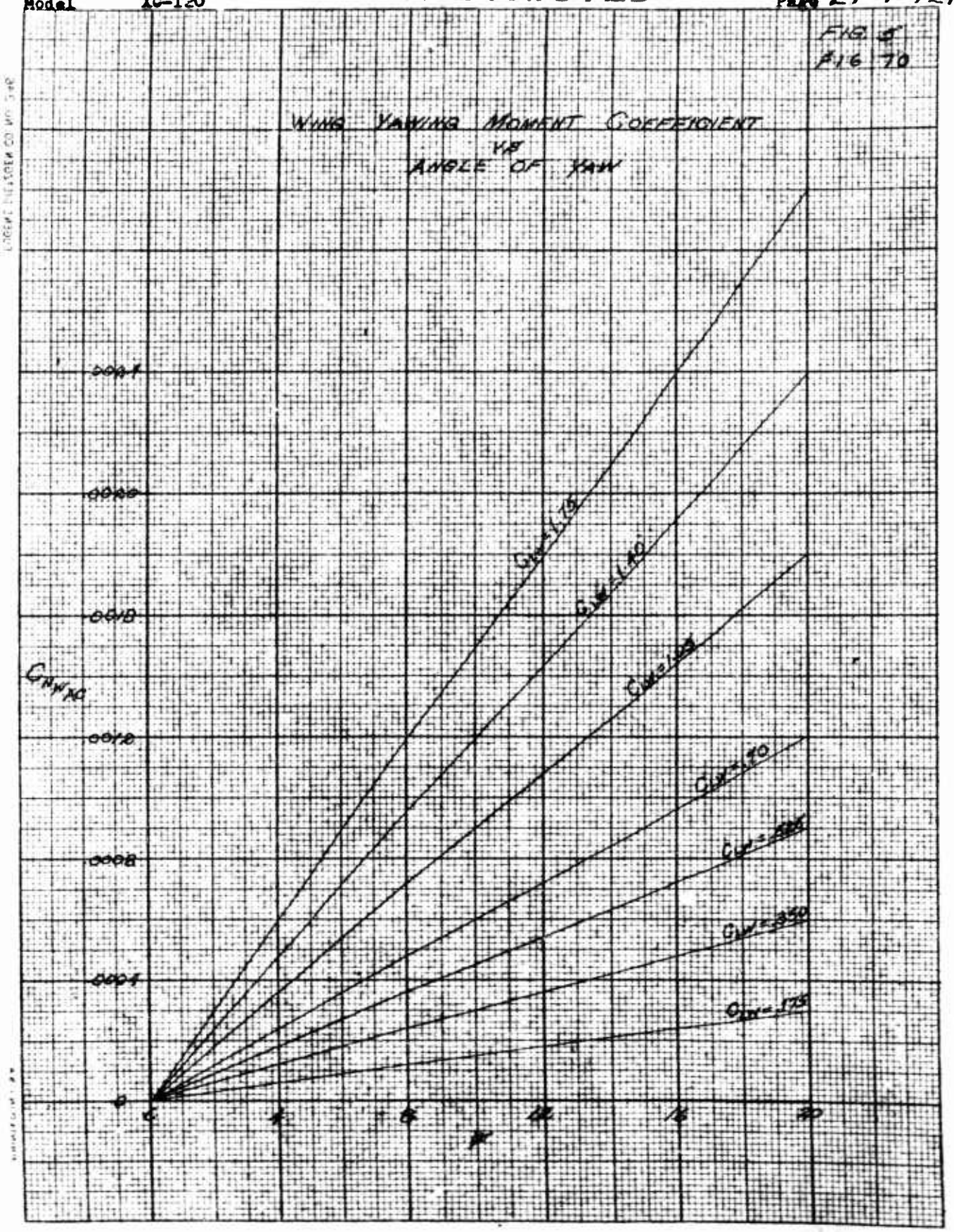
WING YAWING MOMENT COEFFICIENT
VS
ANGLE OF YAW
$C_{N_{W_{XC}}}$
.0014
.0016
.0018
.0012
.0008
.0004
0
0
4
8
12
16
20
C_{L_W}=1.75
C_{L_W}=1.40
C_{L_W}=1.05
C_{L_W}=.70
C_{L_W}=.525
C_{L_W}=.350
C_{L_W}=.175

PART I-D-2

2. WING FLAPPED

The following table and figures summarize the power-off aerodynamic characteristics of the flapped wing.

$a_{wf} = C_{L_{WF}\alpha_c}$	.0842 per degree
α_c ($L_{WF} = 0$)	-5.15°
A C_{wf}	25.6% MAC_w
$C_{M_{WF_{AC}}}$	-.1497
Positive $C_{L_{WF\ max}}$	1.762

For characteristics in yaw see discussion of Part II-A-2-m.

FIG. 6

LIFT CURVE OF THE WING
$\delta_f = 40.0°$

$\alpha_c = \alpha_{TL} + 7.0°$ $C_{L_{MAX}} = 1.762$

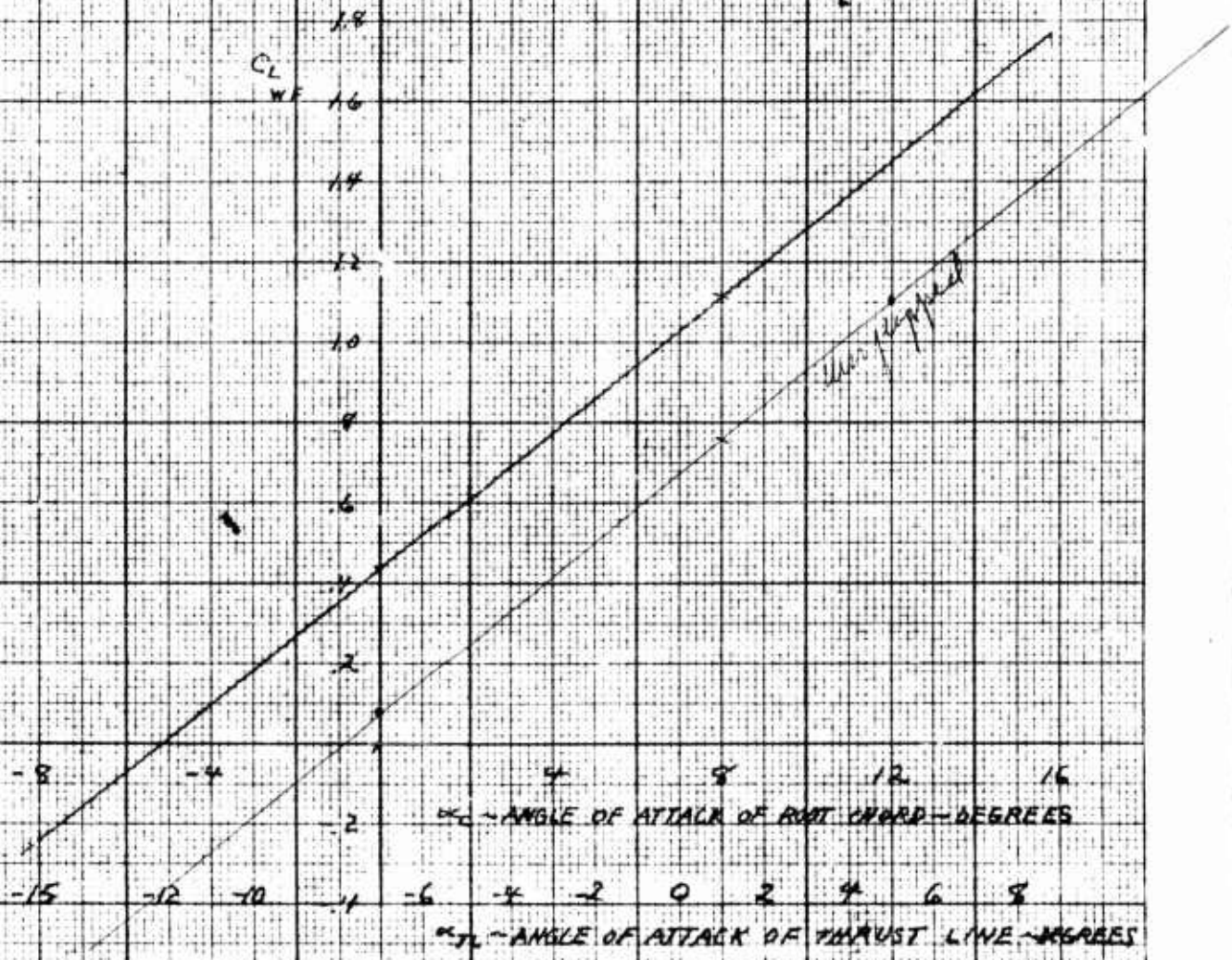

FIG. 28
FIG. 29

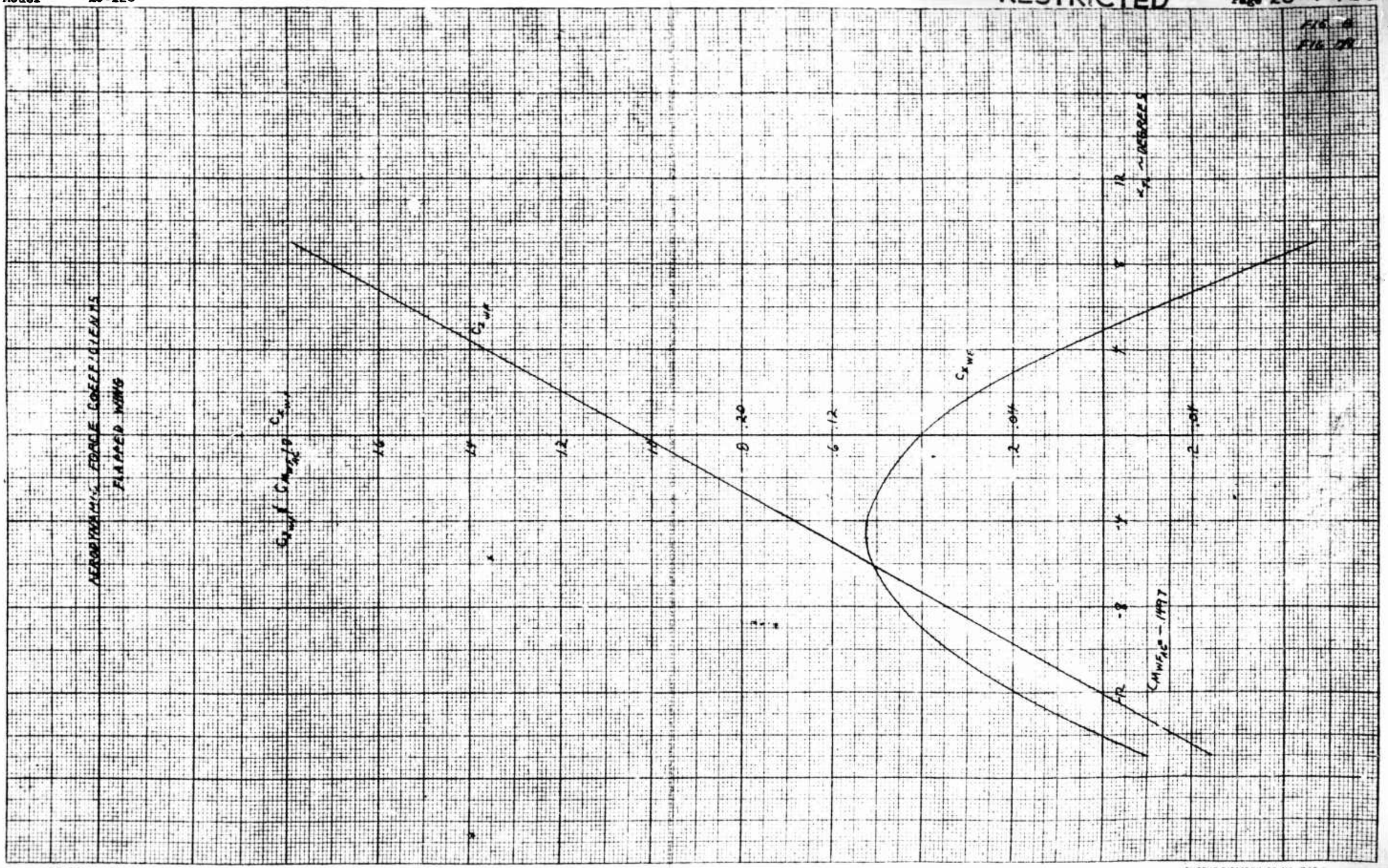
AERODYNAMIC FORCE COEFFICIENTS
FLAPPED WING
$C_{L_{WF}}$
$C_{L_{WF}} \pm C_{M_{WF_{AC}}}$
$C_{L_{WF}}$
$C_{M_{WF_{AC}}} = .1497$
α_F ~ DEGREES
1.8
1.6
1.4
1.2
1.0
.8
.6
.4
.2
.20
.12
.04
.04
.12
.20
12
8
4
0
-4
-8
-12

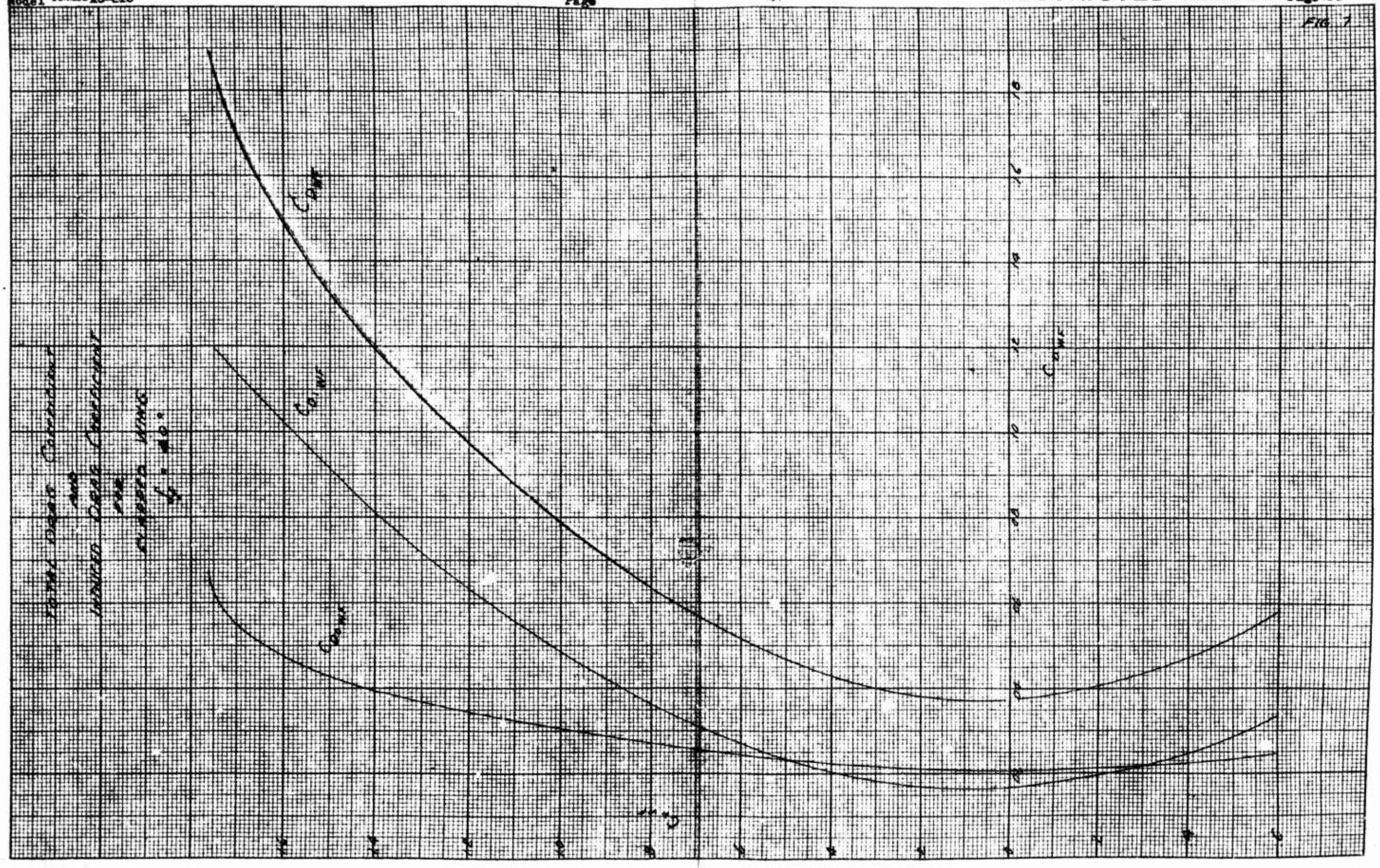
FIG. 7
TOTAL DRAG COEFFICIENT
AND
INDUCED DRAG COEFFICIENT
FOR
FLAPPED WING
$C_{D_{TOT}}$
$C_{D_{IND}}$
$C_{D_{TOT}}$
$C_{D_{IND}}$
C_L

PART I-D-3

3. AILERONS

The following tables and figures summarize the power-off aerodynamic characteristics of the ailerons. Note that the aerodynamic characteristics are different for up and down aileron deflections.

DOWN AILERON

$C_{L_W}\ \delta_a$	.00572 per degree
$c_m\ \delta_a$	-.0069 per degree
$C_{H_a}\ \delta_a$	-.0054 per degree
$c_l\ \delta_a$	.0316 per degree
$\alpha_c\ \delta_a$	-.0680 per degree
$C_{H_a}\ \alpha_{s\ ave}$	-.0012 per degree

UP AILERON

$C_{L_W}\ \delta_a$	.00607 per degree
$c_m\ \delta_a$	-.0073 per degree
$C_{H_a}\ \delta_a$	-.0016 per degree
$c_l\ \delta_a$	.0336 per degree
$\alpha_c\ \delta_a$	-.0722 per degree
$C_{H_a}\ \alpha_{s\ ave}$	-.0012 per degree

FIG 9

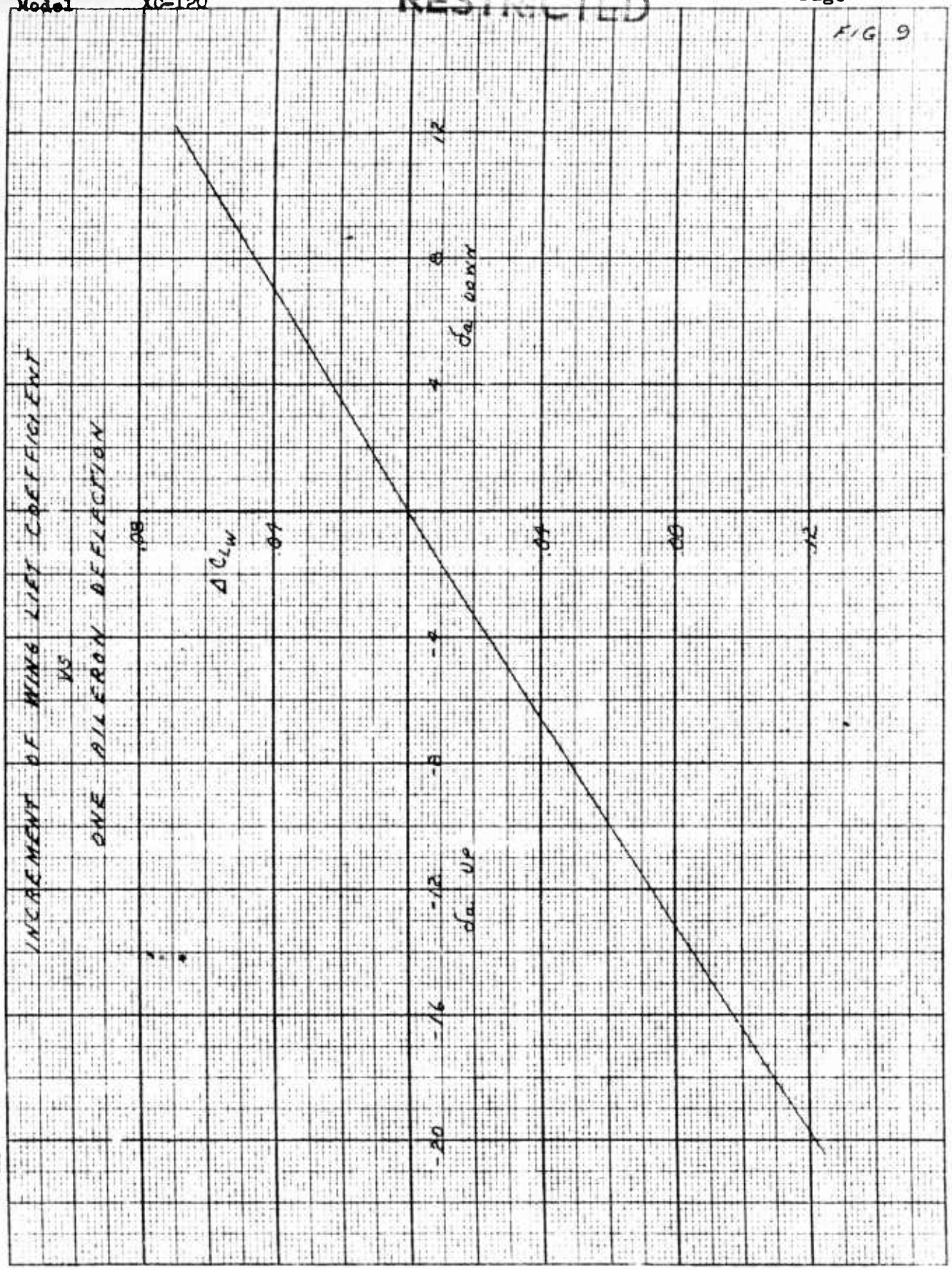
INCREMENT OF WING LIFT COEFFICIENT
VS
DIFF AILERON DEFLECTION
ΔC_{L_W}
.08
.04
.04
.08
.12
δ_a up
δ_a down
-20
-16
-12
-8
-4
4
8
12

FIG. 10

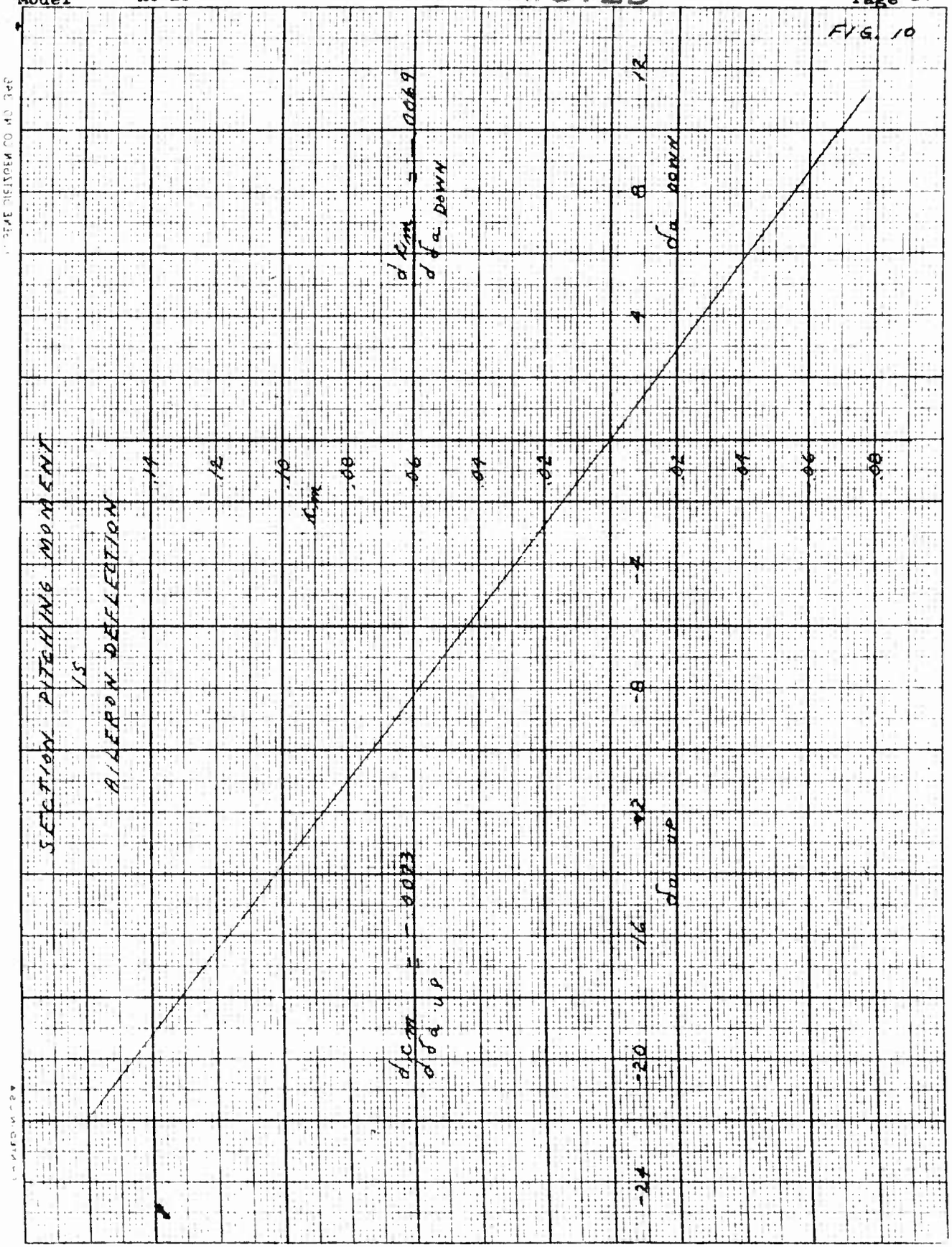
SECTION PITCHING MOMENT
VS
AILERON DEFLECTION
C_m
.14
.12
.10
.08
.06
.04
.02
-.02
-.04
-.06
-.08
$\frac{dC_m}{d\delta_a} = -.0073$
δ_a UP
-24
-20
-16
-12
-8
-4
4
8
12
$\frac{dC_m}{d\delta_a} = -.0069$
δ_a DOWN

FIG. 11

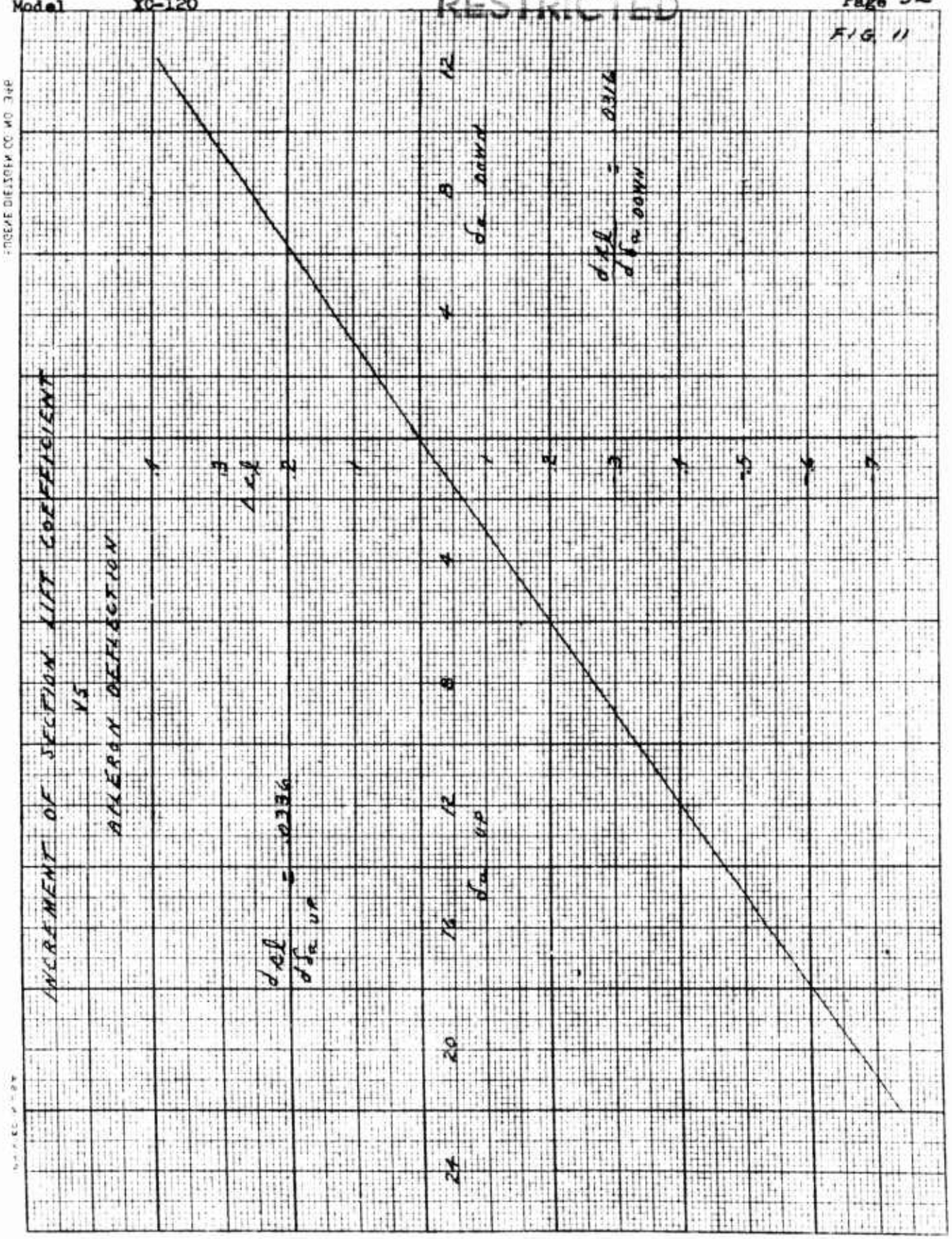
INCREMENT OF SECTION LIFT COEFFICIENT
VS
AILERON DEFLECTION
Δc_l
$\frac{dc_l}{d\delta_a}$ UP = .0336
$\frac{dc_l}{d\delta_a}$ DOWN = .0316
δ_a UP
δ_a DOWN
1
2
3
4
5
6
7
8
12
16
20
24

FIG 12

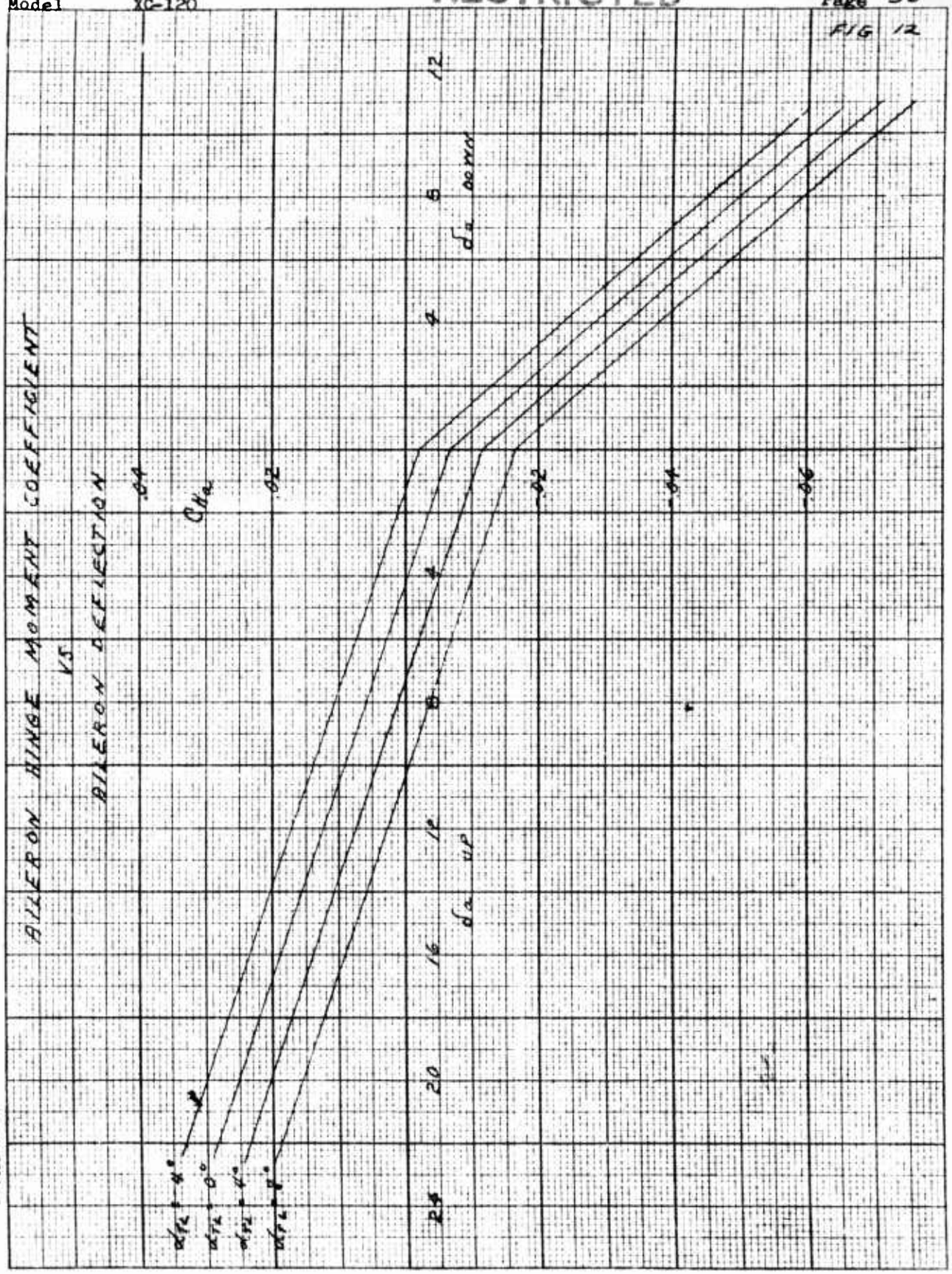
AILERON HINGE MOMENT COEFFICIENT
VS
AILERON DEFLECTION
C_{H_a}
.04
.02
-.02
-.04
-.06
δ_a UP
δ_a DOWN
24
20
16
12
8
4
0
4
8
12
$\alpha_{FL} = 4°$
$\alpha_{FL} = 0°$
$\alpha_{FL} = -4°$
$\alpha_{FL} = -8°$

PART I-D-4

4. AILERON TABS

The following tables and figures summarize the power-off aerodynamic characteristics of the aileron trim and balance tabs.

TRIM TAB	
$c_{l_{\delta_{a_{tt}}}}$	.01248 per degree
$\alpha_{c_{\delta_{a_{tt}}}}$	-.0045 per degree
$C_{H_{a_{\delta_{a_{tt}}}}}$	-.0009 per degree
$C_{H_{a_{tt}}}$	-.0022 per degree

BALANCE TAB	
$c_{l_{\delta_{a_{bt}}}}$	.01144 per degree
$\left(\frac{p\,B_w}{2\,V}\right)_{\delta_{a_{bt}}}$	.0000935 per degree
$C_{H_{a_{\delta_{a_{bt}}}}}$	-.0021 per degree
$C_{H_{a_{bt}\,\delta_{a_{bt}}}}$	-.0017 per degree

FIG 13

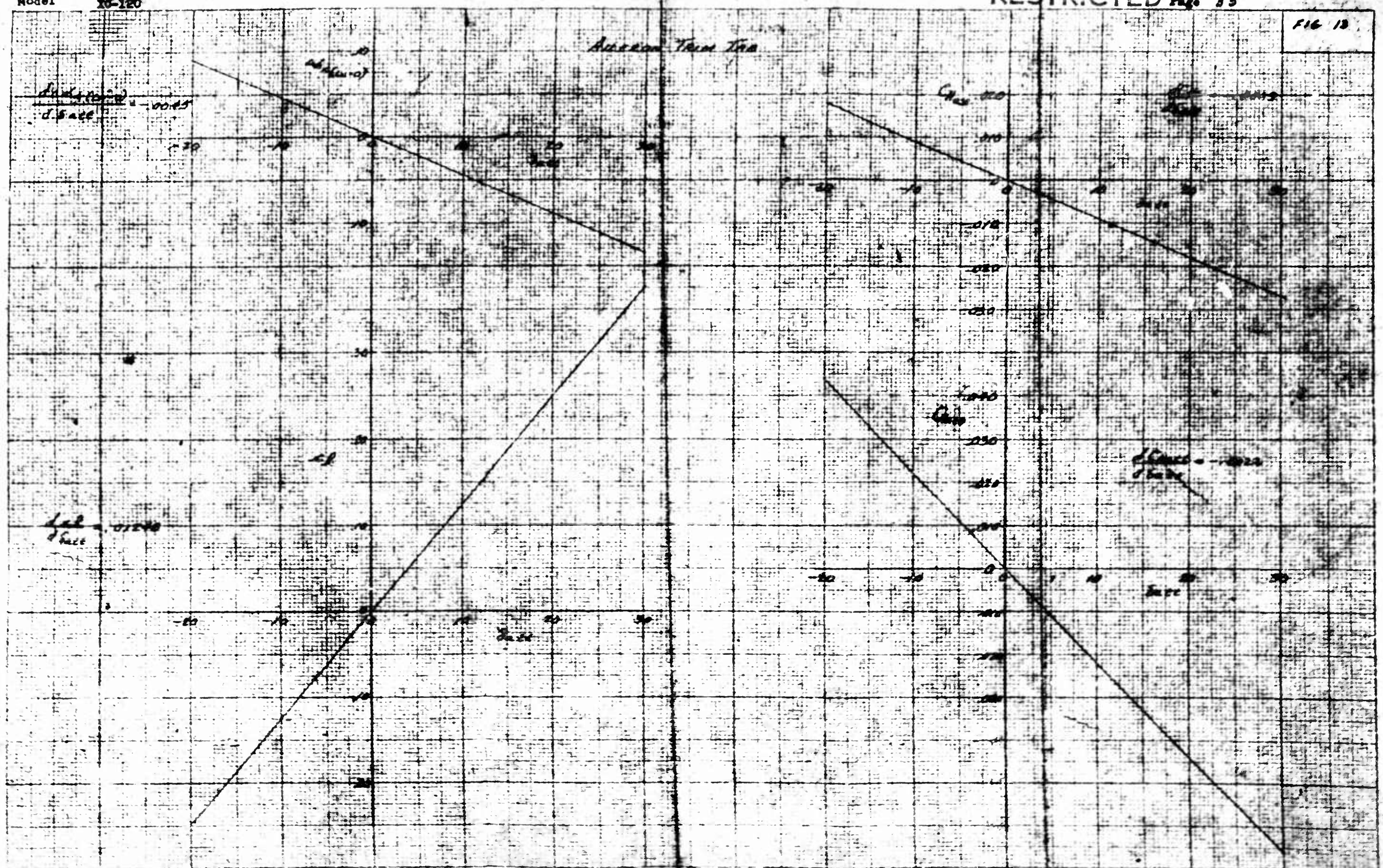

FIG 14

AILERON BALANCE TAB DEFLECTION
VS
AILERON DEFLECTION

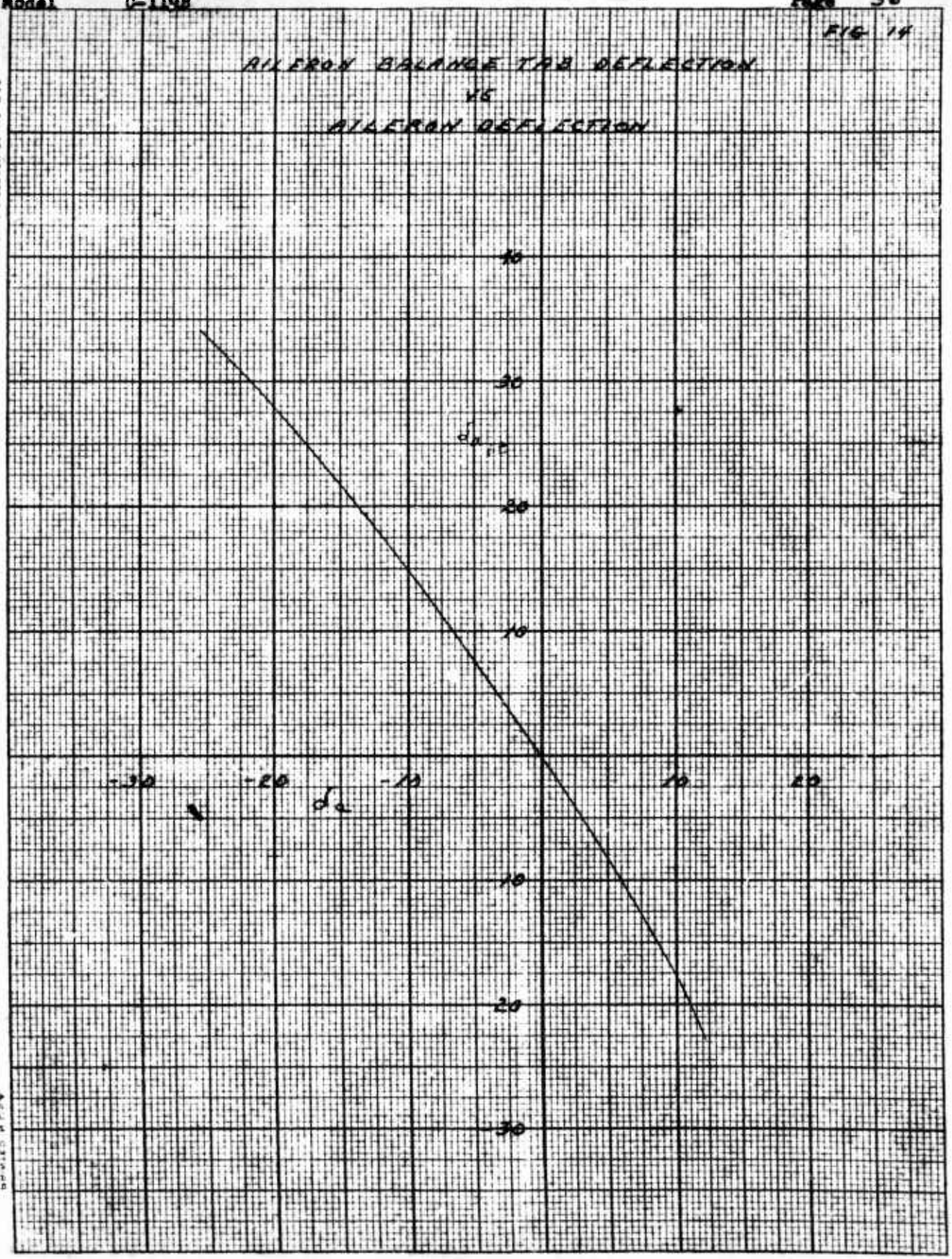

RESTRICTED

FIG 15

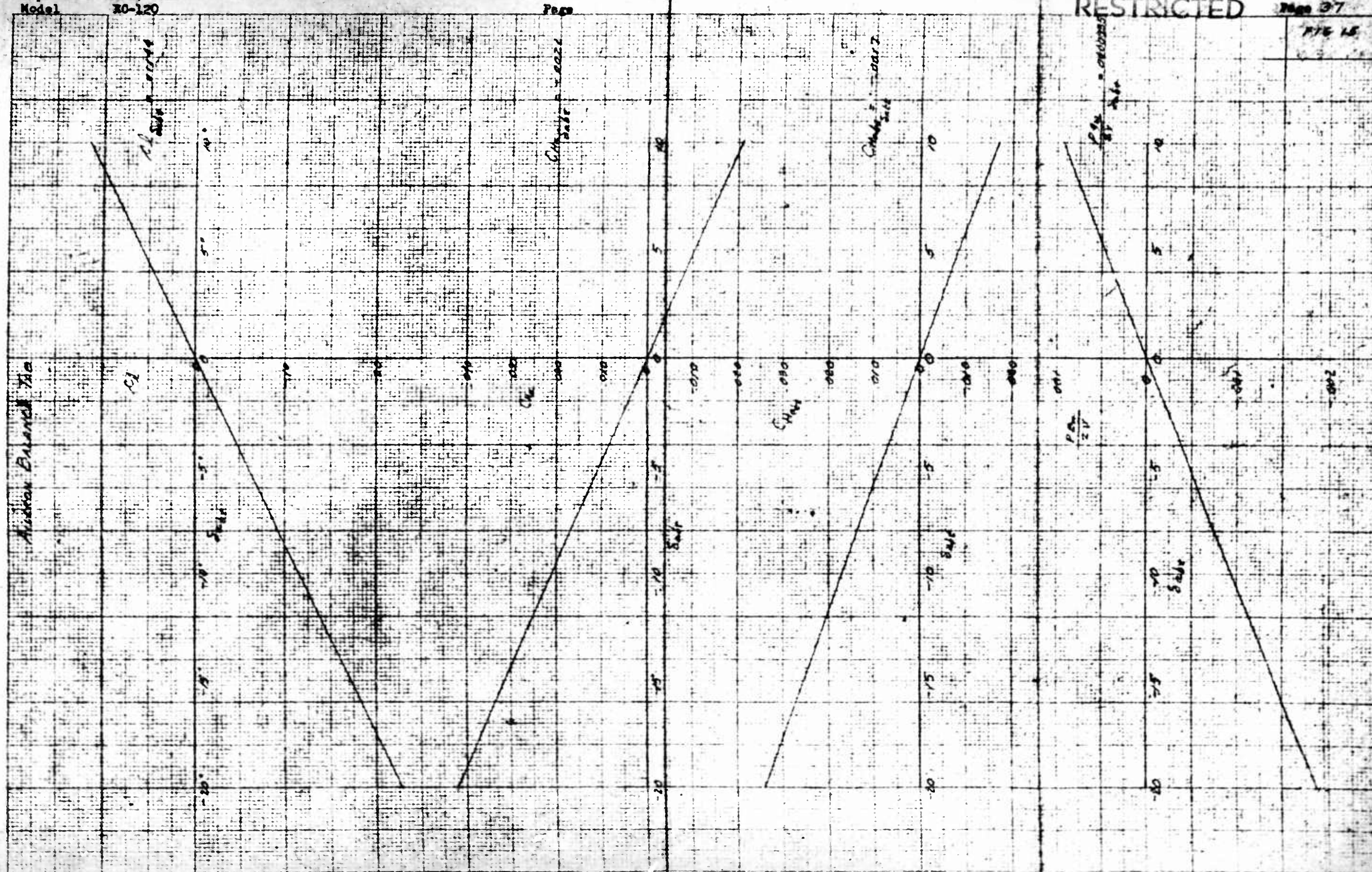

PART I-D-5

5. **FUSELAGE**

The following figures summarize the power-off aerodynamic characteristics of the fuselage (crew nacelle - pack combination)

C_{D_F} at $\alpha_f = 0^\circ$ = .09914 based on

the maximum cross sectional area of the fuselage.

Characteristics in yaw - see discussion in Part II-A-5g.

FIG 16
FIG 73

VARIATION OF FUSELAGE LIFT COEFFICIENT
WITH
FUSELAGE ANGLE OF ATTACK

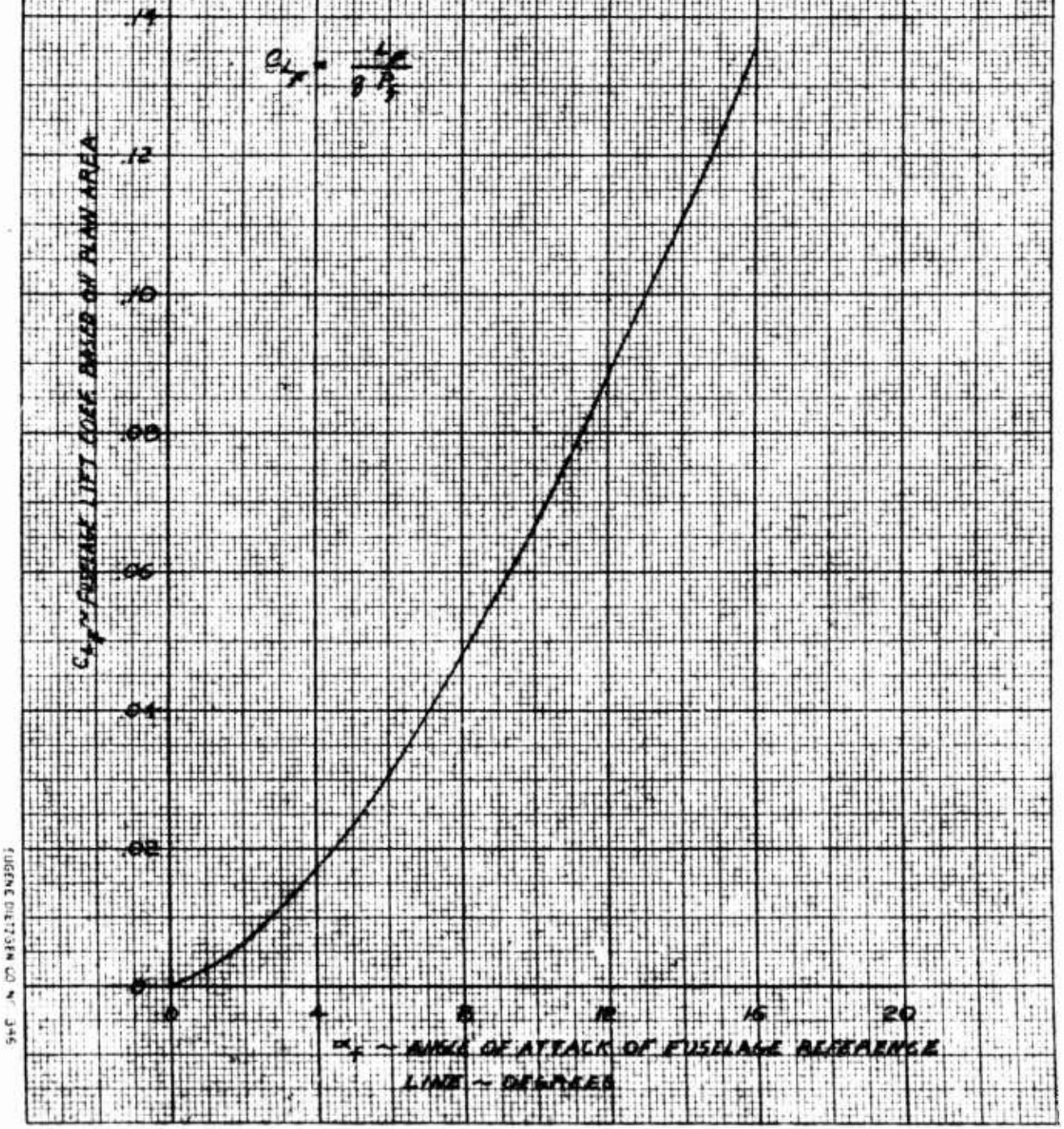

FIG 17
FIG 75

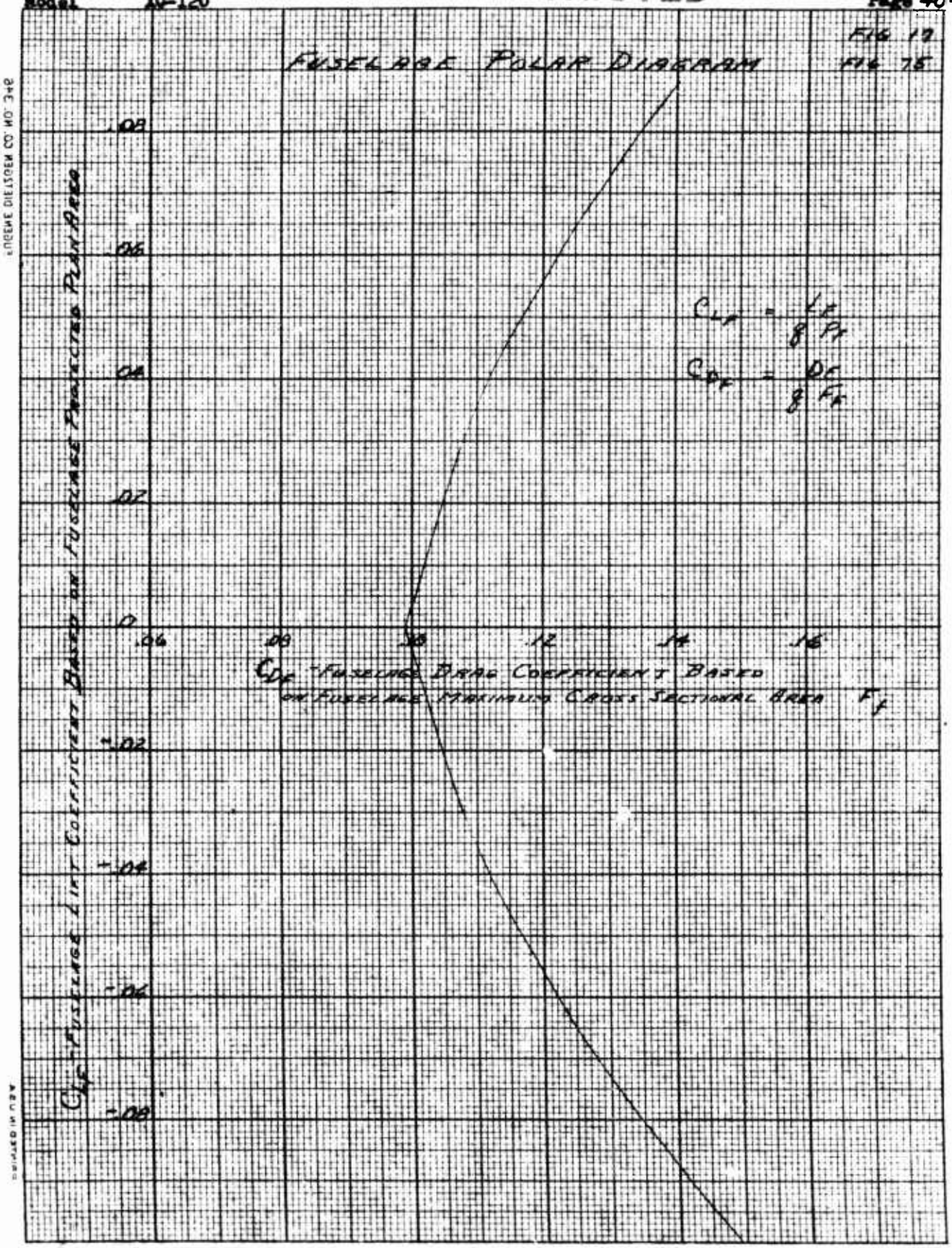
FUSELAGE POLAR DIAGRAM
$C_{L_F} = \frac{L_F}{q F_F}$
$C_{D_F} = \frac{D_F}{q F_F}$
.08
.06
.04
.02
0
-.02
-.04
-.06
-.08
.06
.08
.10
.12
.14
.16
C_{L_F} - FUSELAGE LIFT COEFFICIENT BASED ON FUSELAGE PROJECTED PLAN AREA
C_{D_F} - FUSELAGE DRAG COEFFICIENT BASED ON FUSELAGE MAXIMUM CROSS SECTIONAL AREA F_F

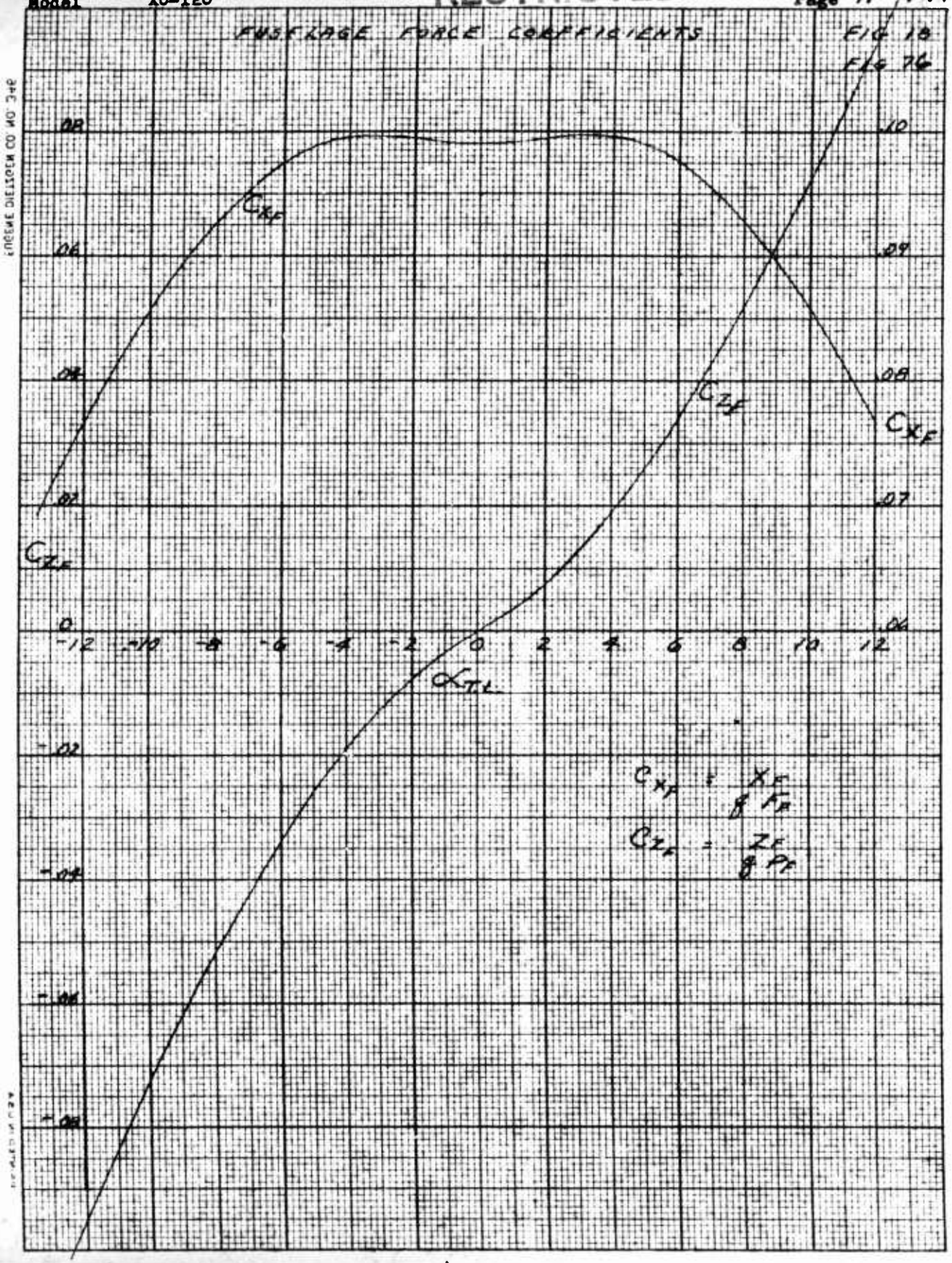
FUSELAGE FORCE COEFFICIENTS
FIG 18
FIG 76
C_{X_F}
C_{Z_F}
α_{TL}
$C_{X_F} = \frac{X_F}{q\,A_F}$
$C_{Z_F} = \frac{Z_F}{q\,A_F}$
.10
.09
.08
.07
.06
.08
.06
.04
.02
0
-.02
-.04
-.06
-.08
-12
-10
-8
-6
-4
-2
0
2
4
6
8
10
12

RESTRICTED

FIG. 19
FIG. 77

FUSELAGE PITCHING MOMENT COEFFICIENT
ABOUT THE QUARTER LENGTH POINT

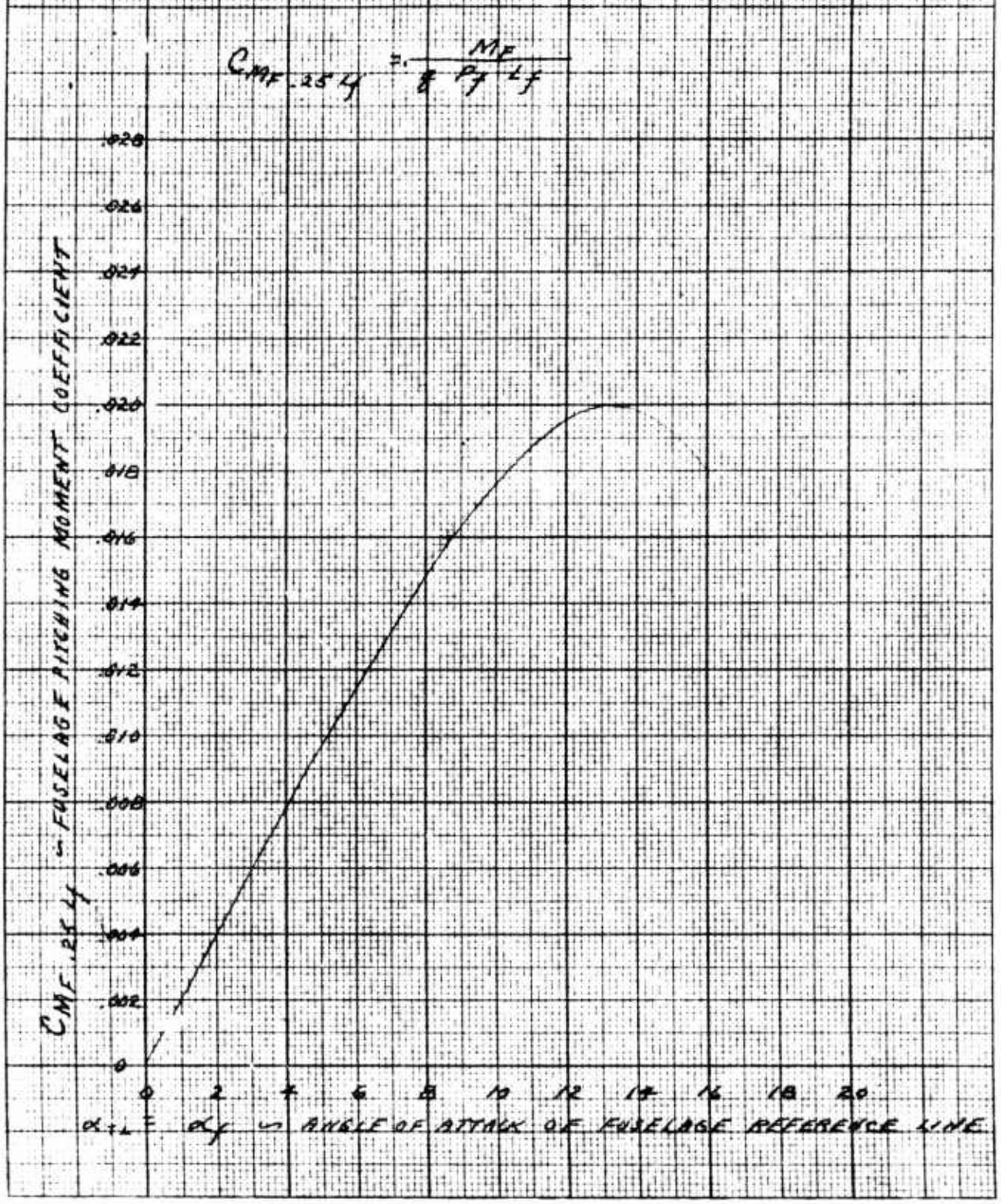

PART I-D-5A

5A. CREW NACELLE

The following figures summarize the power-off aerodynamic characteristics of the crew nacelle.

C_{D_N} at $\alpha_n = 0^\circ = .12286$ based on the maximum cross sectional area of the crew nacelle.

RESTRICTED

FIG 20
FIG 79

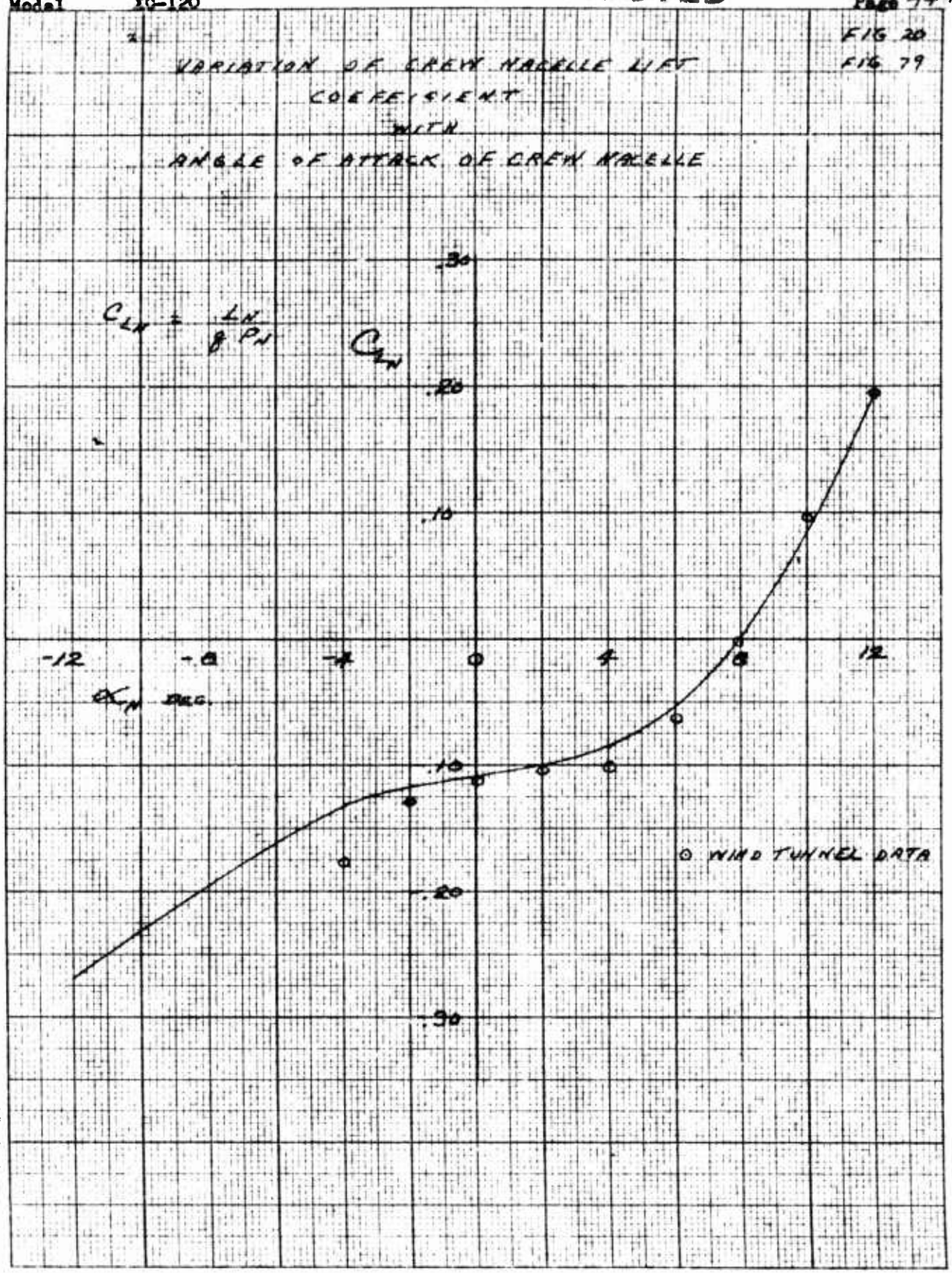

RESTRICTED

FIG. 21
FIG. 81

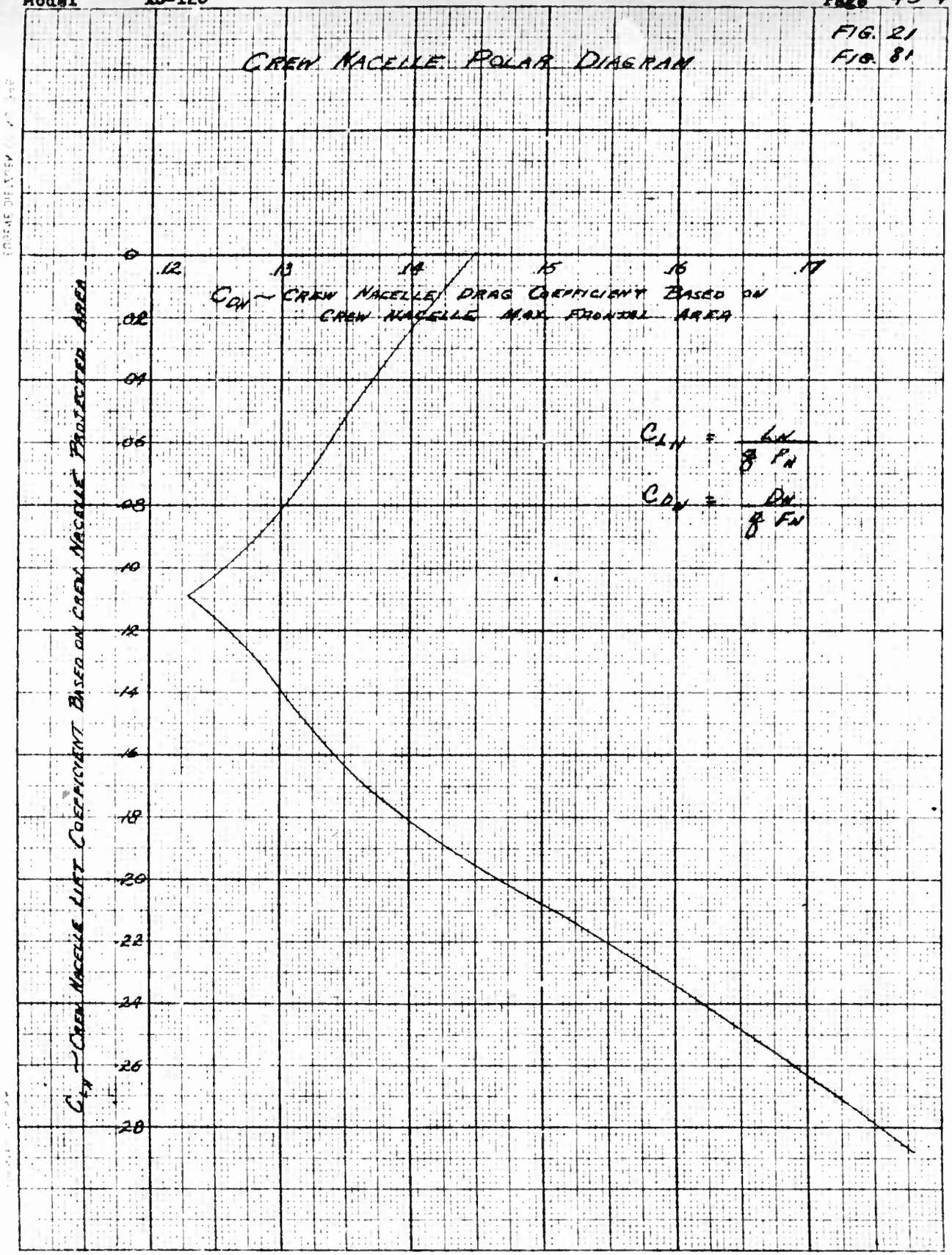

RESTRICTED

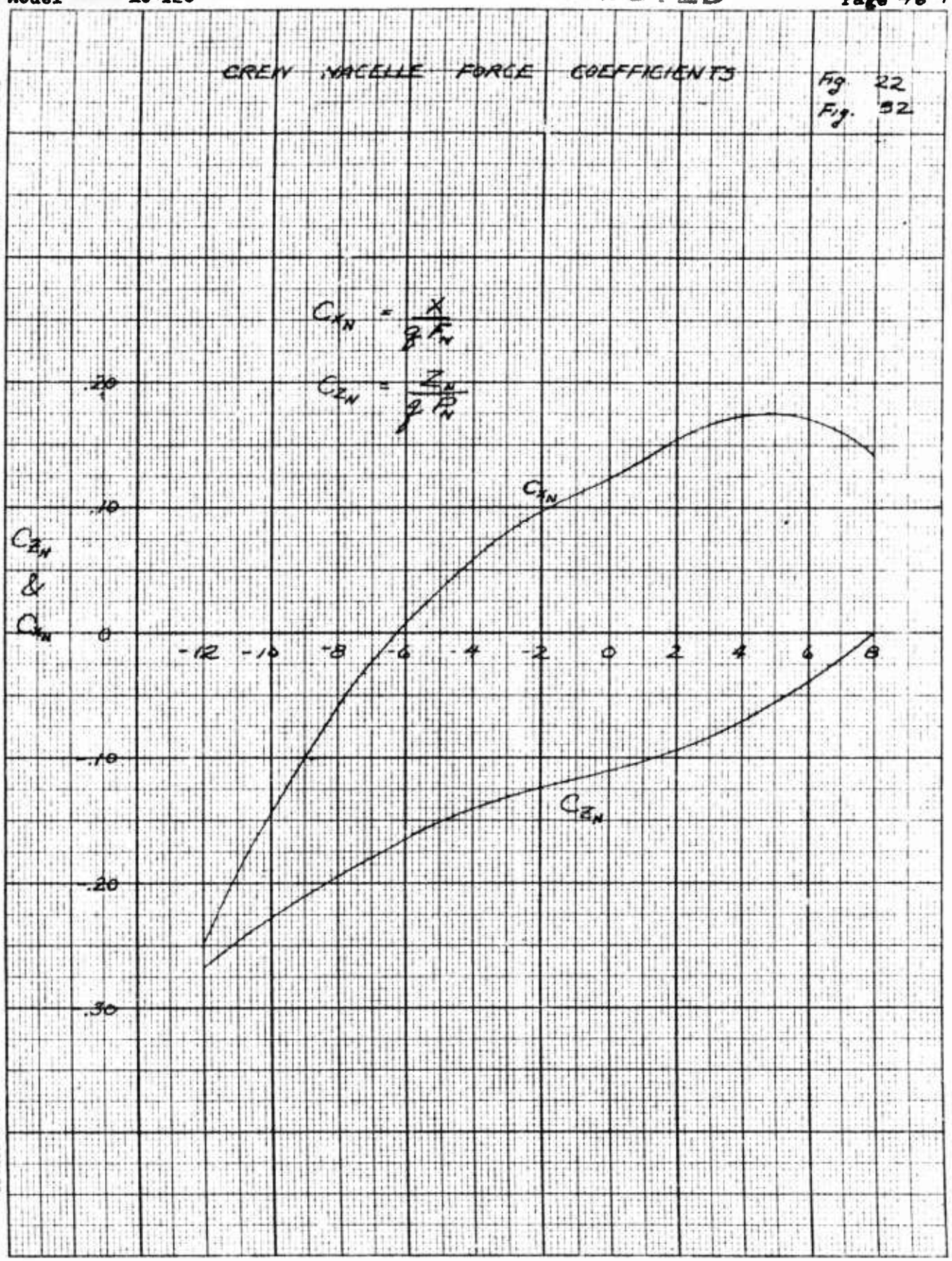
CREW NACELLE FORCE COEFFICIENTS
Fig. 22
Fig. 32
$C_{X_N} = \frac{X}{q F_N}$
$C_{Z_N} = \frac{Z_N}{q F_N}$
C_{Z_N} & C_{X_N}
.20
.10
0
-.10
-.20
-.30
-12
-10
-8
-6
-4
-2
0
2
4
6
8
C_{X_N}
C_{Z_N}

FIG. 23
FIG. 83

CREW NACELLE PITCHING MOMENTS

$$C_{M_{N.25L_N}} = \frac{M_{N.25L_N}}{q\,P_N\,L_N}$$

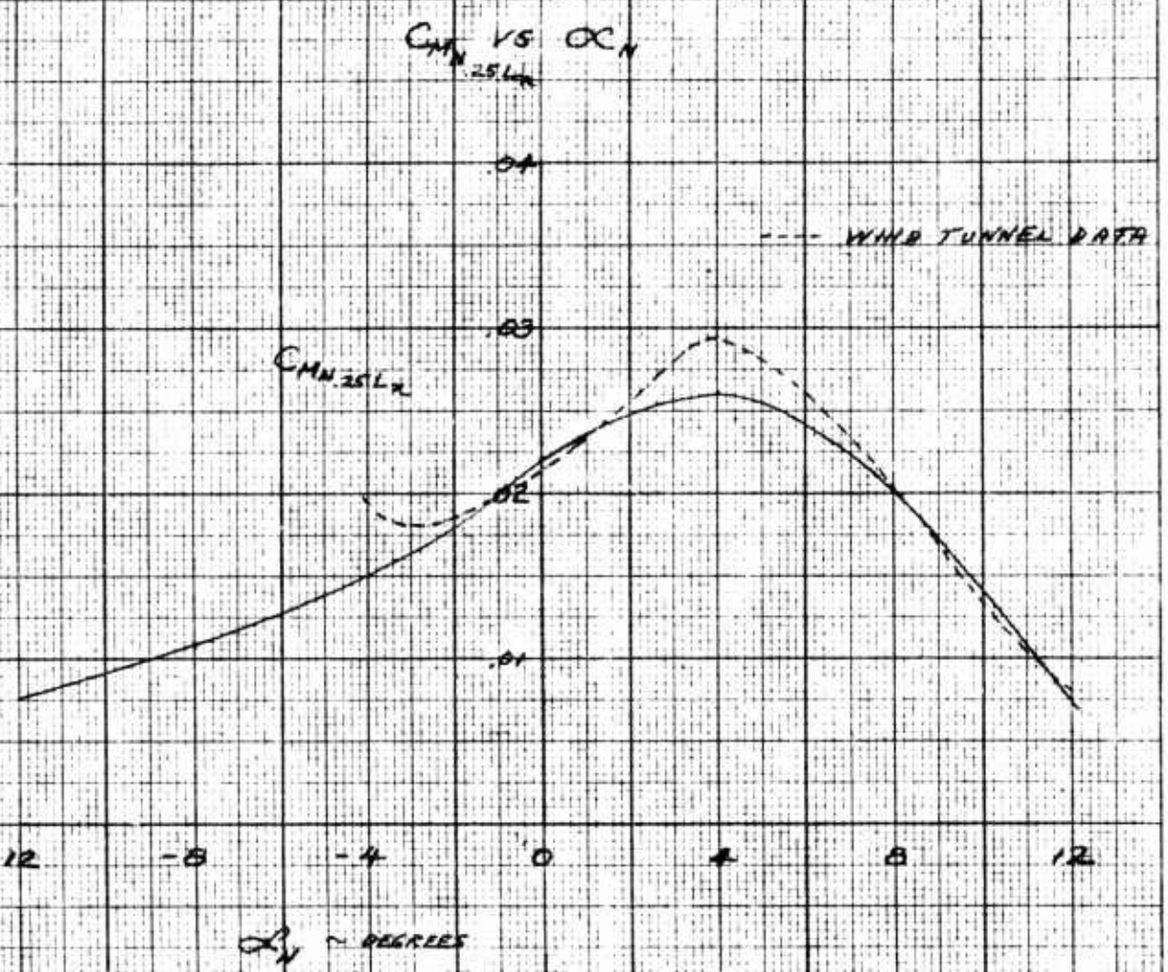

FIG 24
FIG 84

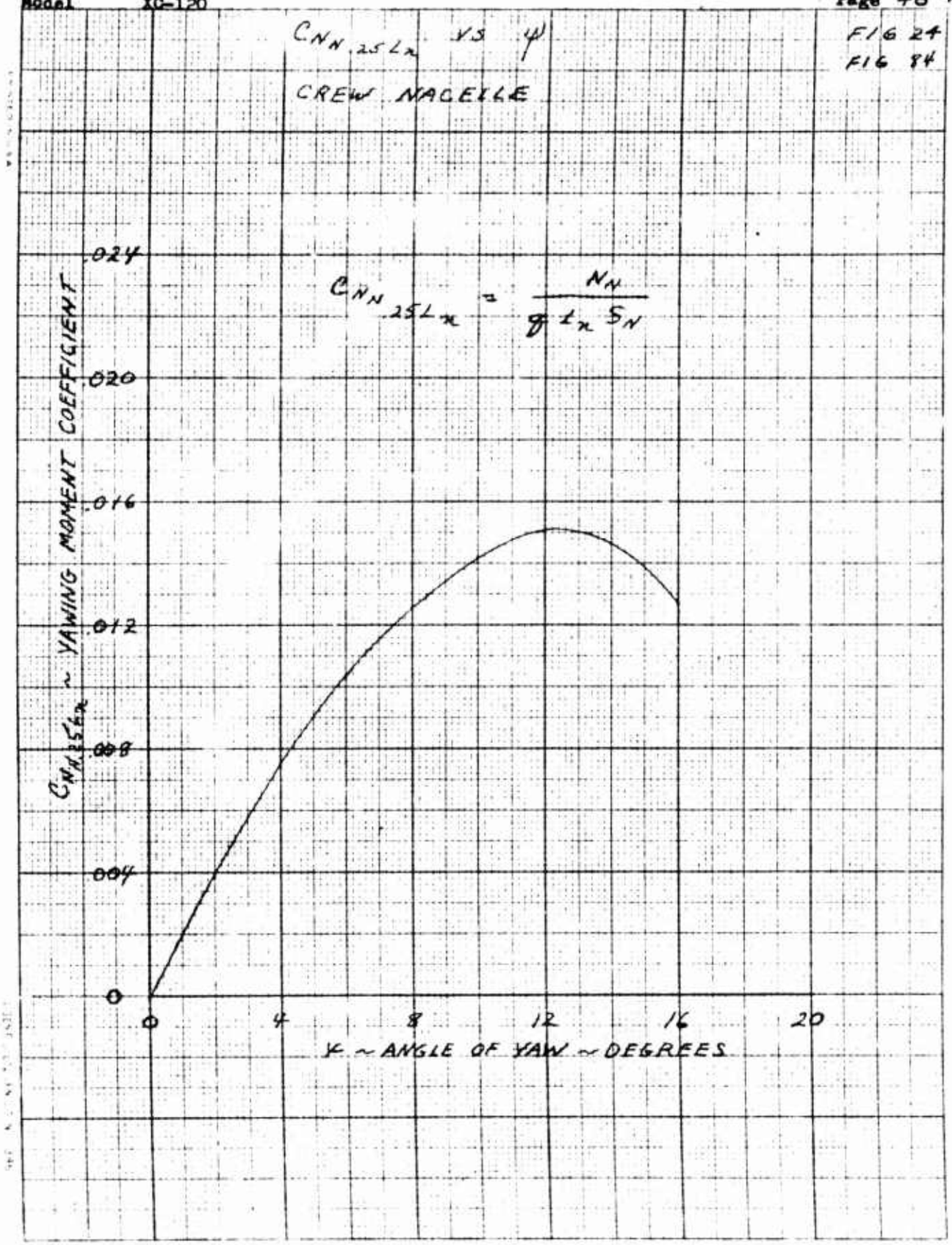
$C_{N_{N.25L_x}}$ VS ψ
CREW NACELLE
$C_{N_{N.25L_x}} = \frac{N_N}{q\, L_x\, S_N}$
$C_{N_{N.25L_x}}$ ~ YAWING MOMENT COEFFICIENT
.024
.020
.016
.012
.008
.004
0
0
4
8
12
16
20
ψ ~ ANGLE OF YAW ~ DEGREES

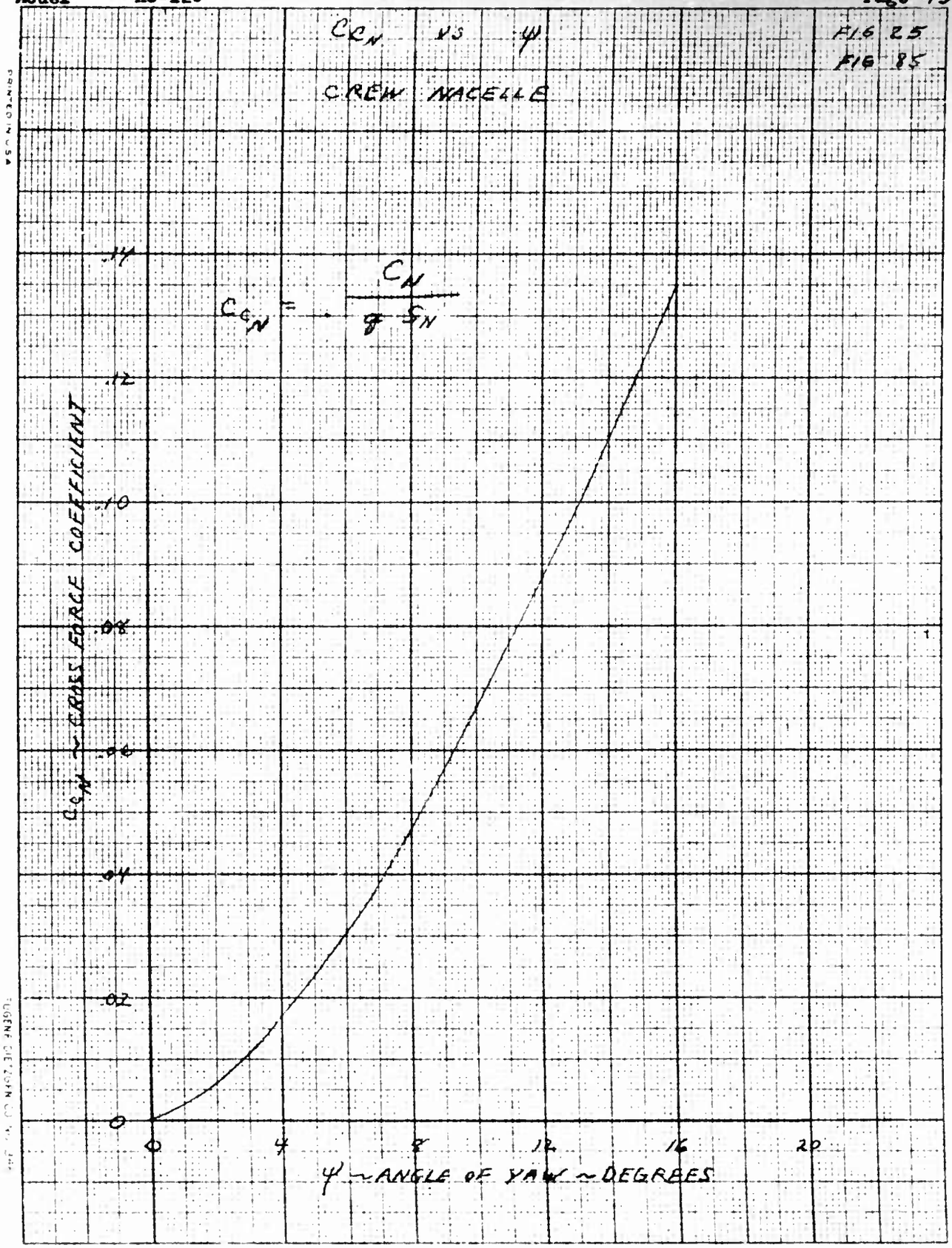
C_{C_N} vs ψ
FIG 25
FIG 85
CREW NACELLE
$C_{C_N} = \frac{C_N}{q\,S_N}$
C_{C_N} ~ CROSS FORCE COEFFICIENT
.14
.12
.10
.08
.06
.04
.02
0
0
4
8
12
16
20
ψ ~ ANGLE OF YAW ~ DEGREES

PART I-D-6

6. BOOM

The following figures summarize the power-off aerodynamic characteristics of the boom. Note that the data shown are for one boom only.

C_{D_B} at $\alpha_b = 0°$ = .18844 based on the maximum cross sectional area of one boom.

Characteristics in yaw - see discussion in Part II-A-6-g.

RESTRICTED

FIG 26
FIG 87

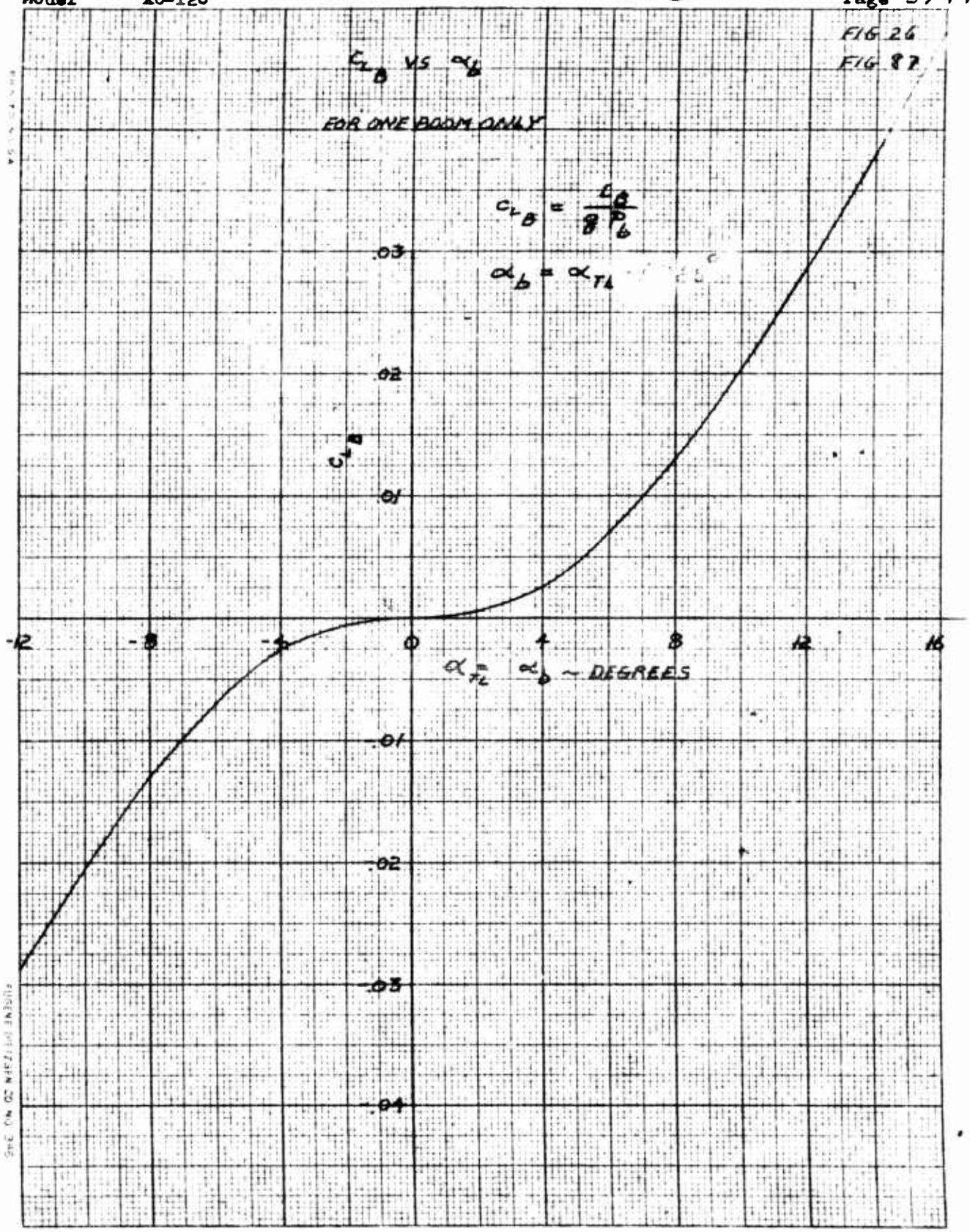

RESTRICTED

FIG 21
FIG 69

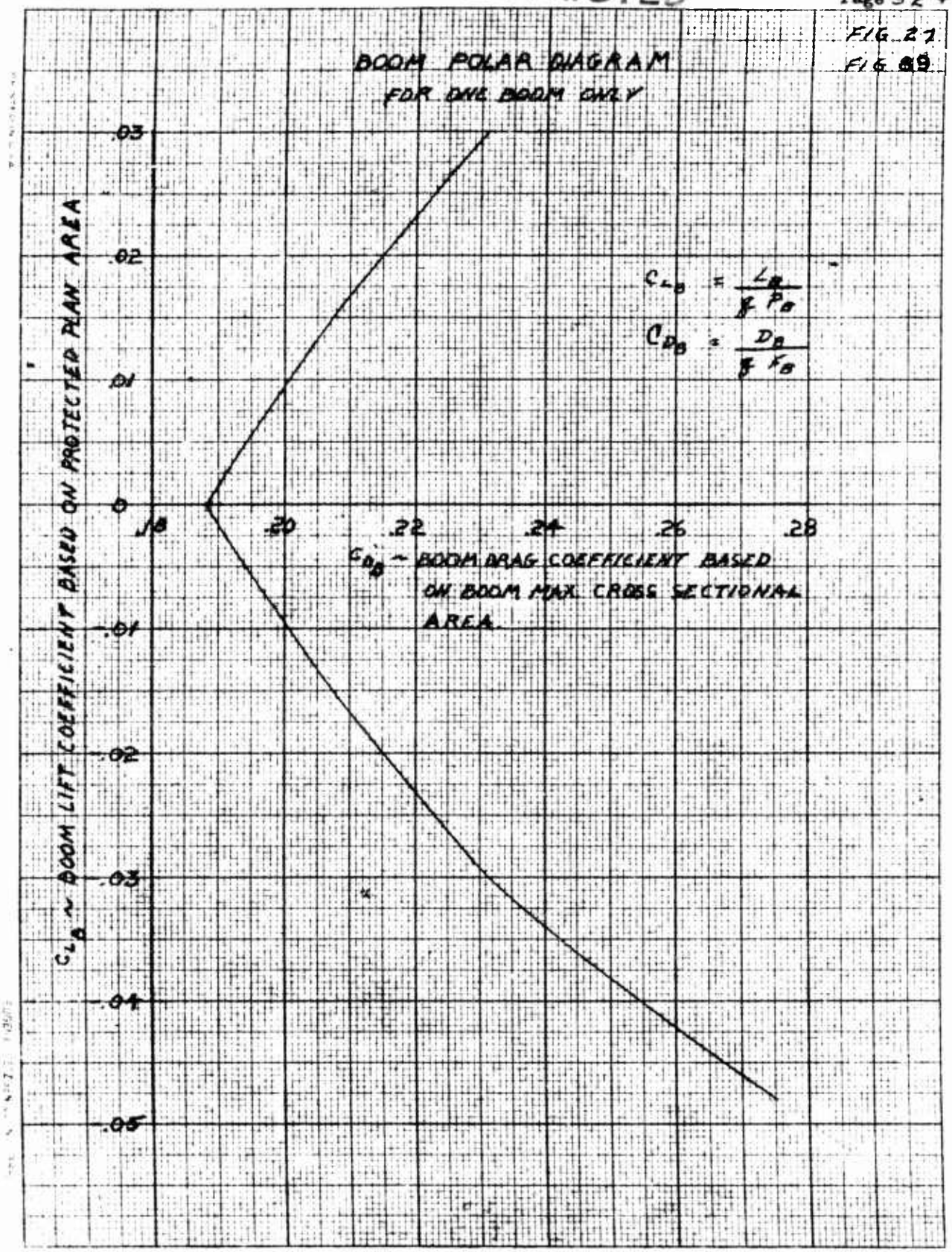

RESTRICTED

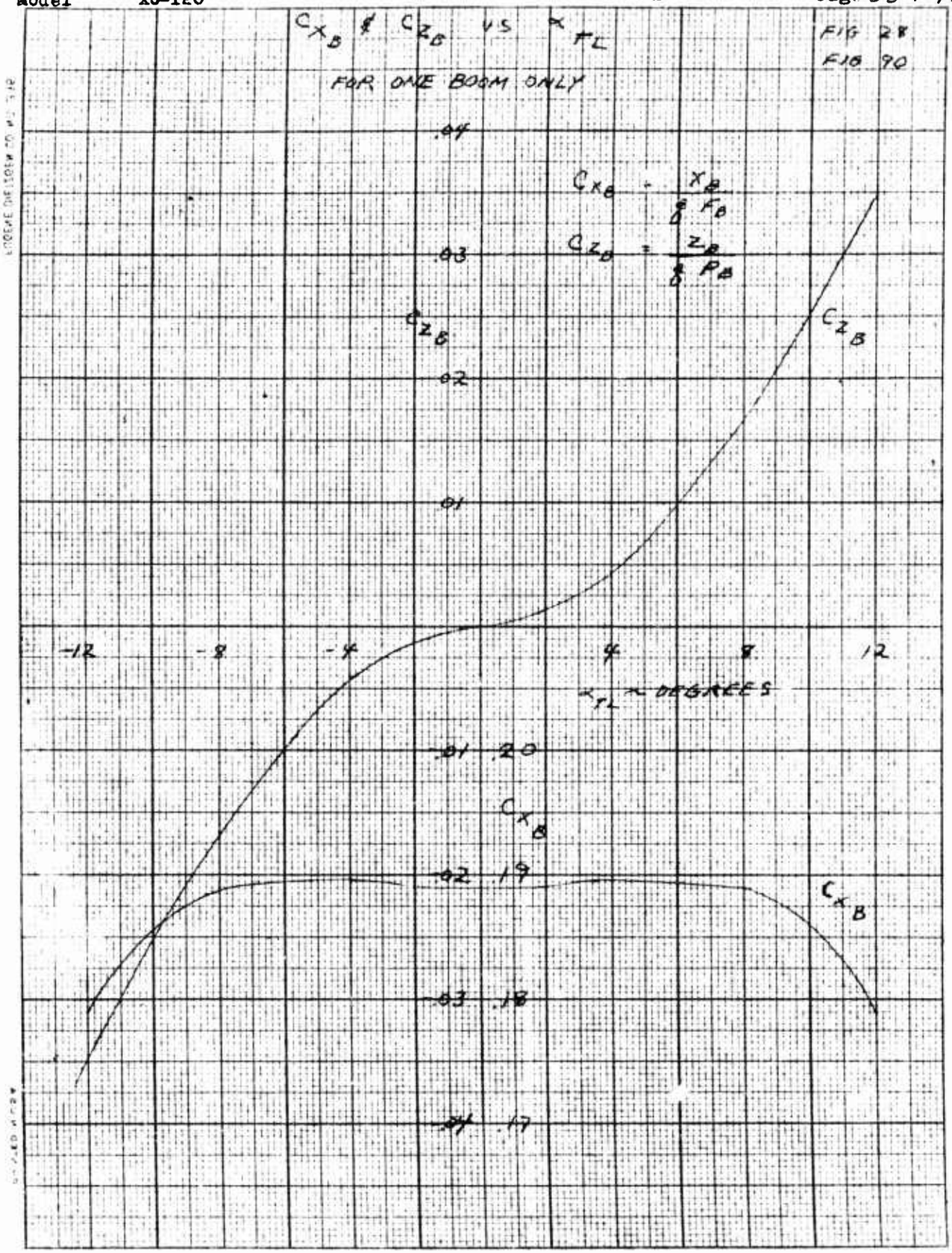
C_{X_B} & C_{Z_B} vs α_{TL}
FIG 28
FIG 90
FOR ONE BOOM ONLY
$C_{X_B} = \frac{X_B}{\frac{\rho}{2} F_B}$
$C_{Z_B} = \frac{Z_B}{\frac{\rho}{2} F_B}$
.04
.03
.02
.01
-.01
-.02
-.03
-.04
.20
.19
.18
.17
-12
-8
-4
4
8
12
α_{TL} ~ DEGREES
C_{Z_B}
C_{X_B}

PITCHING MOMENT COEFFICIENT OF ONE BODY ABOUT THE QUARTER LENGTH POINT

FIG. 29
FIG. 91

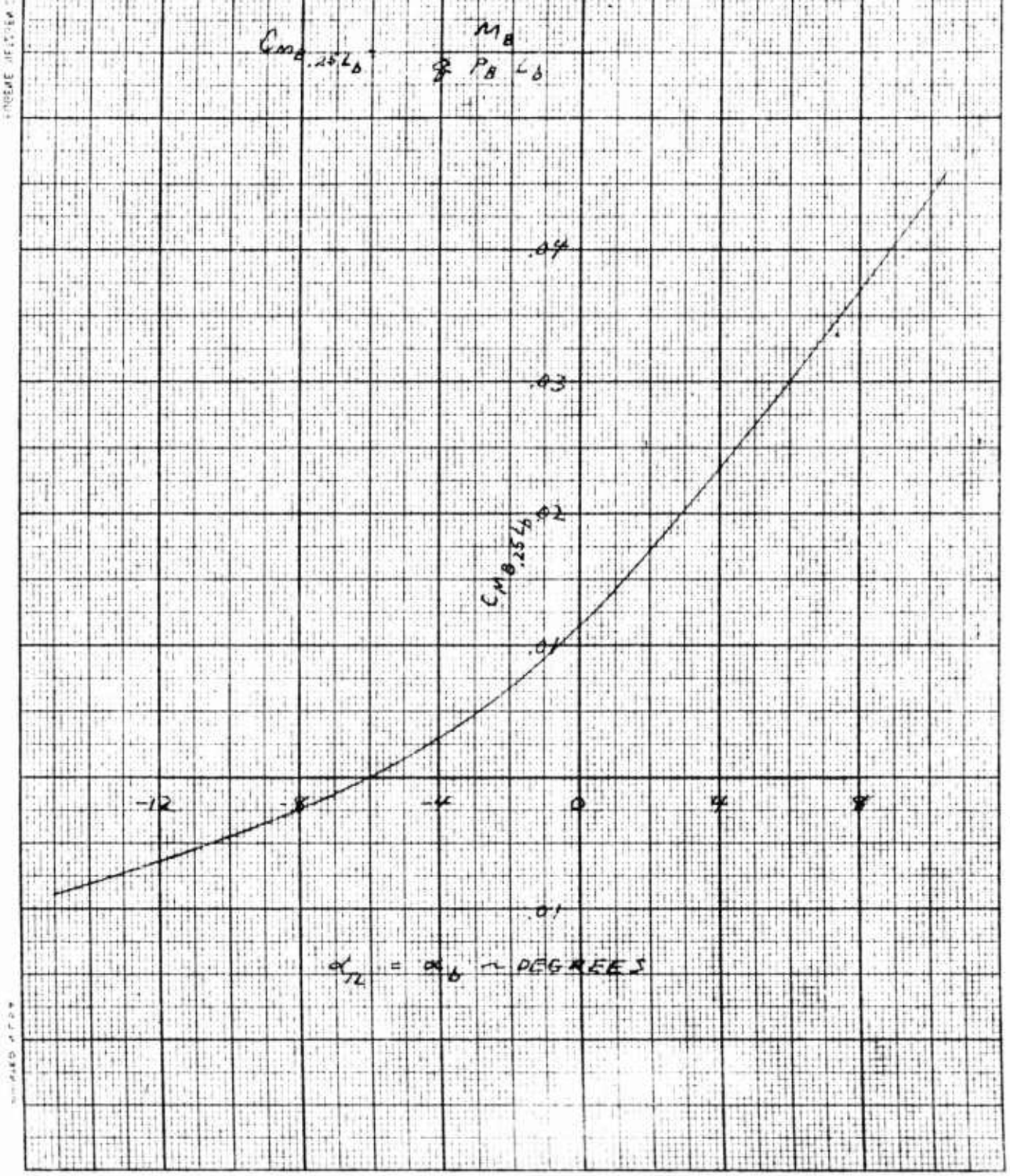

FIG 30
FIG 92

YAWING MOMENT OF BOOM ABOUT QUARTER LENGTH POINT
FOR ONE BOOM ONLY

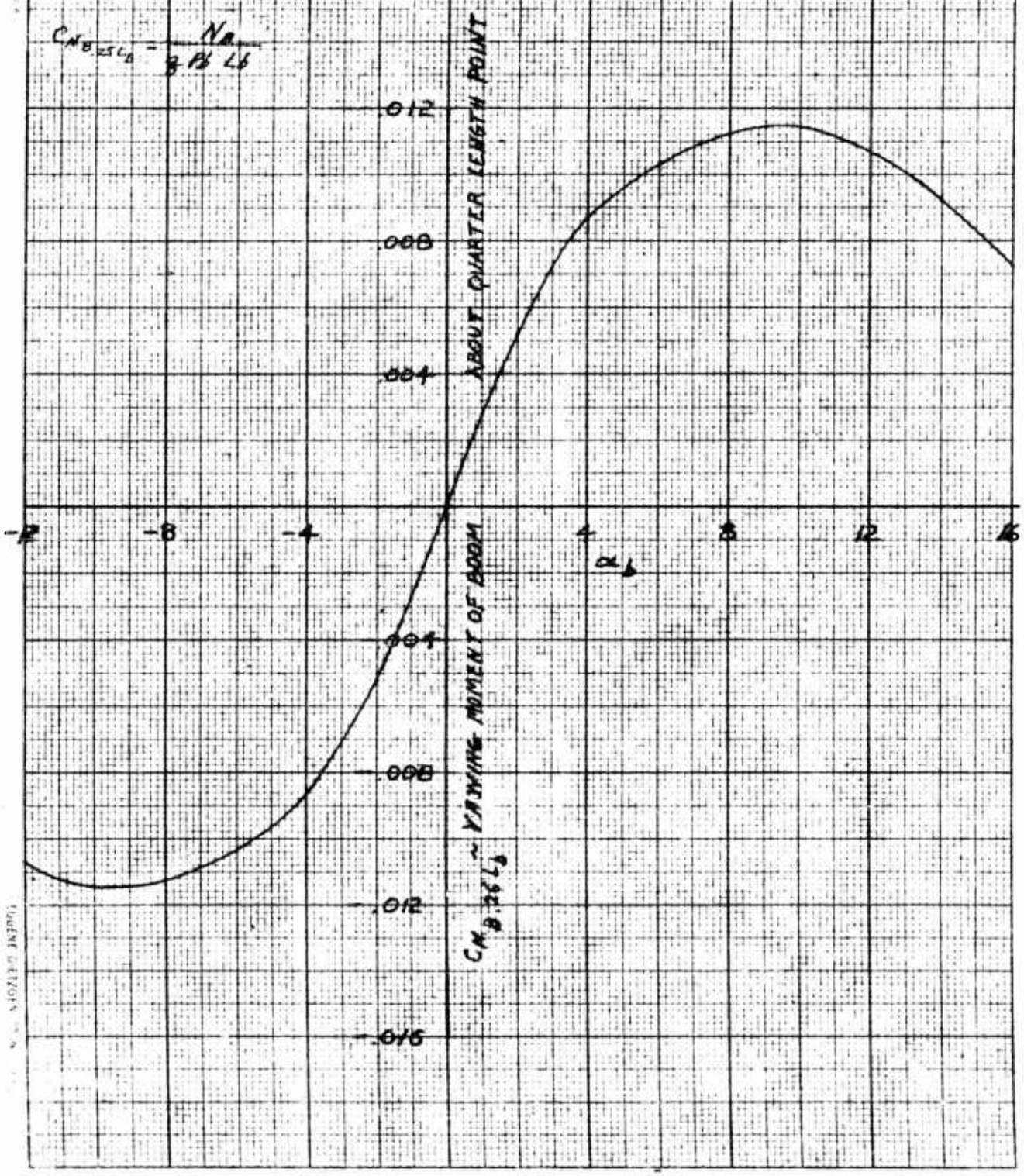

FIG. 31
FIG. 93

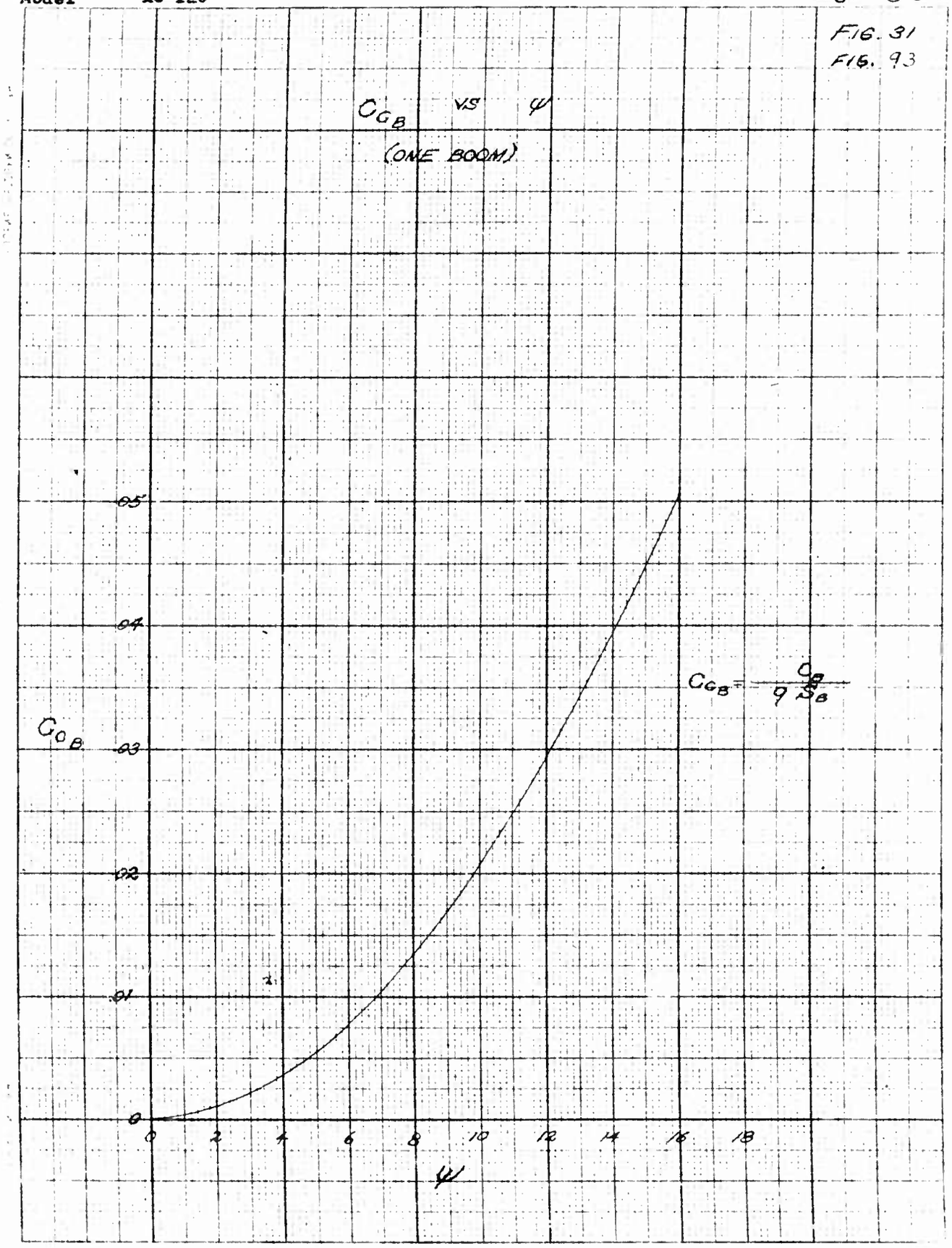
C_{G_B} VS ψ
(ONE BOOM)
$C_{G_B} = \frac{C_g}{q S_B}$
C_{G_B}
.05
.04
.03
.02
.01
0
0
2
4
6
8
10
12
14
16
18
ψ

PART I-D-7

7. HORIZONTAL TAIL

The following table and figures summarize the power-off aerodynamic characteristics of the horizontal tail.

$C_{L\alpha_{ht}}$	.0530 per degree
$\alpha_{ht\delta_e}$	-.545 per degree
η_{ht} for lift only	.85
$C_{M_{HT\delta_e}}$ about ΔC_{ht}	-.0073 per degree
ΔC_{ht}	25% of c_{ht_c}
q_{ht}/q	1.00
$C_{H_{e\delta_e}}$	-.0018 per degree
$C_{H_{e\alpha_{ht}}}$	-.0007 per degree
i_{ht}	+1.0°

Yawing moment due to yaw assumed to be negligible.

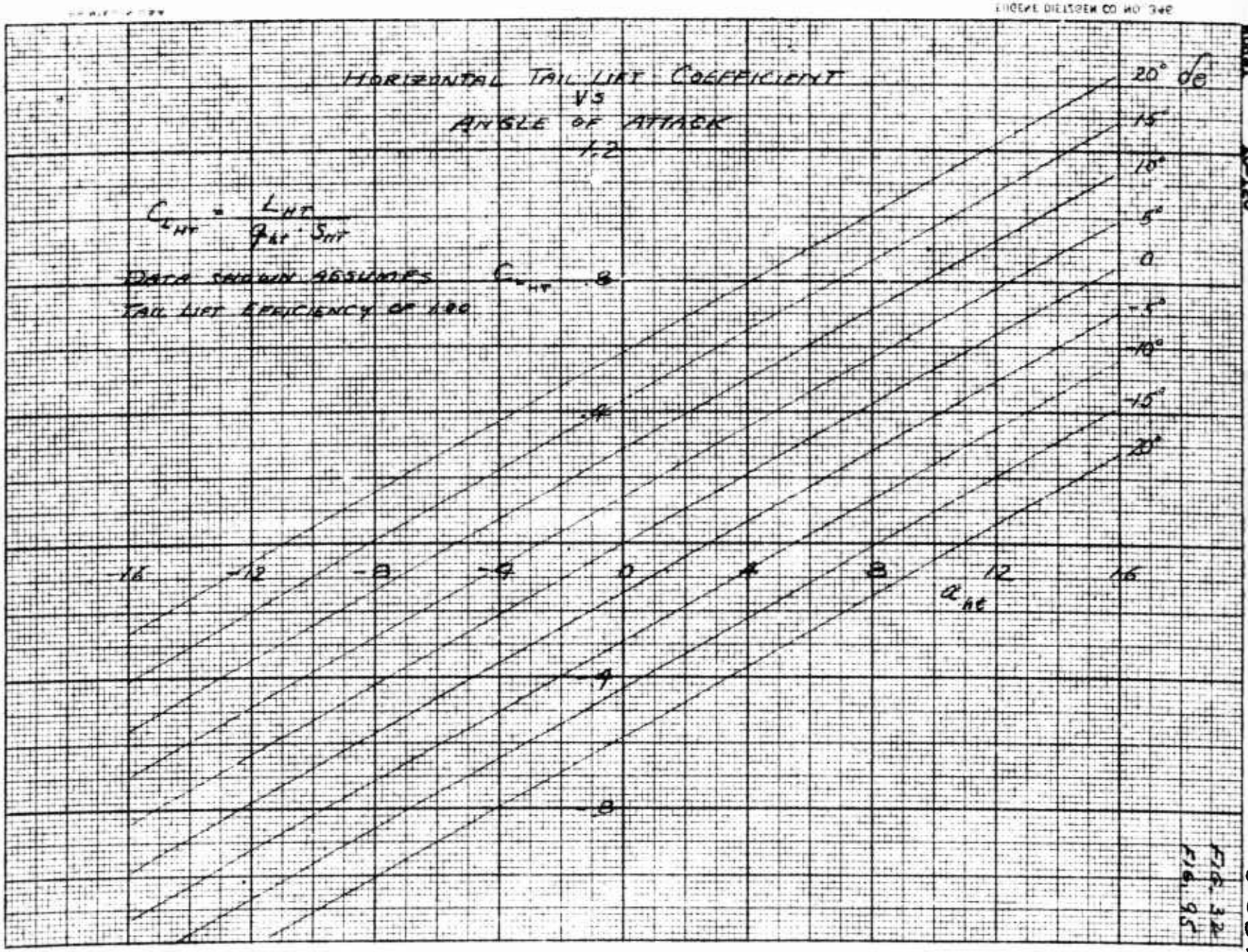
HORIZONTAL TAIL LIFT COEFFICIENT
VS
ANGLE OF ATTACK
$C_{L_{HT}} = \frac{L_{HT}}{q_{ht} \cdot S_{HT}}$
DATA SHOWN ASSUMES $C_{L_{HT}}$ .8
TAIL LIFT EFFICIENCY OF 1.00
1.2
.4
-.4
-.8
-16
-12
-8
-4
0
4
8
12
16
α_{ht}
20° δ_e
15°
10°
5°
0
-5°
-10°
-15°
-20°

RESTRICTED

FIG 33
FIG 97

POLAR DIAGRAM OF HORIZONTAL TAIL

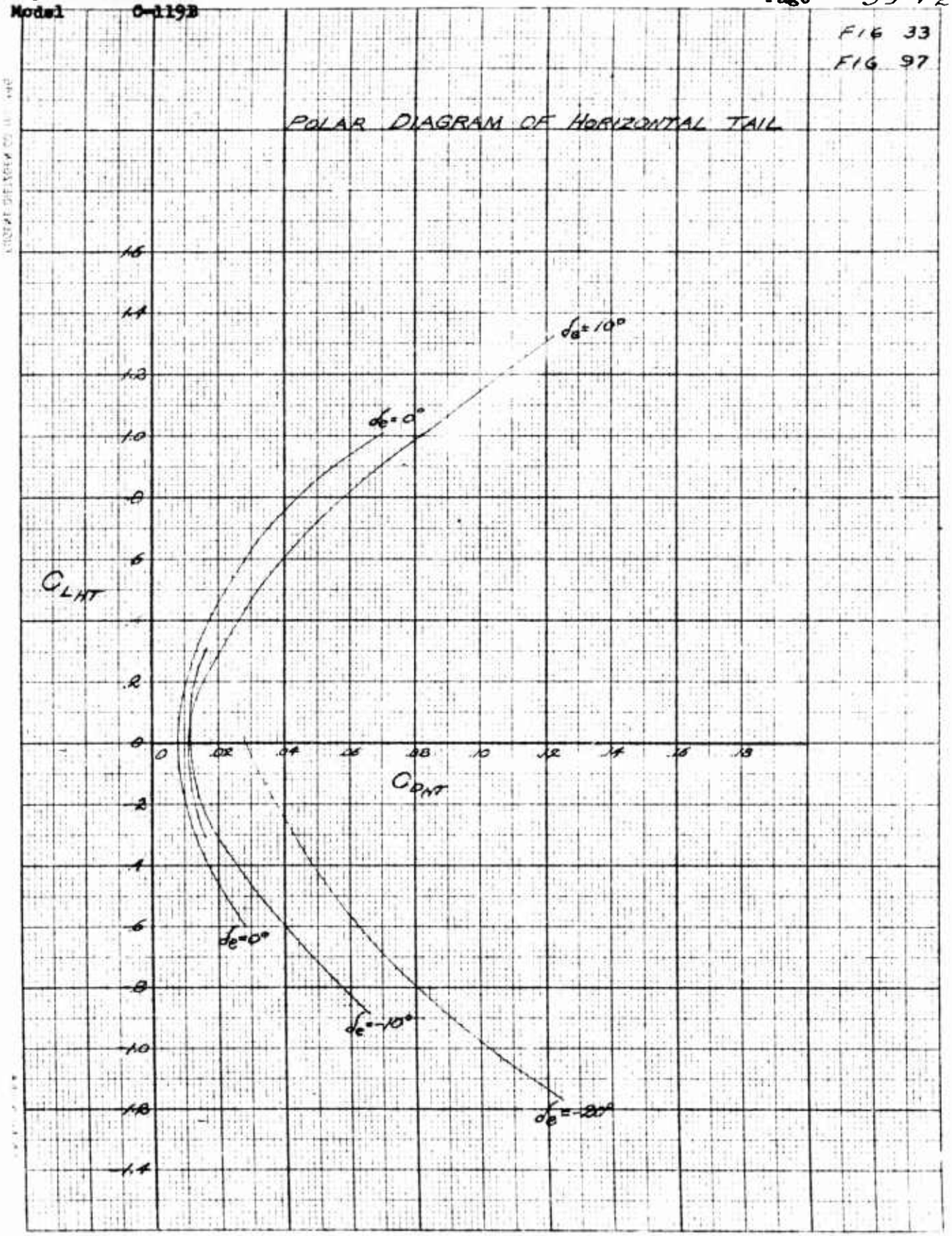

FIG 34
FIG 98

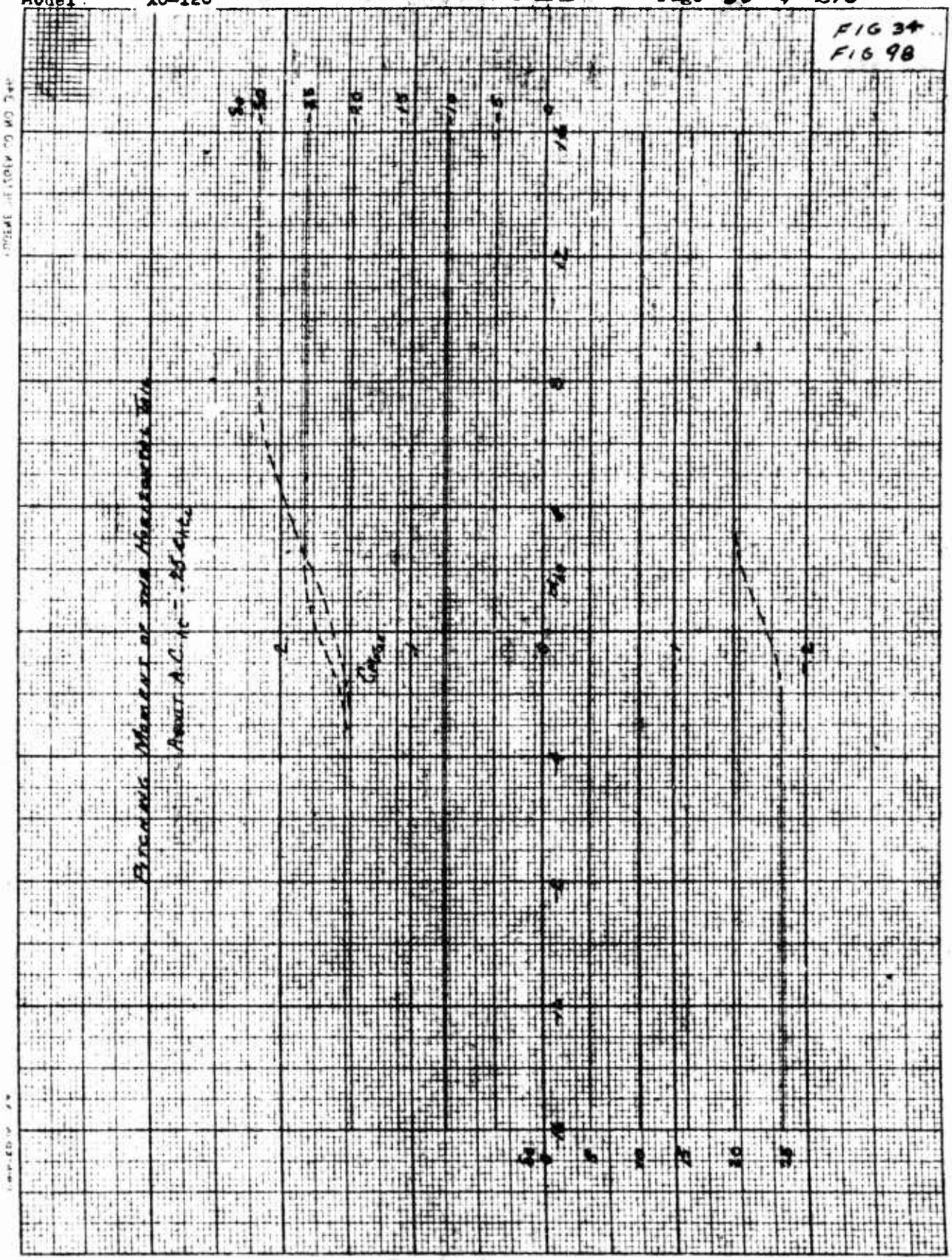
Bending Moment of the Horizontal Tail
About A.C. H.C. = 25.4 in.
Cases
-30
-25
-20
-15
-10
-5
0
5
10
15
20
25

FIG. 35
FIG. 100

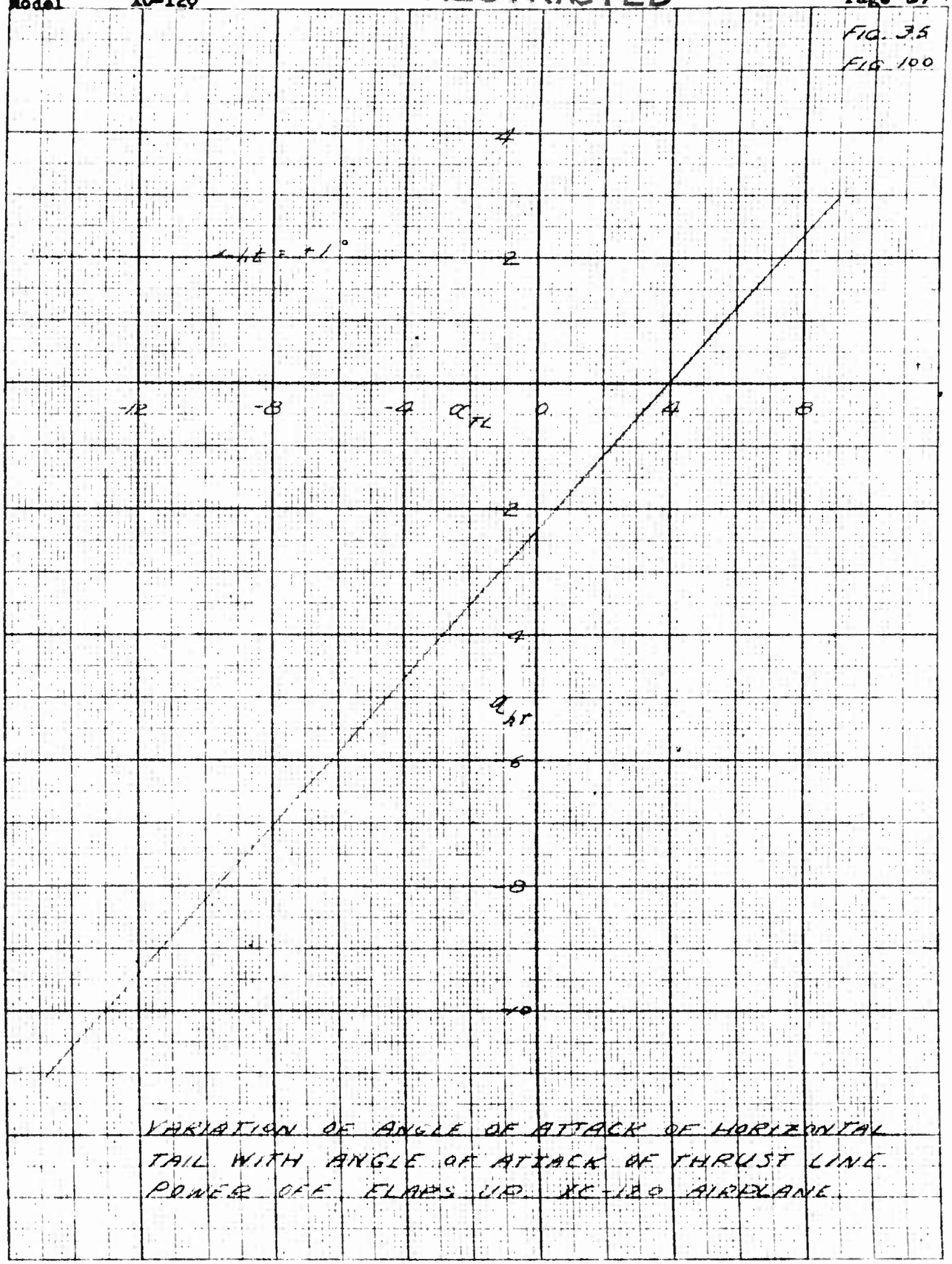

VARIATION OF ANGLE OF ATTACK OF HORIZONTAL TAIL WITH ANGLE OF ATTACK OF THRUST LINE POWER OFF, FLAPS UP. XC-120 AIRPLANE.

RESTRICTED

FIG. 36
FIG. 101

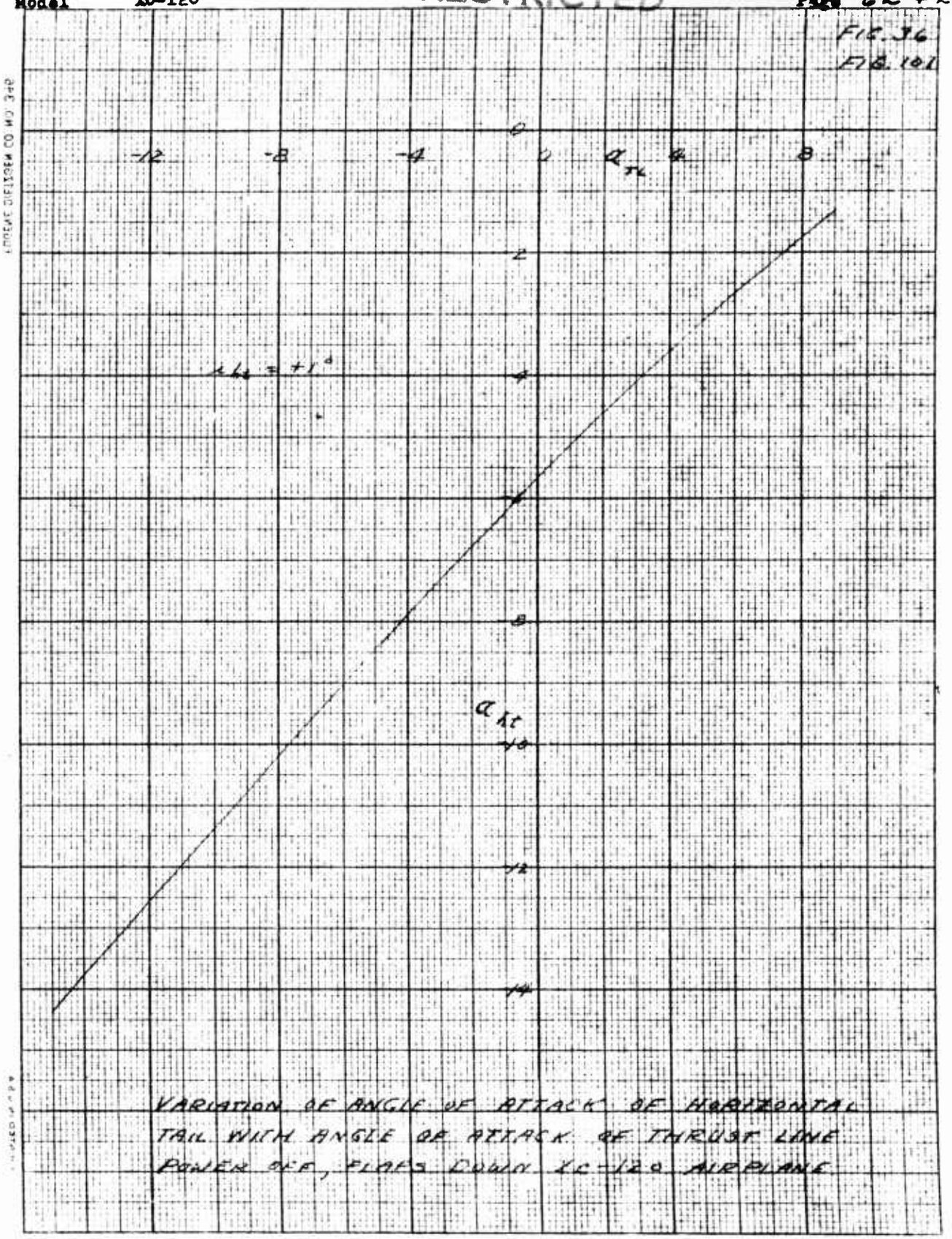

VARIATION OF ANGLE OF ATTACK OF HORIZONTAL TAIL WITH ANGLE OF ATTACK OF THRUST LINE POWER OFF, FLAPS DOWN XC-120 AIRPLANE

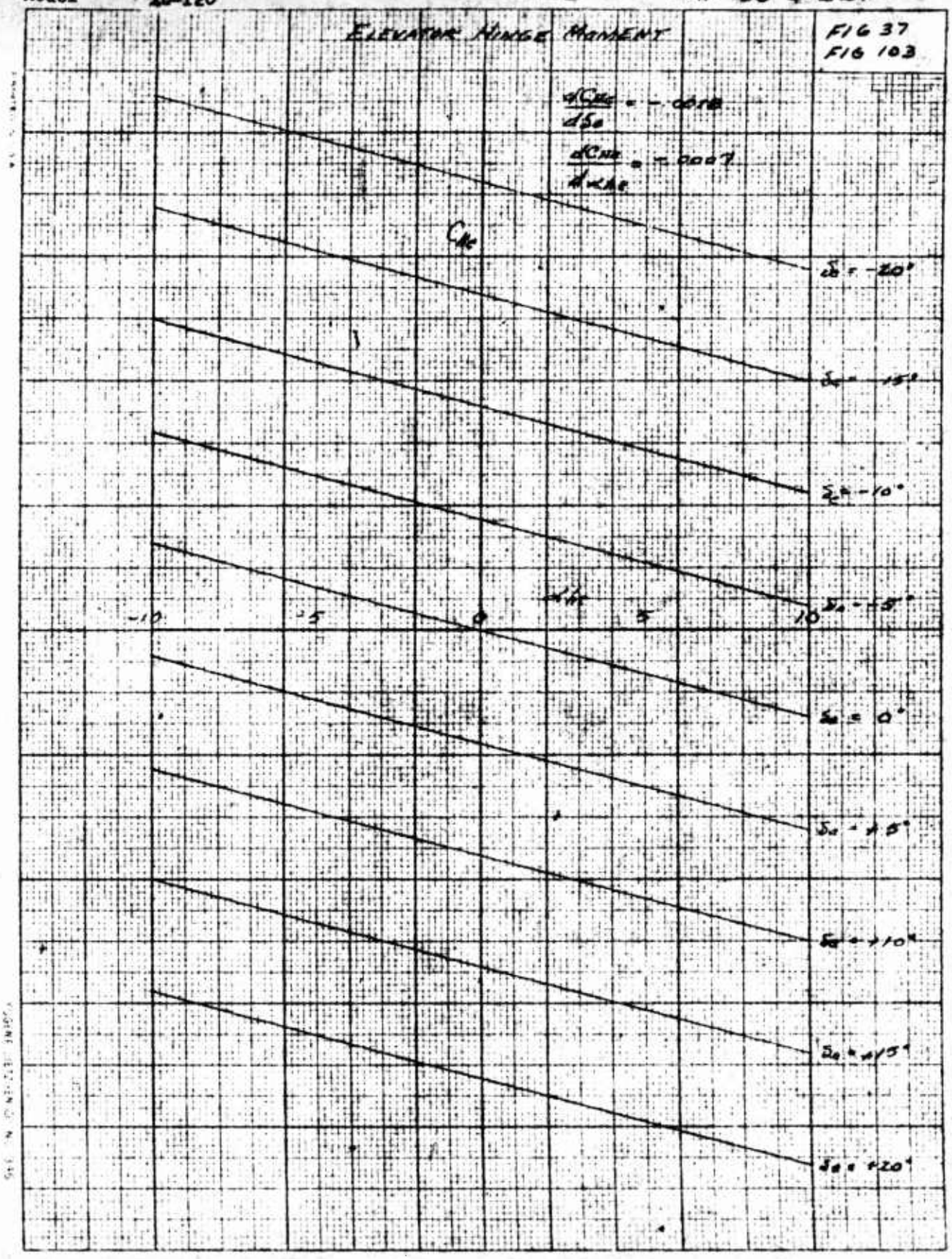
ELEVATOR HINGE MOMENT
FIG 37
FIG 103
$\frac{dC_{H_e}}{d\delta_e} = -.0018$
$\frac{dC_{H_e}}{d\alpha_{h_e}} = -.0007$
C_{H_e}
$\delta_e = -20°$
$\delta_e = -15°$
$\delta_e = -10°$
$\delta_e = -5°$
$\delta_e = 0°$
$\delta_e = +5°$
$\delta_e = +10°$
$\delta_e = +15°$
$\delta_e = +20°$
-10
-5
0
5
10
α_{h_e}

PART I-D-5

5. **ELEVATOR TABS**

The following tables and figures summarize the power-off aerodynamic characteristics of the elevator trim and spring tabs.

TRIM TAB

$C_{L_{ET}} \delta_{e_{tt}}$	.00238 per degree
$C_{H_e} \delta_{e_{tt}}$	-.0034 per degree
$C_{H_{e_{tt}}} \delta_{e_{tt}}$	-.0060 per degree
$\alpha_{ht} \delta_{e_{tt}}$	-.0385 per degree

SPRING TAB

$C_{L_{ET}} \delta_{e_{st}}$	.00172 per degree
$C_{H_e} \delta_{e_{st}}$	-.0025 per degree
$C_{H_{e_{st}}} \delta_{e_{st}}$	-.0060 per degree
$\alpha_{ht} \delta_{e_{st}}$	-.0278 per degree

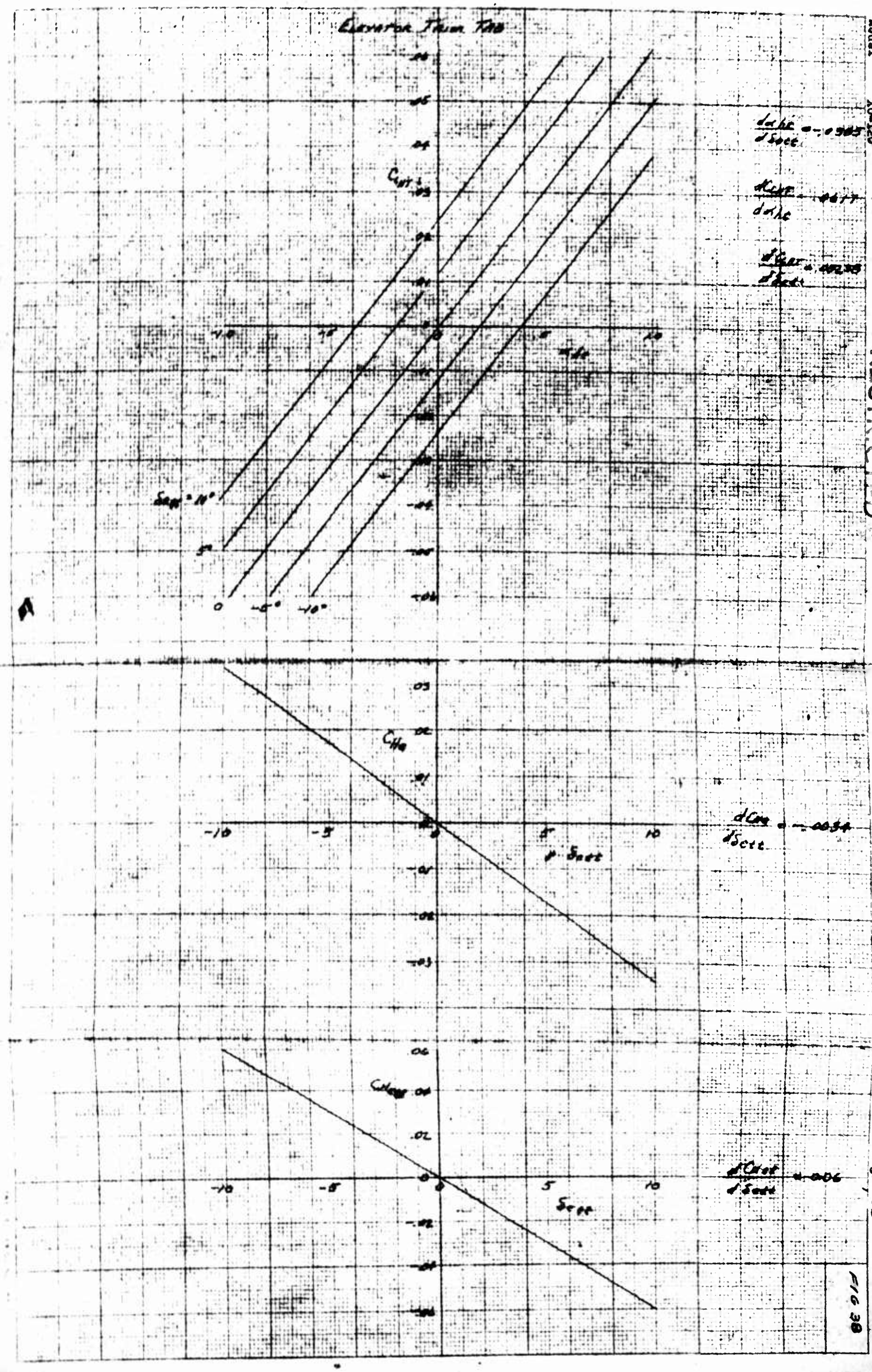

RESTRICTED

FIG 38

RESTRICTED

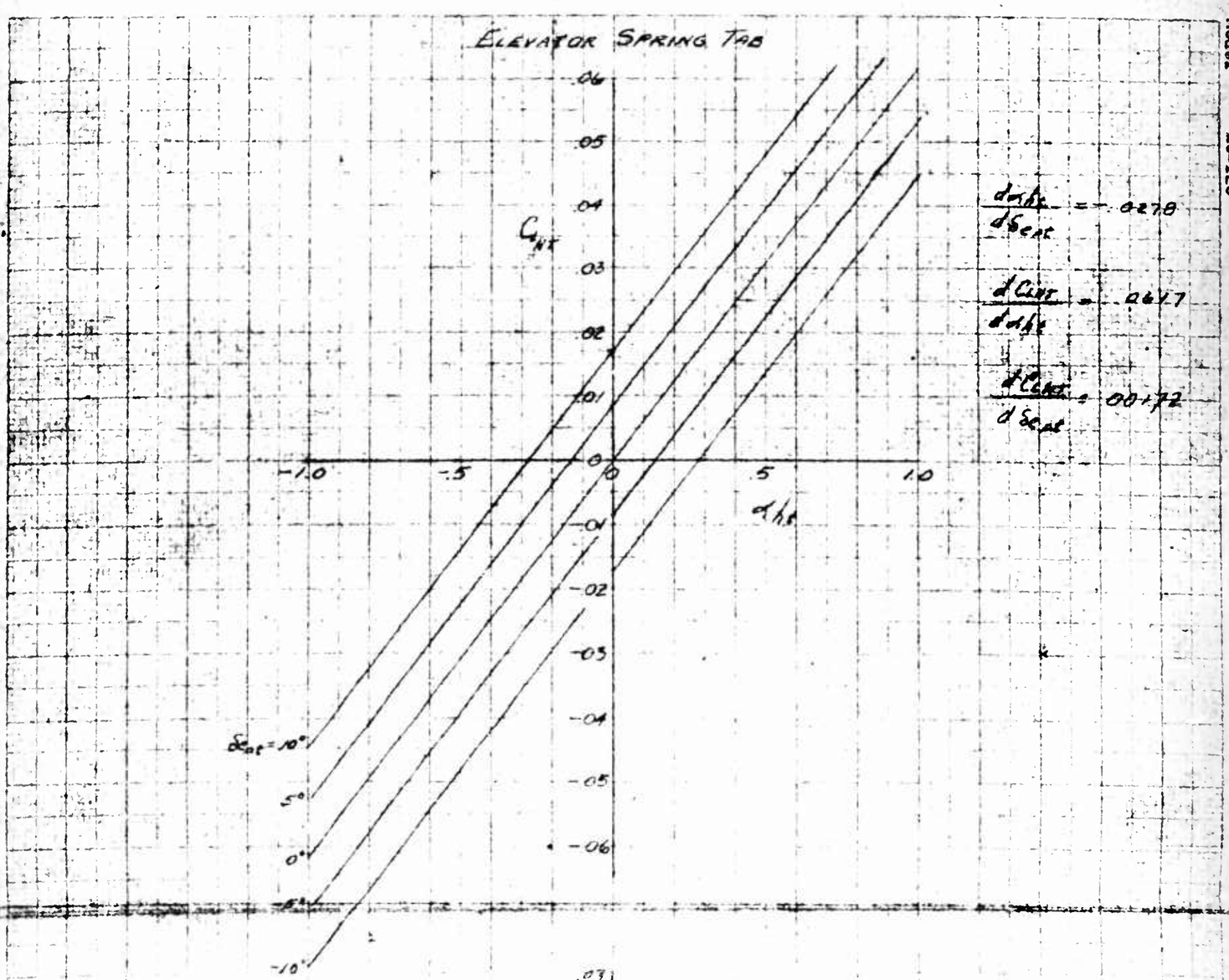

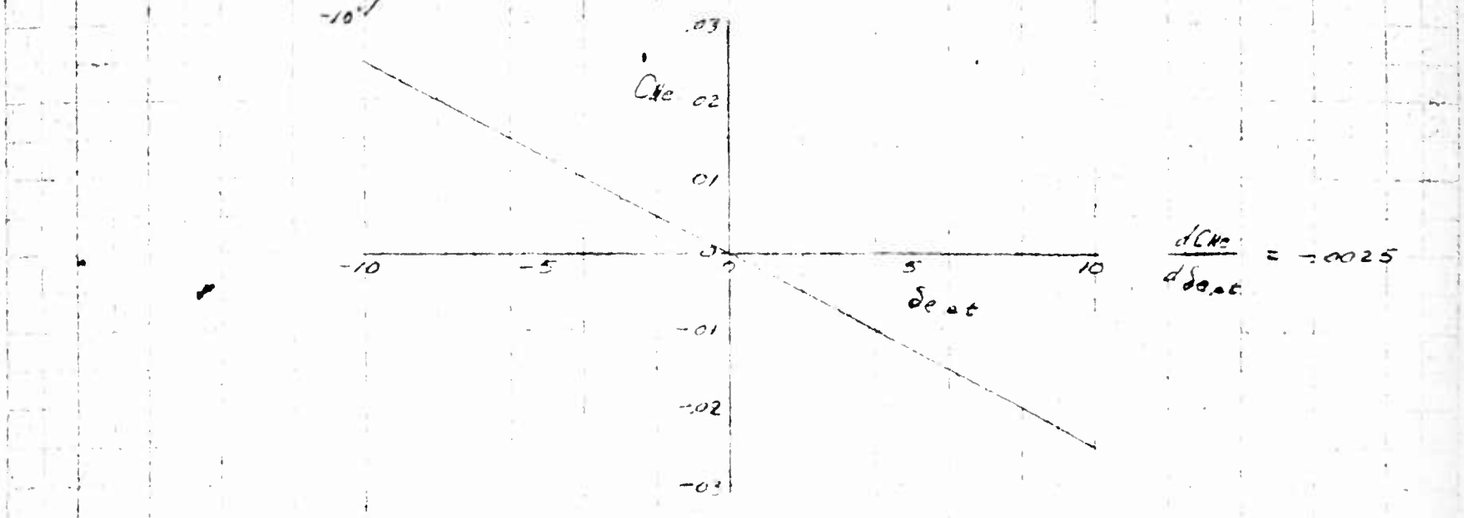

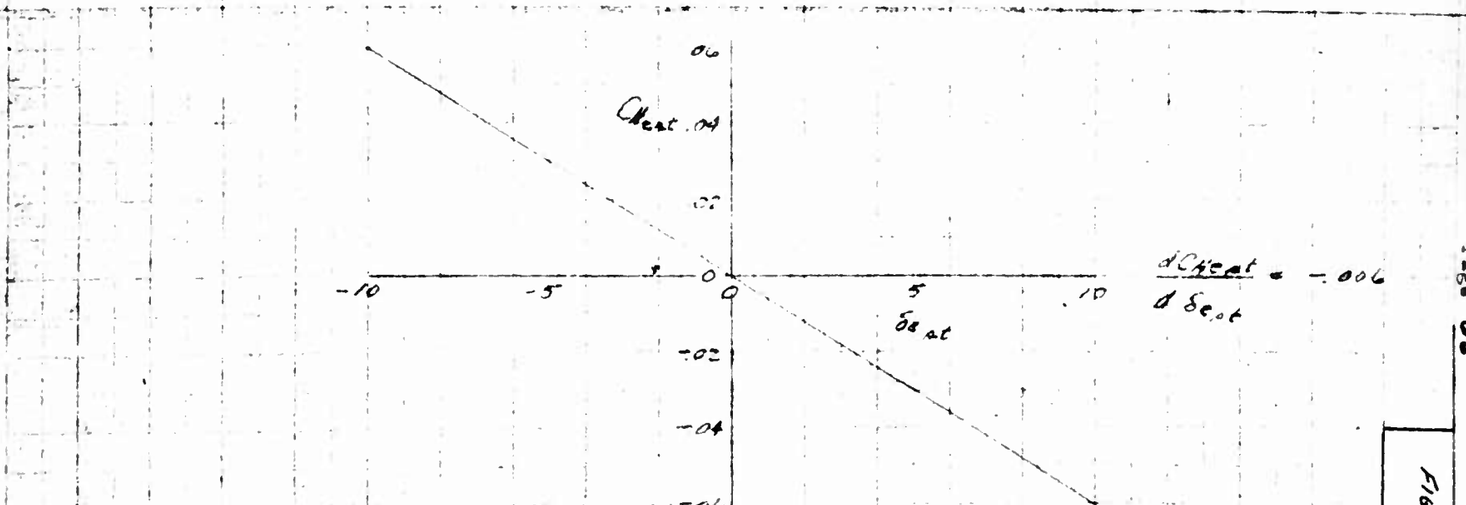

Fig 39

PART I-D-9

9. VERTICAL TAIL

The following table and figures summarize the power-off aerodynamic characteristics of the vertical tail.

$C_{C_{\alpha_{vt}}}$	.0560 per degree
$\alpha_{vt}\,\delta_r$	-.480 per degree
η_{vt} for side force only	.75
$C_{H_{VT}}\,\delta_r$ about AC_{vt}	-.00314 per degree
q_{vt}/q	1.00
$\sigma\psi$ flaps up	.107 per degree
$\sigma\psi$ flaps down	.072 per degree
$C_{H_r}\,\delta_r$	-.0049 per degree
$C_{H_r}\alpha_{vt}$	-.0015 per degree

RESTRICTED

FIG 40
FIG 105

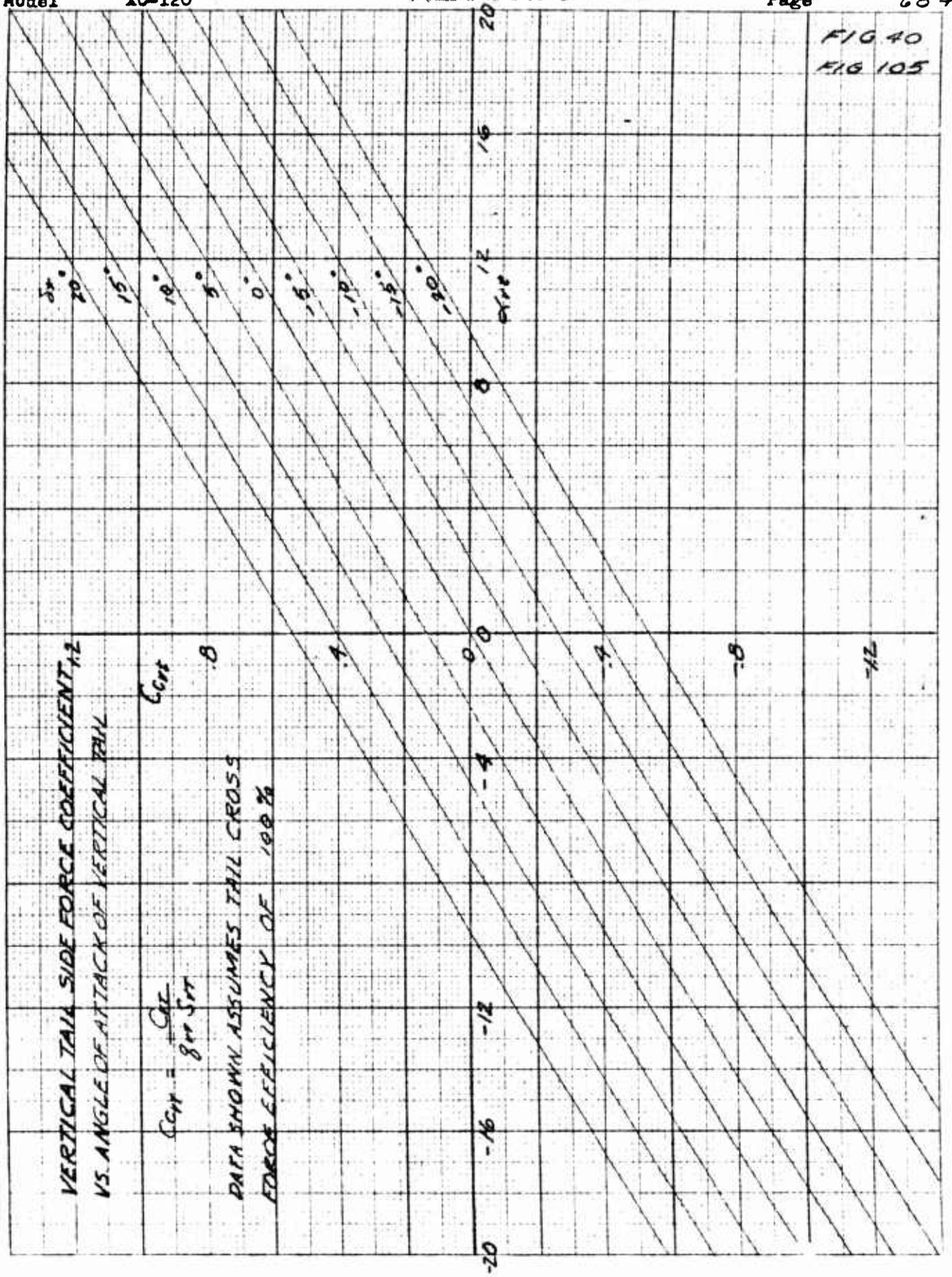

RESTRICTED

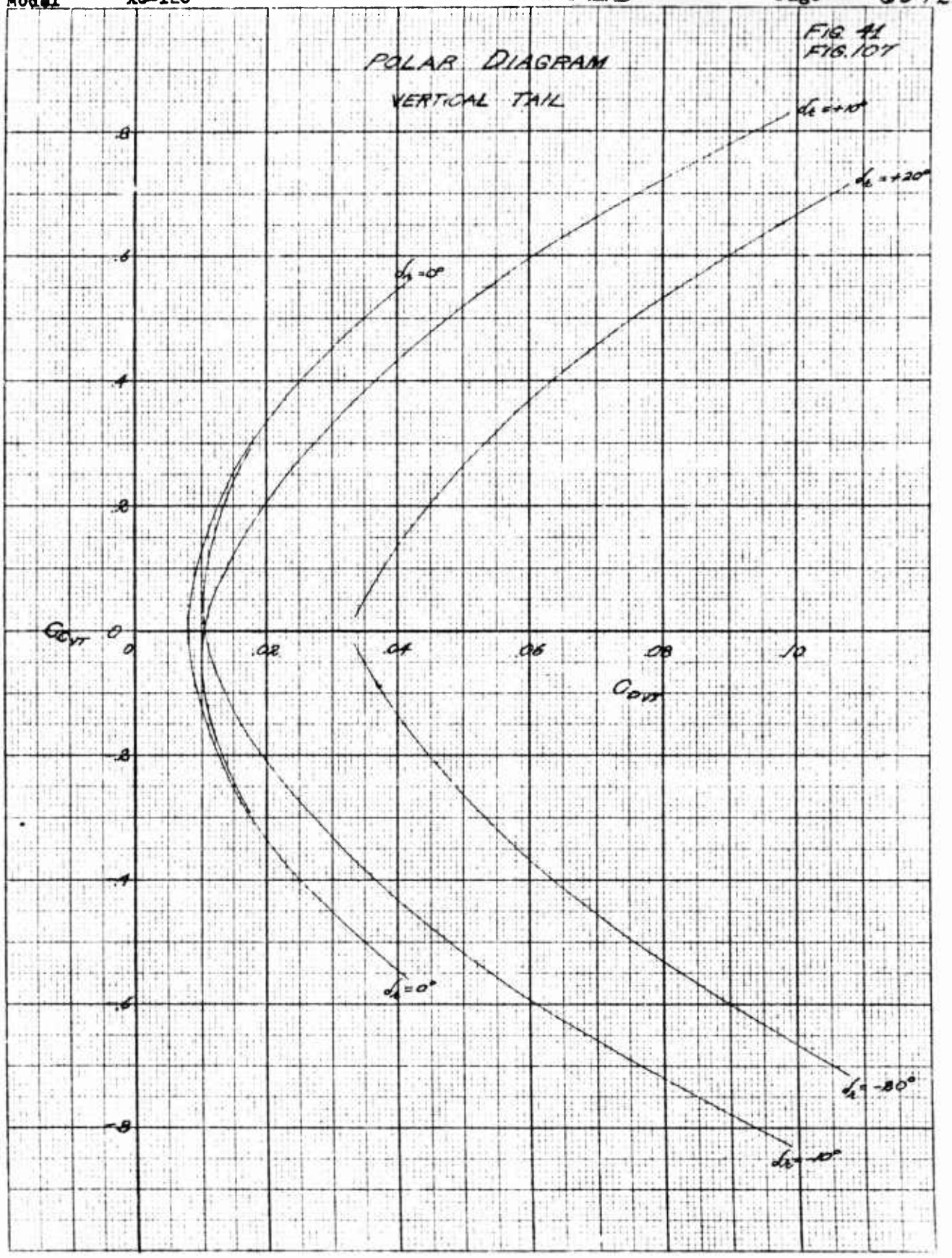
FIG. 41
FIG. 107
POLAR DIAGRAM
VERTICAL TAIL
$C_{L_{VT}}$
$C_{D_{VT}}$
.8
.6
.4
.2
0
-.2
-.4
-.6
-.8
0
.02
.04
.06
.08
.10
$\delta_L = +10°$
$\delta_L = +20°$
$\delta_L = 0°$
$\delta_L = 0°$
$\delta_L = -20°$
$\delta_L = -10°$

RESTRICTED

FIG. 42
FIG 108

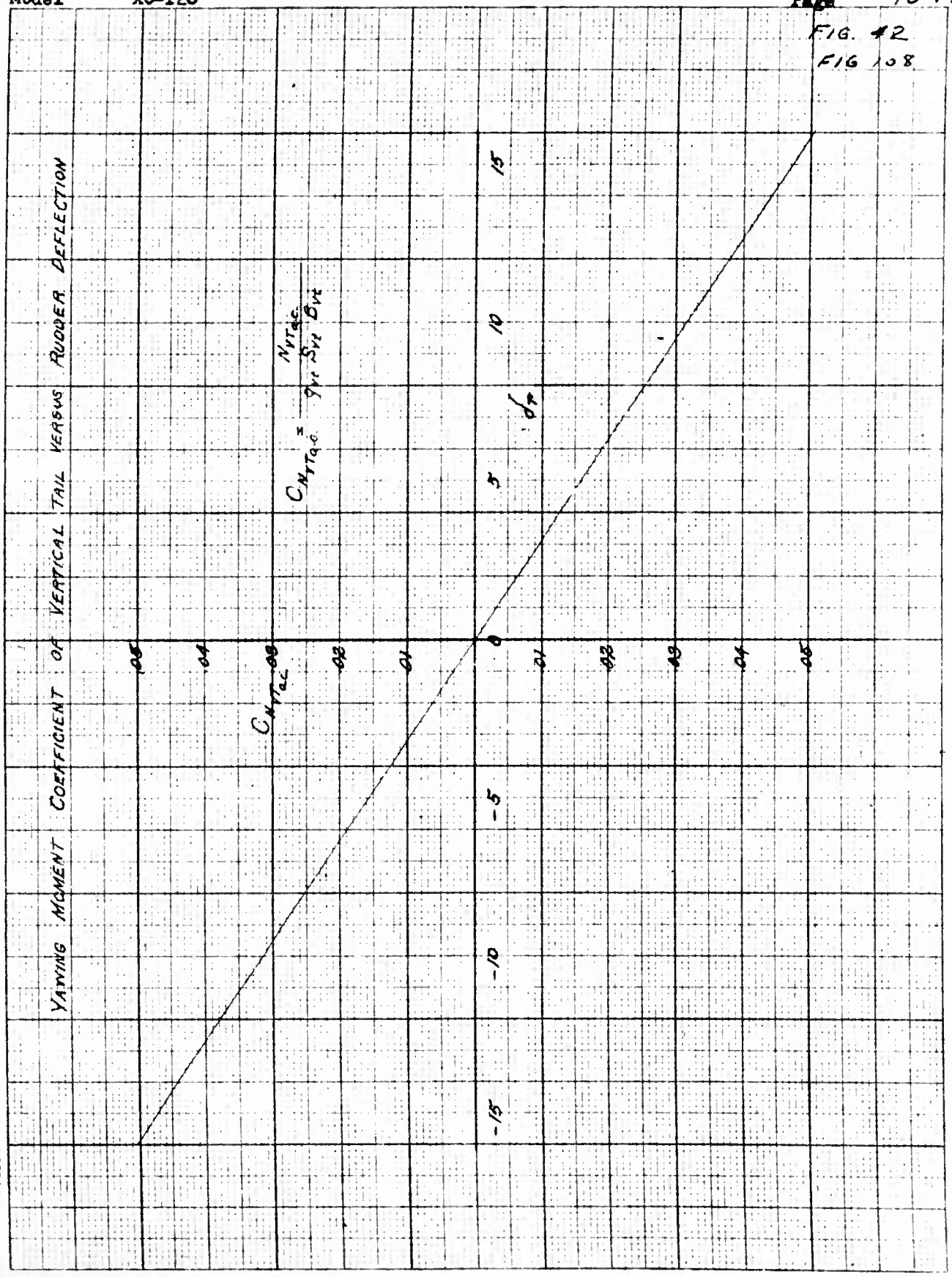

FIG. 43
FIG 10.9

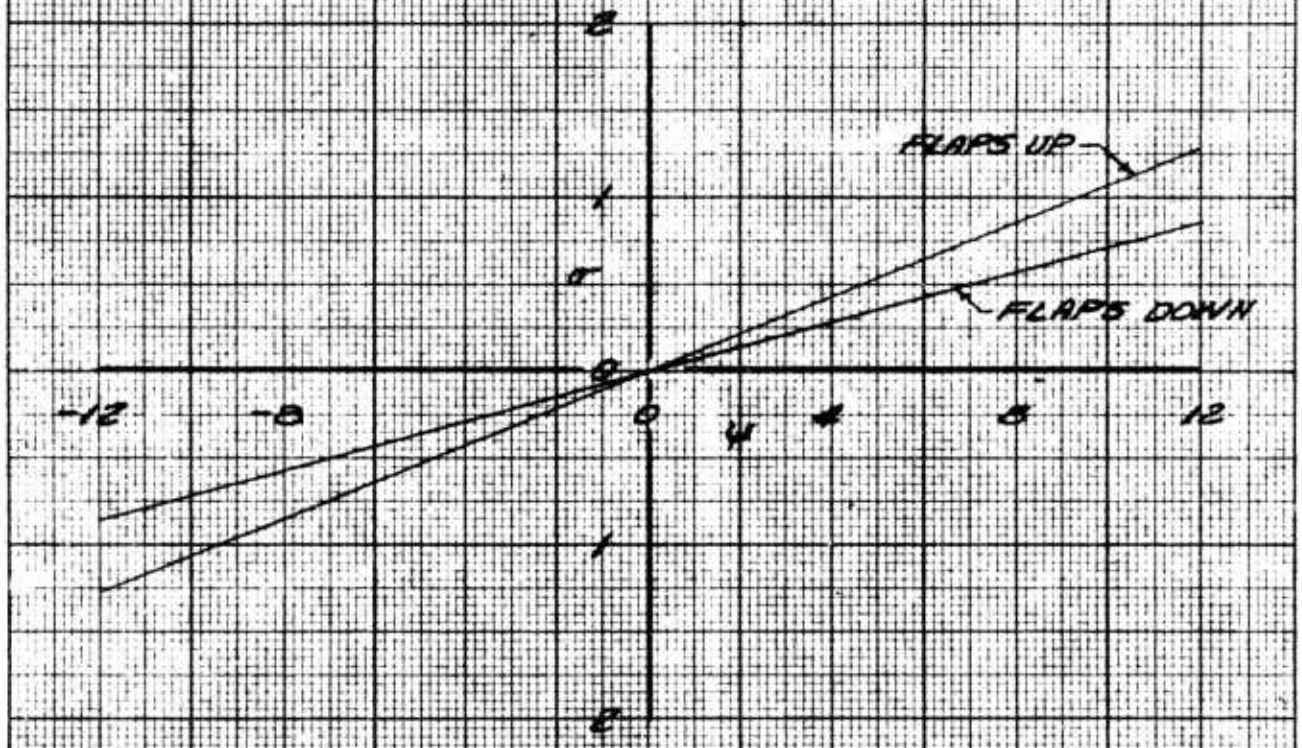

VARIATION OF SIDESLIPPING ANGLE WITH ANGLE OF YAW, POWER OFF, XC-120 AIRPLANE.

FIG. 44

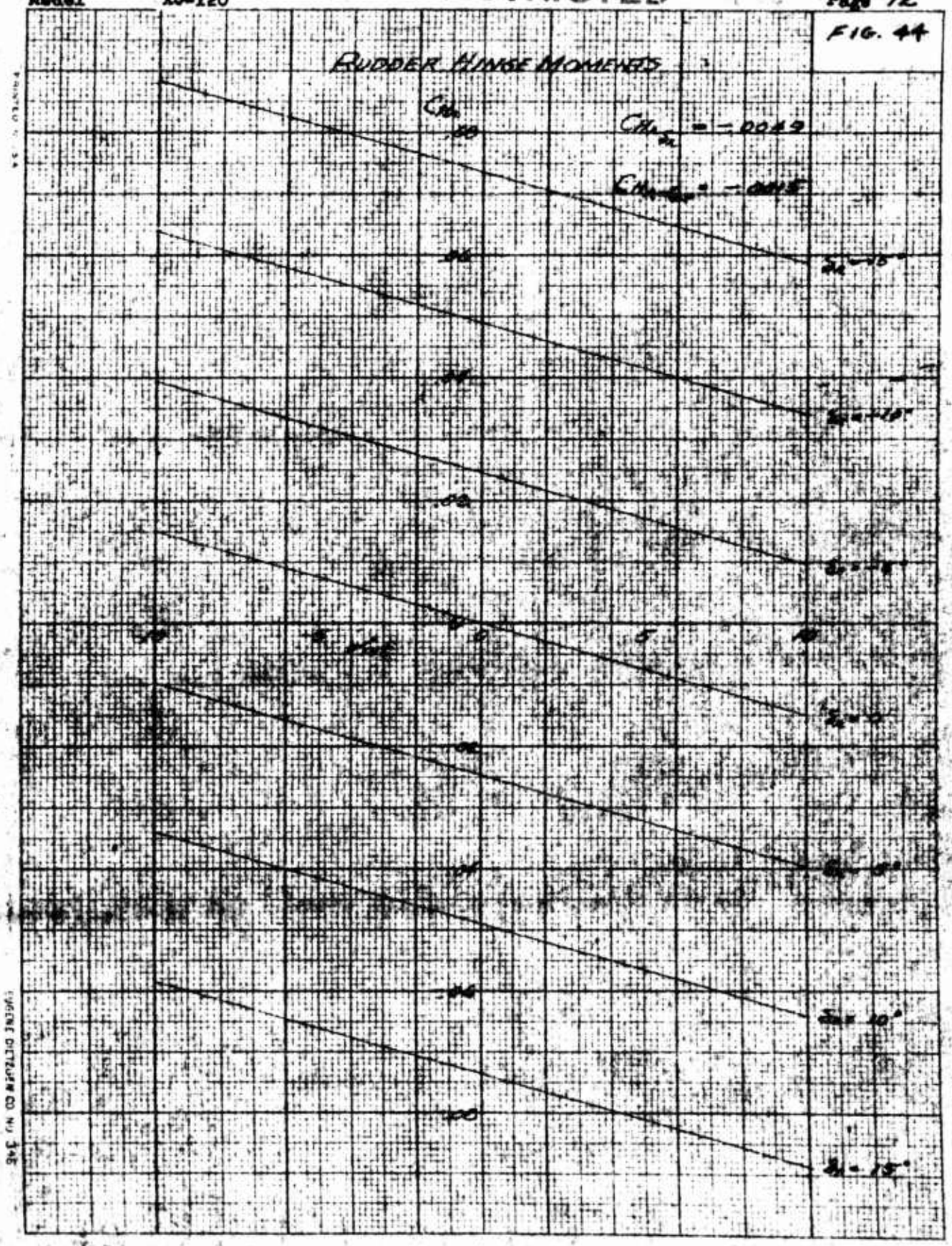
RUDDER HINGE MOMENTS
C_{H_δ}
$C_{H_{\delta_R}} = -.0049$
$C_{H_{\delta_R-\delta_L}} = -.0015$
$\delta_R = -10°$
$\delta_R = -15°$
$\delta_R = -5°$
$\delta_R = 0$
$\delta_R = 5°$
$\delta_R = 10°$
$\delta_R = 15°$

PART I-D-10

10. RUDDER TABS

The following tables and figures summarize the power-off aerodynamic characteristics of the rudder trim and spring tab. Note that there is one rudder trim and spring tab on each rudder.

RUDDER TRIM TAB

$C_{C_{VT}\delta_{r_{tt}}}$	.00277 per degree
$C_{H_{r}\delta_{r_{tt}}}$	-.0034 per degree
$C_{H_{r_{tt}}\delta_{r_{tt}}}$	-.0043 per degree
$\alpha_{vt}\delta_{r_{tt}}$	-.0608 per degree

RUDDER SPRING TAB

$C_{C_{VT}\delta_{r_{st}}}$	.00166 per degree
$C_{H_{r}\delta_{r_{st}}}$	-.0021 per degree
$C_{H_{r_{st}}\delta_{r_{st}}}$	-.0043 per degree
$\alpha_{vt}\delta_{r_{st}}$	-.0364 per degree

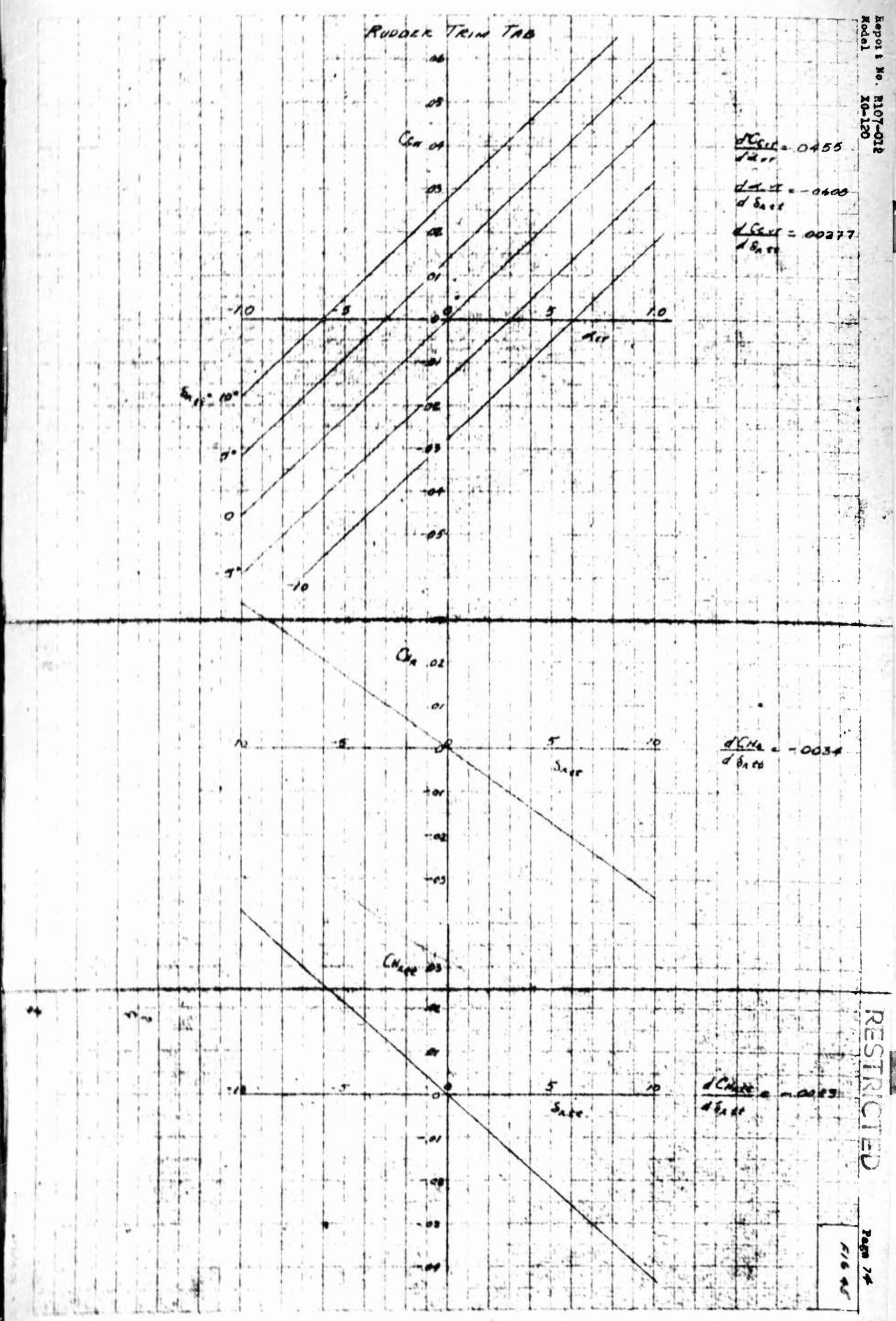
RUDDER TRIM TAB
C_{L_R}
α_{eff}
$\delta_{R_{eff}} = 10°$
5°
0
-5°
$\frac{dC_{L_R}}{d\alpha_{eff}} = .0455$
$\frac{d\alpha_{eff}}{d\delta_{R_{eff}}} = -.0600$
$\frac{dC_{L_R}}{d\delta_{R_{eff}}} = .00277$
C_{H_R}
$\delta_{R_{eff}}$
$\frac{dC_{H_R}}{d\delta_{R_{eff}}} = -.0034$
$C_{H_{R_{eff}}}$
$\frac{dC_{H_{R_{eff}}}}{d\delta_{R_{eff}}} = -.0083$

RESTRICTED

RESTRICTED

FIG. 46

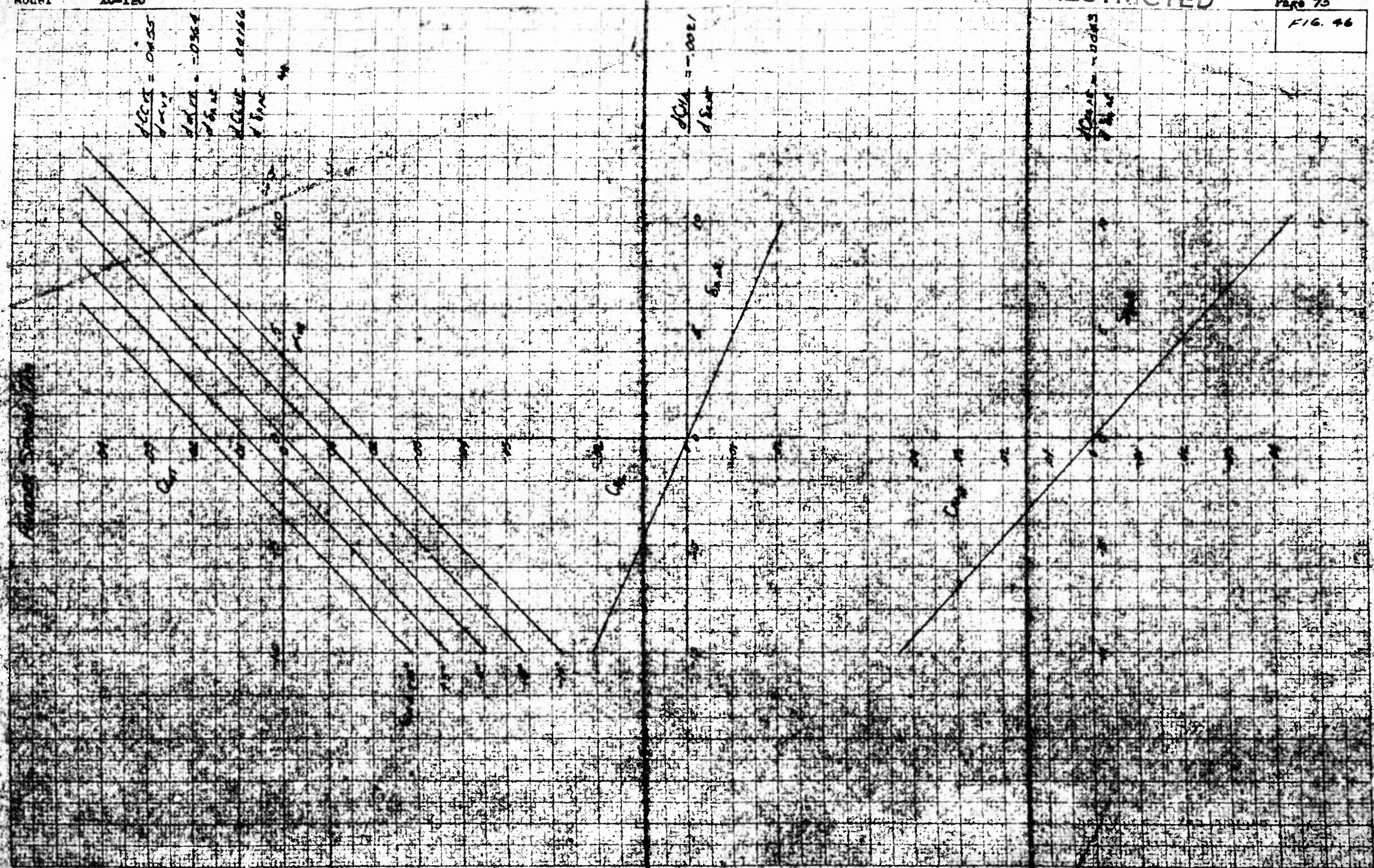

PART I-D-11

11. LANDING GEAR

The following data are the basic power-off aerodynamic characteristics of the landing gear.

C_{D_G} (one) = .0328 based on wing area

RESTRICTED

FIG. 47
FIG. 112

LANDING GEAR FORCE COEFFICIENTS
FOR
ONE LANDING GEAR

$$C_{X_G} = \frac{X_G}{q\,S_W}$$

$$C_{Z_G} = \frac{Z_G}{q\,S_W}$$

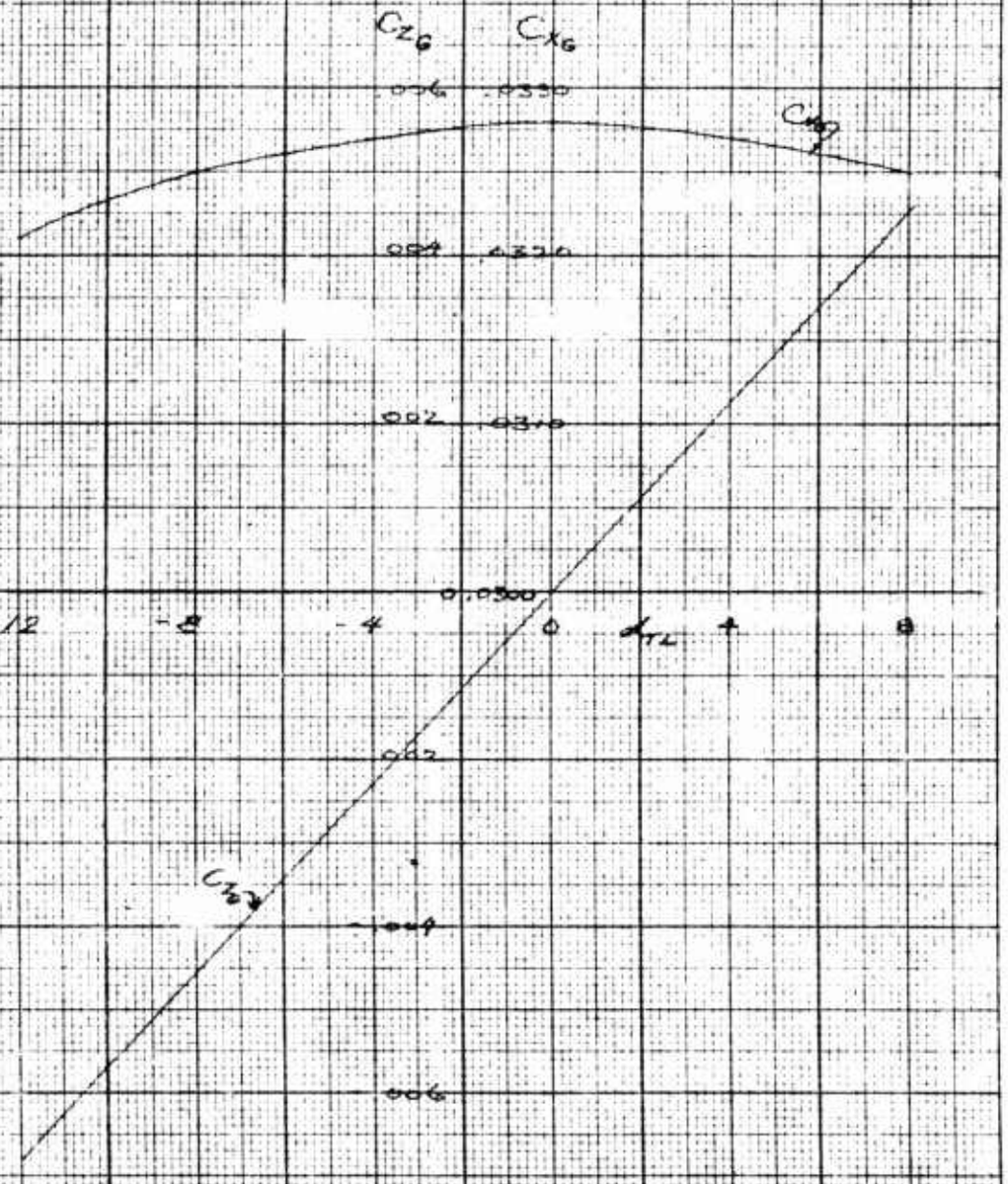

Part I-E

Summary of Aerodynamic Characteristics Power On

This section summarizes the power-on aerodynamic characteristics of the component parts of the airplane. All of the power-on characteristics have been determined for military power at sea level.

PART I-B-1

1. Wing Unflapped

The power on aerodynamic characteristics of the unflapped wing are the same as for power off as shown in Part I-D-1 except that there is an incremental lift and drag due to the slipstream effects on the portion of the wing immersed in the slipstream of the propeller.

The following figures show these incremental values which are to be added to the power off values to obtain the total power on characteristics.

For the effects of power on the pitching and yawing characteristics of the unflapped wing see discussion in Parts II-B-1-a, and II-B-1-f respectively.

FIG. 48
FIG. 114

$\Delta C_{L_{W1}}$ vs α_{TL}
XC-120 FLAPS UP

$$\Delta C_{L_{W1}} = \frac{\Delta L_{W1}}{q\, S_W}$$

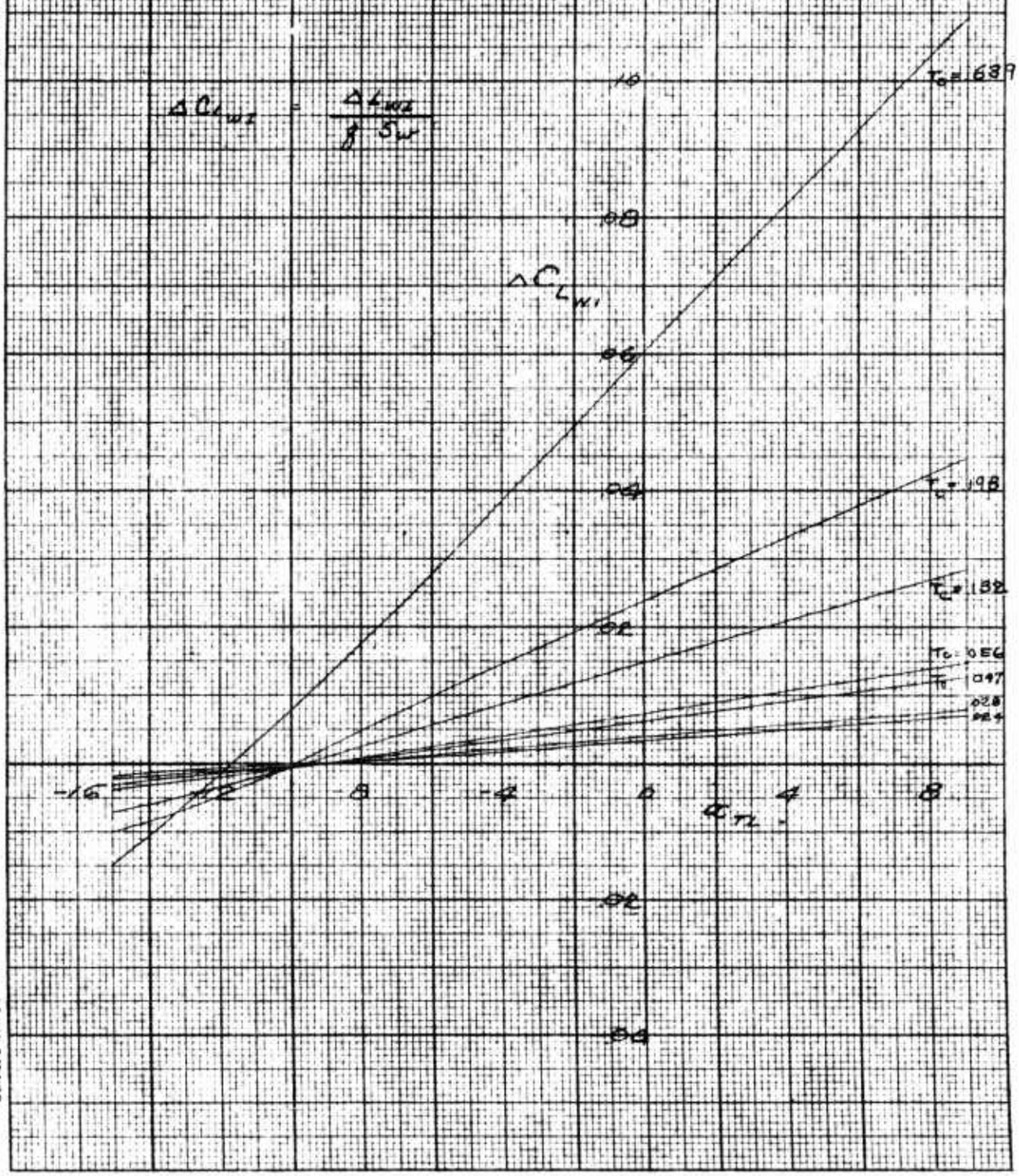

FIG 49
FIG 118

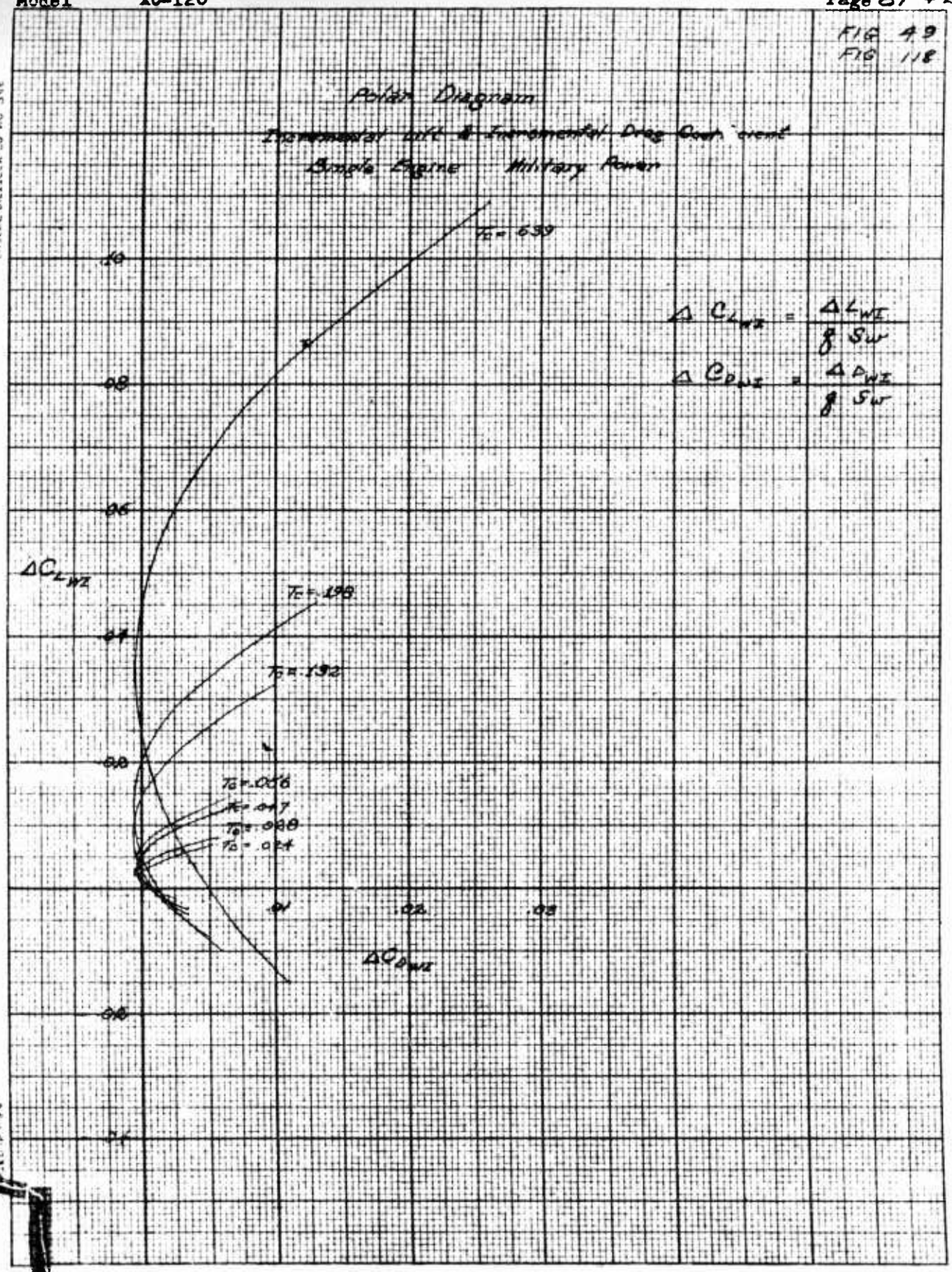

RESTRICTED

FIG 50
FIG 121

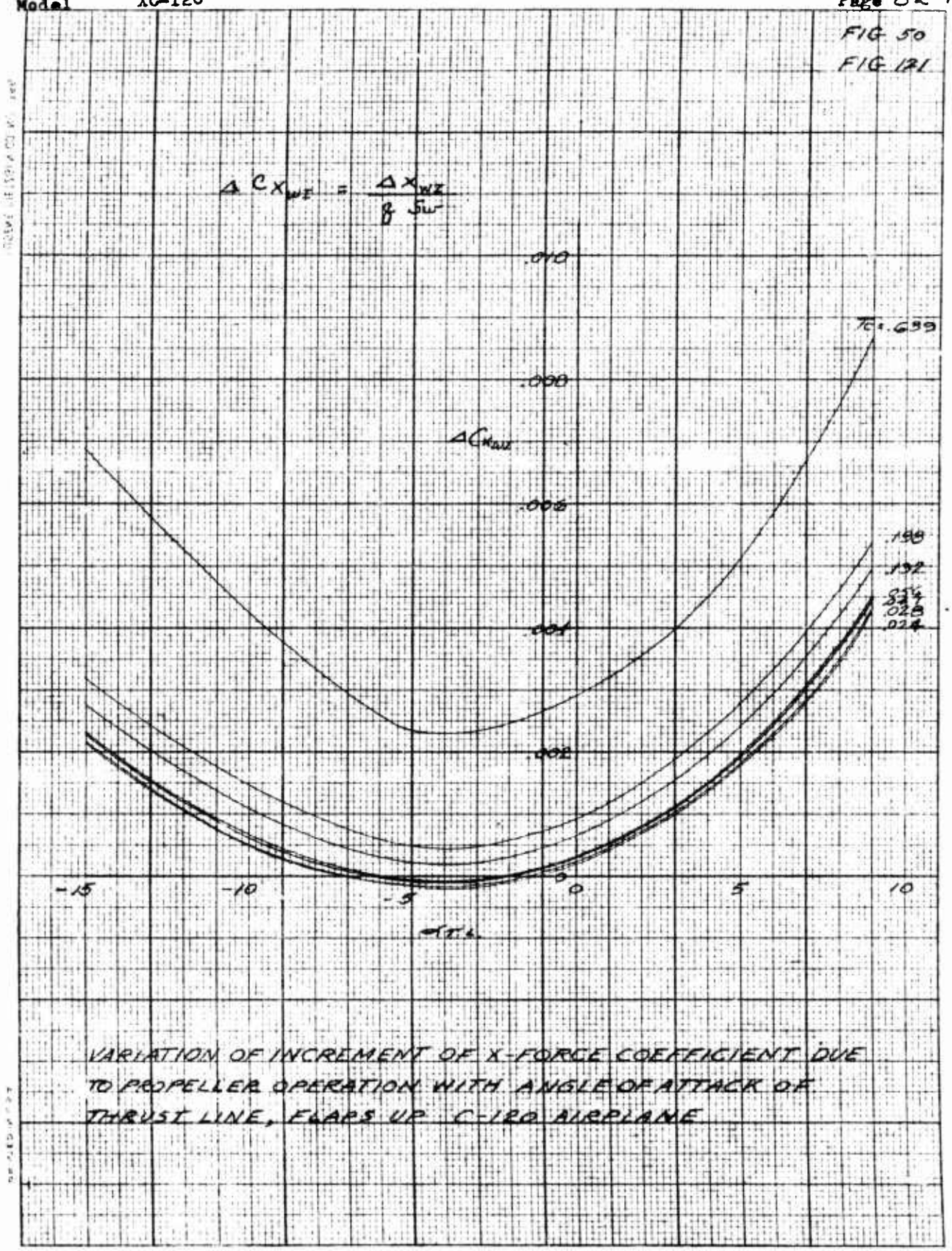

VARIATION OF INCREMENT OF X-FORCE COEFFICIENT DUE TO PROPELLER OPERATION WITH ANGLE OF ATTACK OF THRUST LINE, FLAPS UP C-120 AIRPLANE

RESTRICTED

FIG 61
FIG 122

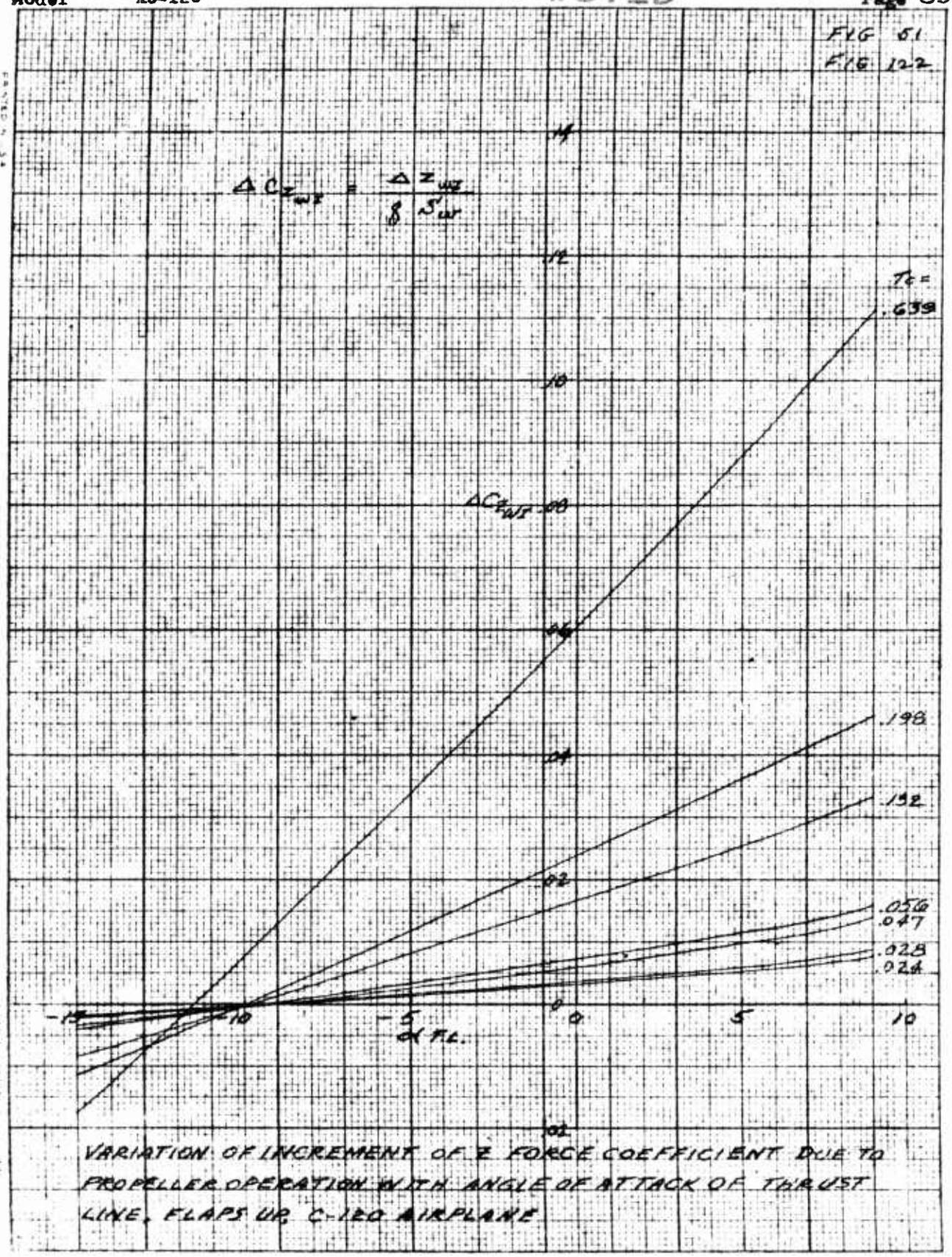

VARIATION OF INCREMENT OF Z FORCE COEFFICIENT DUE TO PROPELLER OPERATION WITH ANGLE OF ATTACK OF THRUST LINE, FLAPS UP, C-120 AIRPLANE

PART I-E-2

2. Wing Flapped

The power on aerodynamic characteristics of the flapped wing are the same as for power off as shown in Part I-D-2 with the exception that there is an incremental lift and drag due to slipstream effects on the portion of the wing immersed in the propeller slipstream.

The following figures shown these incremental values which are to be added to the power off values to obtain the total power on characteristics.

For the effects of power on the yawing characteristics of the flapped wing, see discussion in Part II-B-2-f.

FIG 52
FIG 124

$\Delta C_{m_{WFI}}$ vs α_{TL}

MILITARY POWER - FLAPPED WING

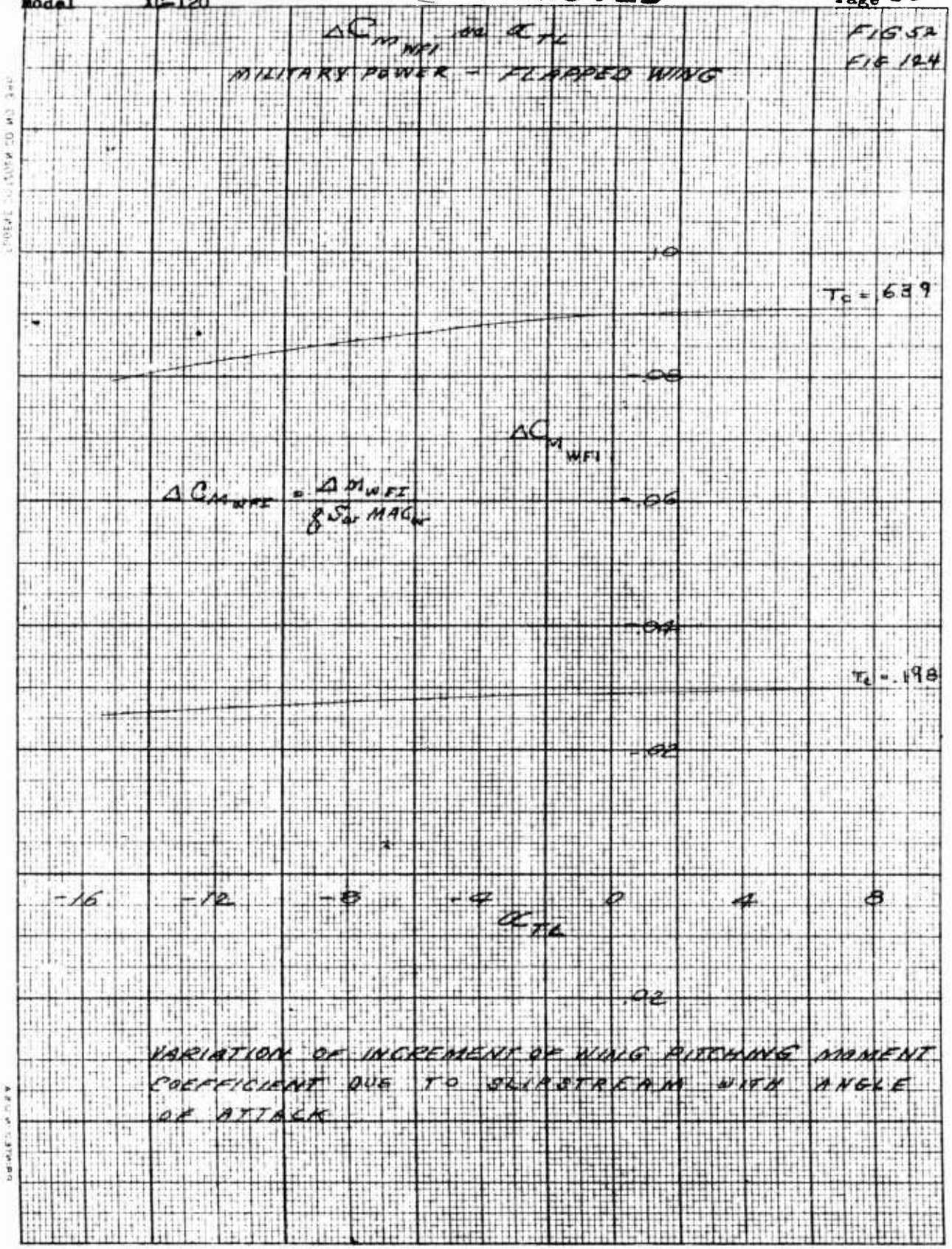

VARIATION OF INCREMENT OF WING PITCHING MOMENT COEFFICIENT DUE TO SLIPSTREAM WITH ANGLE OF ATTACK

FIG 53
FIG 126

$\Delta C_{L_{WF1}}$ vs. α_{TL}

MILITARY POWER — FLAPPED WING

$$\Delta C_{L_{WFE}} = \frac{\Delta L_{WFE}}{q\, S_W}$$

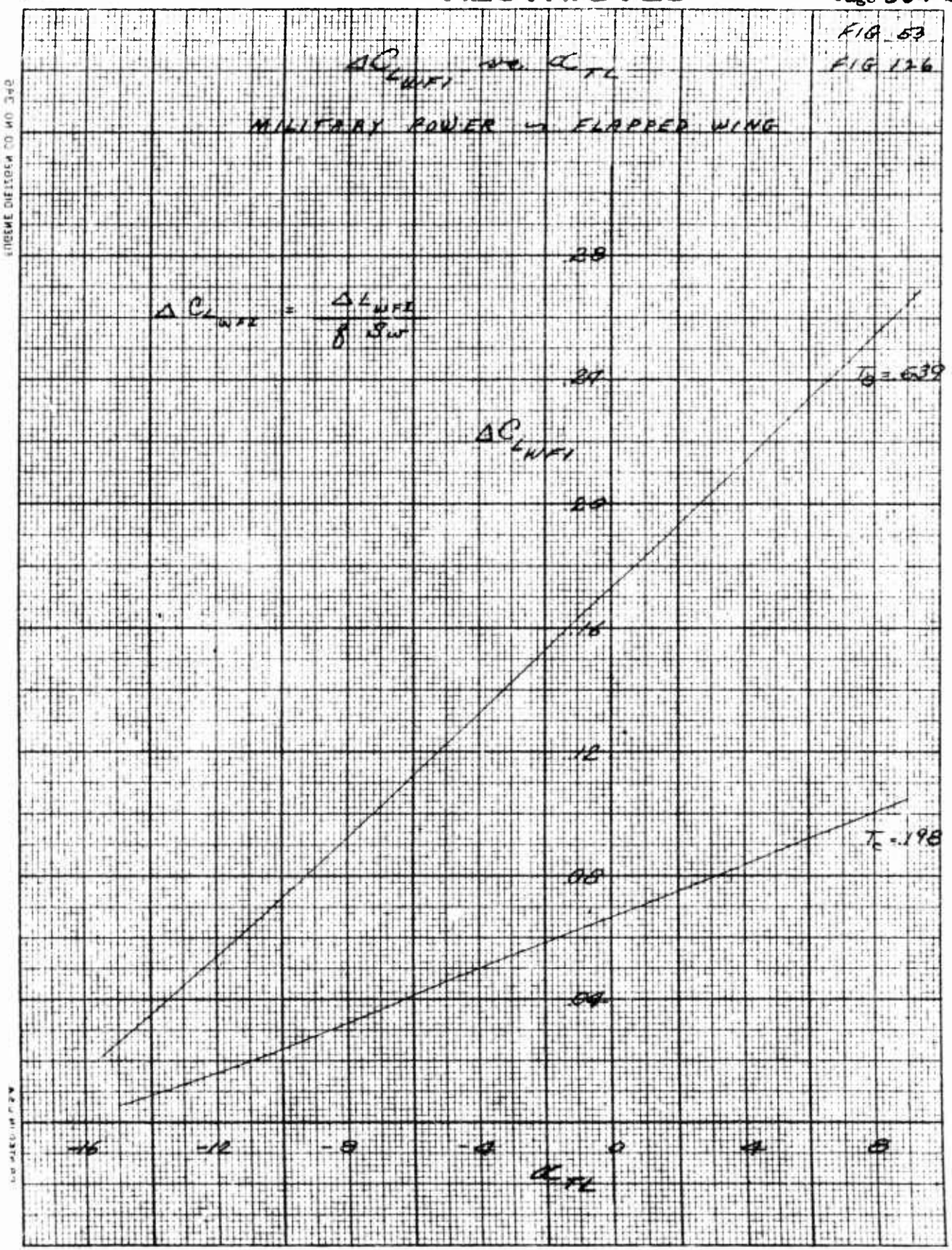

FIG 38
FIG 138

POLAR DIAGRAM
INCREMENTAL LIFT VS INCREMENTAL DRAG

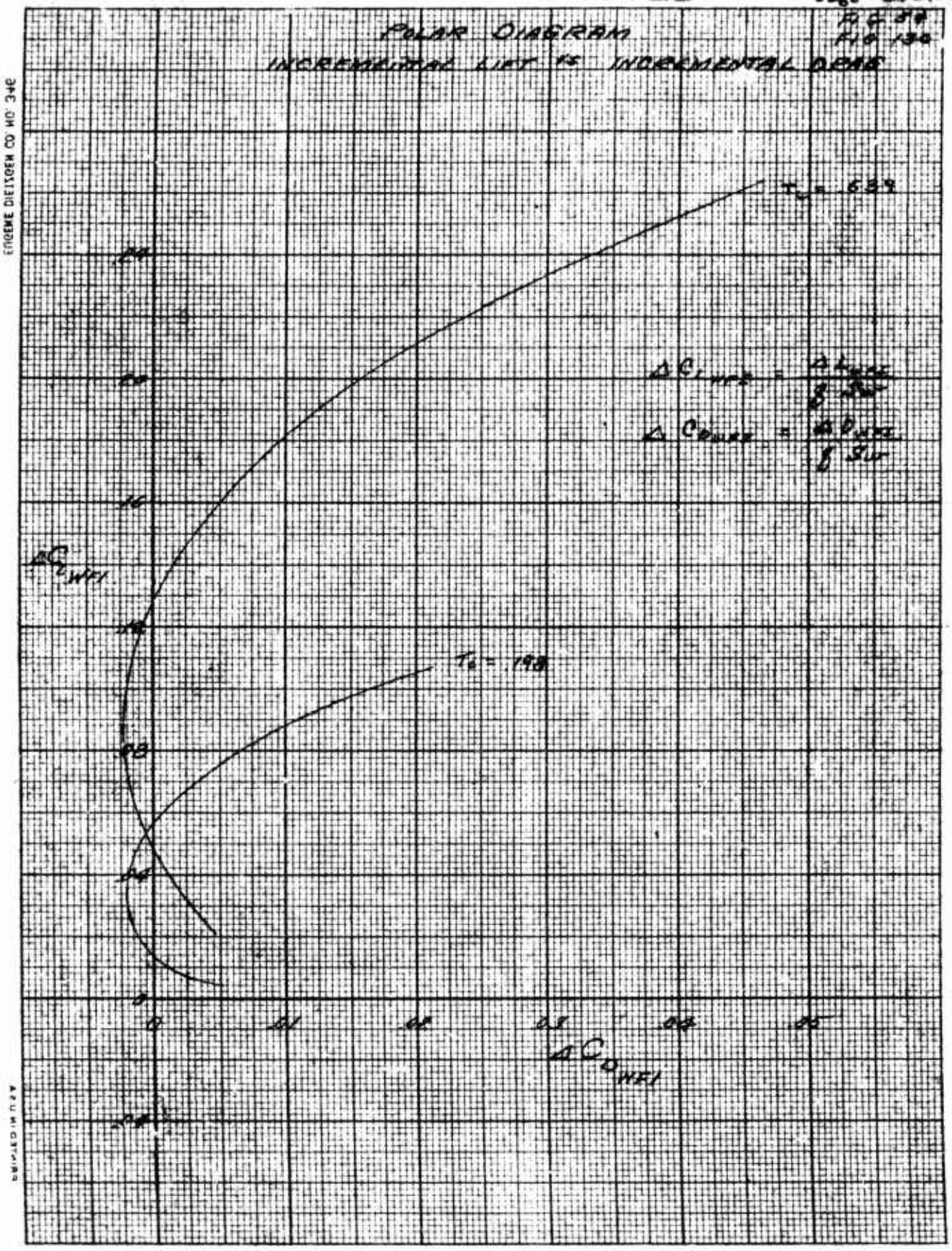

ENGINEERING DIETZGEN CO. NO. 340

RESTRICTED

FIG 85
FIG 188

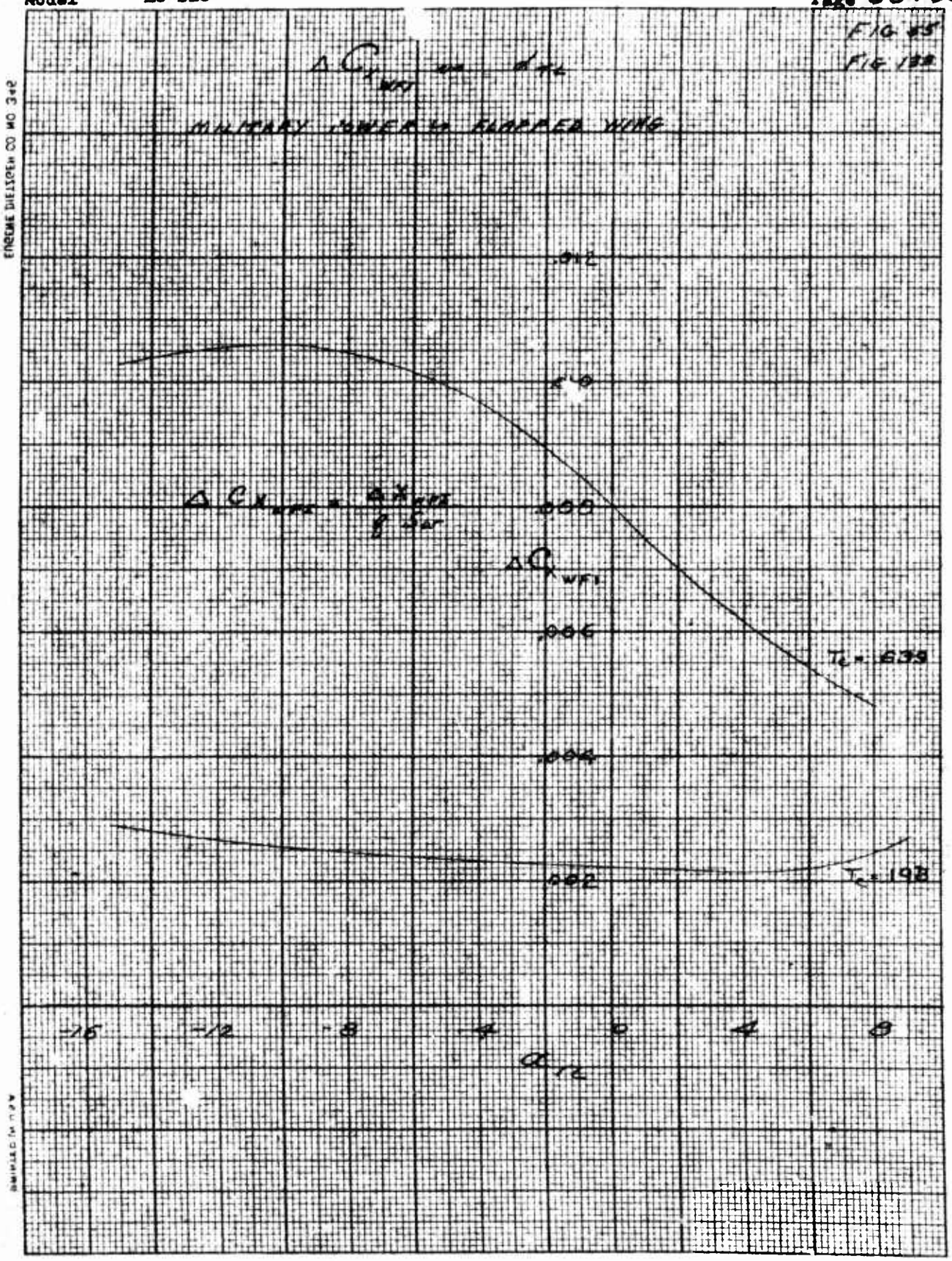

RESTRICTED

FIG 56
FIG 134

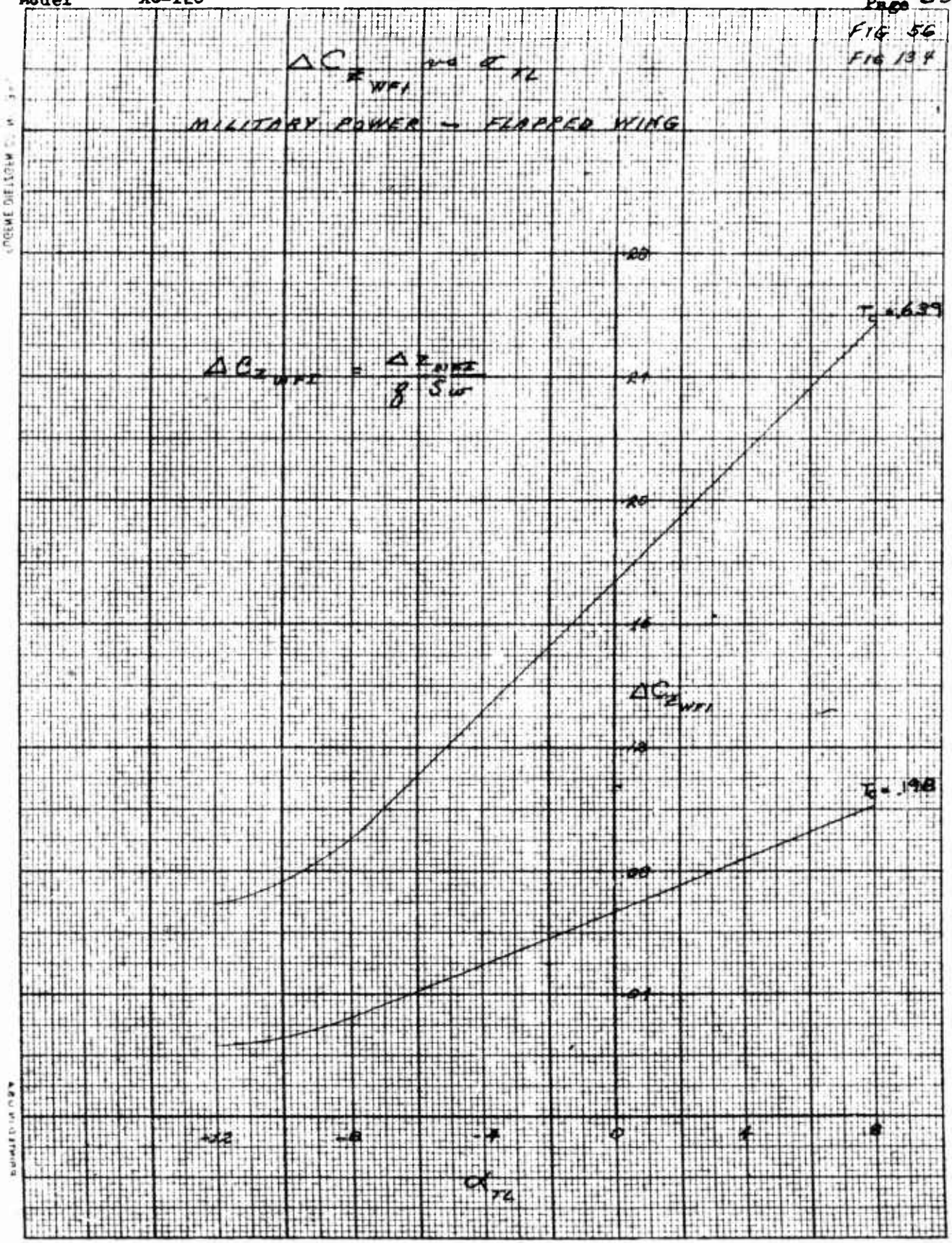

PART I-B-3

3. Ailerons

The power on aerodynamic characteristics of the ailerons are the same as for power off as shown in Part I-D-3.

PART I-E-4

4. Aileron Tabs

The power on aerodynamic characteristics of the aileron tabs are the same as for power off as shown in Part I-D-4

PART I-E-5

5. Fuselage

The power on aerodynamic characteristics of the fuselage are the same as for power off as shown in Part I-D-5.

5A. Crew Nacelle

The power on aerodynamic characteristics of the crew nacelle are the same as for power off as shown in Part II-D-5A.

PART I-E-6

6. **Booms**

The power on aerodynamic characteristics of the booms are the same as for power off as shown in Part I-D-6

PART I-E-7

7. **Power Plant**

The brake horsepower characteristics of the Pratt & Whitney R-4360-20 engine is shown on the following figure for both normal rated power and for military rated power at various altitudes.

The power on characteristics of the component parts have been determined for military power at sea level.

FIG 57

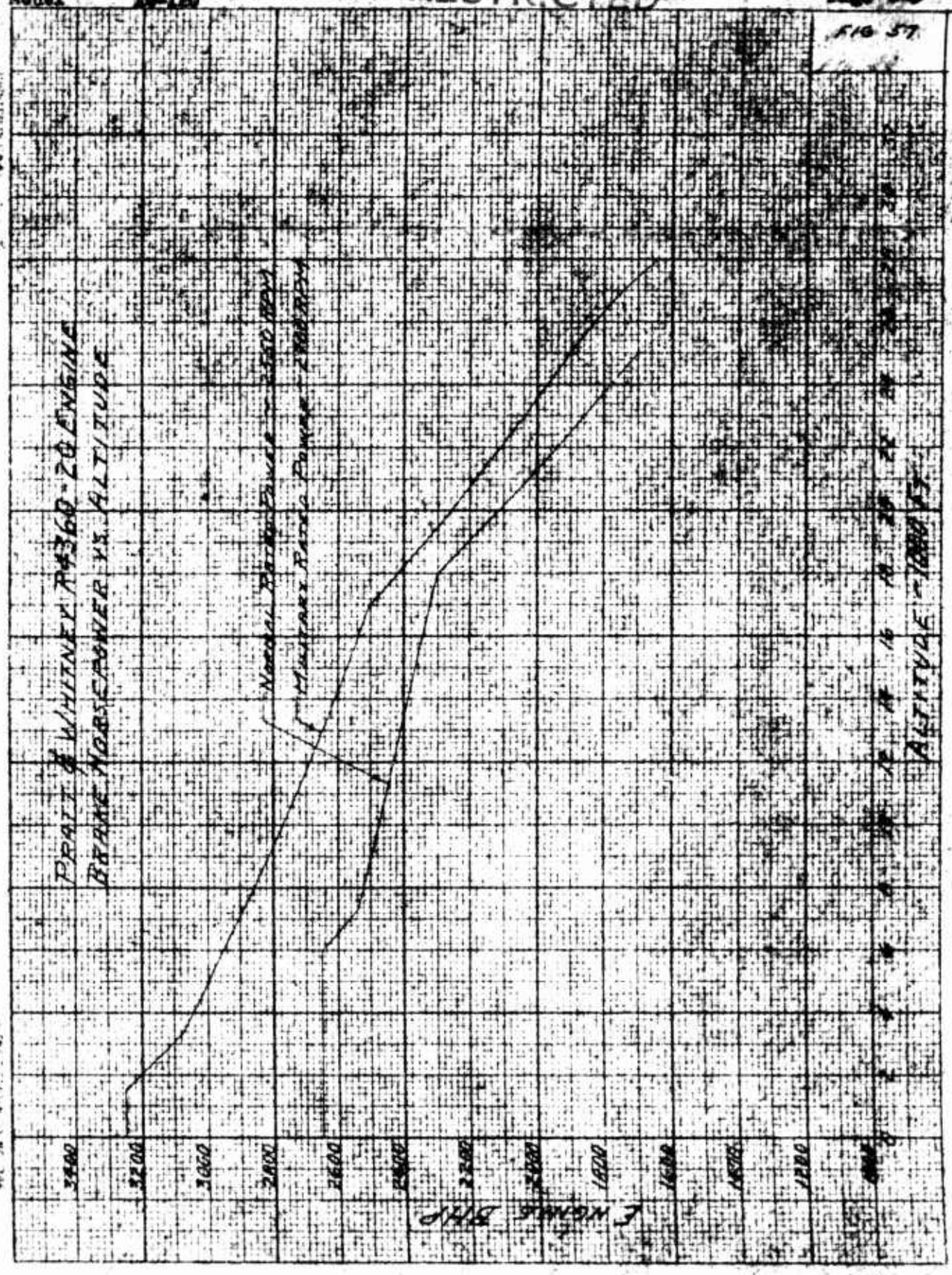
PRATT & WHITNEY R-4360-20 ENGINE
BRAKE HORSEPOWER VS. ALTITUDE
NORMAL RATED POWER ~ 2250 RPM
MILITARY RATED POWER ~ 2500 RPM
ALTITUDE ~ 1000 FT
BHP NORMAL
3400
3200
3000
2800
2600
2400
2200
2000
1800
1600
1400
1200
1000
0
2
4
6
8
10
12
14
16
18
20
22
24
26
28
30
32

PART I-E-5

8. Propeller

The following figures summarize the aerodynamic characteristics of one propeller-engine combination with military power at sea level.

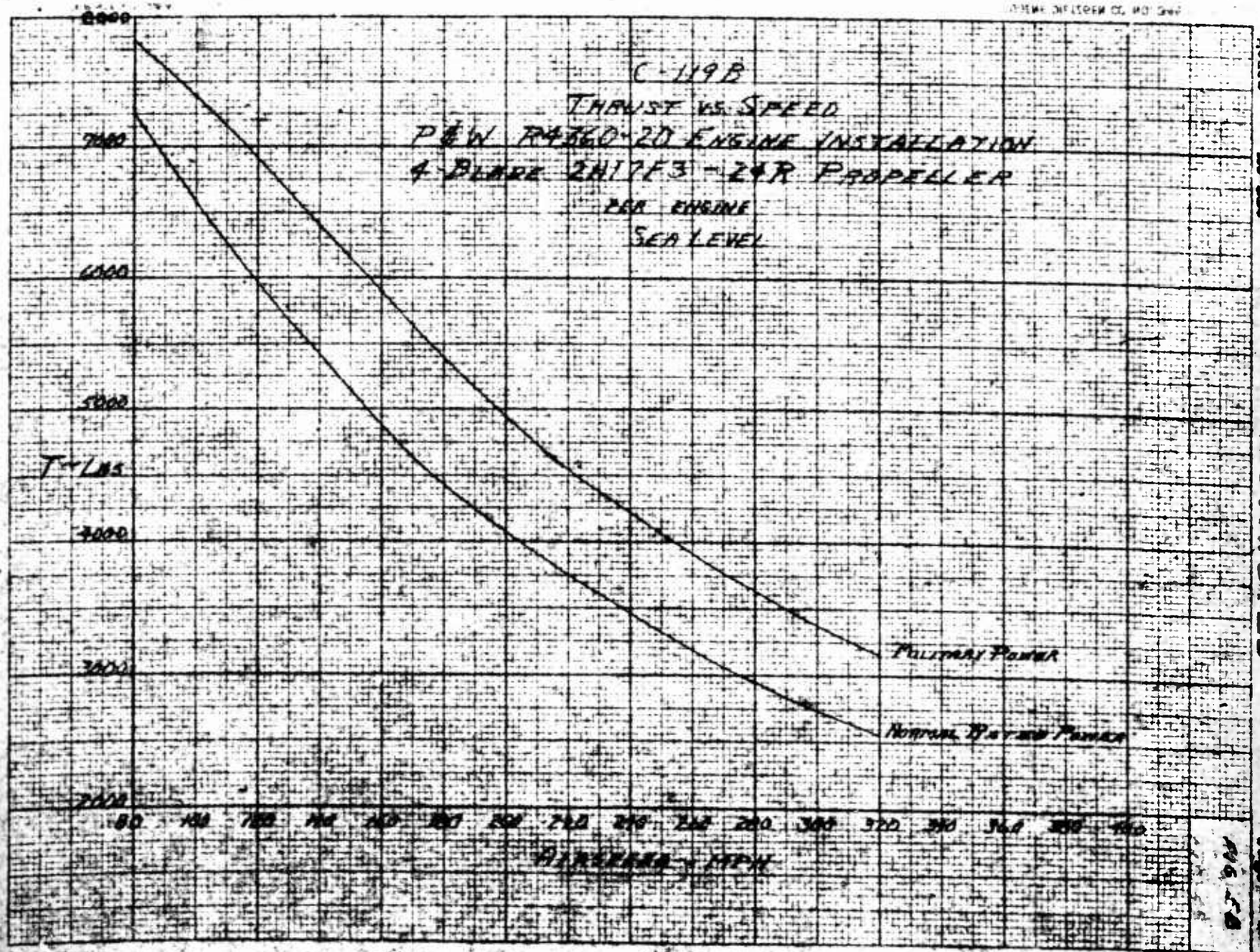
C-119B
THRUST VS. SPEED
P&W R4360-20 ENGINE INSTALLATION
4 BLADE 2H17F3-24R PROPELLER
PER ENGINE
SEA LEVEL
T-LBS
8000
7000
6000
5000
4000
3000
2000
MILITARY POWER
NORMAL RATED POWER
80
100
120
140
160
180
200
220
240
260
280
300
320
340
360
380
400
AIRSPEED - MPH

RESTRICTED

FIG 59

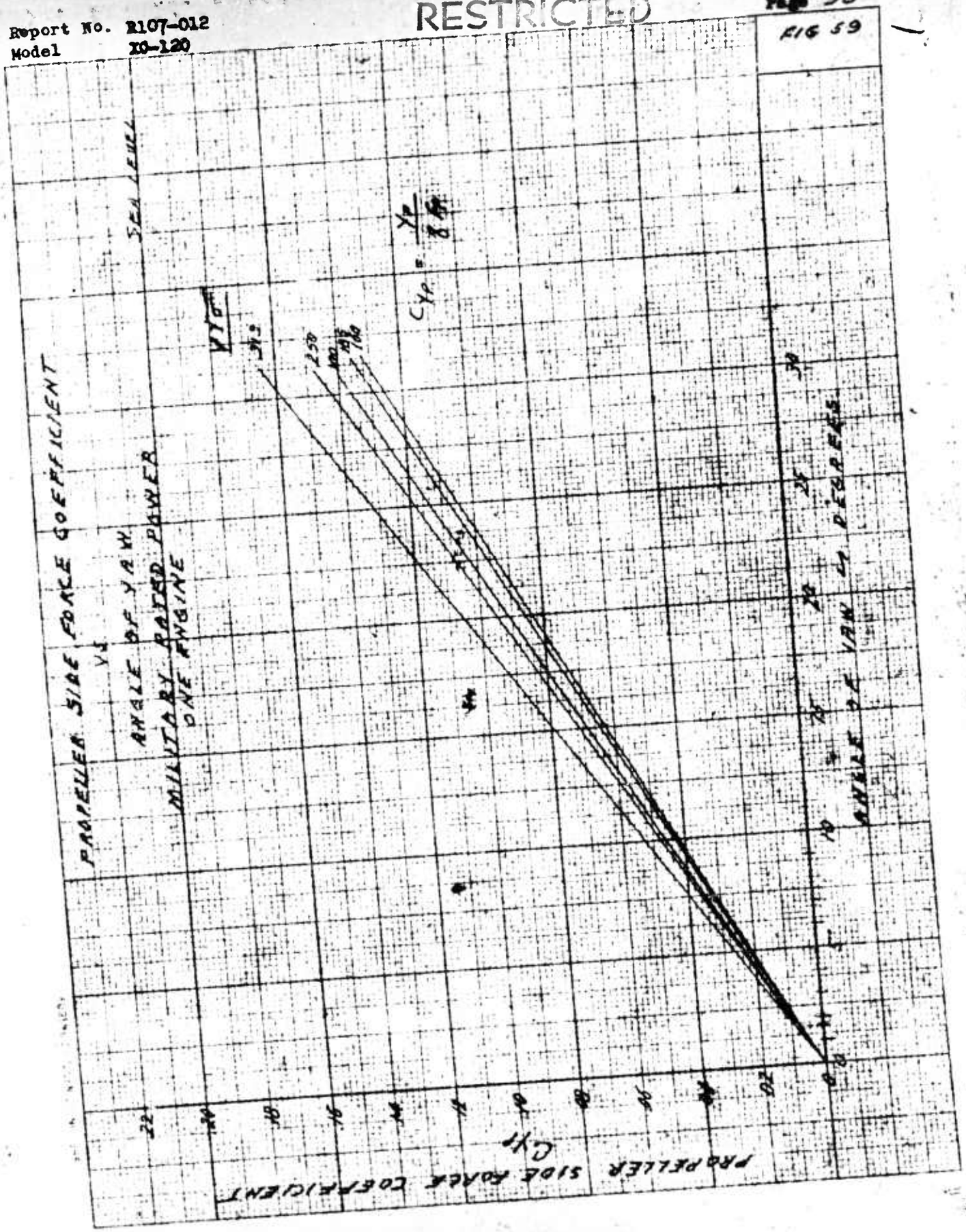
PROPELLER SIDE FORCE COEFFICIENT
VS
ANGLE OF YAW
MILITARY RATED POWER
ONE ENGINE
SEA LEVEL
$C_{Y_P} = \frac{Y_P}{qS_P}$
$\frac{V}{V_{TOT}}$
250
PROPELLER SIDE FORCE COEFFICIENT
C_{Y_P}
ANGLE OF YAW ψ DEGREES

FIG 60

VARIATION OF PROPELLER NORMAL FORCE COEFFICIENT WITH THRUST COEFFICIENT

MID LEVEL

$C_{N_p} = \frac{N_p}{\rho n^2 D^4}$

C_{N_p}

C_T ~ THRUST COEFFICIENT

$\alpha_{FUS} = 0$

$\alpha_{FUS} = -4$

$\alpha_{FUS} = -8$

$\alpha_{FUS} = -12$

FIG 61

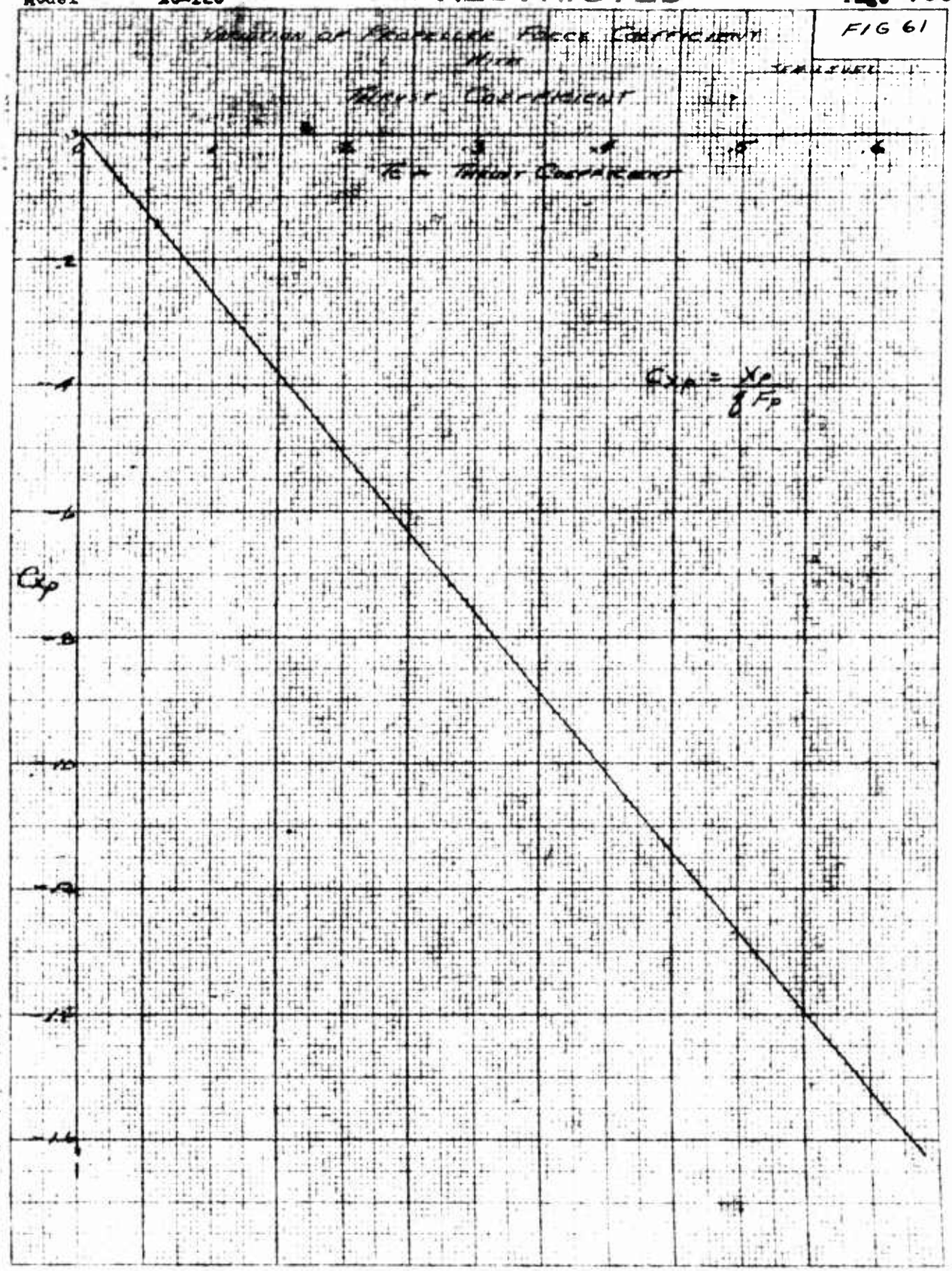
Variation of Propeller Force Coefficient
With
Thrust Coefficient
Thrust Coefficient
$C_{x_p} = \frac{X_p}{q F_p}$
C_{x_p}
0
-.2
-.4
-.6
-.8
-1.0
-1.2
-1.4
.1
.2
.3
.4
.5
.6

PART I-E-9

9. Horizontal Tail

The power on aerodynamic characteristics of the horizontal tail are the same as for power off as shown in Part I-D-7. However, the downwash and dynamic pressure at the horizontal tail changes with power on.

The following data and figures show the power effects on the dynamic pressure at the horizontal tail and the angle of attack of the horizontal tail.

q_{ht}/q for flaps down = 1.00

FIG. 62
FIG. 127

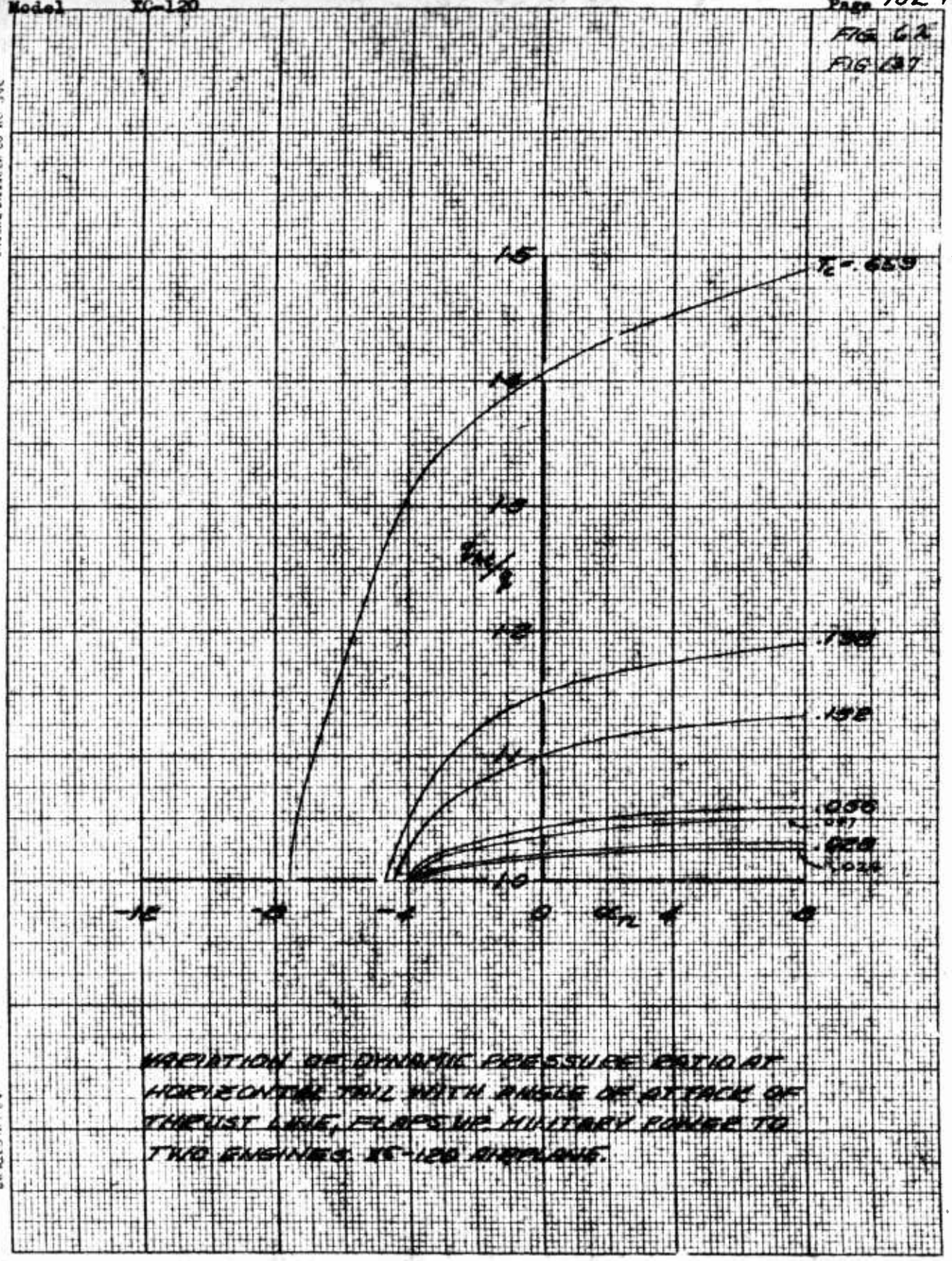

VARIATION OF DYNAMIC PRESSURE RATIO AT HORIZONTAL TAIL WITH ANGLE OF ATTACK OF THRUST LINE, FLAPS UP, MILITARY POWER TO TWO ENGINES. XC-120 AIRPLANE.

FIG. 63
FIG. 139

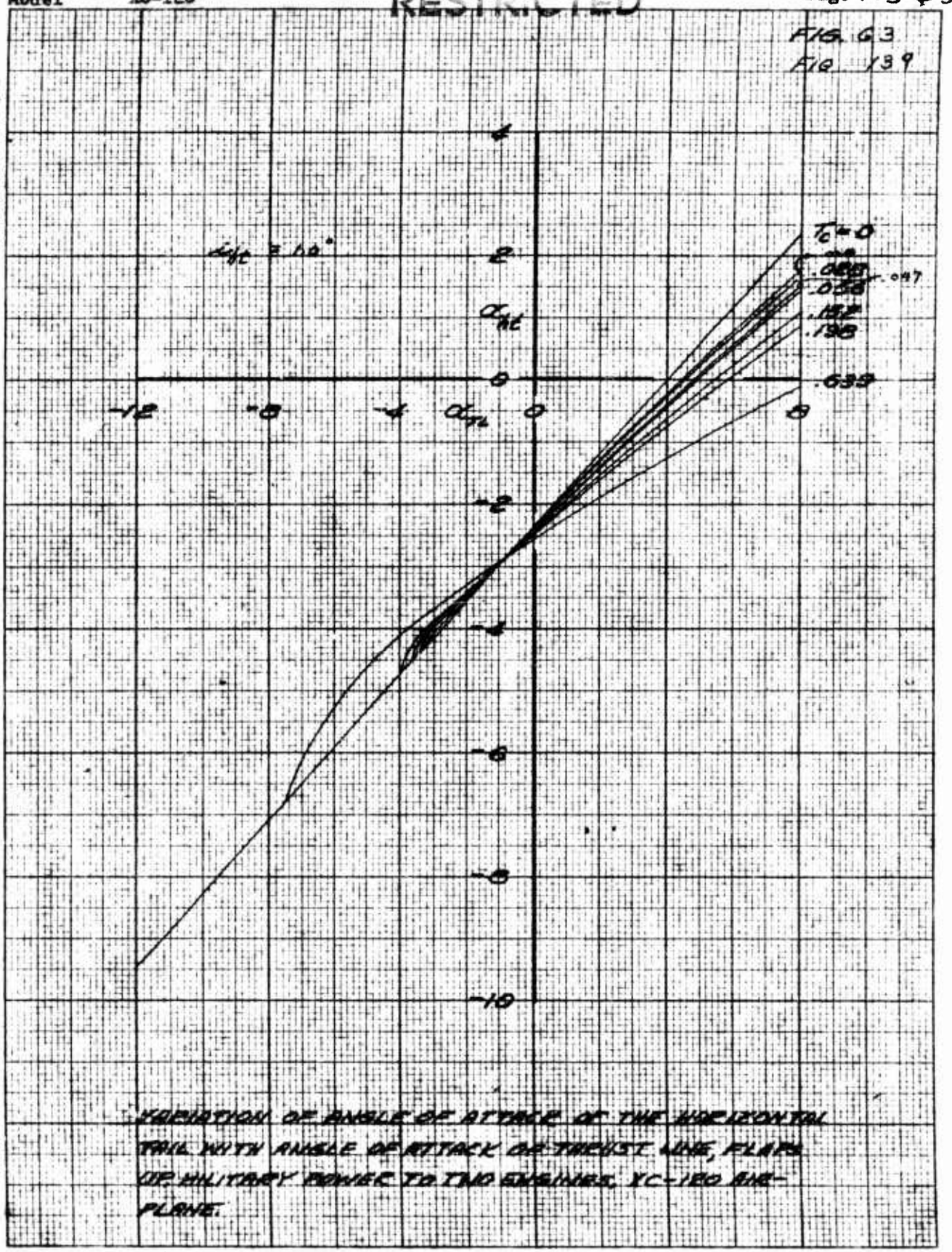

VARIATION OF ANGLE OF ATTACK OF THE HORIZONTAL TAIL WITH ANGLE OF ATTACK OF THRUST LINE, FLAPS UP, MILITARY POWER TO TWO ENGINES, XC-120 AIRPLANE.

RESTRICTED

FIG 64
FIG 141

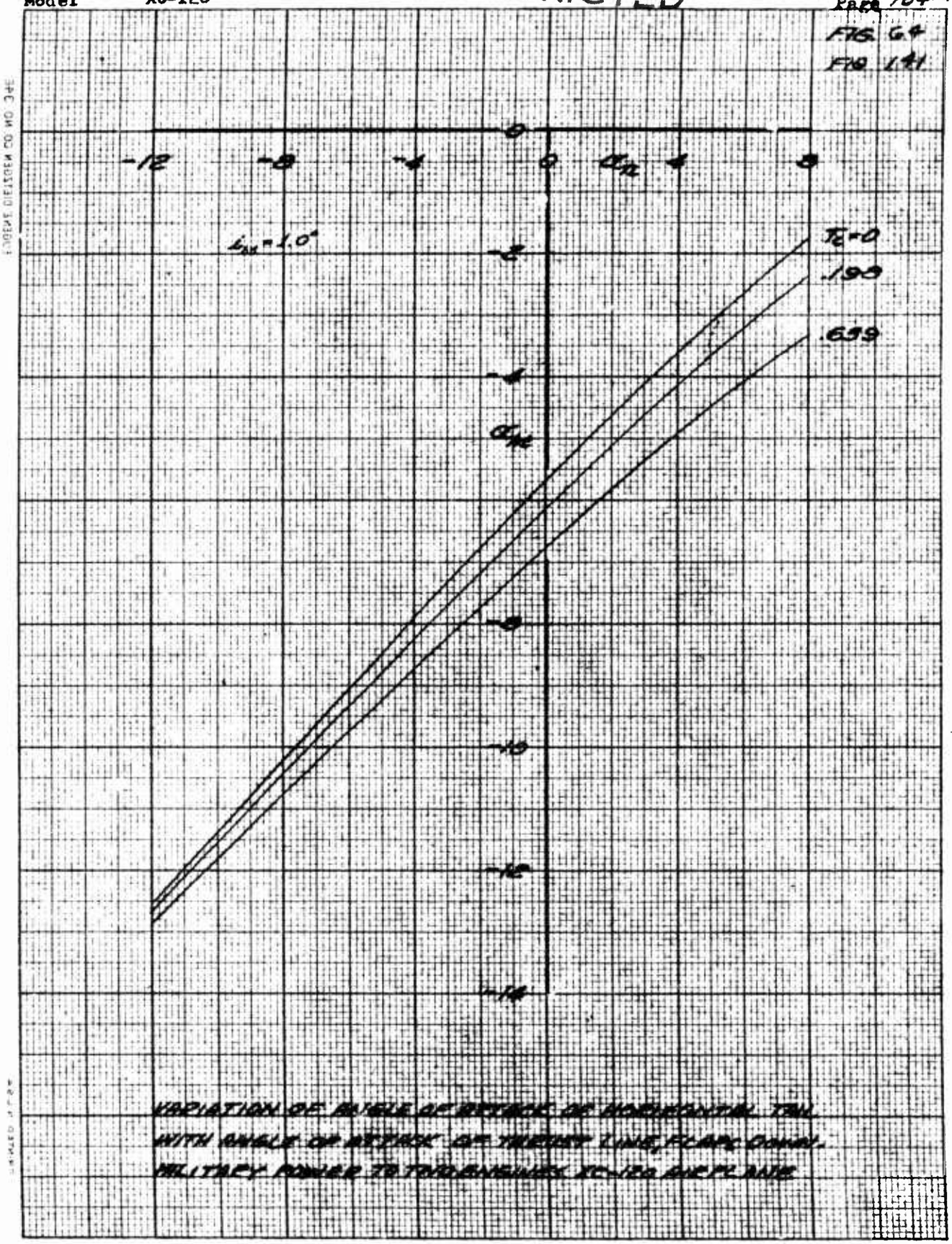

VARIATION OF ANGLE OF ATTACK OF HORIZONTAL TAIL WITH ANGLE OF ATTACK OF THRUST LINE, FLAPS DOWN. MILITARY POWER TO TWO ENGINES XC-120 AIRPLANE

PART I-E-10

10. Elevator Tabs

The power on aerodynamic characteristics of the elevator tabs are the same as for power off as shown in Part I-D-5

PART I-E-11

11. Vertical Tail

The power on aerodynamic characteristics of the vertical tail are the same as for power off as shown in Part I-D-9. However, the sidewash and dynamic pressure at the vertical tail changes with power on. The following figures show the power effects on the dynamic pressure and sidewash at the vertical tail for flaps up and flaps down conditions at various speeds.

FIG 68
FIG 142

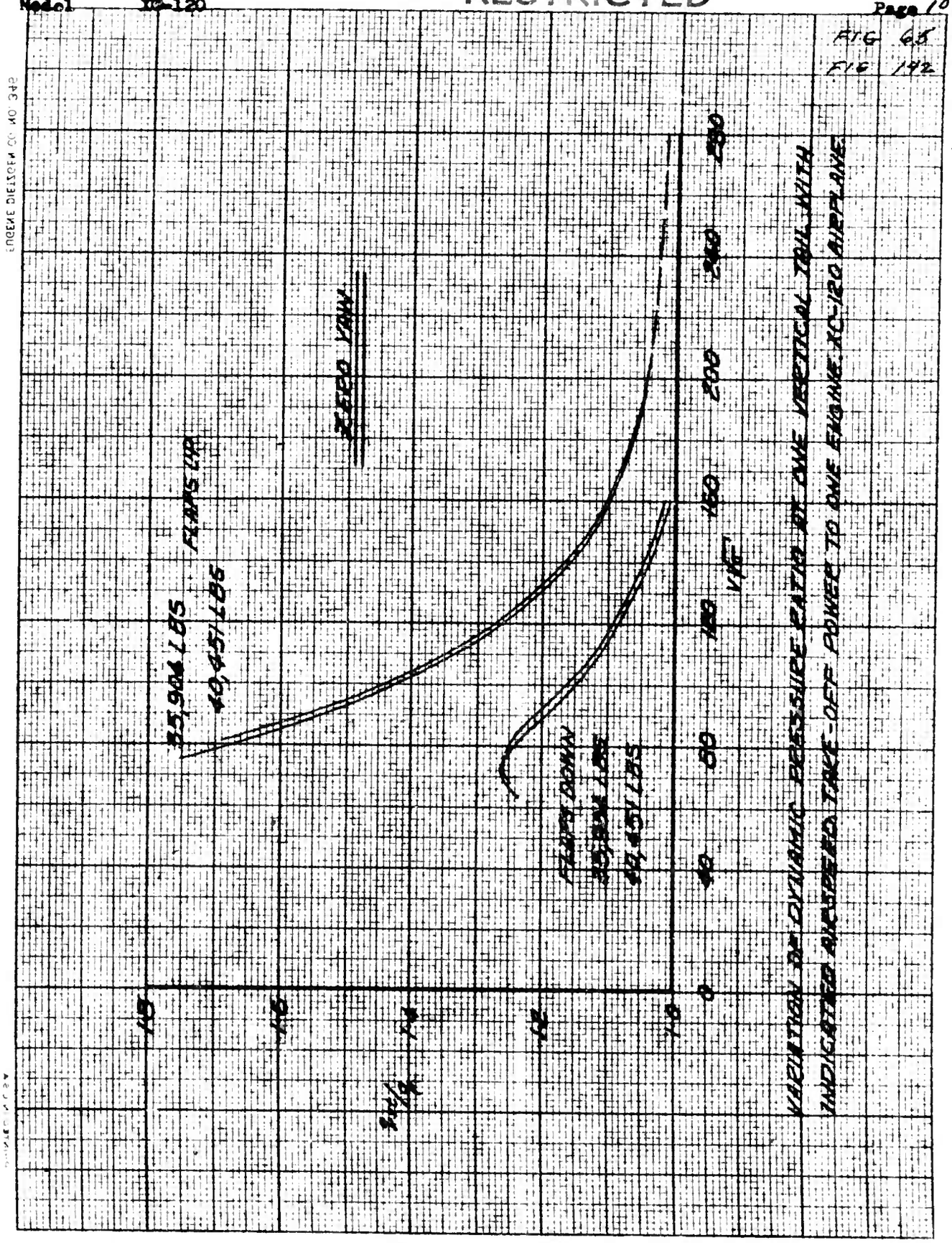

FIG. 66
Fig. 143

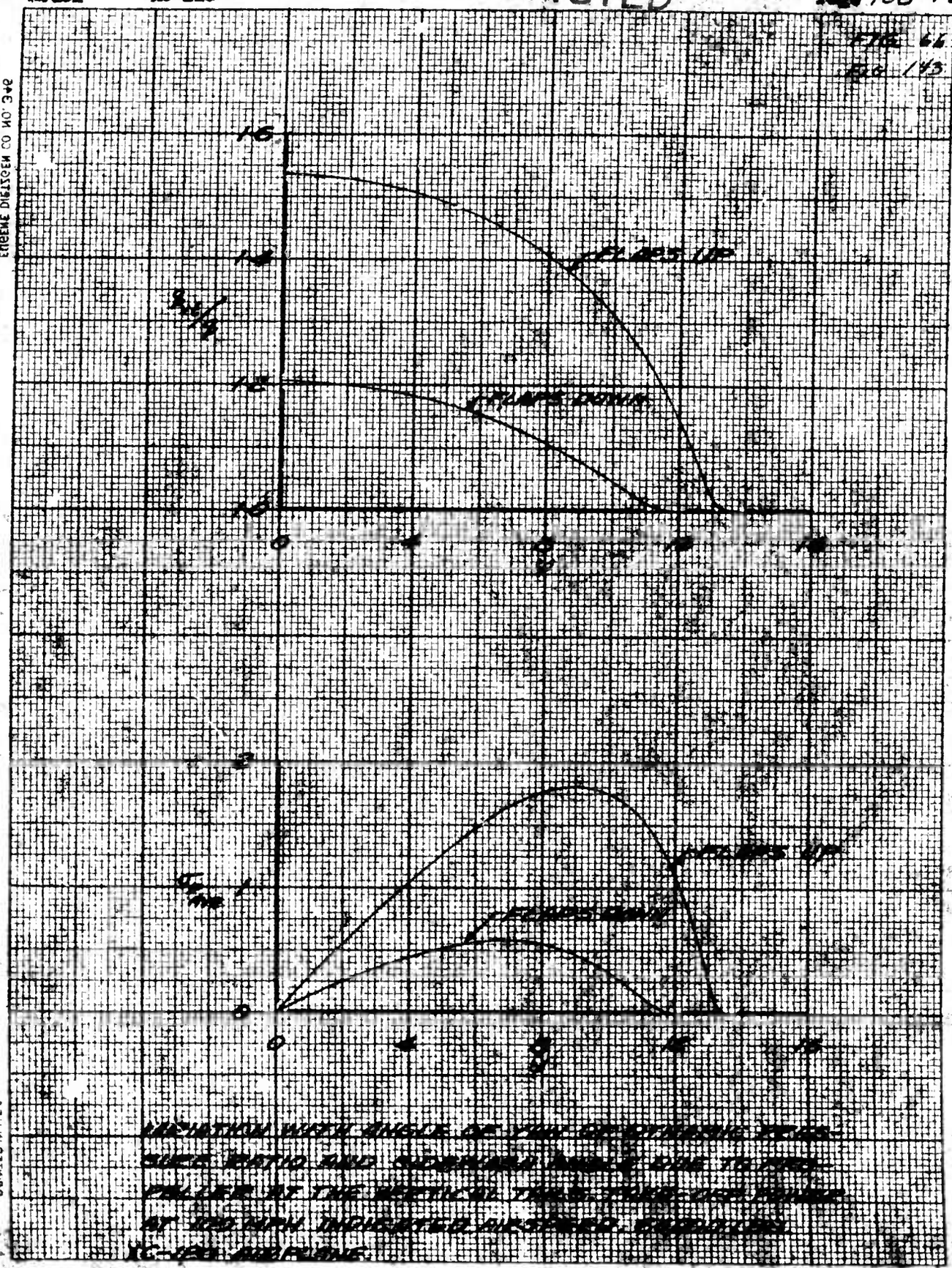

VARIATION WITH ANGLE OF ATTACK OF THE AERODYNAMIC FORCE RATIO AND ELEVATOR HINGE MOMENT DUE TO DEFLECTION OF THE ELEVATOR TRIM TAB AND FLAPS AT TRIM INDICATED AIRSPEED EQUAL TO 120 MILES PER HOUR.

ENGINE DIVISION CO NO. 345
PRINTED IN U.S.A.

FIG 67
FIG 144

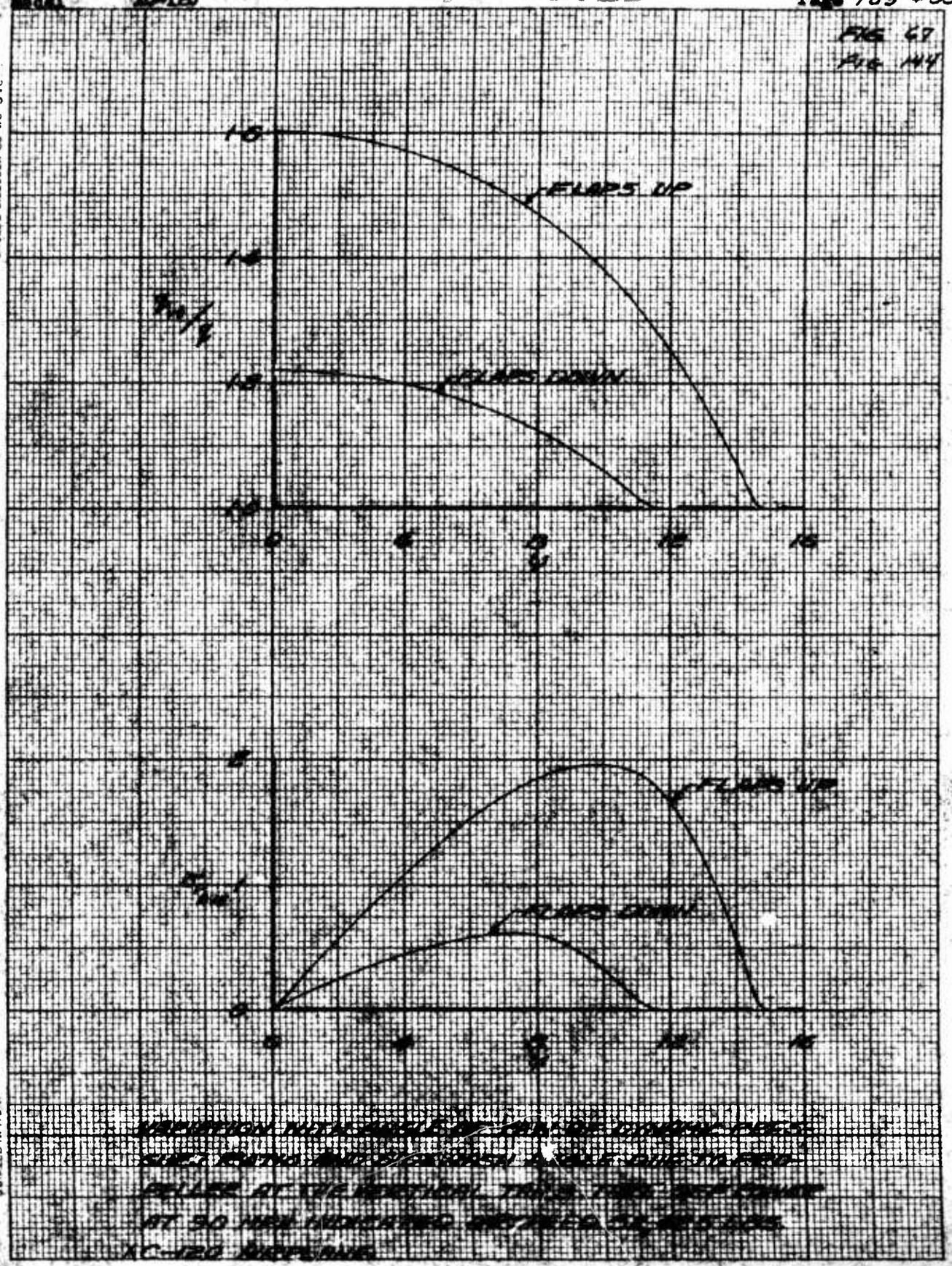

[illegible]
[illegible]
[illegible]
[illegible]
[illegible]
XC-120 [illegible]

PART I-E-12

12. Rudder Tabs

The power on aerodynamic characteristics of the rudder tabs are the same as for power off as shown in Part I-D-10.

PART I-E-13

13. Landing Gear

The power on aerodynamic characteristics of the landing gear are the same as for power off as shown in Part I-D-11.

PART II-A

CALCULATION OF AERODYNAMIC CHARACTERISTICS

A. POWER-OFF

This portion of the report presents the aerodynamic characteristics of the various component parts of the airplane neglecting all power effects.

PART II-A-1

1. WING UNFLAPPED

Since the unflapped wing is exactly the same as that of the C-119B airplane with the exception that the angle of incidence of the wing root chord with respect to the thrust line is 7.0°; (On the C-119B this angle is 3.0°) all the aerodynamic characteristics are the same as those presented in reference (1) except where the change in angle of incidence is a determining factor.

Therefore, since this change does not affect the following sections, all calculations and figures presented therein in reference (1) apply to the XC-120 unflapped wing.

Part II-A-1-b	Part II-A-1-i
Part II-A-1-c	Part II-A-1-j
Part II-A-1-d	Part II-A-1-k
Part II-A-1-f	Part II-A-1-l
Part II-A-1-g	Part II-A-1-m
Part II-A-1-h	Part II-A-1-n

The following sections are affected by the change in angle of incidence and the revisions are presented herein.

Part II-A-1-a	Part II-A-1-o
Part II-A-1-e	Part II-A-1-p

All coefficients shown in this section are based on free stream dynamic pressure, wing area, and/or wing chord (MAC_w).

For convenience all aerodynamic characteristics are presented completely in the summary whether affected by the change in angle of incidence or not.

PART II-A-1-a

a. WING DRAWING

A wing drawing with pertinent dimensions used in calculating MAC_w is shown on the following page.

Report No. R107-012
Model XC-120

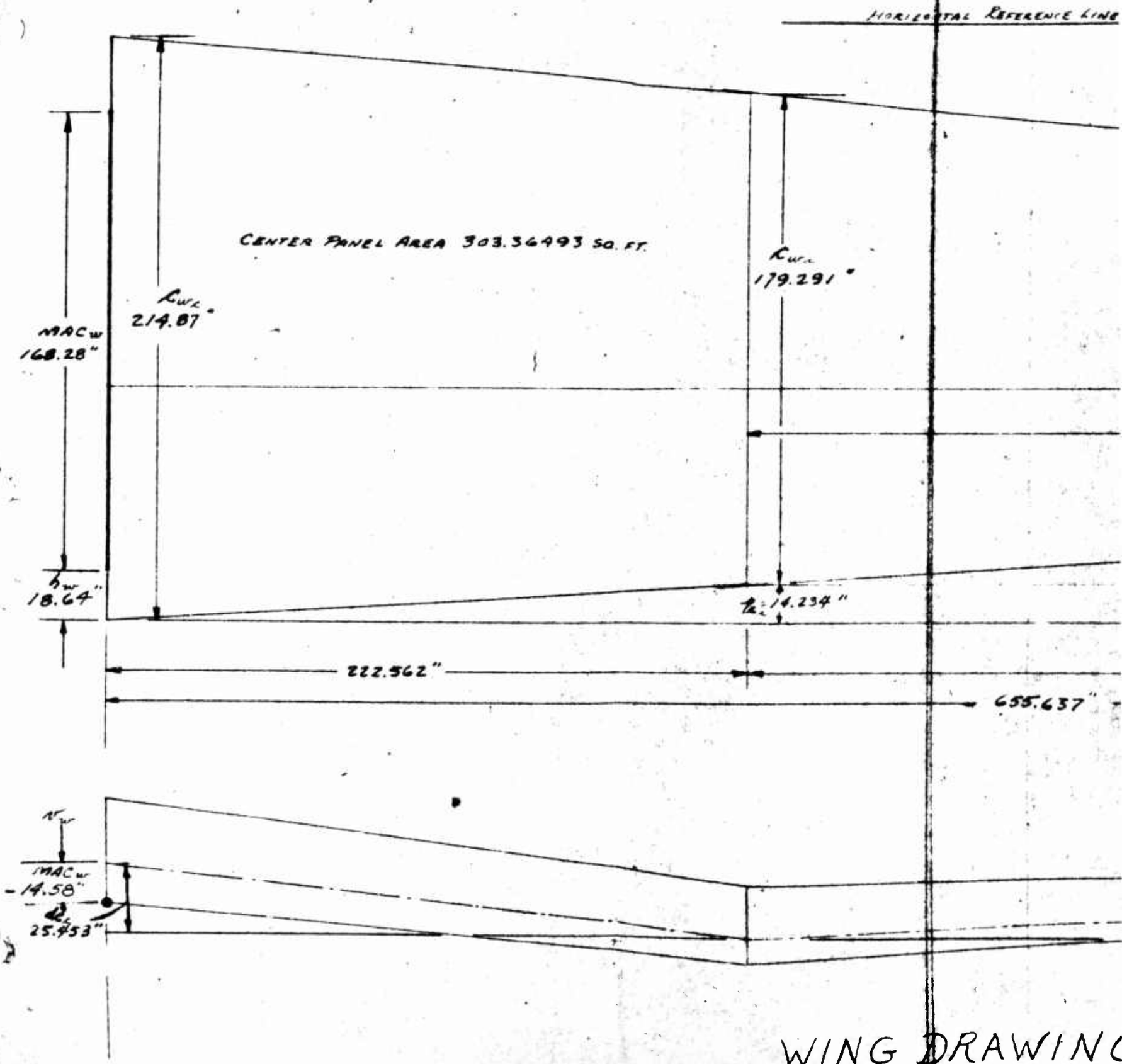

WING DRAWING

RESTRICT

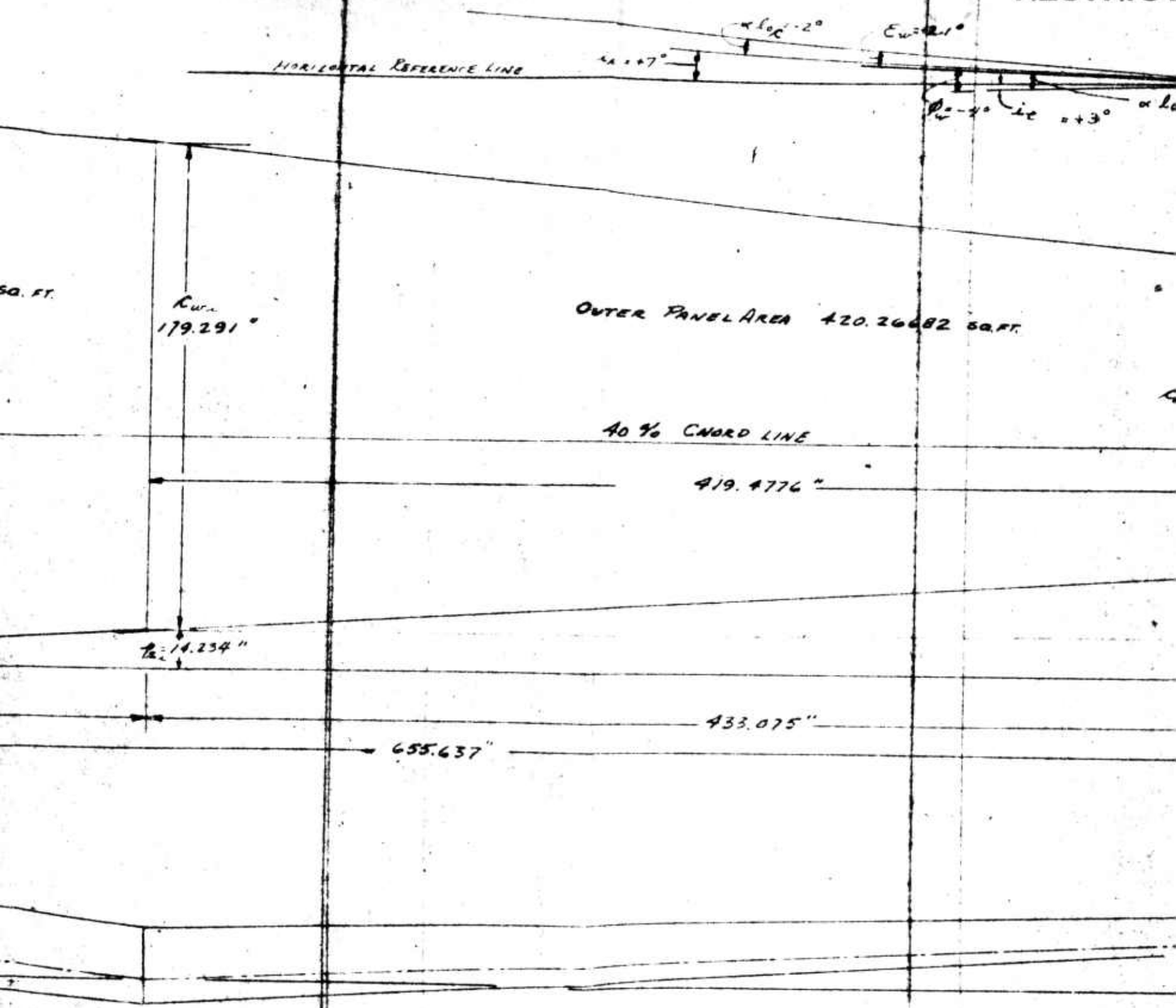

WING DRAWING

FIG 68

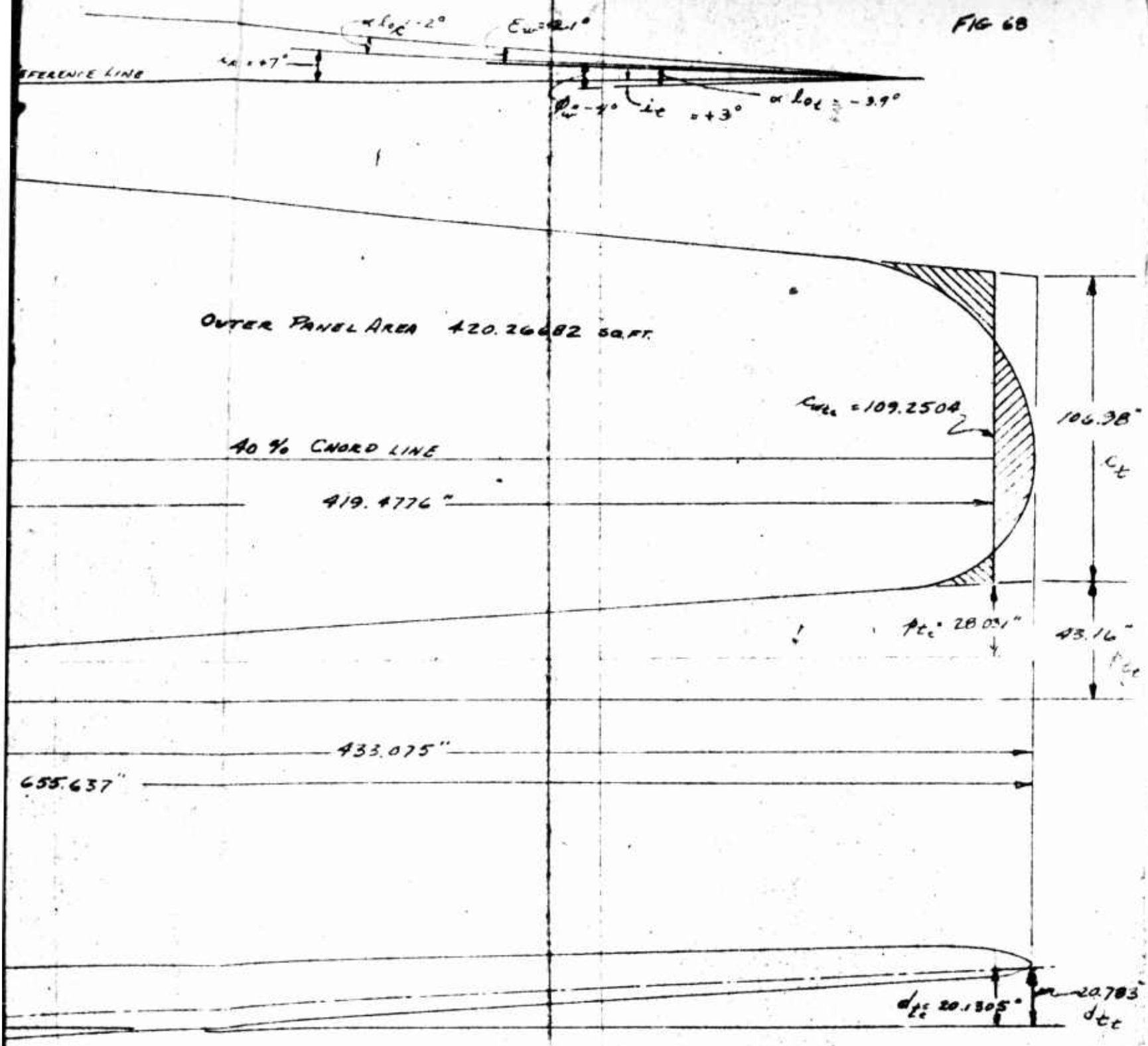
$\alpha_{l_{0_c}} = -2°$
$\epsilon_w = 2.1°$
$\alpha_{l_0} = +7°$
FERENCE LINE
$\phi_w = -4°$
$i_t = +3°$
$\alpha_{l_{0_t}} = -3.9°$
OUTER PANEL AREA 420.26682 SQ.FT.
$c_{t_c} = 109.2504$
106.38"
c_t
40 % CHORD LINE
419.4776"
$t_{t_c} = 28.051"$
43.16"
t_{t_t}
433.075"
655.637"
$d_{t_c} = 20.1305"$
20.783"
d_{t_t}

AWING

PART II-A-1-e

e. AERODYNAMIC TWIST

The aerodynamic twist is defined as the geometric twist angle less the difference between the angles of zero lift of the root chord and tip chord sections.

$$\epsilon_w = \phi_w - \left[(\alpha_{l_{0_c}}) - (\alpha_{l_{0_t}})\right]$$

$$\phi_w = -\left[(i_c) - (i_t)\right]$$

$$\phi_w = -\left[7^\circ - 3^\circ\right] = -4.0^\circ$$

$$\epsilon_w = -4.0^\circ - \left[(-3.9^\circ) - (-2.0)\right]$$

$$\epsilon_w = -2.1^\circ$$

PART II-A-1-o

o. Aerodynamic Force Coefficients

Having determined the C_{L_W} and C_{D_W} for the complete range of flight conditions from maximum positive C_{L_W} to maximum negative C_{L_W}, the coefficients were resolved to obtain a C_{Z_W} and C_{X_W} perpendicular and parallel, respectively, to the airplane thrust line.

Where

$$C_{Z_W} = C_{L_W} \cos \alpha_{TL} + C_{D_W} \sin \alpha_{TL}$$

$$C_{X_W} = C_{D_W} \cos \alpha_{TL} - C_{L_W} \sin \alpha_{TL}$$

$$\alpha_c = \alpha_{TL} + i_c = \alpha_{TL} + 7^\circ$$

$$\alpha_{TL} = \alpha_c - 7^\circ$$

Figure 69 shows C_{X_W}, C_{Z_W}, and $C_{M_{WAC}}$ versus α_{TL}.

MODEL XO-120 PREPARED BY CHECKED BY APPROVED BY

DATE July 9, 1945

REVISED

Subject:— BASIC AERODYNAMIC DATA

PART II-A-1-0

AERODYNAMIC FORCE COEFFICIENTS

WING UNLADEN

1	2	3	4	5	6	7	8	9	10	11	12
α_a Deg.	α_{WL} Deg.	C_{L_W}	C_{D_W}	$C_{m_{WL}}$	$C_{m_{WL}}$	3 x 6	4 x 5	4 x 6	3 x 5	C_{L_W}	C_{D_W}
15	8	1.396	.0990	.1392	.9903	1.346	.0138	.0960	.1895	1.3615	-.0915
11	4	1.021	.0525	.0686	.9976	1.019	.0037	.0524	.0712	1.0227	-.0151
7	0	.6846	.0270	0	1.000	.6850	0	.0270	0	.6850	.0270
3	-4	.3477	.0180	-.0698	.9976	.3470	-.0008	.0119	-.0245	.3462	.0365
-1	-8	.0110	.0070	-.1392	.9903	.0106	-.0010	.0069	-.0015	.0096	.0056
-5	-12	-.3260	.0120	-.2080	.9781	-.3188	-.0025	.0118	-.0079	-.3213	.0087

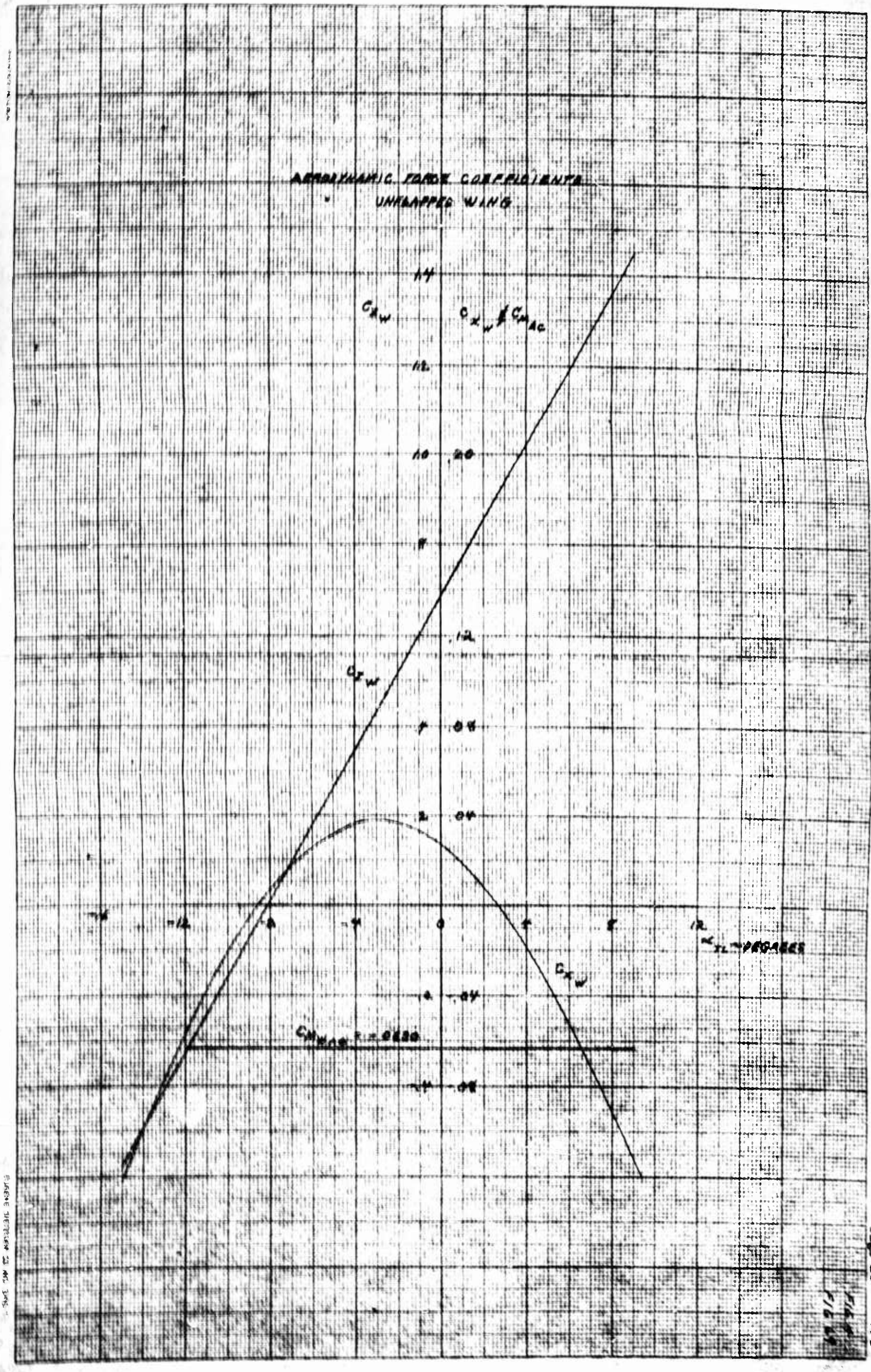
AERODYNAMIC FORCE COEFFICIENTS
UNFLAPPED WING
C_{N_W}
C_{X_W} & $C_{M_{AC}}$
C_{Z_W}
C_{X_W}
$C_{M_{W_{AC}}} = .0230$
α_{IL} - DEGREES

RESTRICTED

PART II-A-1-p

p. WING CHARACTERISTICS IN YAW

The rate of change of wing yawing moment coefficient due to angle of yaw has been determined in Part II-A-1-p reference (1).

$$C_{N_{W_\psi}} / \alpha_{c_0} = .0000075 \text{ per degree}$$

Figure 70 on the following page presents a plot of wing yawing moment coefficient versus angle of yaw for various wing lift coefficients.

PART II-A-2

2. FLAPPED WING

The flapped wing is exactly the same as that of the C-119B airplane except for the change in incidence so that all of the aerodynamic characteristics are the same as those presented in reference (1) except where the change in incidence is a determining factor. Since this change does not affect the following sections, all calculations and figures presented therein in reference (1) apply to the XC-120 airplane.

Part II-A-2-a	Part II-A-2-f
Part II-A-2-b	Part II-A-2-g
Part II-A-2-c	Part II-A-2-h
Part II-A-2-d	Part II-A-2-i
Part II-A-2-e	Part II-A-2-j

The following sections are affected by the change in incidence and the revisions are presented herein.

Part II-A-2-l	Part II-A-2-m

For convenience, all aerodynamic characteristics are presented completely in the summary, whether affected by the change in angle of incidence or not.

FIG 8
R16 70

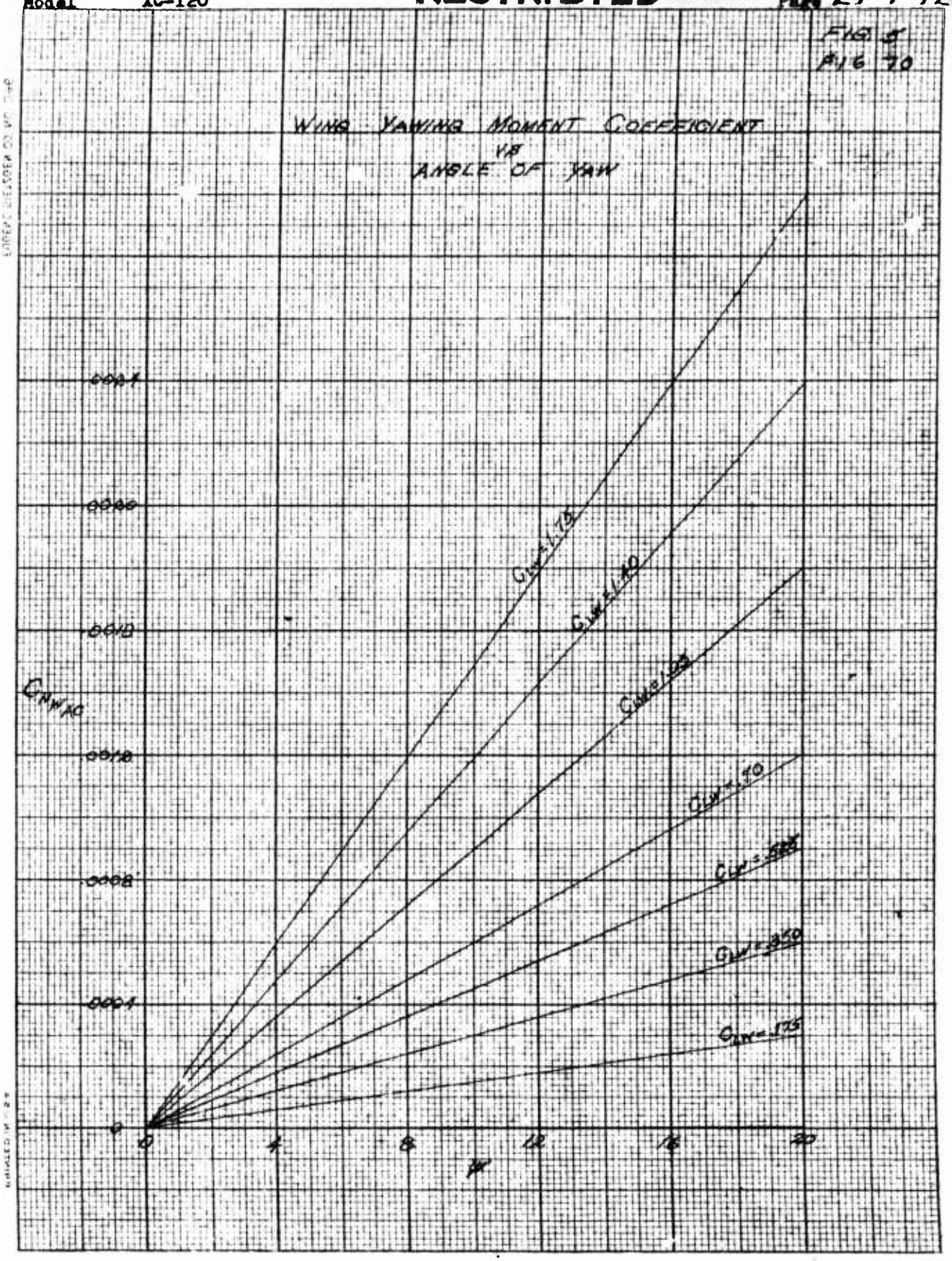
WING YAWING MOMENT COEFFICIENT
VS
ANGLE OF YAW
$C_{N_{W_{AC}}}$
.0004
.0006
.0010
.0008
.0002
0
0
4
8
12
16
20
ψ
$C_{L_W}=1.75$
$C_{L_W}=1.40$
$C_{L_W}=1.05$
$C_{L_W}=.70$
$C_{L_W}=.35$
$C_{L_W}=.175$

PART II-A-2-L

L. AERODYNAMIC FORCE COEFFICIENTS

The aerodynamic force coefficients were determined for the flapped wing in the same manner as for the unflapped wing in Part II-A-1-O. Figure 71 presents a plot of $C_{X_{WF}}$, $C_{Z_{WF}}$, and $C_{M_{WF_{AC}}}$, versus angle of attack of the airplane thrust line.

FA-800-23

AERODYNAMIC FORCE COEFFICIENTS - FLAPPED WING

1	2	3	4	5	6	7	8	9	10	11
α_o	α_{TL}	$C_{L_{WF}}$	$C_{D_{WF}}$	$\sin\alpha_{TL}$	$\cos\alpha_{TL}$	$C_{L_{WF}} \times \cos\alpha_{TL}$	$C_{D_{WF}} \times \sin\alpha_{TL}$	$C_{D_{WF}} \times \cos\alpha_{TL}$	$C_{L_{WF}} \times \sin\alpha_{TL}$	$C_{Z_{WF}}$
15	8	1.6966	.1692	.13917	.99027	1.6801	.0235	.1676	.2361	1.7036
11	4	1.3598	.1150	.06976	.99756	1.3565	.0080	.1147	.0949	1.3645
7	0	1.0230	.0809	0	1.0000	1.0230	0	.0809	0	1.0230
3	-4	.6862	.0560	-.06976	.99756	.6845	-.0039	.0559	-.0479	.6806
0	-7	.4336	.0439	-.12187	.99255	.4304	-.0054	.0436	-.0528	.4250
-1	-8	.3494	.0410	-.13917	.99027	.3460	-.0057	.0406	-.0486	.3403
-5	-12	.0126	.0370	-.20791	.97815	.0123	-.0077	.0362	-.0026	.0046
12										
9 - 10										
$C_{X_{WF}}$										
-.0685										
.0198										
.0809										
.1038										
.0964										
.0892										
.0388										

FIG. 8
FIG. 72

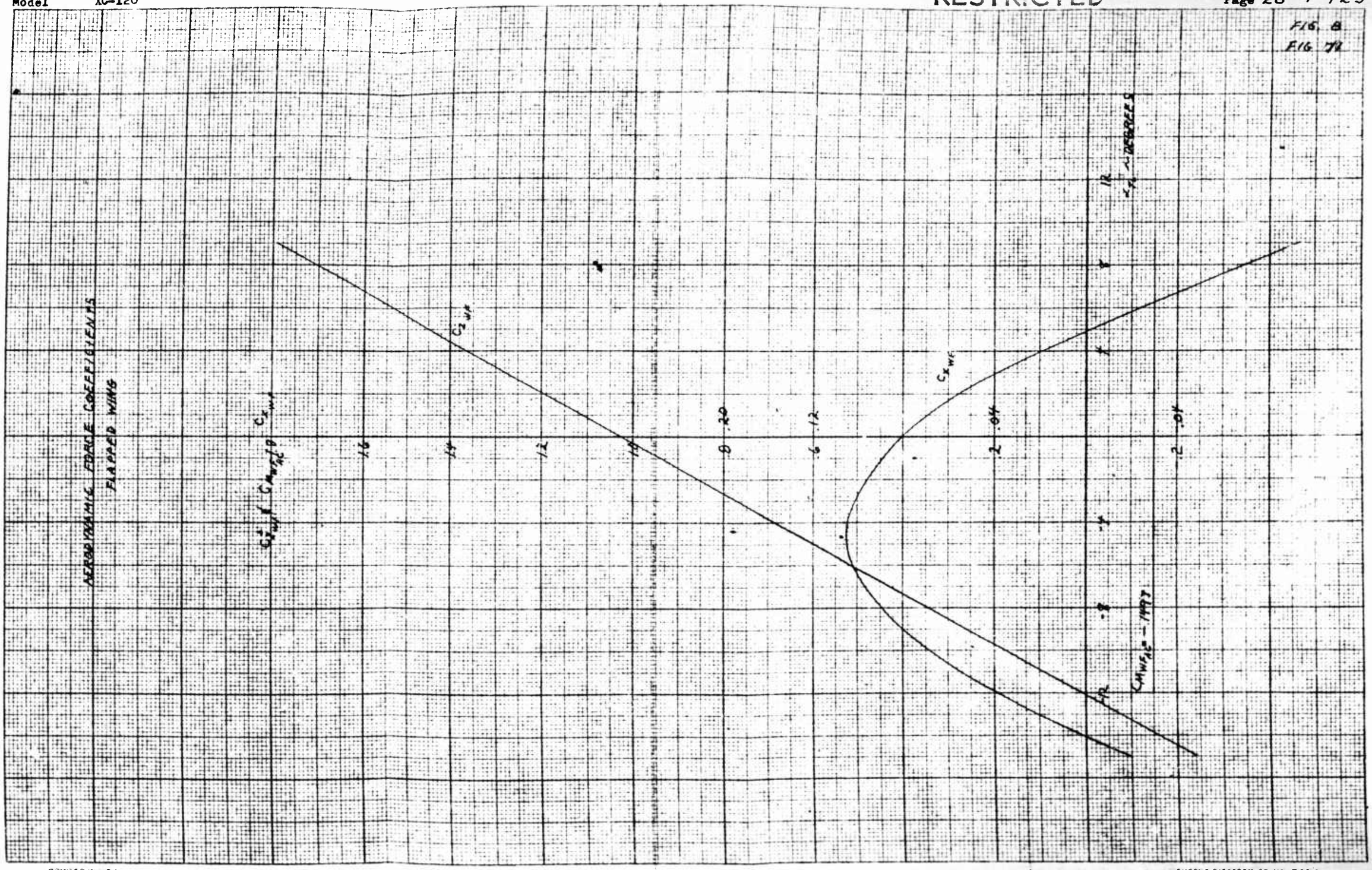
AERODYNAMIC FORCE COEFFICIENTS
FLAPPED WING
$C_{L_{WF}}$
$C_{X_{WF}}$
$C_{M_{WF_{AC}}}$
$C_{L_{WF}} \& C_{M_{WF_{AC}}}$
$C_{X_{WF}}$
i_R
α_R ~ DEGREES
$C_{M_{WF_{AC}}} - 1997$
1.6
1.4
1.2
1.0
.8
.6
.4
.2
0
.20
.12
.04
.04
.12
-4
-8
i_R

PART II-A-2-m

m. Characteristics in Yaw

The yawing moment of the flapped wing about the aerodynamic center was assumed to be the same as for the unflapped wing, as presented in figure 70 of Part II-A-1-p, taking into account the fact that the lift coefficient will be different for the same angle of attack.

PART II-A-3

3. AILERONS

Since the ailerons are identical to those on the C-119B airplane, all aerodynamic characteristics are the same as those presented in Part II-A-3 reference (1).

All aerodynamic coefficients are based on aileron area or wing area depending upon the item affected.

For convenience the important aileron characteristics are tabulated below as well as being shown graphically in the summary section.

AILERON AERODYNAMIC CHARACTERISTICS

SYMBOL	ITEM	DOWN AILERON	UP AILERON
$C_{L_W \delta_a}$	$d\,C_{L_W}/d\delta_a$	.00572	.00607
$c_{m \delta_a}$	$d\,c_m/d\delta_a$	-.0069	-.0073
$C_{H_a \delta_a}$	$d\,C_{H_a}/d\delta_a$	-.0054	-.0016
$c_{l \delta_a}$	$d\,c_l/d\delta_a$	.0316	.0336
$\alpha_{o\,\delta_a}$	$d\,\alpha_o/d\,\delta_a$	-.0680	-.0722
$C_{H_a \alpha_{s_{ave.}}}$	$d\,C_{H_a}/d\,\alpha_{s_{ave.}}$	-.0012	-.0012

PART II-A-4

4. AILERON TABS

Since the aileron tabs are exactly the same as those on the C-119B airplane, all aerodynamic characteristics are identical to those shown in Part II-A-4 reference (1).

All aerodynamic characteristics are based on tab area or aileron area depending upon the item affected by the tab.

For convenience, all aileron tab characteristics are tabulated below, as well as being shown graphically in the summary.

AILERON TAB AERODYNAMIC CHARACTERISTICS

SYMBOL	ITEM	TRIM TAB	BALANCE TAB
$c_{l_{\delta_{a\,tab}}}$	$d c_l / d\delta_{a\,tab}$	.01248	.01144
$C_{H_{a_{\delta_{a\,tab}}}}$	$d C_{H_a} / d\delta_{a\,tab}$	-.0009	-.0021
$C_{H_{a\,tab_{\delta_{a\,tab}}}}$	$d C_{H_{a\,tab}} / d\delta_{a\,tab}$	-.0022	-.0017
$\alpha_{c_{\delta_{a\,tab}}}$	$d \alpha_c / d\delta_{a\,tab}$	-.0045	
$\left(\frac{p B_w}{2 V}\right)_{\delta_{a\,tab}}$	$d \left(\frac{p B_w}{2V}\right) \Big/ d\delta_{a_{tab}}$		.0000935

PART II-A-5

5. FUSELAGE

This section presents the calculation made for determining the aerodynamic characteristics of the fuselage.

Throughout this section all coefficients used and calculated are based on an area of the fuselage itself (either planform, frontal or side area as necessary) and no attempt has been made in this section to convert the coefficients. All coefficients are referred to the angle of attack of the fuselage reference line which is exactly parallel to the airplane thrust line. Therefore, all data is plotted versus $\alpha_{T.L.}$

Coefficients are based on various fuselage areas as follows: -

Coefficient	Definition
C_{L_F}	$L_F/q\ P_f$
C_{D_F}	$D_F/q\ F_f$
$C_{M_{F.25L_f}}$	$M_{F.25L_f}/qP_f\ L_f$
C_{X_F}	$X_F/q\ F_f$
C_{Z_F}	$Z_F/q\ P_f$
$C_{N_{F.25L_f}}$	$N_{F.25L_f}/q\ S_f\ L_f$
C_{C_F}	$C_F/q\ S_f$

Total fuselage C_{L_F}, C_{D_F}, and $C_{M_{F.25\ L_f}}$ versus α T.L. are presented in figures 73, 74, and 77 respectively. Figure 76 presents a plot of C_{X_F} and C_{Z_F} versus α T.L. For characteristics in yaw, see explanation of Part II-A-5-g.

PART II-A-5-a

a. FUSELAGE DRAWING

Figure 72 presents a drawing of the fuselage which is the combination of the crew nacelle and the pack. Pertinent dimensions and areas used in this analysis are shown.

Subject:— BASIC AERODYNAMIC DATA

FIG. 72

AREAS

S_f = SIDE AREA = 801.0 □'

P_f PLANFORM AREA = 579.0 □'

F_f = FRONTAL AREA = 175.3 □'

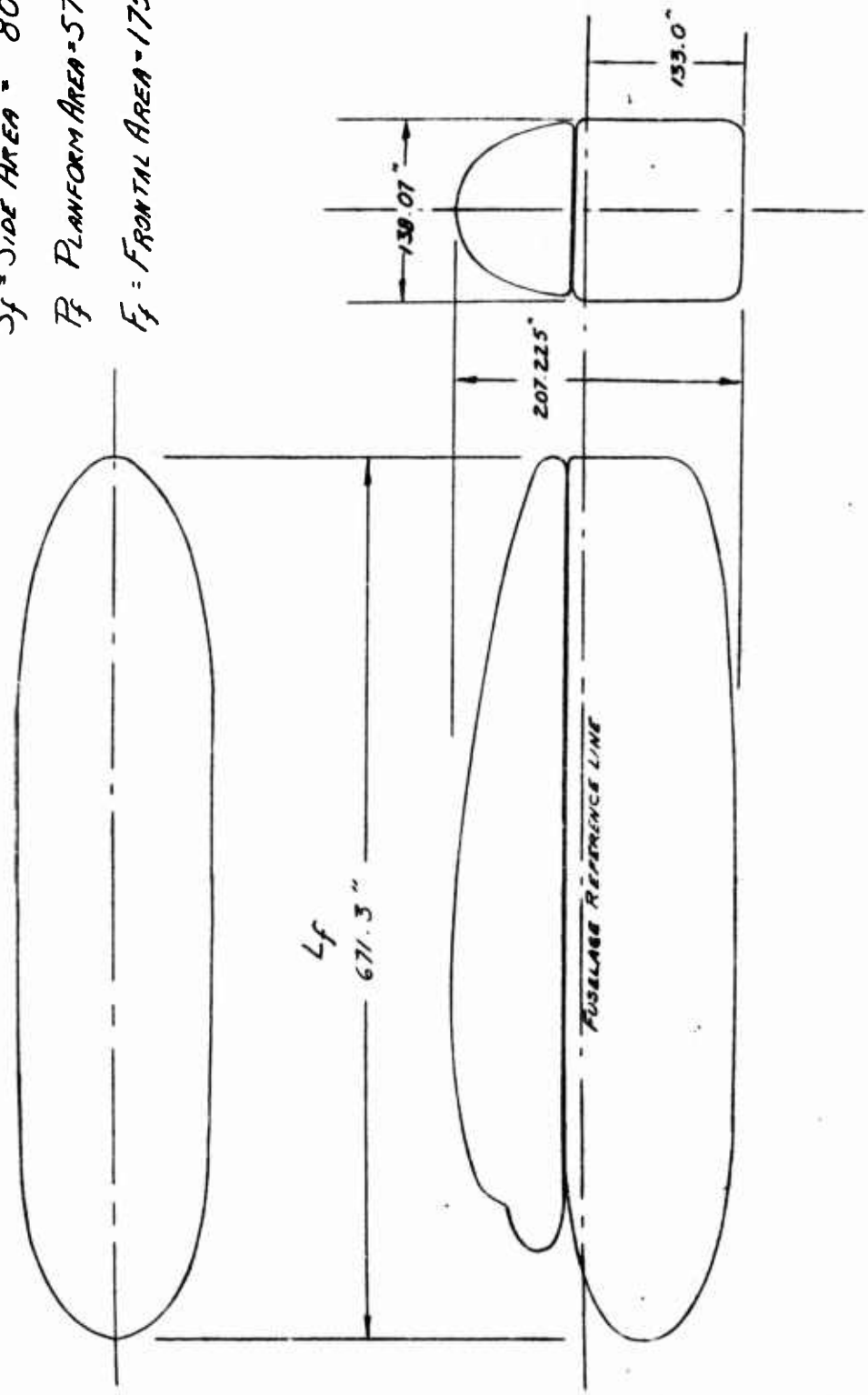

FUSELAGE

PART II-A-5-b

b. LIFT ANALYSIS

The lift coefficient of combination of crew nacelle and pack is taken to be the same as that of the fuselage of the C-119B as reported in reference (1). This is felt to be justified since the shape and proportions of the combination are generally similar to those of the fuselage of the C-119B.

Figure 73 presents a plot of fuselage lift coefficient C_{L_F} versus α_f which is equal to $\alpha_{T.L.}$. This figure is identical with figure 116 of reference (1).

FIG 16
FIG 73

VARIATION OF FUSELAGE LIFT COEFFICIENT
WITH
FUSELAGE ANGLE OF ATTACK

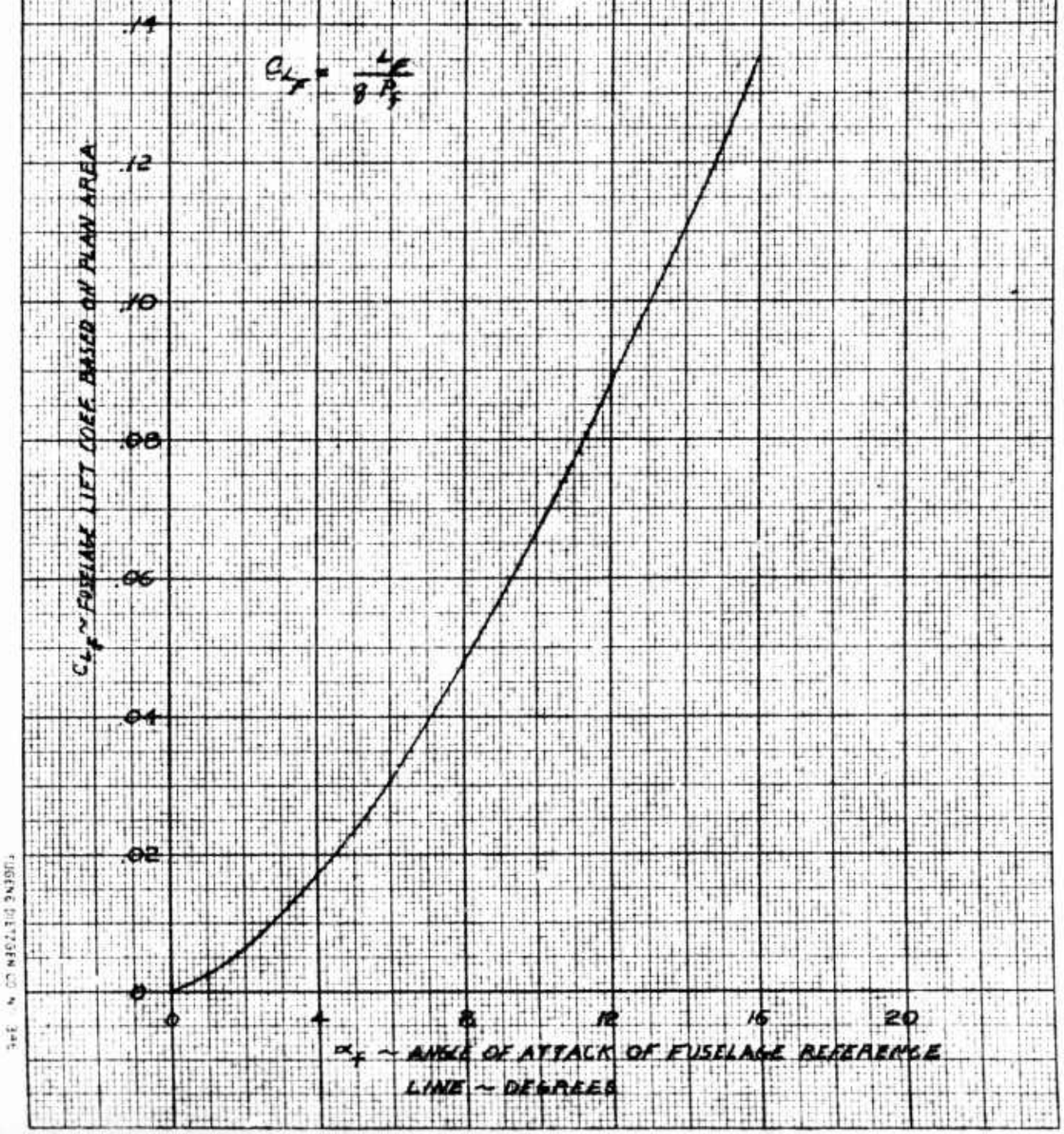

PART II-A-5-c

c. DRAG ANALYSIS

The method of computing drag is the same as that presented in reference (1). All of the basic fuselage general drag curves are the same as those of reference (1).

For the purposes of this report the fuselage is defined as crew nacelle plus pack.

PART II-A-5-c

FUSELAGE DRAG ANALYSIS

ITEM		GENERAL	K_{X_F}	C_{D_F}
Smooth Drag				
Cross-sectional area,	sq. ft.	175.3		
Type of cross section		Irregular rectangular (rounded corners)		
Length (L_f),	ft.	56		
Fineness Ratio = $\frac{.886\ L_f}{F_f}$		3.75		
Speed/altitude of analysis,	mph/ft.	280/8000		
Reynolds Number = $9354(V_{mph})(L_f)\ \frac{\nu}{\nu_0}$		9.15×10^7		
Smooth C_{D_F} figure 117 of reference (1)				.038
Increase of 10% due to rectangular shape				.0038
TOTAL SMOOTH C_{D_F}				.0418
Using figure 118 of reference (1) construct a curve of smooth C_{D_F} versus α_f of fuselage reference line				
Roughness, Leakage & Miscellaneous				
Equipment Allowance for roughness due to rivet heads, dimples, inspection doors, drains and plugs, doors, windows, break due to windshield, door hinges, lap joints, break line of crew nacelle and pack, etc.				
Percent of smooth drag		70		
ΔC_{D_F}				.0292
Allowance for leakage				
Percent of smooth drag		30		
ΔC_{D_F}				.01254
Allowance for interference of wing-fuselage intersection				
Percent of smooth drag		5		
ΔC_{D_F}				.00209

PART II-A-5-c

FUSELAGE DRAG ANALYSIS (Cont.)

ITEM	GENERAL	K_{X_F}	C_{D_F}
Drag of miscellaneous equipment			
Astradome		.0019	.00425
Drift sight		.00032	.000714
Heater exhaust outlets		.00034	.000758
Pitot tubes		.00010	.000223
Relief tube venturi		.00032	.000714
Radio compass antennae		.00168	.003745
Radio altimeter antennae		on boom	
Marker beacon antennae		flush	
IFF antennae		on boom	
Blind landing antennae		.00072	.001603
Liason antennae		.00025	.000558
Beacon transmitter		.00040	.000892
TOTAL ΔC_{D_F} - ROUGHNESS, LEAKAGE, MISCELLANEOUS EQUIPMENT			.05734
This ΔC_{D_F} is added directly to figure as a constant increment at all angles of attack.			
TOTAL C_{D_F} AT ZERO ANGLE OF ATTACK			.09914

NOTE: C_{D_F} above is based on maximum cross sectional area of the fuselage.

$$C_{D_F} = \frac{D_F}{q \; F_f}$$

PART II-A-5-c

C_{D_F} versus α_f

α_f deg.	$C_{D_F} = x / C_{D_F}\alpha = 0$	C_{D_F} - smooth	C_{D_F} - (roughness, leakage, equipment)
0	1.000	.0418	.09914
2	1.044	.04364	.10098
4	1.110	.04640	.10374
6	1.212	.05066	.10800
8	1.393	.05823	.11557
10	1.644	.06872	.12606
12	1.985	.08297	.14031
14	2.458	.10274	.16008
16	3.075	.12854	.18588

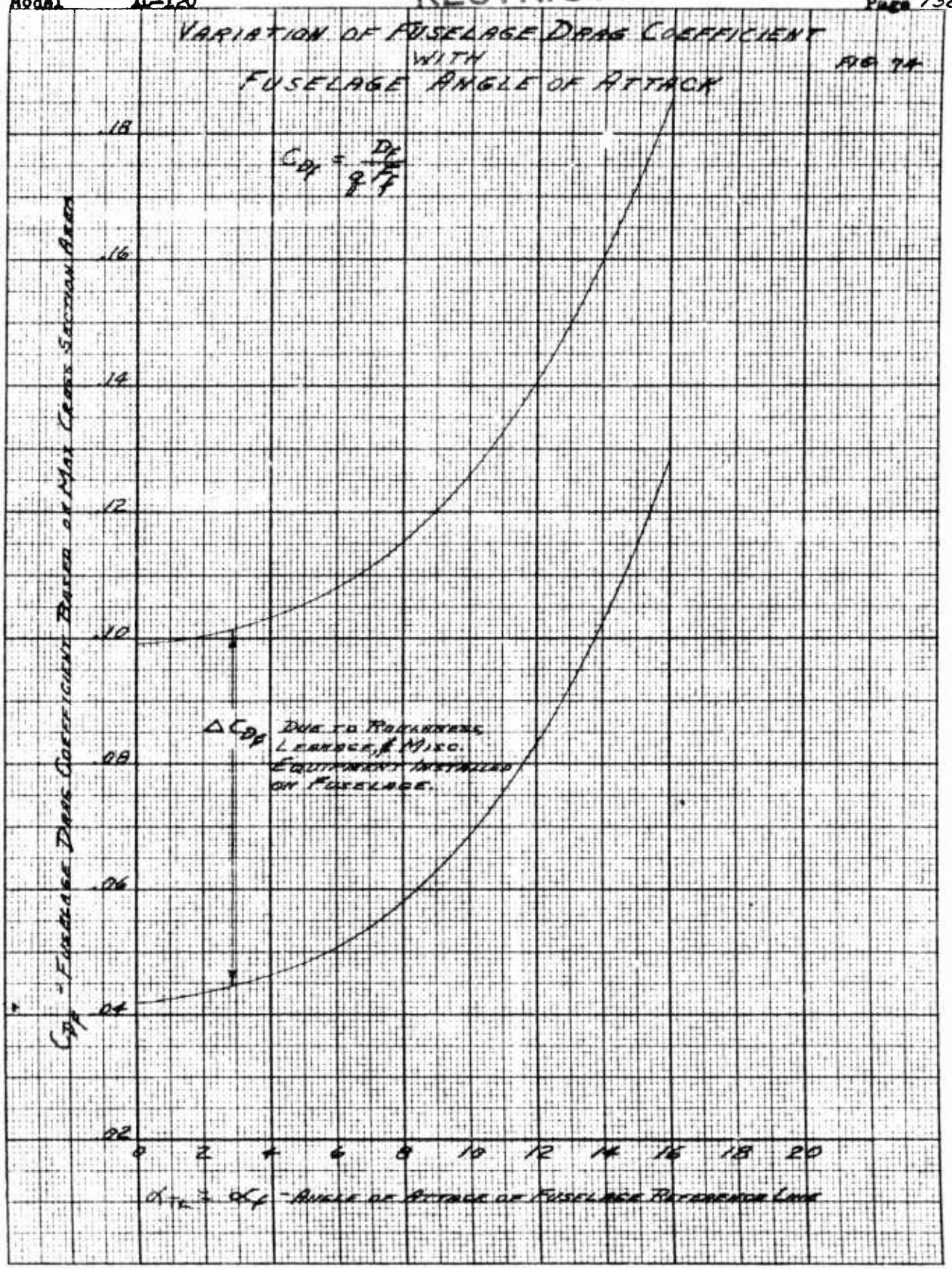
VARIATION OF FUSELAGE DRAG COEFFICIENT
WITH
FUSELAGE ANGLE OF ATTACK
FIG 74
$C_{D_f} = \frac{D_f}{q_f F_f}$
C_{D_f} - FUSELAGE DRAG COEFFICIENT BASED ON MAX CROSS SECTION AREA
.18
.16
.14
.12
.10
.08
.06
.04
.02
ΔC_{D_f} DUE TO MOTOR NACELLE, LANDING GEAR, & MISC. EQUIPMENT INSTALLED ON FUSELAGE.
0
2
4
6
8
10
12
14
16
18
20
$\alpha_{TR} = \alpha_f$ - ANGLE OF ATTACK OF FUSELAGE REFERENCE LINE

PART II-A-5-d

FUSELAGE POLAR DIAGRAM

α_f	C_{D_F} Fig. 74	C_{L_F} Fig. 73
0	.09914	0
2	.10098	.0062
4	.10374	.0167
6	.10800	.0306
8	.11557	.0475
10	.12606	.0668
12	.14031	.0882
14	.16008	.1110
16	.18588	.1354

FIG 12
FIG 75

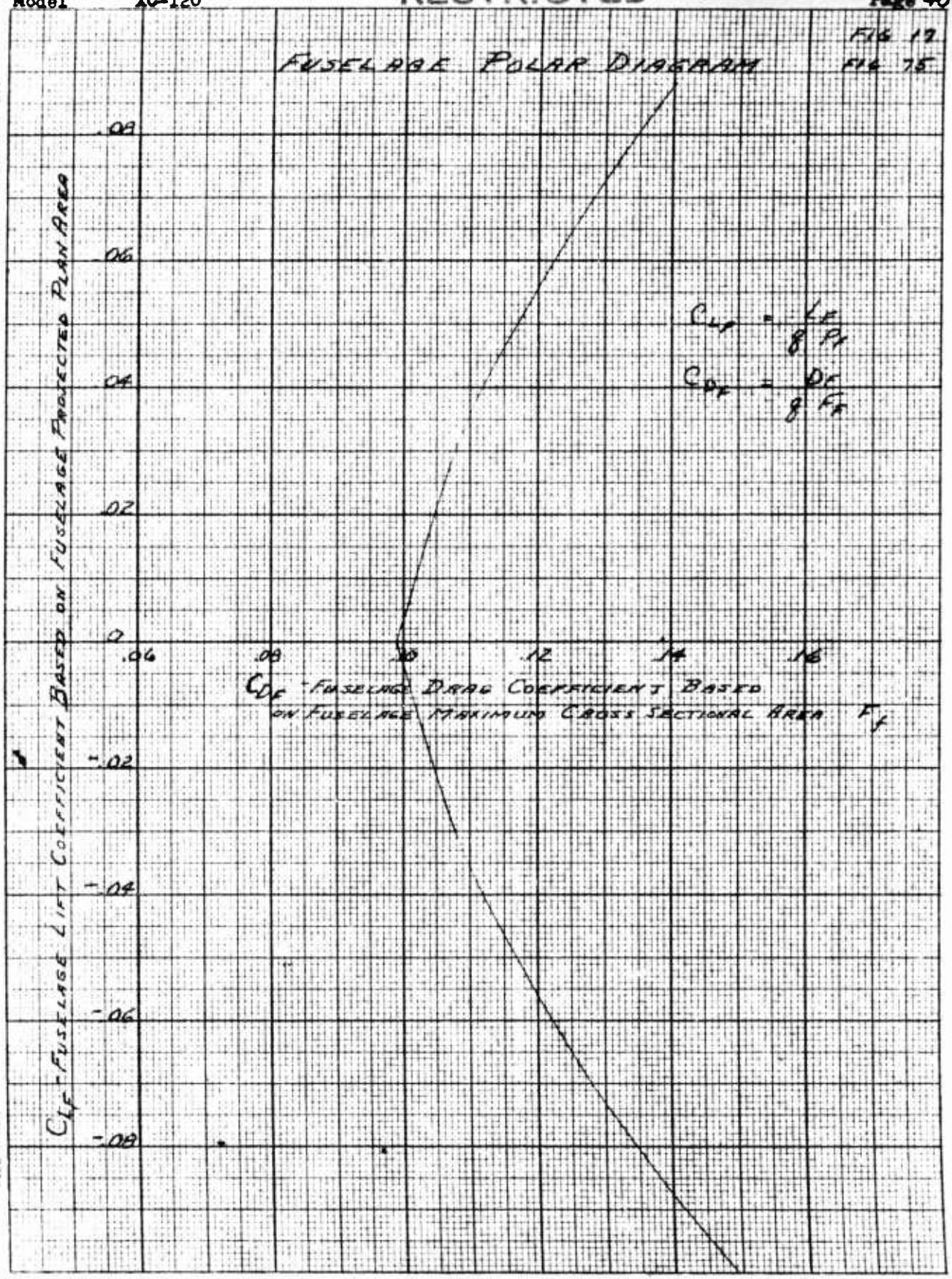
FUSELAGE POLAR DIAGRAM
$C_{L_F} = \frac{L_F}{q F_F}$
$C_{D_F} = \frac{D_F}{q F_F}$
.08
.06
.04
.02
0
-.02
-.04
-.06
-.08
.06
.08
.10
.12
.14
.16
C_{L_F} - FUSELAGE LIFT COEFFICIENT BASED ON FUSELAGE PROJECTED PLAN AREA
C_{D_F} - FUSELAGE DRAG COEFFICIENT BASED ON FUSELAGE MAXIMUM CROSS SECTIONAL AREA F_F

PART II-A-5-e

e. AERODYNAMIC FORCE COEFFICIENTS

Having previously determined the lift and drag characteristics of the fuselage, it is desired to resolve the forces into components parallel and perpendicular to the airplane thrust line. To do this several relations must be determined as below:

$C_{D_F} = \frac{D_f}{q\,F_f}$ F_f = fuselage frontal area in sq. ft. = 175.3

$C_{L_F} = \frac{L_f}{q\,P_f}$ P_f = fuselage plan area in sq. ft. = 579.0

$C_{X_F} = \frac{X_F}{q\,F_f}$ S_f = fuselage side area in sq. ft. = 801.0

$C_{Z_F} = \frac{Z_F}{q\,P_f}$ D_F, L_F, X_F, Z_F, = forces

(fuselage center line) $= \alpha_f$ (fuselage reference line) $= \alpha_{T.L.}$

$$Z_F = L_F \cos\alpha_{T.L.} + D_F \sin\alpha_{T.L.}$$

$$X_F = D_F \cos\alpha_{T.L.} - L_F \sin\alpha_{T.L.}$$

dividing through to coefficient form

$$C_{Z_F} = \frac{L_F}{q\,P_f}\cos\alpha_{T.L.} + \frac{D_F}{q\,P_f}\sin\alpha_{T.L.}$$

$$= C_{L_F}\cos\alpha_{T.L.} + C_{D_F}\frac{F_f}{P_f}\sin\alpha_{T.L.}$$

$$C_{X_F} = \frac{D_F}{q\,F_f}\cos\alpha_{T.L.} - \frac{L_F}{q\,F_f}\sin\alpha_{T.L.}$$

$$= C_{D_F}\cos\alpha_{T.L.} - C_{L_F}\frac{P_f}{F_f}\sin\alpha_{T.L.}$$

The following page presents the calculations necessary to determine C_{X_F} and C_{Z_F}

A plot of C_{Z_F} and C_{X_F} versus $\alpha_{T.L.}$ is presented in figure 76 .

PART II-A-5-e

DETERMINATION OF C_{Z_F} AND C_{X_F} FOR FUSELAGE

$F_f / P_f = .3028$ $P_f / F_f = 3.3029$

①	②	③	④	⑤	⑥	⑦	⑧	⑨	⑩	⑪
α T.L.	Sin α T.L.	Cos α T.L.	C_{D_F}	C_{L_F}					C_{X_F}	C_{Z_F}
					③ x ⑤	② x ④ x .3028	③ x ④	② x ⑤ x 3.3029	⑧ - ⑨	⑥ + ⑦
-12	-.2079	.9782	.1403	-.0882	-.0863	-.0088	.1372	.0606	.0766	-.0951
- 8	-.1392	.9903	.1156	-.0475	-.0470	-.0049	.1145	.0218	.0927	-.0519
- 4	-.0698	.9976	.1037	-.0167	-.0167	-.0022	.1035	.0039	.0996	-.0189
0	0	1.0000	.0991	0	0	0	.0991	0	.0991	0
4	.0698	.9976	.1037	.0167	.0167	.0022	.1035	.0039	.0996	.0189
8	.1392	.9903	.1156	.0475	.0470	.0049	.1145	.0218	.0927	.0519
12	.2079	.9782	.1403	.0882	.0863	.0088	.1372	.0606	.0766	.0951

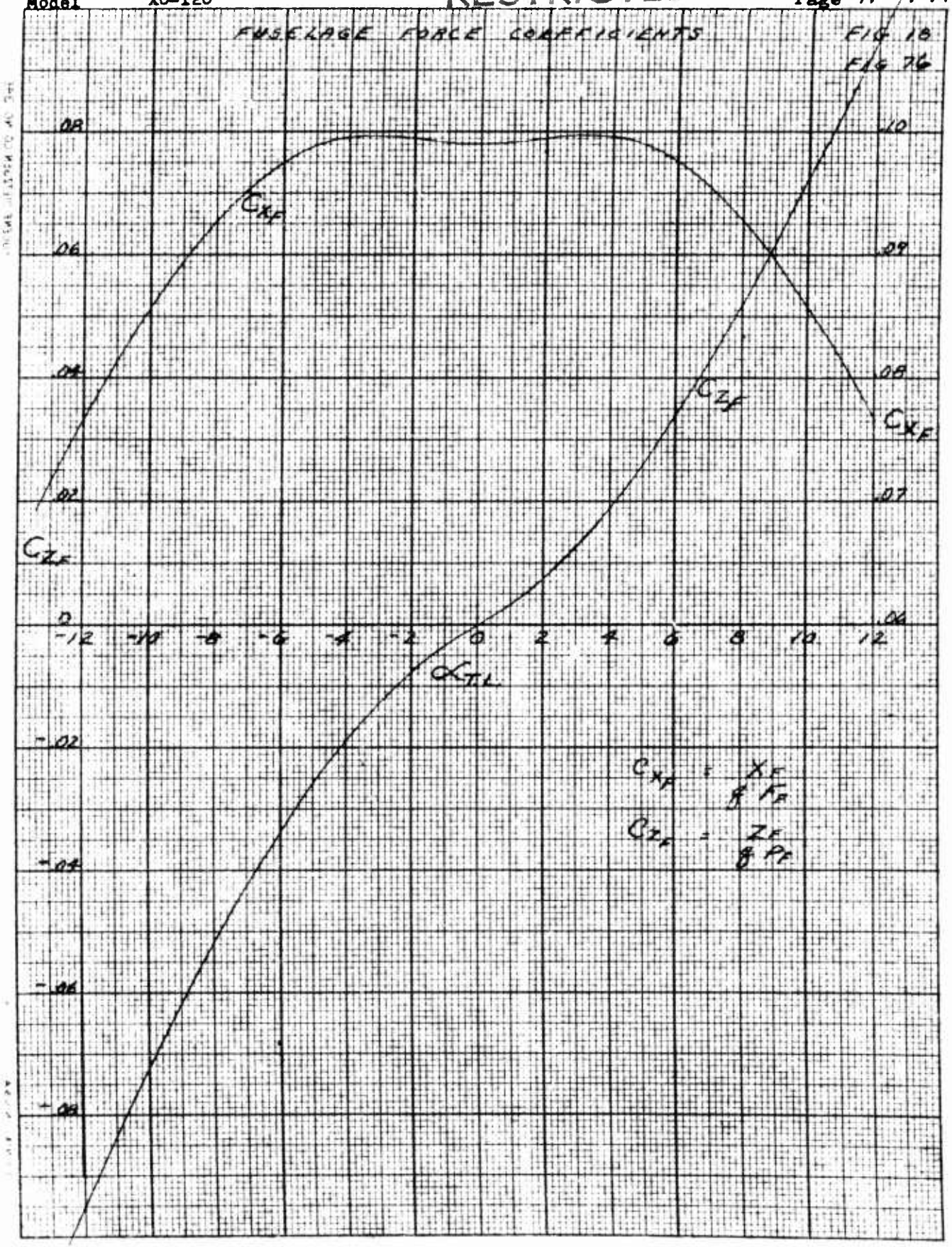
FUSELAGE FORCE COEFFICIENTS
FIG 18
FIG 76
C_{X_F}
C_{Z_F}
α_{TL}
$C_{X_F} = \frac{X_F}{q\,F_F}$
$C_{Z_F} = \frac{Z_F}{q\,F_F}$
.08
.06
.04
.02
0
-.02
-.04
-.06
-.08
.10
.09
.08
.07
.06
-12
-10
-8
-6
-4
-2
0
2
4
6
8
10
12

PART II-A-5-f

f. PITCHING MOMENT ANALYSIS

The pitching moment coefficients for the fuselage (crew nacelle + pack) is based on the data of figure 123 reference (1).

Figure 77 presents a plot of fuselage pitching moment coefficient about the fuselage quarter chord point versus angle of attack of the fuselage reference line which is equal to $\alpha_{T.L.}$.

FIG. 19

FUSELAGE PITCHING MOMENT COEFFICIENT FIG 77
ABOUT THE QUARTER LENGTH POINT

$$C_{M_{F.25\,l_f}} = \frac{M_F}{q\,P_f\,l_f}$$

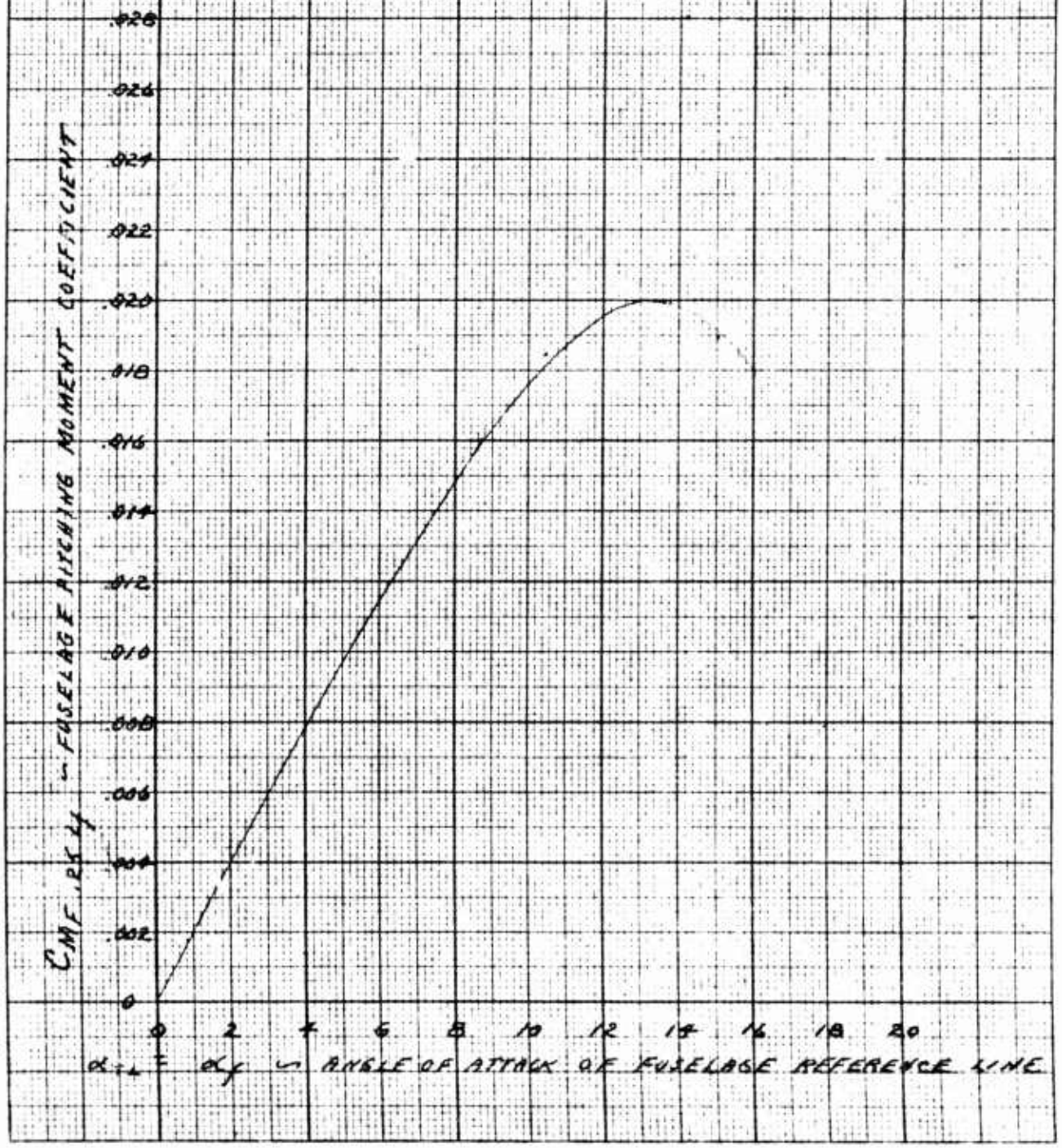

PART II-A-5-g

g. YAWING MOMENT ANALYSIS

The $C_{N_{F.25L_f}}$ fuselage versus ψ is considered to be the same as the $C_{M_{F.25L_f}}$ versus α T.L. except that they are based on difference areas.

$$C_{N_{F.25L_f}} = \frac{N_F}{q\ S_f\ L_f} \quad \text{and} \quad C_{M_{F.25L_f}} = \frac{M_F}{q\ P_f\ L_f}$$

The C_{C_F} fuselage versus ψ is also considered to be the same as the C_{L_F} fuselage versus $\alpha_{T.L.}$ each based on its respective area.

$$C_{C_F} = \frac{C_F}{q\ S_f} \quad \text{and} \quad C_{L_F} = \frac{L_F}{q\ P_f}$$

In other words the lift and pitching moment coefficient curves of figures 73 and 77 are used directly for yaw forces except that the coefficients as picked from the curves are considered to be based on different areas.

It is assumed that the drag coefficients of the fuselage at small angeles of yaw are the same as those at small angles of attack so that for $\psi = \alpha_{T.L.}$ (small angles) C_{D_F} in yaw = C_{D_F} in pitch.

PART II-A-5A

5A. CREW NACELLE

This section presents the calculations made for determining the aerodynamic characteristics of the crew nacelle.

Throughout this section all coefficients used and calculated are based on an area of the crew nacelle itself (either planform, frontal, or side area as necessary) and no attempt has been made in this section to convert the coefficients to wing area. All coefficients are referred to the angle of attack of the crew nacelle reference line which is exactly parallel to the airplane thrust line. Therefore, all data is plotted versus $\alpha_{T.L.}$

Coefficients are based on various crew nacelle areas as follows:

Coefficient	Definition
C_{L_N}	$L_N / q\ F_n$
C_{D_N}	$D_N / q\ F_n$
$C_{M_{N.25\ L_n}}$	$M_{N.25\ L_n} / q\ F_n\ L_n$
C_{X_N}	$X_N / q\ F_n$
C_{Z_n}	$Z_N / q\ F_n$
$C_{N_{N.25\ L_n}}$	$N_{N.25\ L_n} / q\ S_n\ L_n$
C_{C_N}	$C_N / q\ S_n$

Total crew nacelle C_{L_N}, C_{D_N}, and $C_{M_{N.25\ L_n}}$ versus $\alpha_{T.L.}$ are presented in figures 78, 80, and 83 respectively. Figure 82 presents plots of C_{X_N} and C_{Z_N} versus $\alpha_{T.L.}$.

For characteristics in yaw see explanation of part II-A-5A-g.

PART II-A-5A-a

a. CREW NACELLE DRAWING

Figure 78 presents a three-view drawing of the crew nacelle alone. Pertinent dimensions and areas used in this analysis are shown.

Subject:- BASIC AERODYNAMIC DATA

FIG 78

AREAS

S_n = SIDE AREA = 271.0 □'

P_n = PLANFORM AREA = 450.0 □'

F_n = FRONTAL AREA = 58.8 □'

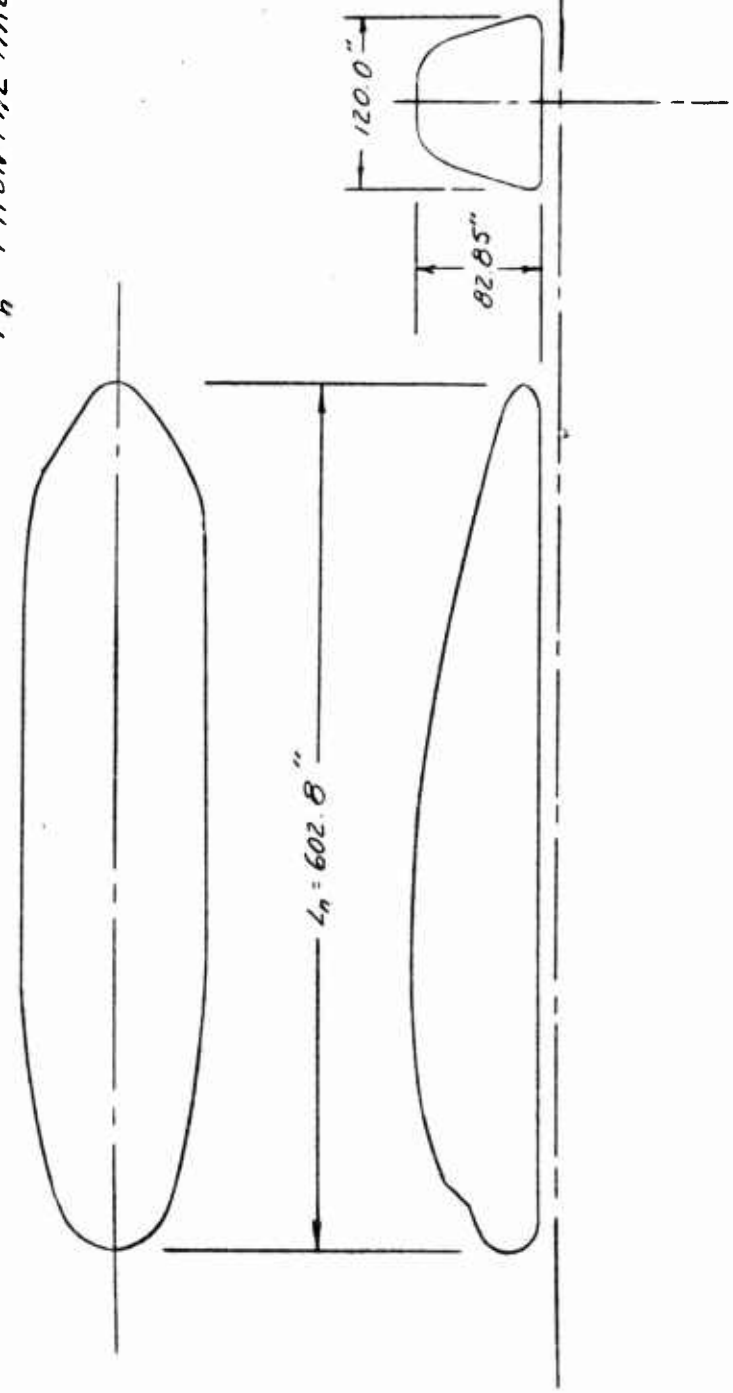

CREW NACELLE

PART II-A-5-A

b. Lift Analysis

The lift coefficient of the crew nacelle alone was determined from wind tunnel data of reference (2) where $C_{L_N} = C_{L_{\text{crew nacelle on}}} - C_{L_{\text{crew nacelle off}}}$

Values thus obtained were converted to crew nacelle planform area and included any interference effects. Figure 79 presents a plot of C_{L_N} versus α_N.

FIG 20
FIG 79

VARIATION OF CREW NACELLE LIFT COEFFICIENT WITH ANGLE OF ATTACK OF CREW NACELLE

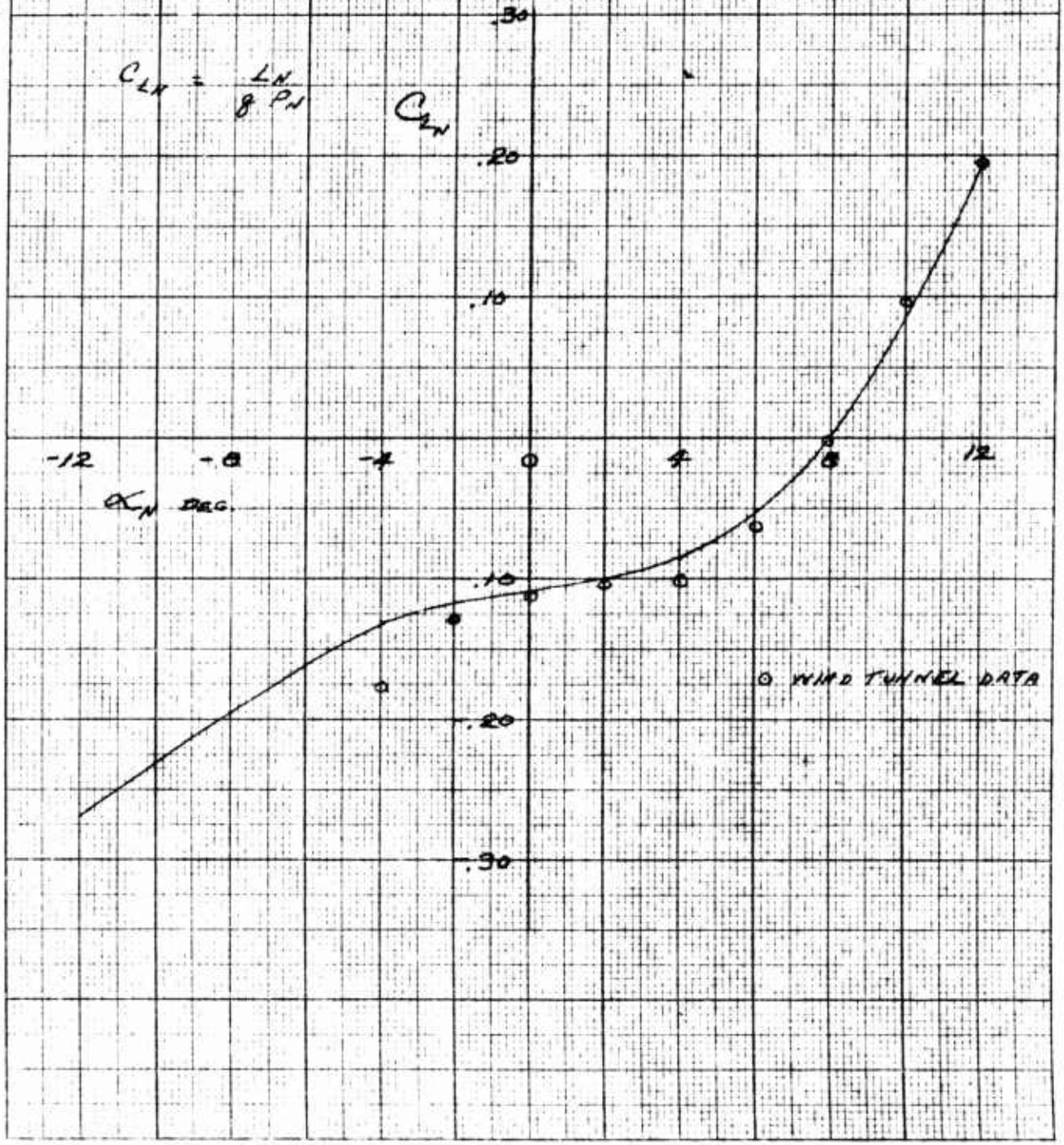

PART II-A-5A-c

c. DRAG ANALYSIS

The method of computing the drag of the crew nacelle is the same as that of reference (1) using the general drag curves for rectangular bodies.

Crew nacelle is defined as fuselage less pack

PART II-A-5A-c

CREW NACELLE DRAG ANALYSIS

ITEM	GENERAL	K_{X_N}	C_{D_N}
Smooth Drag			
Cross-sectional area, sq. ft.	58.8		
Type of cross section	Flat bottom round top		
Length (L_n) ft.	50.2		
Fineness ratio = $\frac{.886\ L_n}{\sqrt{F_n}}$	5.8		
Speed/altitude of analysis, mph/ft.	280/15000		
Reynolds Number = 9354 (Vmph) (L_n) $\frac{\nu}{\nu_o}$	8.2×10^7		
Smooth C_{D_N} figure 117 reference (1)			.0508
Increase of 10% due to body shape			.00508
TOTAL SMOOTH C_{D_N}			.05588
Using figure 118 of reference (1) construct a curve of smooth C_{D_N} versus α_n of crew nacelle reference line (parallel to thrust line)			
Roughness, Leakage, and Miscellaneous Equipment			
Allowance for roughness due to rivet heads, dimples, inspection doors, drains and plugs, doors, windows, break due to windshield, hinges, lap joints, etc.			
Percent of smooth drag	30		
ΔC_{D_N}			.01676
Allowance for leakage			
Percent of smooth drag	15		
ΔC_{D_N}			.00838
Allowance for interference of wing - fuselage intersection			
Percent of smooth drag	5		
ΔC_{D_N}			.00279

PART II-A-5A-c

CREW NACELLE DRAG ANALYSIS (Cont.)

ITEM	GENERAL	K_{X_N}	C_{D_N}
Drag of Miscellaneous Equipment			
Astradome		.0019	.01264
drift sight		.00032	.00213
heater exhaust outlets		.00034	.00226
pitot tubes		.00010	.00067
relief tube venturi		.00016	.00106
radio compass antenna		.00168	.01118
radio altimeter antenna		on boom	
marker beacon antenna		flush	
IFF antenna		on boom	
blind landing antenna		.00072	.00479
liaison antenna		.00025	.00166
beacon transmitter		.00040	.00266
TOTAL ΔC_{D_N} - ROUGHNESS, LEAKAGE, MISCELLANEOUS EQUIPMENT This ΔC_{D_N} is added directly to figure 79 as a constant increment at all angles of attack			.06698
TOTAL C_{D_N} AT ZERO ANGLE OF ATTACK			.12286

Note: C_{D_N} above is based on maximum cross sectional area of the crew nacelle

$$C_{D_N} = \frac{D_N}{q\,F_n}$$

PART II-A-5A-c

C_{D_N} versus α_n

α_n Deg.	$C_{D_N}{}_{\alpha n = X} / C_{D_N}{}_{\alpha = 0}$	$C_{D_N}{}_{smooth}$	C_{D_N} (roughness, leakage, equipment)
0	1.000	.05588	.12286
2	1.044	.05834	.12532
4	1.110	.06203	.12901
6	1.212	.06773	.13471
8	1.393	.07784	.14482
10	1.644	.09187	.15885
12	1.985	.11092	.17790
14	2.458	.13735	.20433
16	3.075	.17183	.23881

FIG. 50

VARIATION OF CREW NACELLE DRAG COEFFICIENT WITH CREW NACELLE ANGLE OF ATTACK

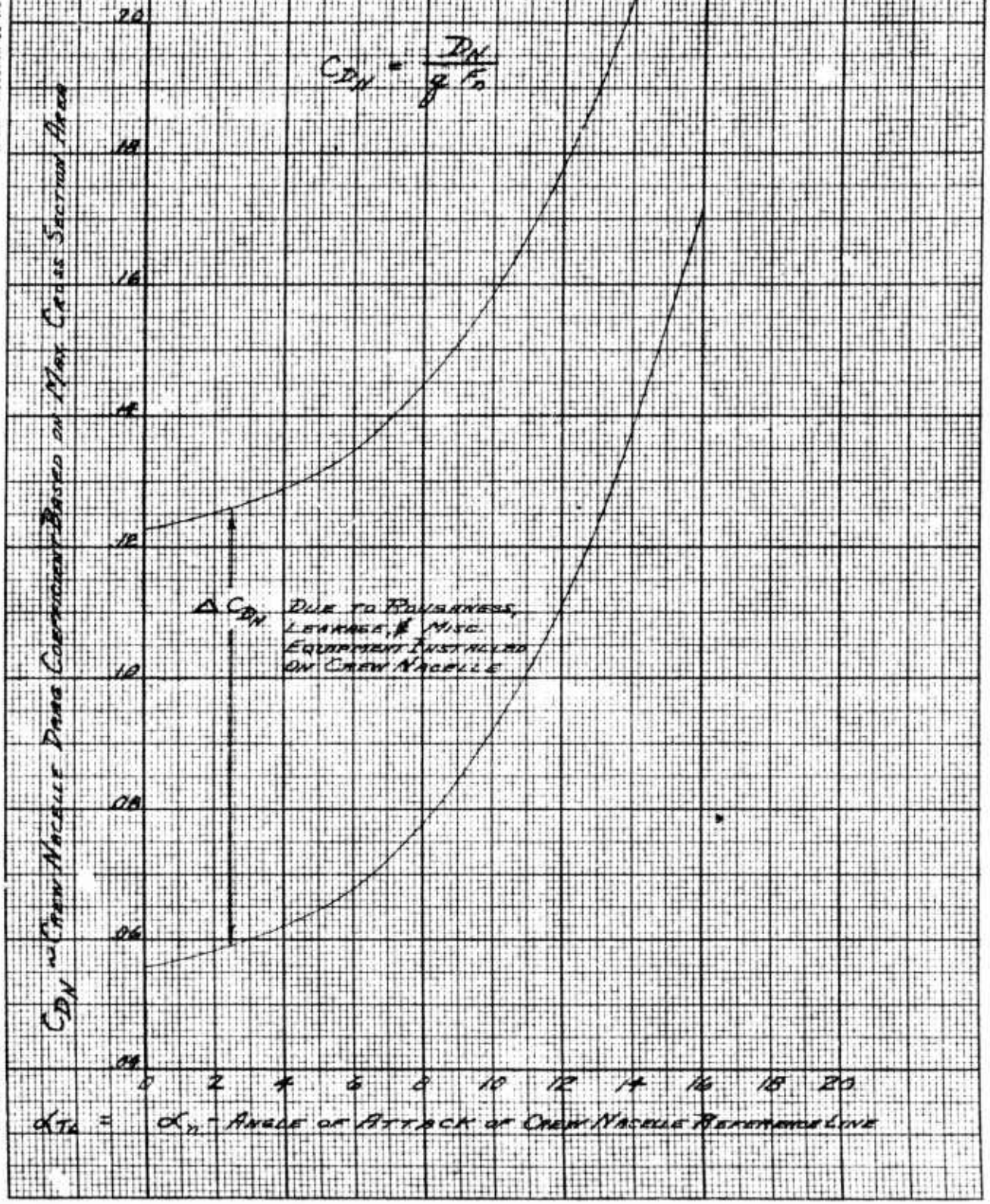

PART II-A-5A-d

CREW NACELLE POLAR DIAGRAM

α_n deg.	C_{L_N} Fig. 79	C_{D_N} Fig. 80
-12	-.269	.17790
-10	-.231	.15885
- 8	-.195	.14482
- 6	-.162	.13471
- 4	-.1325	.12901
- 2	-.117	.12532
0	-.109	.12286
2	-.101	.12532
4	-.086	.12901
6	-.054	.13471
8	.000	.14482

FIG. 21
FIG. 81

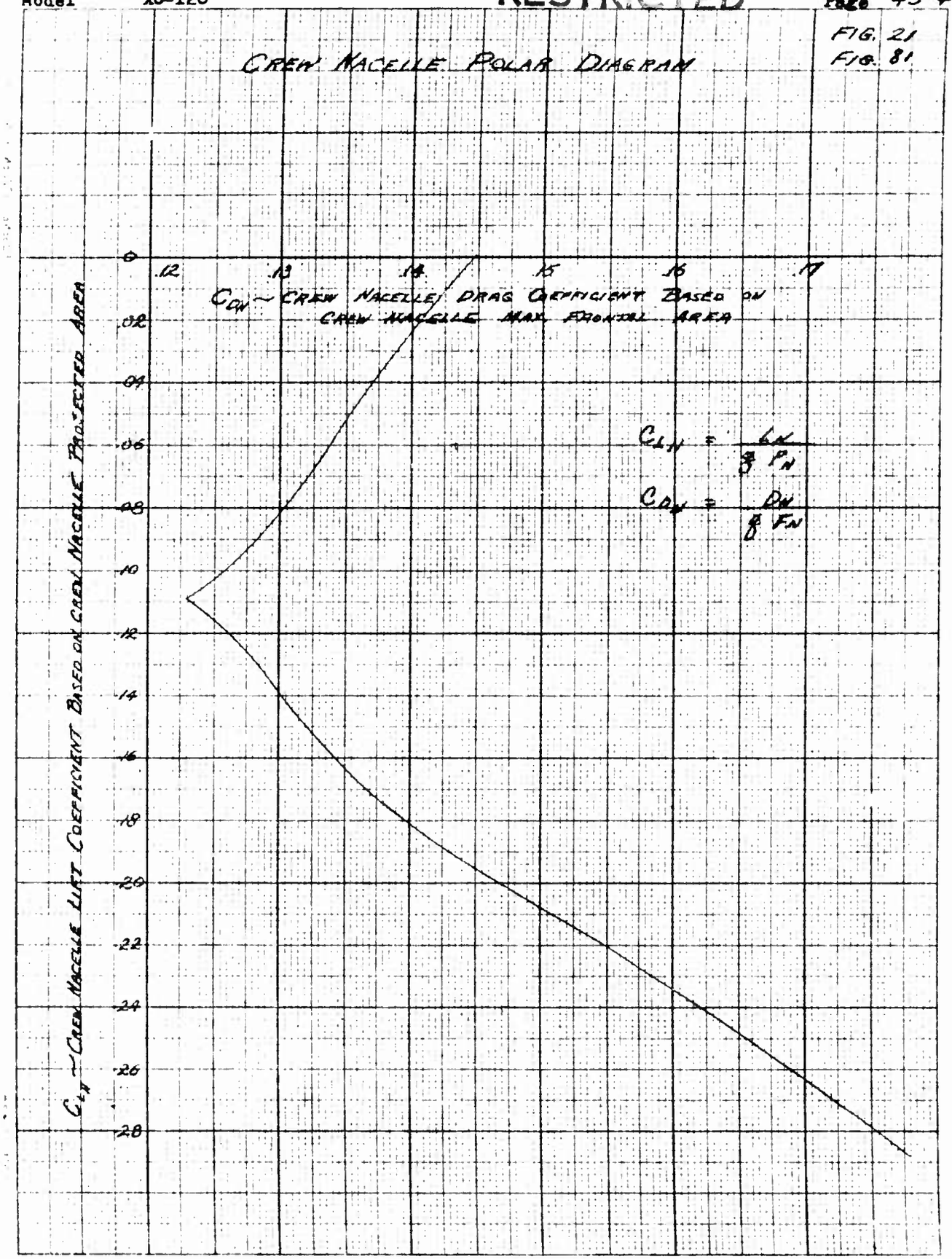
CREW NACELLE POLAR DIAGRAM
C_{DN} ~ CREW NACELLE DRAG COEFFICIENT BASED ON CREW NACELLE MAX FRONTAL AREA
$C_{LN} = \frac{L_N}{q F_N}$
$C_{DN} = \frac{D_N}{q F_N}$
C_{LN} ~ CREW NACELLE LIFT COEFFICIENT BASED ON CREW NACELLE PROJECTED AREA
0
.02
.04
.06
.08
.10
.12
.14
.16
.18
.20
.22
.24
.26
.28
.12
.13
.14
.15
.16
.17

PART II-A-5A-e

e. AERODYNAMIC FORCE COEFFICIENTS

Having previously determined the lift and drag characteristics of the fuselage, it is desired to resolve the forces into components parallel and perpendicular to the airplane thrust line. To do this several relations must be determined as below:

$C_{D_N} = \frac{D_N}{q\,F_n}$ F_n = crew nacelle frontal area in sq.ft. = 58.5

$C_{L_N} = \frac{L_N}{q\,P_n}$ P_n = crew nacelle plan area in sq.ft. = 450.0

$C_{X_N} = \frac{X_N}{q\,F_n}$ S_n = crew nacelle side area in sq.ft. = 271.0

$C_{Z_N} = \frac{Z_n}{q\,P_n}$ D_N, L_N, X_N, Z_N are forces on the crew nacelle

α (crew nacelle center line) = α_n (crew nacelle reference line) = $\alpha_{T.L.}$

$$Z_N = L_N \cos\alpha_{T.L.} + D_N \sin\alpha_{T.L.}$$

$$X_N = D_N \cos\alpha_{T.L.} - L_N \sin\alpha_{T.L.}$$

dividing through to coefficient form

$$C_{Z_N} = \frac{L_N}{q\,P_n}\cos\alpha_{T.L.} - \frac{D_N}{q\,P_n}\sin\alpha_{T.L.}$$

$$= C_{L_N}\cos\alpha_{T.L.} - C_{D_N}\frac{F_n}{P_n}\sin\alpha_{T.L.}$$

$$C_{X_N} = \frac{D_N}{q\,F_n}\cos\alpha_{T.L.} - \frac{L_N}{q\,F_n}\sin\alpha_{T.L.}$$

$$= C_{D_N}\cos\alpha_{T.L.} - C_{L_N}\frac{P_n}{F_n}\sin\alpha_{T.L.}$$

The following page presents the calculations necessary to determine C_{Z_N} and C_{X_N}.

A plot of C_{X_N} and C_{Z_N} versus $\alpha_{T.L.}$ is presented in figure 82.

FA-800-23

DETERMINATION OF C_{X_N} AND C_{Z_N} OF CREW NACELLE

1	2	3	4	5	6	7	8	9	10	11
α_{TL}	Sin α_{TL}	Cos α_{TL}	C_{D_N}	C_{L_N}	③ x ⑤	② x ④ x .1307	③ x ④	② x ⑤ x 7.6531	C_{X_N} ⑧ - ⑨	C_{Z_N} ⑥ - ⑦
-12	-.2079	.9782	.1779	-.268	-.262	-.0048	.1734	.426	-.2526	-.2668
- 8	-.1392	.9903	.1448	-.195	-.193	-.0026	.1433	.207	-.0637	-.1956
- 4	-.0698	.9976	.1290	-.131	-.1304	-.0117	.1285	.0696	.0589	-.1421
0	0	1.0000	.1229	-.110	-.110	0	.1229	0	.1229	-.110
4	.0698	.9976	.1290	-.065	-.0827	.0117	.1285	-.0457	.1742	-.0710
8	.1392	.9903	.1448	0	0	.0026	.1433	0	.1433	-.0026

RESTRICTED

CREW NACELLE FORCE COEFFICIENTS

Fig 22
Fig. 82

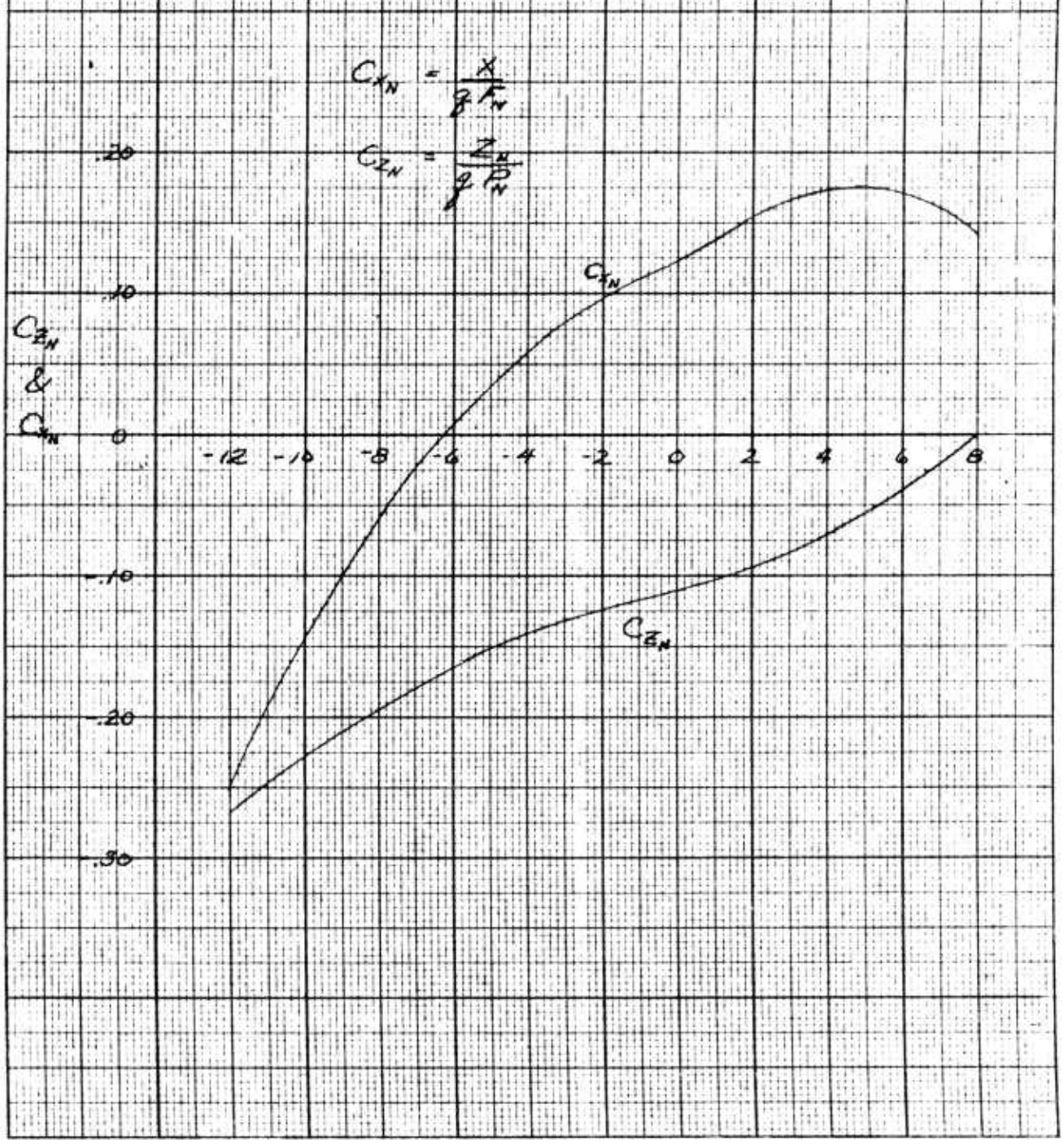

PART II-A-5A-f

f. Pitching Moment Analysis

The pitching moment coefficient of the crew nacelle alone about the quarter length point are obtained from wind tunnel data of reference (2) where

$$C_{M_N} = C_{M\ \text{crew nacelle on}} - C_{M\ \text{crew nacelle off}}$$

Values thus obtained, converted to the quarter length point of the crew nacelle and based on crew nacelle planform area and crew nacelle length are presented in figure 83 as $C_{M_{N.25L_n}}$ versus α_n.

RESTRICTED

FIG 23

CREW NACELLE PITCHING MOMENTS

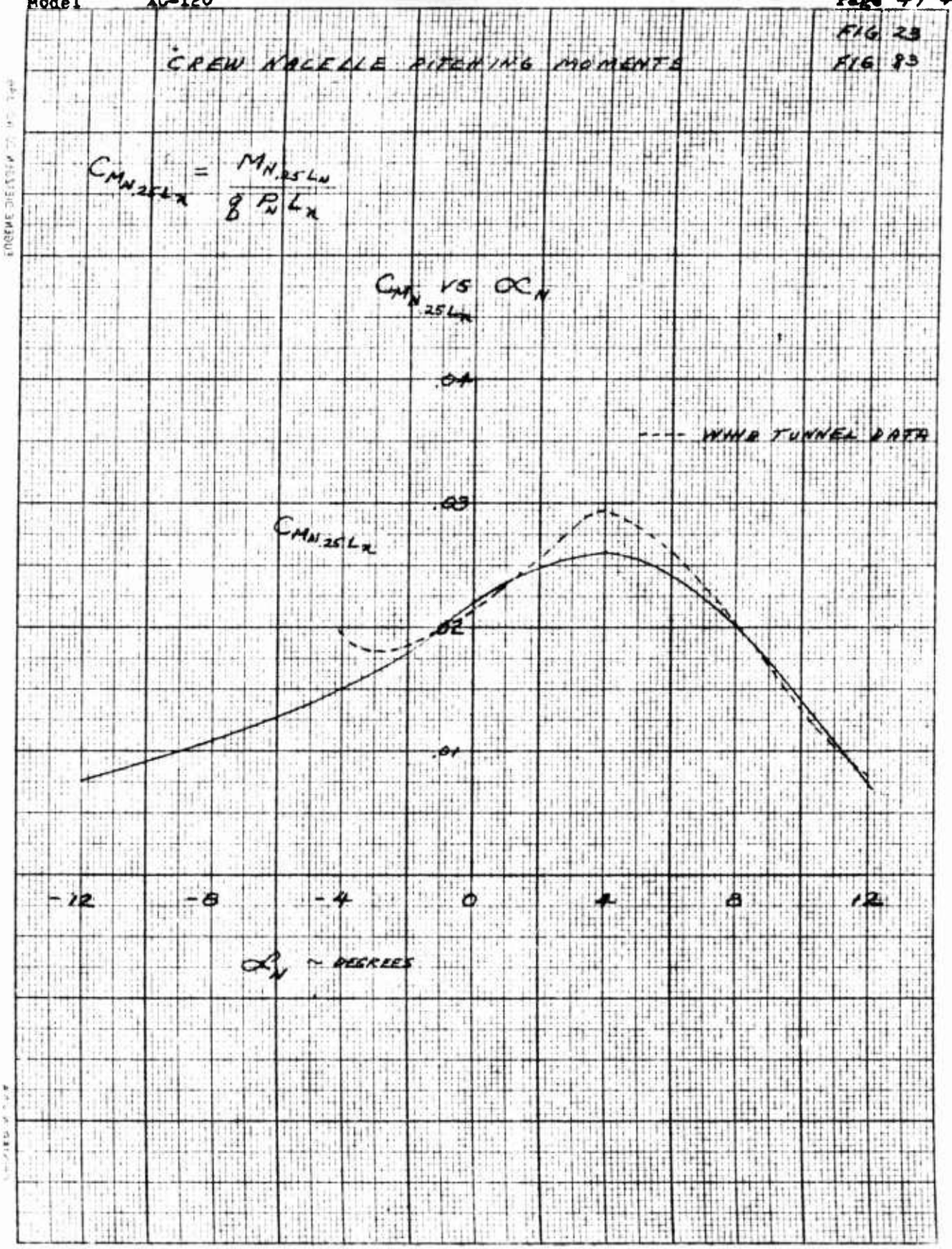

PART II-A-5A-g

g. Yawing Moment Analysis

The crew nacelle yawing moment coefficients are obtained from fuselage pitching moment data of figure 123, reference (1) for a crew nacelle fineness ratio of 5.80 and are based on crew nacelle length and side area.

The crew nacelle side force coefficients are obtained from fuselage lift coefficient data of figure 115 reference (1) and are based on crew nacelle side area.

It is assumed that the drag coefficient of the crew nacelle at small angles of yaw are the same as those at small angles of attack so that for $\psi = \alpha_{TL}$ (small angles)

$$C_{D_N} \text{ in yaw} = C_{D_N} \text{ in pitch}$$

FIG 24
FIG 84

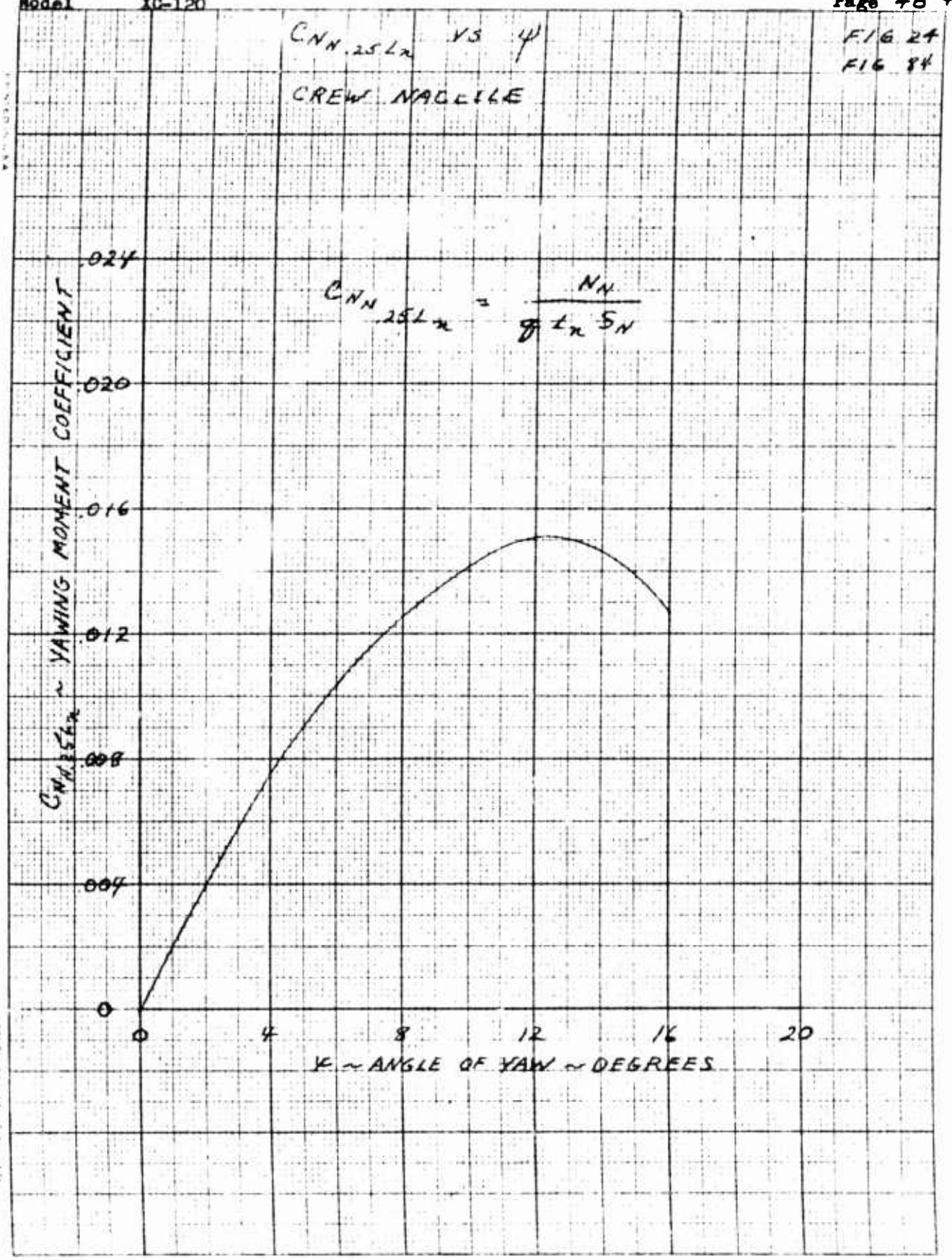
$C_{N_{N.25L_n}}$ VS ψ
CREW NACELLE
$C_{N_{N.25L_n}} = \frac{N_N}{q\, t_n\, S_N}$
$C_{N_{N.25L_n}}$ ~ YAWING MOMENT COEFFICIENT
.024
.020
.016
.012
.008
.004
0
0
4
8
12
16
20
ψ ~ ANGLE OF YAW ~ DEGREES

RESTRICTED

FIG 25
FIG 85

C_{C_N} VS ψ

CREW NACELLE

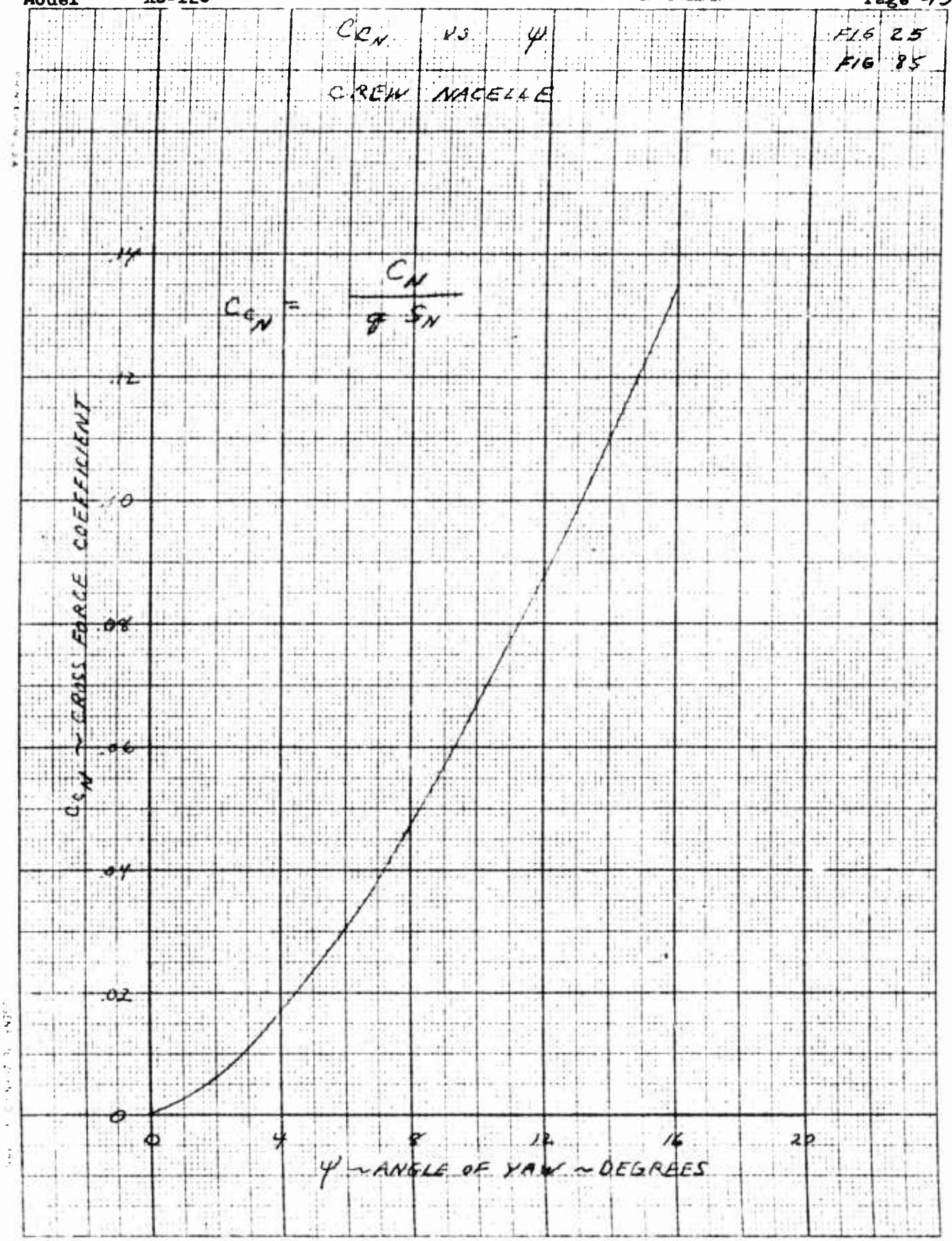

PART II-A-6

6. BOOM

This section presents the calculations for determining the aerodynamic characteristics of one boom. All coefficients in this section are based on an area of the boom itself (either planform, frontal or side area as necessary) and no attempt is made to convert the coefficients to wing area. Coefficients are based on various boom areas as follows:

Coefficient	Definition
C_{L_B}	$L_B/q\ F_b$
C_{D_B}	$D_B/q\ F_b$
$C_{M_{B.25\ L_b}}$	$M_{B.25L_b}/q\ F_b\ L_b$
C_{X_B}	$X_B/q\ F_b$
C_{Z_B}	$Z_B/q\ F_b$
$C_{N_{B.25\ L_b}}$	$N_{B.25L_b}/q\ S_b\ L_b$
C_{C_B}	$C_B/q\ S_b$

It should be noted that all coefficients are presented versus α_b and that $\alpha_{T.L.} = \alpha_b$

Total boom C_{L_B}, C_{D_B} and $C_{M_{B.25L_b}}$ versus α_b are presented in figures 87, 88, and 91 respectively. Figure 90 presents plots of C_{X_B} and C_{Z_B} versus $\alpha_{T.L.}$. For characteristics in yaw see explanation of Part II-A-6-g.

PART II-A-6-a

a. BOOM DRAWING

Figure 86 presents a three-view drawing of the boom alone. Pertinent dimensions and areas used in the analysis are shown.

MODEL X0-120 | PREPARED BY | CHECKED BY | APPROVED BY

DATE 7/9/48

REVISED

Subject:— BASIC AERODYNAMIC DATA

FIG 86.

Boom Frontal Area F_b = 10.76 Sq. Ft.
Boom Planform Area P_b = 312.5 Sq. Ft.
Boom Side Area S_b = 363.2 Sq. Ft.

Boom

PART II-A-6-b

b. LIFT ANALYSIS

The lift coefficient of the boom is the same as that of reference (1) Part II-A-6-b. Figure 87 presents a plot of boom lift coefficient versus angle of attack of boom centerline for boom alone.

FIG 26
FIG 87

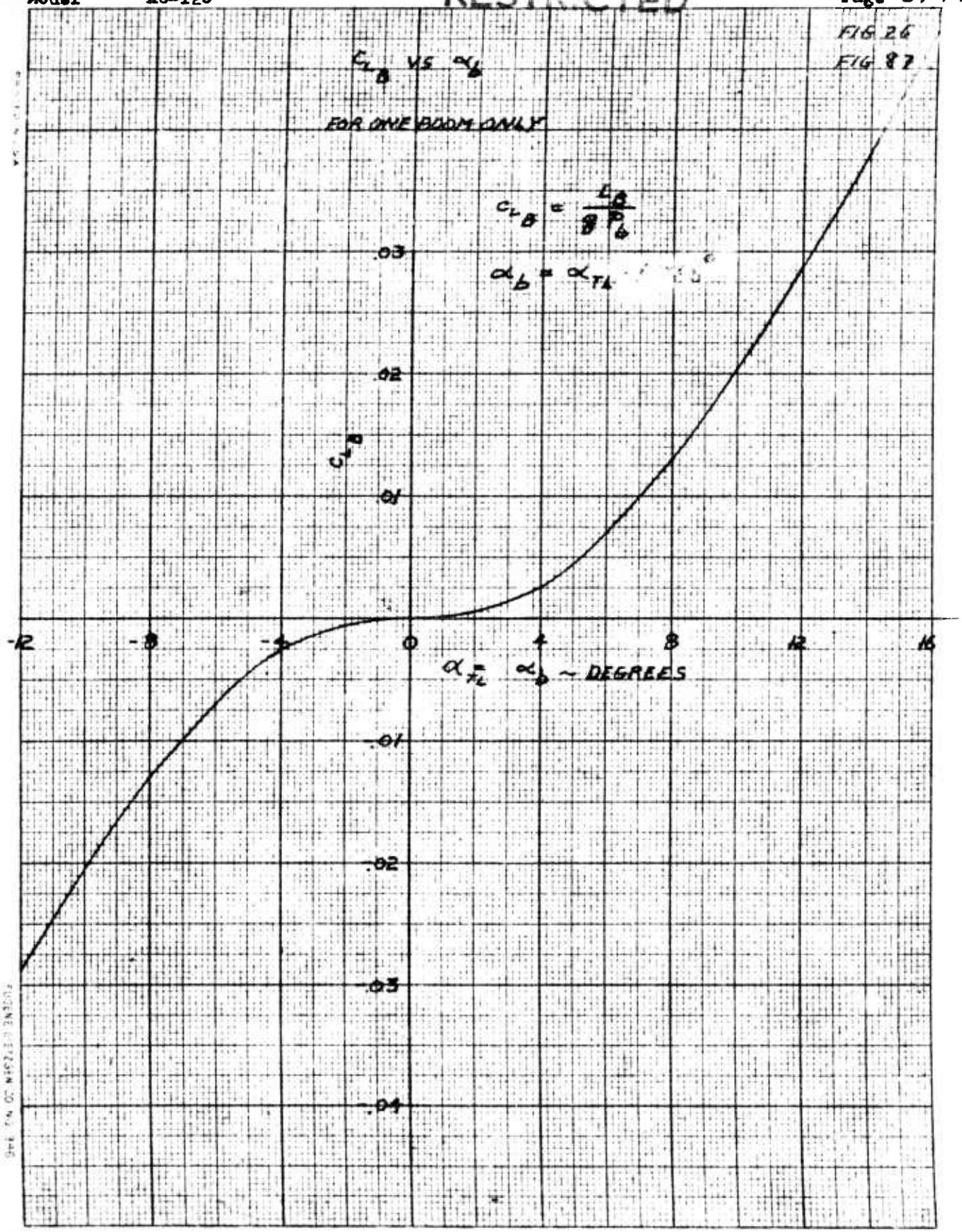
C_{L_B} VS α_b
FOR ONE BOOM ONLY
$C_{L_B} = \frac{L_B}{q S_b}$
$\alpha_b = \alpha_{TL}$
.03
.02
.01
C_{L_B}
-.01
-.02
-.03
-.04
-12
-8
-4
0
4
8
12
16
$\alpha_{TL} = \alpha_b$ ~ DEGREES

PART II-A-6-c

c. DRAG ANALYSIS

The drag of the boom was determined by the same method of analysis as reference (1), using the same generalized drag curves. The variation of smooth drag with angle of attack was determined from figure 115 for round fuselages.

PART II-A-6-c

BOOM DRAG ANALYSIS (ONE BOOM)

ITEM		GENERAL	K_{X_B}	C_{D_B}
Smooth Drag				
Cross sectional area (F_b),	sq. ft.	40.76		
Type of cross section		Round		
Length (L_b)	ft.	68.1		
Fineness ratio = $\frac{.886\ L_b}{\sqrt{F_b}}$		9.46		
Speed/altitude for analysis,	mph/ft.	280/18000		
Reynolds Number		11.11×10^7		
Smooth C_{D_B} from figure 117 reference (1)				.0798
TOTAL SMOOTH C_{D_B}				.0798
Using figure 118 of reference (1) (round) construct a curve of smooth C_{D_B} versus α of boom center line				
Roughness, Leakage, and Miscellaneous Equipment				
Allowance for roughness due to rivet heads, dimples, inspection doors, gear doors, small drains and plugs etc.				
Percent of smooth drag		40		
ΔC_{D_B}				.03192
Allowance for leakage through boom, engine compartment, etc.				
Percent of smooth drag		25		
ΔC_{D_B}				.01997
Allowance for interference of wing-boom intersection				
Percent of smooth drag		5		
ΔC_{D_B}				.00399
Addition of cowl to streamlined body				
Cross sectional area at engine ℄.	sq.ft.	30.2		
C_D due to cowl (on area above)		.015		
C_{D_B}				.01111
Fairing for landing gear				
Frontal area,	sq.ft.	3.5		
C_D on frontal area		0.1		
ΔC_{D_B}				.0086

PART II-A-6-c

BOOM DRAG ANALYSIS (ONE BOOM) (Cont.)

ITEM	GENERAL	K_{X_B}	C_{D_B}
Roughness, Leakage, and Miscellaneous Equipment (Cont.)			
Radio altimeter antenna ΔC_{D_B}		.00027	.00259
IFF antenna ΔC_{D_B}		.0001	.00096
Engine cooling air (cowl flaps closed) ΔC_{D_B}			.02370
Oil cooling air (flap closed) ΔC_{D_B}			.0058
TOTAL ΔC_{D_B} DUE TO ROUGHNESS, LEAKAGE, MISCELLANEOUS EQUIPMENT			.10564
This ΔC_{D_B} is added directly to figure as a constant increment at all angles of attack			
TOTAL C_{D_B} AT ZERO ANGLE OF ATTACK			.18844

Note: C_{D_B} above is based on maximum cross sectional area of the boom

$$C_{D_B} = D_B / q F_b$$

RESTRICTED

FIG. 88

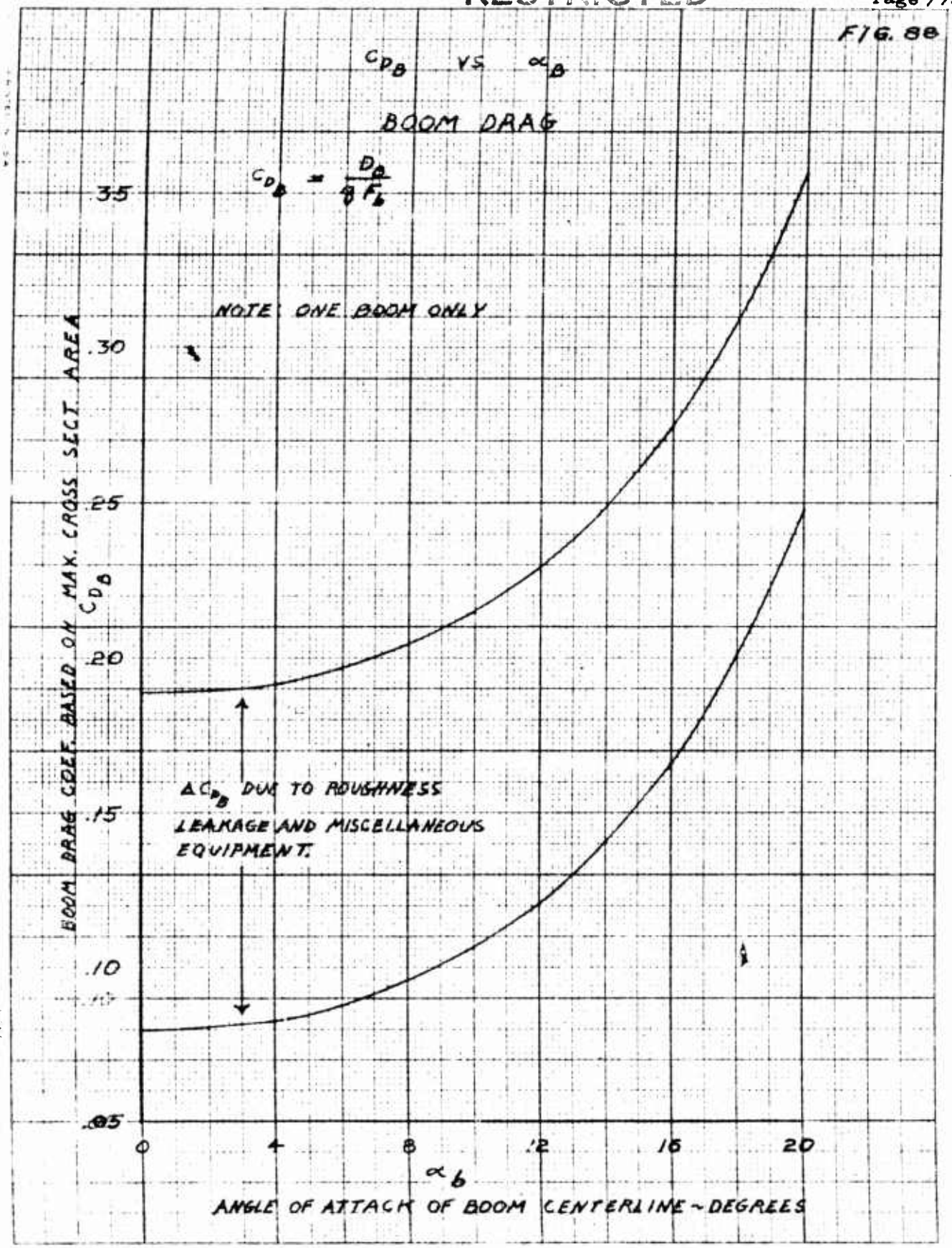

RESTRICTED

FIG 27
FIG 29

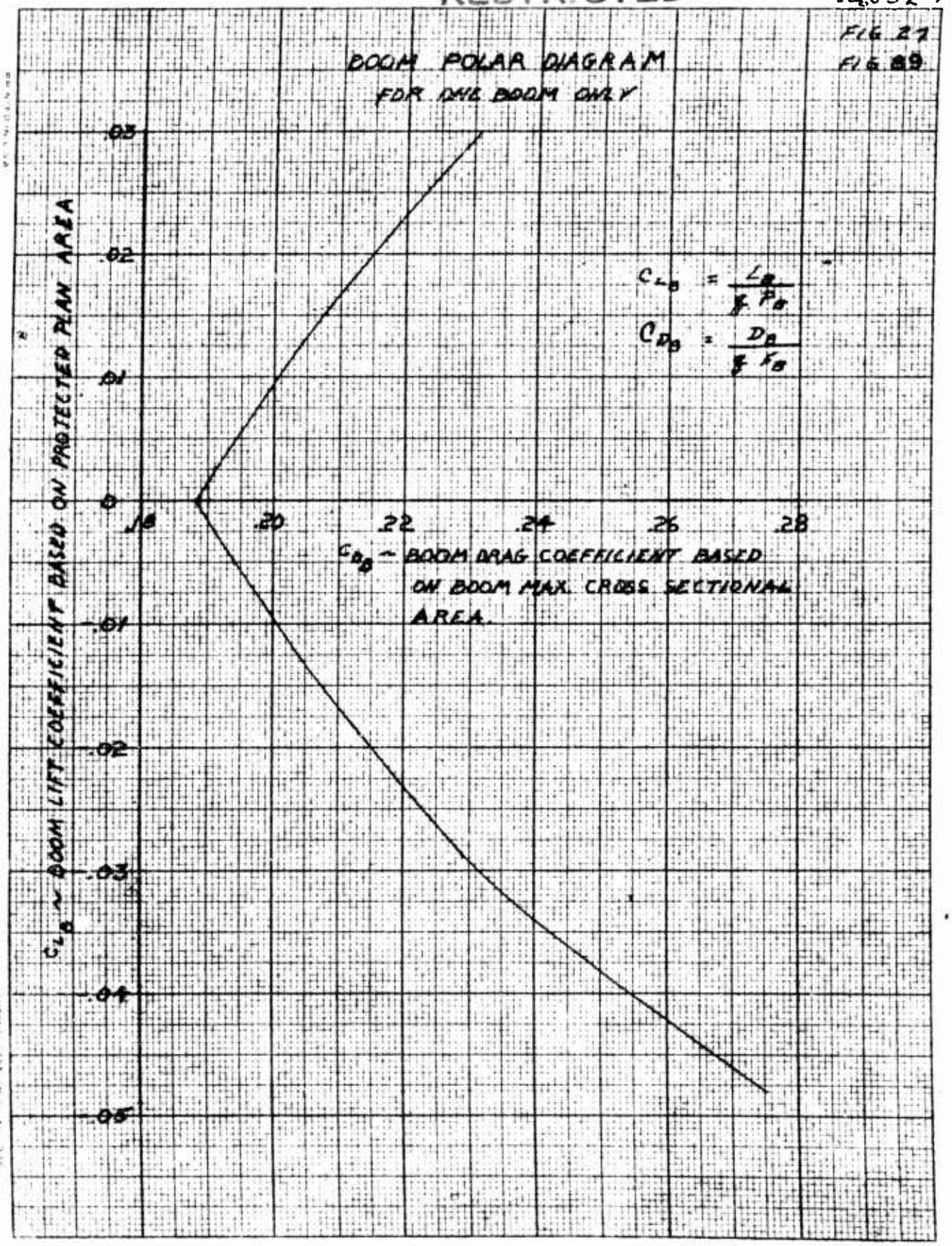

PART II-A-6-e

e. AERODYNAMIC FORCE COEFFICIENTS

Having determined lift and drag of the boom, the forces must be resolved parallel and perpendicular to the airplane thrust line. The necessary relations are tabulated below:

$$C_{D_B} = \frac{D_B}{q\,F_b}$$

$$C_{L_B} = \frac{L_B}{q\,P_b}$$

$$C_{X_B} = \frac{X_B}{q\,F_b}$$

$$C_{Z_B} = \frac{Z_B}{q\,P_b}$$

F_b = boom frontal area in sq. ft. = 40.76

P_b = boom planform area in sq. ft. = 312.5

S_b = boom side area in sq. ft. = 363.2

D_B, L_B, Z_B, X_B, = forces

α_b (boom center line) = $\alpha_{T.L.}$

$$C_{Z_B} = C_{L_B} \cos \alpha_{T.L.} + C_{D_B} \frac{F_b}{P_b} \sin \alpha_{T.L.}$$

$$C_{X_B} = C_{D_B} \cos \alpha_{T.L.} - C_{L_B} \frac{F_b}{P_b} \sin \alpha_{T.L.}$$

The following page presents the calculations necessary to determine C_{Z_B} and C_{X_B} and figure 90 presents a plot of these coefficients versus $\alpha_{T.L.}$

PART II-A-6-e

DETERMINATION OF C_{L_B} AND C_{Z_B} FOR ONE BOOM

$$\frac{F_b}{P_b} = .1305 \qquad \frac{P_t}{F_b} = 7.66$$

1	2	3	4	5	6	7	8	9	10	11	12
α_{TL}	α_b	$\sin\alpha_{TL}$	$\cos\alpha_{TL}$	C_{D_B}	C_{L_B}	C_{D_B} $\cos\alpha_{TL}$	C_{L_B} $\sin\alpha_{TL}$ x 7.66	C_{D_B} $\sin\alpha_{TL}$ x .1305	C_{L_B} $\cos\alpha_{TL}$	C_{X_B}	C_{Z_B}
	1	Sin 1	Cos 1			4 x 5	6 x 3 x 7.66	5 x 3 x .1305	6 x 4	7 - 8	9 + 10
-12	-12	-.208	.98	+.230	-.029	.225	.0462	-.00625	-.0284	.179	-.0347
-8	-8	-.139	.99	+.205	-.013	.203	.01385	-.00372	-.0129	.189	-.0166
-4	-4	-.0698	.998	+.191	-.0025	.191	.00134	-.00174	-.0025	.1897	-.00424
-2	-2	-.0344	1	.189	-.0005	.189	.000132	-.00085	-.0005	.189	-.00135
2	2	.0344	1	.189	1.0005	.189	.000132	+.00085	+.0005	.189	+.00135
0	0	0	1.0	+.189	0	.189	0	0	0	.189	0
4	4	-.0698	.998	+.191	+.0025	.191	.00134	+.00174	+.0025	.1897	+.00424
8	8	-.139	.99	+.205	+.013	.203	.01385	+.00372	+.0129	.189	+.0166
12	12	-.208	.98	+.230	+.029	.225	.0462	+.00625	+.0284	.179	+.0347

RESTRICTED

RESTRICTED

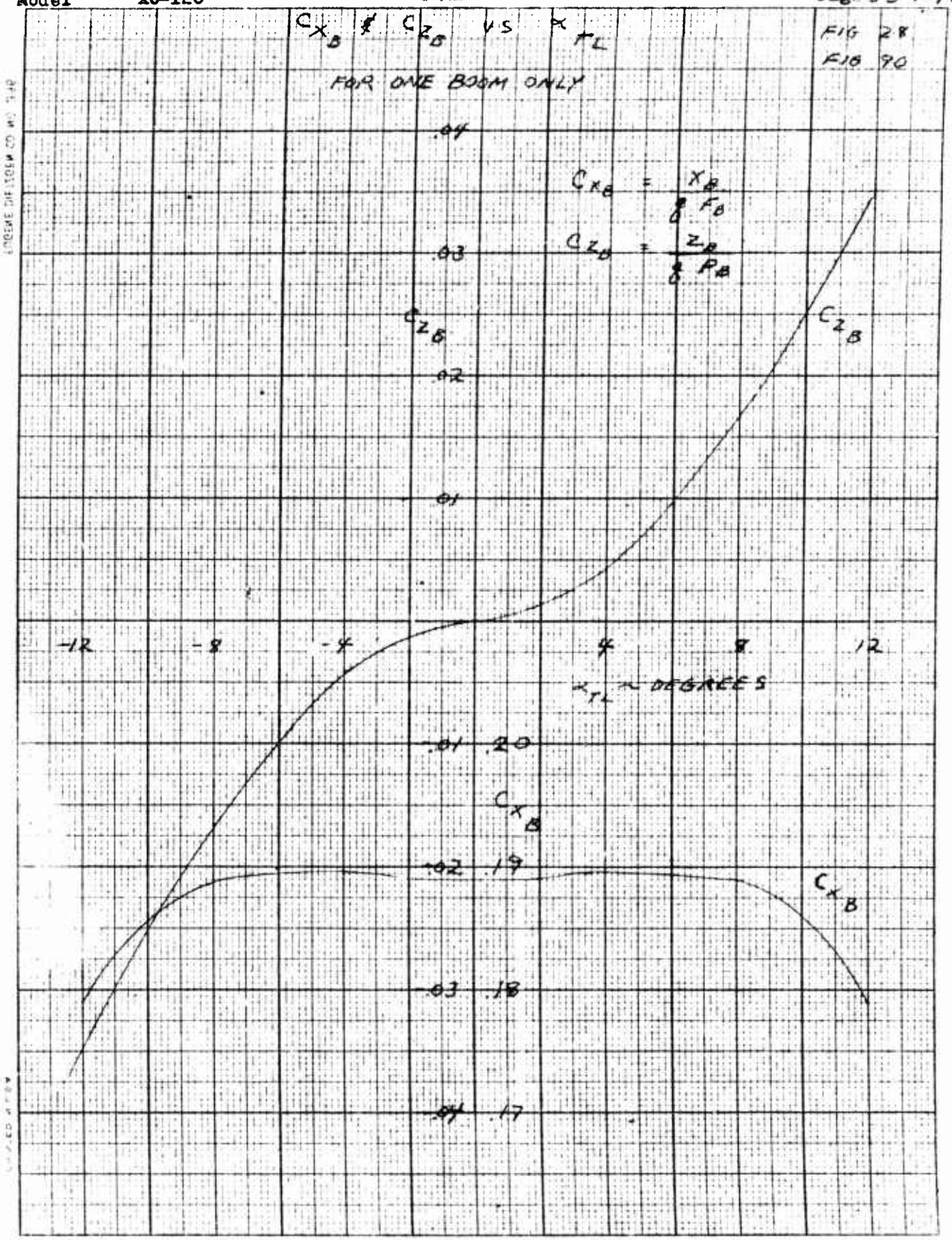
C_{X_B} & C_{Z_B} vs α_{TL}
FIG 28
FIG 90
FOR ONE BOOM ONLY
$C_{X_B} = \frac{X_B}{q_0 F_B}$
$C_{Z_B} = \frac{Z_B}{q_0 P_B}$
.04
.03
.02
.01
C_{Z_B}
-12
-8
-4
4
8
12
α_{TL} ~ DEGREES
.01 .20
C_{X_B}
.02 .19
.03 .18
.04 .17

PART II-A-6

f. Pitching Moment Analysis

The pitching moment coefficient of one boom alone about the quarter length point of the boom was determined from wind tunnel data of reference (2) where

$C_{M_B} = C_M$ (wing, booms, and vertical tails from the wind tunnel data) $- C_M$ (computed values for wing and vertical tails from reference (3))

Values thus obtained include any interference effects and are for two booms.

Converted to the quarter length point of the boom, and based on one boom area, and boom length, figure 91 on the following page presents the variation of one boom pitching moment coefficient versus angle of attack of the boom.

RESTRICTED

PITCHING MOMENT COEFFICIENT OF ONE BOOM ABOUT THE QUARTER LENGTH POINT

FIG. 29
FIG. 91

$C_{m_{B_{.25L_b}}} = \frac{M_B}{q\, P_B\, L_b}$

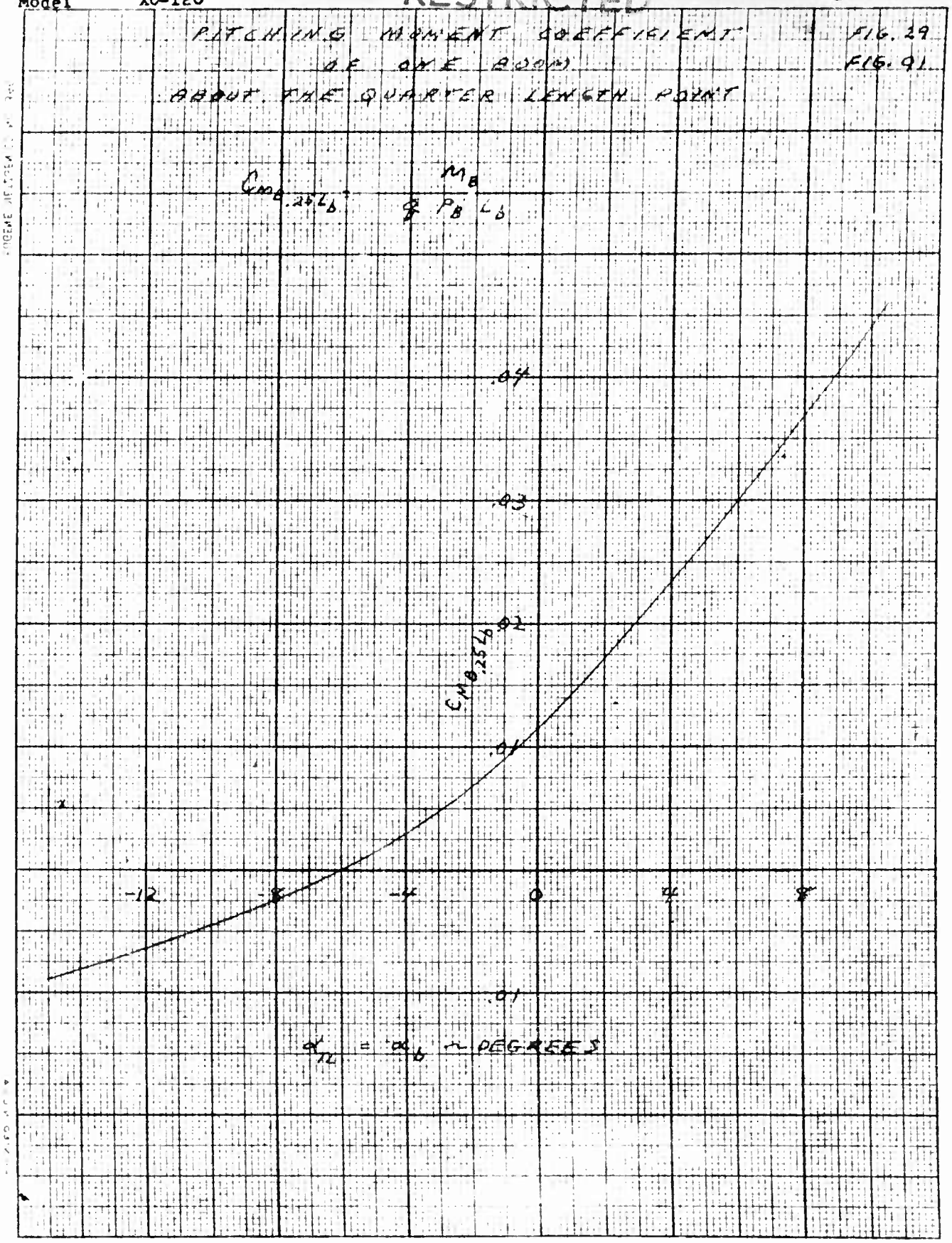

PART II-A-6

g. Yawing Moment Analysis

The boom yawing moment coefficients are obtained from fuselage pitching moment data of figure 123 reference (1) for a boom fineness ratio of 9.46 and are based on boom length and side area.

The boom side force coefficients are obtained from fuselage lift coefficient data on figure 115 reference (1) and are based on boom side area.

It is assumed that the drag coefficients of the boom at small angles of yaw are the same as those at small angles of attack so that for $\psi = \alpha_{TL}$(small angles)

$$C_{D_B} \text{ in yaw} = C_{D_B} \text{ in pitch}$$

FIG 30
FIG 92

YAWING MOMENT OF BOOM ABOUT QUARTER LENGTH POINT
FOR ONE BOOM ONLY

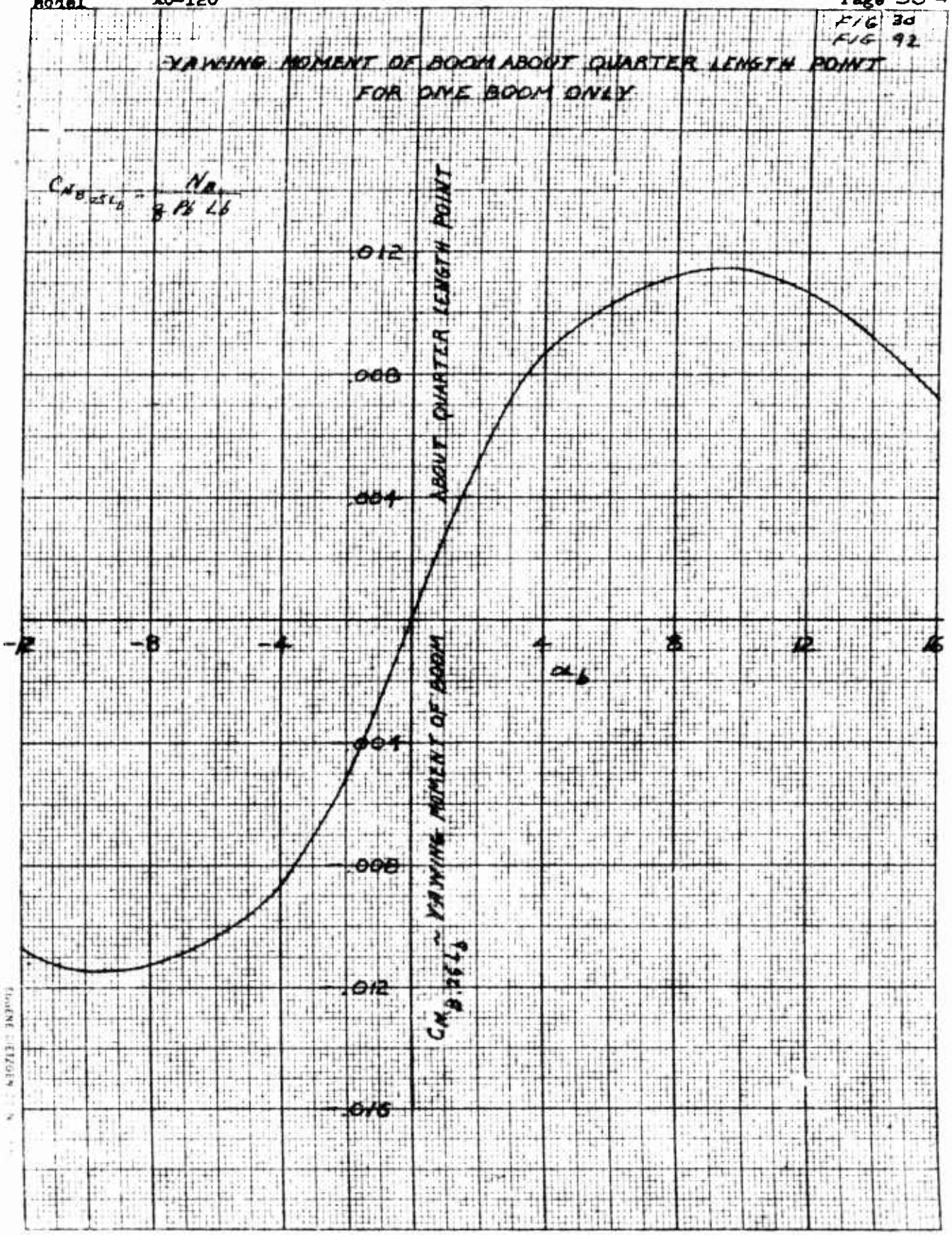

RESTRICTED

FIG. 31
FIG. 93

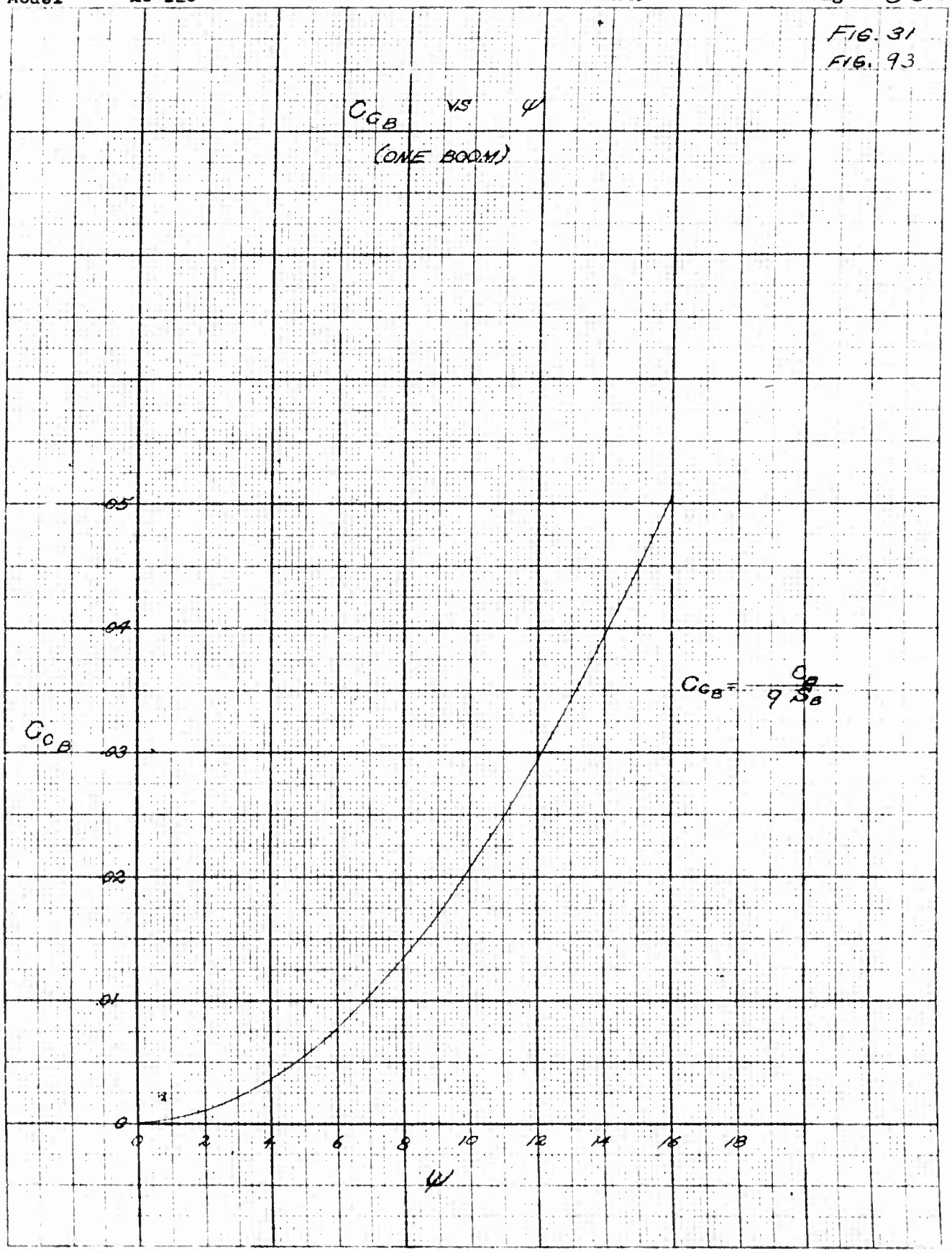

PART II-A-7

7. Horizontal Tail

It is the purpose of this section to determine the aerodynamic characteristics of the Model XC-120 horizontal tail, power off.

The characteristics as determined herein are the results of calculations and/or wind tunnel data. All coefficients are based on total horizontal tail area and/or chord and presented versus the angle of attack of the horizontal tail. The relationship of the horizontal tail to the rest of the airplane is discussed in the downwash section. This relation is made by use of the following angular relationship.

$$\alpha_{ht} = \alpha_{TL} + i_{ht} - \epsilon_{ht}$$

where

$$i_{ht} = +1.0^{\circ}$$

The final characteristics of the horizontal tail may be found in the following figure or sections.

Lift	Figure 95
Drag	Figure 96
Polar Diagram	Figure 97
Force Coefficient	See discussion section e
Pitching Moments	Figure 98
Yawing Moments	See discussion section g
Dynamic Pressure	See discussion section h
Downwash	Figures 100 and 101
Elevator Hinge Moments	Figure 103

PART II-A-7-a

a. Horizontal Tail Drawing

Figure 94 on the following page presents a drawing of the horizontal tail with all pertinent dimensions noted.

RESTRICTED

FIG. 94

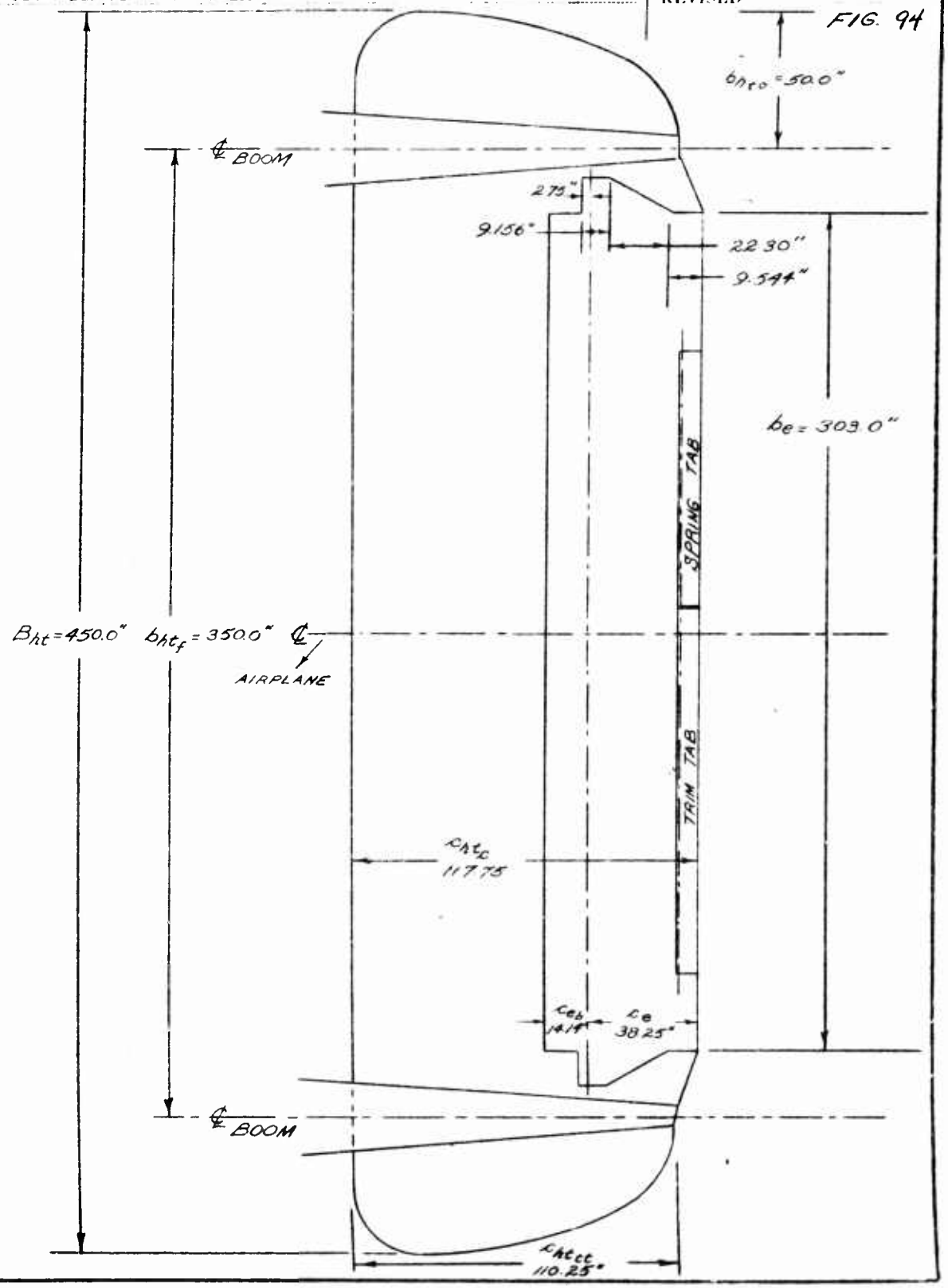

PART II-A-7

b. Lift Analysis

It is the purpose of this section to determine the lift characteristics of the horizontal tail. The section characteristics as well as the three dimensional characteristics are determined for each of the lift parameters.

Lift Curve Slope

For the flapped section between the fins:

S_{ht_f} = 286.2 sq. ft.

$A_{ht_f} = \frac{(350/12)^2}{286.2} = 2.96$

Airfoil thickness in percent of chord = 13%

Trailing edge angle ϕ = 12.27°

gap between elevator and stabilizer = .625 in.

gap ratio $\frac{gap}{chord} = \frac{.625}{117.25} = .0053$

gap location in percent of chord = $\frac{65.36}{117.75} = 55.5\%$

section c_{l_α} = .0995 figure 42 reference (15), correction from section data to sealed gap .98, figure 44 reference (15) correction from sealed gap to open gap = .855, figure 43 reference (15)

c_{l_α} corrected for open gap = .0955 x .98 x .855 = .0834

$\frac{A_{ht_f}}{c_{l_\alpha}} = \frac{2.96}{.0834} = 35.5$ $\frac{\sqrt{S_{vt}}}{b_{ht_f}} = \frac{\sqrt{99.6}}{350/12} = .342$

$\frac{C_{L_\alpha}}{c_{l_\alpha}} = .696$ figure 47, reference (15)

$C_{L_\alpha} = .696 \times .0834 = .0580$

For the tip sections outboard of the fins:

PART II-A-7-b (Cont.)

Assume that the tip sections outboard of the tips act as a single unit so that

$$S_{ht_o} = 60 \text{ sq. ft.}$$

$$A_{ht_o} = \frac{(100/12)^2}{60} = 1.16$$

Airfoil thickness in percent of chord = 14%
trailing edge angle ϕ = 16°

section c_{l_α} = .0980 figure 42 reference (15)

$$\frac{A_{ht_o}}{c_{l_\alpha}} = \frac{1.16}{.0980} = 11.85$$

$$\frac{C_{L_\alpha}}{c_{l_\alpha}} = .300 \quad \text{figure 45 reference (15)}$$

$$C_{L_\alpha} = .300 \times .0980 = .0294$$

<u>For the complete horizontal tail:</u>

Taking a weighted average based on areas we obtain

$$c_{l_{\alpha ht}} = \frac{.0834 \times 286.2 + .0980 \times 60}{346.2} = .0860$$

$$C_{L_{\alpha ht}} = \frac{.0580 \times 286.2 + .0294 \times 60}{346.2} = .0530$$

<u>Summary of lift curve slope data</u>

	Section Data c_{l_α}	Three Dimensional Data C_{L_α}
Between fins	.0834	.0580
Outboard	.0995	.0294
Complete Tail	.0860	.0530

Wind tunnel data, reference (14) shows a C_{L_α} of the complete tail to be equal to .0450

PART II-A-7 (Cont.)

The efficiency of the horizontal tail, η_{ht} is thus

$$\frac{.0450}{.0530} = .85$$

Lift-effectiveness Parameter

For the flapped section between the fins:

$$\text{Elevator-chord ratio} = \frac{c_e}{c_{ht}} = \frac{38.25}{117.75} = .325$$

section α/δ plain sealed $= -.615$ figure 49 reference (15)
correction from sealed to open gap $= 1.11$ figure 6 reference (9)

$K_1 = .070$ for blunt nose figure 3 reference (9)

where balance chord ratio $\frac{c_{eb}}{c_e} = \frac{14.14}{38.25} = .37$

and $\frac{t/2}{c_e} = \frac{8.75/2}{38.25} = .113$

section α/δ open gap $= -.615 \times 1.11 = -.682$

$$c_{l_{\delta_e}} = .0834 \times .682 = .0568$$

Assuming that the three dimensional value of α/δ varies directly with the percent of elevator span to the tail span between the fins

$$\alpha/\delta = -.682 \times .87 = -.594$$

For the tip sections outboard of the fins:

As the elevators are only on the section between fins, they are considered to affect that section only and therefore the section and three dimensional values of α/δ for the tip sections are equal to zero.

For the complete horizontal tail:

PART II-A-7 (Cont.)

Taking a weighted average based on areas we obtain

$$C_{L\delta_e} = \frac{.058 \times .594 \times 286.2 + .0294 \times 0 \times 60}{346.2} = .0284$$

$$\frac{\alpha_{ht}}{\delta_e} = -\frac{C_{L\delta}}{C_{L\alpha}} = -\frac{.0284}{.0530} = -.538$$

Wind tunnel data, reference (14) shows $\frac{\alpha_{ht}}{\delta_e}$ for the complete tail to equal -.545. Therefore, the wind tunnel value will be used for further analysis.

Summary of lift effectiveness parameter data

	Section data α/δ_e	Three dimensional data α_{ht}/δ_e
Between fins	-.682	-.594
Outboard	0	0
Complete tail		-.545

Summary of Lift Analysis

$$C_{L\alpha_{ht}} = .0530$$

$$\alpha_{ht\delta_e} = -.545$$

$$C_{L_{HT}} = (C_{L\alpha_{ht}})\,\alpha_{ht} + (C_{L\alpha_{ht}})(-\alpha_{ht\delta_e})\,\delta_e$$

$$C_{L_{HT}} = (.0530\alpha_{ht}) + (.0530 \times .545 \times \delta_e)$$

$$C_{L_{HT}} = .0530\alpha_{ht} + .0289\delta_e$$

For all calculations assume tail lift efficiency $\eta_{ht} = .85$ (from wind tunnel data).

Figure 95 presents the variation of $C_{L_{HT}}$ for various elevator deflections versus angle of attack of the horizontal tail.

FIG. 32
FIG. 95

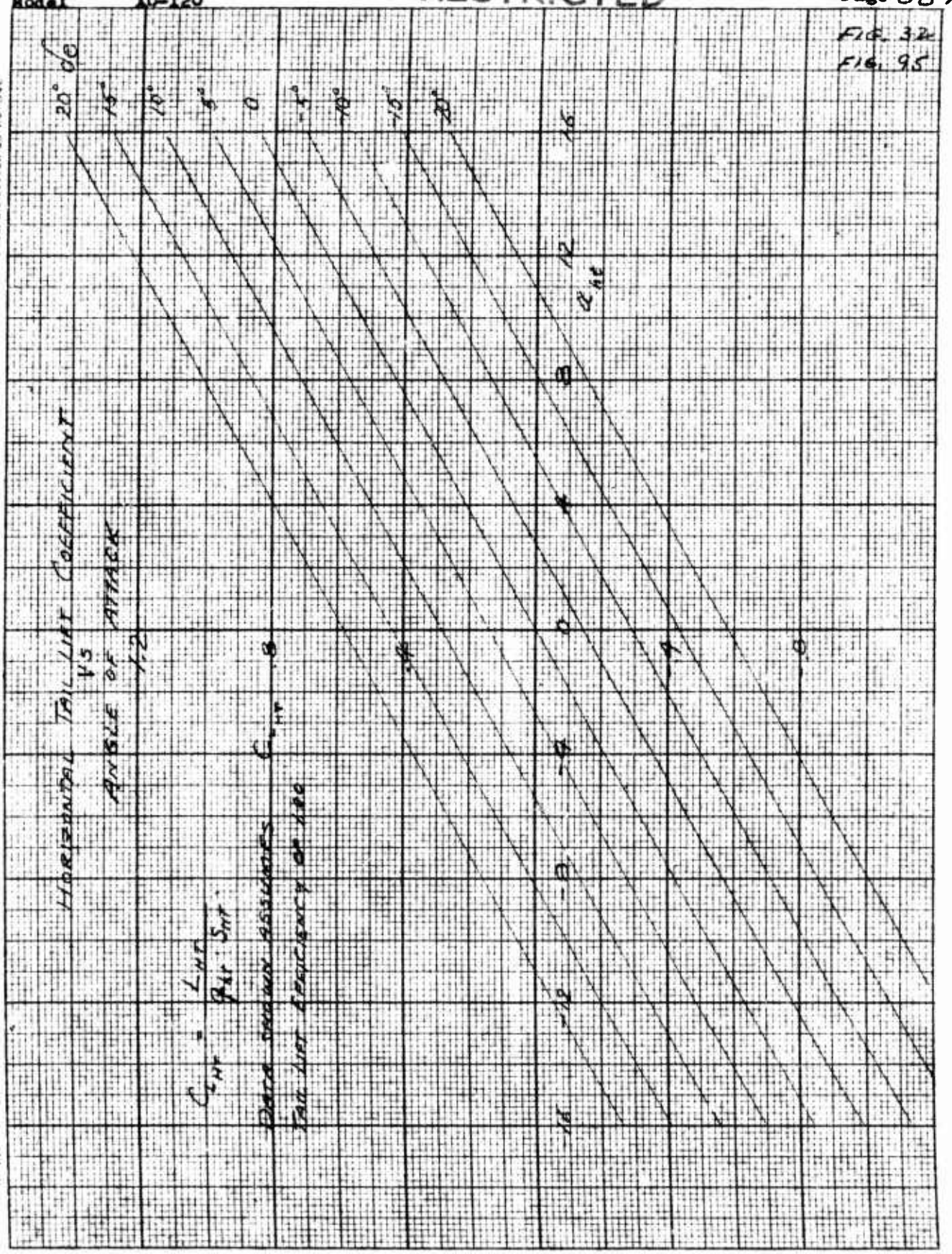
HORIZONTAL TAIL LIFT COEFFICIENT
VS
ANGLE OF ATTACK
$C_{L_{HT}} = \frac{L_{HT}}{q_{HT} S_{HT}}$
DATA REDUCED ASSUMING
TAIL LIFT EFFICIENCY OF 1.00
$C_{L_{HT}}$
α_{HT}
20° de
15°
10°
5°
0
-5°
-10°
-15°
-20°
1.2
.8
.4
0
-.4
-.8
-1.2
-1.6
.16
.12
.8
.4
0

PART II-A-7-c

c. Drag Analysis

It is the purpose of this section to determine the drag characteristics of the horizontal tail.

In determining this drag, the induced drag was first calculated for various α_{ht} and δ_e and then added to the profile drag for the same conditions of α_{ht} and δ_e to obtain the total drag.

Induced Drag

From reference (11) the induced drag is

$$C_{D_{I_{HT}}} = \frac{C_{L_{HT}}^2}{\pi A_{ht_u}} + C_{L_{HT}} \Delta c_{l_e} v + \Delta c_{l_e}^2 w$$

where u, v and w are factors obtained from figure 8 of reference (11)
and Δc_{l_e} is the increment of section lift coefficient due to elevator deflection.

$$\Delta c_{l_e} = c_{l_{\delta_e}} \times \delta_e = .0568 \delta_e$$

The effective aspect ratio of the horizontal tail for calculation of induced drag will not correspond to that for the lift analysis because of the end plate effect of the vertical fins on the center section.

For the Center Section between Fins

$$\left(C_{D_{I_{HT}}}\right)_f = \frac{\left(C_{L_{HT}}\right)_f^2}{A_{ht_f}} \times \frac{1}{1 + 1.66\left(\frac{R_{vt}}{b_{ht_f}}\right)} \quad \text{from reference (10)}$$

Assuming that the effectiveness of the fins as end plates is reduced by reason of their chord being less than that of the horizontal tail and that the effect varies linearly with values of this ratio from 1.0 to 0

$$\frac{c_{vtc}}{c_{ht}} = \frac{97.5}{117.75} = .827$$

$$\frac{R_{vt}}{b_{ht_f}} = .572$$

PART II-A-7 (Cont.)

Then

$$\left(\frac{B_{vt}}{b_{ht_f}}\right)_{effective} = .572 \times .827 = .473$$

$$A_{ht_f} = 2.96$$

$$\left(C_{D_{I_{HT}}}\right)_f = \frac{\left(C_{L_{HT}}\right)_f^2}{2.96} \times \frac{1}{1 + 1.66 \times .473}$$

$$\left(C_{D_{I_{HT}}}\right)_f = \frac{\left(C_{L_{HT}}\right)_f^2}{5.3}$$

If we set $\left(C_{D_{I_{HT}}}\right)_f = \dfrac{\left(C_{L_{HT}}\right)_f^2}{A_{ht_f\ effective}}$

Then $A_{ht_f\ effective} = 5.3$ (for drag analysis)

<u>For the Tip Sections</u>

As the end plate effect does not apply to the tip sections

$A_{ht\ effective} = 1.16$ (for lift and drag analysis)

$$\left(C_{D_{I_{HT}}}\right)_o = \frac{\left(C_{L_{HT}}\right)^2}{1.16}$$

<u>For the Complete Horizontal Tail</u>

If we set

$$\left(C_{D_{I_{HT}}}\right) = \frac{\left(C_{L_{HT}}\right)^2}{A_{ht\ effective}}$$

$A_{ht\ effective}$ is the effective aspect ratio of the horizontal tail for drag analysis

$$C_{D_{I_{HT}}} = \left(C_{D_{I_{HT}}}\right)_f + \left(C_{D_{I_{HT}}}\right)_o$$

where for any α_{ht}

PART II-A-7

$$C_{L_{HT_f}} = C_{L_{HT}} \left(\frac{.0580}{.0530} \times \frac{286.2}{346.2} \right)$$

$$C_{L_{HT_o}} = C_{L_{HT}} \left(\frac{.0294}{.0520} \times \frac{60}{346.2} \right)$$

Then

$$C_{D_{I_{HT}}} = \frac{C_{L_{HT}}^2 \left(\frac{.0580}{.0530} \times \frac{286.2}{346.2} \right)^2}{5.3} + \frac{C_{L_{HT}}^2 \left(\frac{.0294}{.0530} \times \frac{60}{346.2} \right)^2}{1.16}$$

$$C_{D_{I_{HT}}} = \frac{C_{L_{HT}}^2}{6.16}$$

and

$$A_{ht_{effective}} = 6.16 \quad \text{(for drag analysis)}$$

Assuming that the ratio of b_e(effective) to $b_{ht_f(effective)}$ will be the same as $\frac{b_e}{b_{ht_f}}$

$$b_{e_{effective}} = .87\ b_{ht_{f\ effective}}$$

$$b_{ht_{f\ effective}} = 5.3 \times 9.8125 = 52.0 \text{ ft.}$$

then

$$b_{e\ effective} = .87 \times 52.0 = 45.3 \text{ ft.}$$

$$B_{ht_{effective}} = 52.0 + 8.333 = 60.333 \text{ ft.}$$

$$\frac{b_e}{B_{ht}}_{effective} = \frac{45.3}{60.333} = .74$$

From figure 5 of reference (11) for a taper ratio of 1.0

$$u = .987$$
$$v = -.0052$$
$$w = .0064$$

PART II-A-7 (Cont.)

Then

$$C_{D_{I_{HT}}} = \left(\frac{C_{L_{HT}}}{6.16 \times .987}\right) + \left(C_{L_{HT}} \times .0568\,\delta_e \times (-.0052)\right) + \left((.0568\,\delta_e)^2 \times .0064\right)$$

$$C_{D_{I_{HT}}} = .0523\, C_{L_{HT}}^2 - .000295\, C_{L_{HT}}\,\delta_e + .000021\,\delta_e^2$$

Calculations of induced drag for various angles of attack and elevator deflections are made in the tables immediately following.

PART II-A-7

CALCULATION OF INDUCED DRAG $C_{D_{I_{HT}}}$

$$C_{D_{I_{HT}}} = .0523(C_{L_{HT}})^2 - .000295\, C_{L_{HT}}\, \delta_e + .000021\, \delta_e^2$$

$$C_{L_{HT}} = (.0530\,\alpha_{ht} + .0289\,\delta_e).85$$

$\delta_e = 0°$

α_{ht}	$C_{L_{HT}}$	$C_{L_{HT}}\delta_e$	$-.000295\, C_{L_{HT}}\delta_e$	$\overline{C_{L_{HT}}}^2$	$.0523(\overline{C_{L_{HT}}})^2$	$C_{D_{I_{HT}}}$
-11.2	-.5940	0	0	.3530	.0185	.0185
- 8.4	-.4450	0	0	.1980	.0104	.0104
-5.6	-.2970	0	0	.0881	.0046	.0046
-2.8	-.1485	0	0	.0221	.0012	.0012
0	0	0	0	0	0	0
2.8	.1485	0	0	.0221	.0012	.0012
5.6	.2970	0	0	.0881	.0046	.0046
11.2	.5940	0	0	.3530	.0185	.0185
14.0	.7425	0	0	.5510	.0288	.0288
16.8	.8910	0	0	.7939	.0415	.0415
19.6	1.040	0	0	1.0816	.0566	.0566

$\delta_e = 5°$

$.000021\, \delta_e^2 = .00053$

-11.2	-.4491	-2.2455	+.0007	+0.2017	.0105	.0117
- 8.4	-.3007	-1.5035	+.0004	+0.0904	.0047	.0056
-5.6	-.1523	-0.7615	+.0002	+0.0232	.0012	.0019
-2.8	-.0039	-0.0195	+.0000	+0.0000	.0000	.0005
0	+.1445	+0.7225	-.0002	+0.0209	.0011	.0014
2.8	+.2929	+1.4645	-.0004	+0.0858	.0045	.0046
5.6	+.4413	+2.2065	-.0007	+0.1947	.0102	.0100
8.4	+.5897	+2.9485	-.0009	+0.3477	.0182	.0178
11.2	+.7381	+3.6905	-.0011	+0.5448	.0285	.0279
14.0	+.8865	+4.4325	-.0013	+0.7859	.0411	.0403
16.8	+1.0349	+5.1745	-.0015	+1.0710	.0560	.0550
19.6	+1.1833	+5.9165	-.0017	+1.4002	.0732	.0720

PART II-A-7

CALCULATION OF INDUCED DRAG (Cont.)

$\delta_e = 10°$

$.000021\,\delta_e^2 = .0021$

α_{ht}	$C_{L_{HT}}$	$C_{L_{HT}}\delta_e$	$-.000295\,C_{L_{HT}}\delta_e$	$\overline{C_{L_{HT}}}^2$	$.0523(C_{L_{HT}})^2$	$C_{D_{I_{HT}}}$
-11.2	-.3046	-3.0460	+.0009	+0.0928	.0048	.0078
- 8.4	-.1562	-1.5620	+.0005	+0.0244	.0013	.0039
- 5.6	-.0078	-0.0780	+.0002	+0.0001	.0000	.0023
- 2.8	+.1406	+1.4060	-.0004	+0.0198	.0010	.0027
0	+.2890	+2.8900	-.0009	+0.0835	.0044	.0056
2.8	+.4374	+4.3740	-.0013	+0.1913	.0100	.0108
5.6	+.5858	+5.8580	-.0017	+0.3432	.0179	.0183
8.4	+.7342	+7.3420	-.0022	+0.5390	.0282	.0281
11.2	+.8826	+8.8260	-.0026	+0.7790	.0407	.0402
14.0	+1.0310	+10.3100	-.0030	+1.0630	.0556	.0547
16.8	+1.1794	+11.7940	-.0035	+1.3310	.0727	.0713
19.6	+1.3278	+13.2780	-.0039	+1.7631	.0922	.0904

$\delta_e = -5°$

$.000021\,\delta_e^2 = .00053$

-11.2	-.7381	+3.6905	-.0011	+0.5448	.0285	.0279
- 8.4	-.5897	+2.9485	-.0009	+0.3477	.0182	.0178
- 5.6	-.4413	+2.2065	-.0007	+0.1947	.0102	.0100
- 2.8	-.2929	+1.4645	-.0004	+0.0858	.0045	.0046
0	-.1445	+0.7225	-.0002	+0.0209	.0011	.0014
2.8	+.0039	-0.0195	+.0000	+0.0000	.0000	.0005
5.6	+.1523	-0.7615	+.0002	+0.0232	.0012	.0019
8.4	+.3007	-1.5035	+.0004	+0.0904	.0047	.0056
11.2	+.4491	-2.2455	+.0007	+0.2017	.0105	.0117
14.0	+.5975	-2.9875	+.0009	+0.3570	.0187	.0201
16.8	+.7459	-3.7295	+.0011	+0.5564	.0291	.0307
19.6	+.8943	-4.4715	+.0013	+0.7998	.0418	.0436

PART II-A-7

CALCULATION OF INDUCED DRAG (Cont.)

$\delta_e = -10°$

$.000021\ \delta_e^2 = .0021$

α_{ht}	$C_{L_{HT}}$	$C_{L_{HT}}\ \delta_e$	$-.000295\ C_{L_{HT}}\ \delta_e$	$\overline{C_{L_{HT}}}^2$	$.0523(\overline{C_{L_{HT}}})^2$	$C_{D_{I_{HT}}}$
-11.2	-.8830	8.830	-.0026	.7805	.0408	.0403
- 8.4	-.7340	7.340	-.0022	.5399	.0283	.0282
- 5.6	-.5860	5.860	-.0017	.3430	.0180	.0184
- 2.8	-.4375	4.375	-.0013	.1915	.0103	.0111
0	-.2890	2.890	-.0009	.0835	.0044	.0056
2.8	-.1405	1.405	-.0004	.0197	.0010	.0027
5.6	+.0080	-.080	0	.0001	0	.0021
8.4	.1560	-1.560	.0005	.0243	.0013	.0039
11.2	.3050	-3.050	.0009	.0930	.0049	.0079
14.0	.4535	-4.535	.0013	.2060	.0108	.0142
16.8	.6020	-6.020	.0018	.3620	.0190	.0229
19.6	.7510	-7.510	.0022	.5640	.0295	.0338

$\delta_e = -15°$

$.000021\ \delta_e^2 = .0047$

-11.2	-1.0275	15.40	-.0045	1.055	.0552	.0554
- 8.4	- .8785	13.18	-.0039	.7710	.0403	.0411
- 5.6	- .7305	10.96	-.0032	.5330	.0279	.0294
- 2.8	- .5820	8.73	-.0026	.3380	.0177	.0198
0	- .4335	6.51	-.0019	.1880	.0098	.0126
2.8	- .2850	4.275	-.0013	.0811	.0042	.0076
5.6	- .1365	2.048	-.0006	.0186	.0010	.0051
8.4	.0115	- .1725	.0001	.0001		.0048
11.2	.1605	-2.406	.0007	.0257	.0014	.0068
14.0	.3090	-4.635	.0014	.0954	.0095	.0156
16.8	.4575	-6.860	.0020	.2095	.0110	.0177
19.6	.6065	-9.100	.0027	.3675	.0192	.0266

PART II-A-7

CALCULATION OF INDUCED DRAG (Cont.)

$\delta_e = -20°$ $.000021\ \delta_e^2 = .0084$

α_{ht}	$C_{L_{HT}}$	$C_{L_{HT}}\delta_e$	$-.000295\ C_{L_{HT}}\delta_e$	$C_{L_{HT}}^2$	$.0523(C_{L_{HT}})^2$	$C_{D_{I_{HT}}}$
-11.2	-1.1720	+23.4400	-.0069	+1.3736	.0718	.0733
- 8.4	-1.0230	+20.4600	-.0060	+1.0465	.0547	.0571
- 5.6	- .8750	+17.5000	-.0052	+0.7656	.0400	.0432
- 2.8	- .7265	+14.5300	-.0043	+0.5278	.0276	.0317
0	-. 5780	+11.5600	-.0034	+0.3341	.0175	.0225
2.8	- .4295	+ 8.5900	-.0025	+0.1845	.0096	.0155
5.6	- .2810	+ 5.6200	-.0017	+0.0790	.0041	.0108
8.4	- .1330	+ 2.6600	-.0008	+0.0177	.0009	.0085
11.2	.0160	- 0.3200	+.0001	+0.0003	.0000	.0085
14.0	.1645	- 3.2900	+.0010	+0.0271	.0014	.0108
16.8	.3130	- 6.2600	+.0018	+0.0980	.0051	.0153
19.6	.462	- 9.2400	+.0027	+0.2134	.0112	.0223

$\delta_e = -25°$ $.000021\ \delta_e^2 = .0131$

-11.2	-1.3165	+26.3300	-.0078	1.730	.0905	.0958
- 8.4	-1.1675	+23.3500	-.0069	1.360	.0712	.0774
- 5.6	-1.0195	+20.3900	-.0060	1.035	.0542	.0613
- 2.8	- .8710	+17.4200	-.0051	.758	.0397	.0477
0	- .7225	+14.4500	-.0043	.521	.0272	.0360
2.8	- .5740	+11.4800	-.0034	.329	.0172	.0269
5.6	- .4255	+ 8.5100	-.0025	.181	.0095	.0201
8.4	- .2775	+ 5.5500	-.0016	.077	.0043	.0158
11.2	- .1285	+ 2.5700	-.0008	.016	.0008	.0131
14.0	.0200	- 0.4000	+.0001	.0004	0	.0132
16.8	.1685	- 3.3700	+.0010	.0284	.0015	.0156
19.6	.3175	- 6.3500	+.0019	.1005	.0053	.0203

PART II-A-7

Profile Drag

The profile drag of the horizontal tail has been determined in Part II-A-7 of reference (1) for various angles of attack of the horizontal tail and elevator deflection.

PART II-A-7

Total Horizontal Tail Drag

The total horizontal tail drag is obtained by the addition of induced and profile drag as shown in the following table.

Figure 96 presents a plot of total horizontal tail drag versus angle of attack of the horizontal tail for various elevator deflections.

PART II-A-7-c

TOTAL HORIZONTAL DRAG

$\delta_e = 0°$

α_{ht}	$C_{D_{o_{HT}}}$	$C_{D_{I_{HT}}}$	$C_{D_{HT}}$
-11.2	.0096	.0185	.0281
- 8.4	.0089	.0104	.0193
- 5.6	.0085	.0046	.0131
- 2.8	.0082	.0012	.0094
0	.0081	0	.0081
2.8	.0082	.0012	.0094
5.6	.0085	.0046	.0131
8.4	.0089	.0104	.0193
11.2	.0096	.0185	.0281
14.0	.0106	.0288	.0394
16.8	.0121	.0415	.0536
19.6	.0145	.0566	.0711

$\delta_e = 5°$

α_{ht}	$C_{D_{o_{HT}}}$	$C_{D_{I_{HT}}}$	$C_{D_{HT}}$
-11.2	.0090	.0117	.0207
- 8.4	.0085	.0056	.0141
- 5.6	.0084	.0019	.0103
- 2.8	.0090	.0005	.0095
0	.0096	.0014	.0110
2.8	.0112	.0046	.0158
5.6	.0126	.0100	.0226
8.4	.0135	.0178	.0313
11.2	.0154	.0279	.0433
14.0	.0173	.0403	.0576
16.8	.0187	.0550	.0737
19.6	.0211	.0720	.0931

$\delta_e = 10°$

-11.2	.0087	.0078	.0165
- 8.4	.0085	.0039	.0124
- 5.6	.0090	.0023	.0113
- 2.8	.0108	.0027	.0135
0	.0145	.0056	.0201
2.8	.0176	.0108	.0284
5.6	.0206	.0183	.0389
8.4	.0231	.0281	.0511
11.2	.0257	.0402	.0659
14.0	.0273	.0547	.0820
16.8	.0294	.0713	.1007
19.6	.0317	.0904	.1221

$\delta_e = -5°$

-11.2	.0154	.0279	.0433
- 8.4	.0135	.0178	.0313
- 5.6	.0126	.0100	.0226
- 2.8	.0112	.0046	.0158
0	.0096	.0014	.0110
2.8	.0090	.0005	.0095
5.6	.0084	.0019	.0103
8.4	.0085	.0056	.0141
11.2	.0090	.0117	.0207
14.0		.0201	
16.8		.0307	
19.6		.0436	

PART II-A-7-c

TOTAL HORIZONTAL DRAG (Cont.)

$\delta_e = -10°$

α_{ht}	$C_{D_{o_{HT}}}$	$C_{D_{I_{HT}}}$	$C_{D_{HT}}$
-11.2	.0257	.0403	.0660
- 8.4	.0230	.0282	.0512
- 5.6	.0201	.0184	.0385
- 2.8	.0176	.0111	.0287
0	.0145	.0056	.0201
2.8	.0108	.0027	.0135
5.6	.0090	.0021	.0111
8.4	.0085	.0039	.0124
11.2	.0087	.0079	.0166

$\delta_e = -15°$

α_{ht}	$C_{D_{o_{HT}}}$	$C_{D_{I_{HT}}}$	$C_{D_{HT}}$
-11.2	.0379	.0554	.0933
- 8.4	.0349	.0411	.0760
- 5.6	.0320	.0294	.0614
- 2.8	.0280	.0198	.0478
0	.0228	.0126	.0354
2.8	.0169	.0076	.0245
5.6	.0122	.0051	.0173
8.4	.0100	.0048	.0148
11.2	.0092	.0068	.0160

$\delta_e = -20°$

α_{ht}	$C_{D_{o_{HT}}}$	$C_{D_{I_{HT}}}$	$C_{D_{HT}}$
-11.2	.0511	.0733	.1244
- 8.4	.0482	.0571	.1053
- 5.6	.0455	.0432	.0887
- 2.8	.0421	.0317	.0738
0	.0385	.0225	.0610
2.8	.0344	.0155	.0499
5.6	.0300	.0108	.0408
8.4	.0246	.0085	.0351
11.2	.0195	.0085	.0280

$\delta_e = -25°$

α_{ht}	$C_{D_{o_{HT}}}$	$C_{D_{I_{HT}}}$	$C_{D_{HT}}$
2.8	.0500	.0269	.0769
5.6	.0459	.0201	.0660
8.4	.0404	.0158	.0562
11.2	.0346	.0131	.0477

RESTRICTED

FIG 96

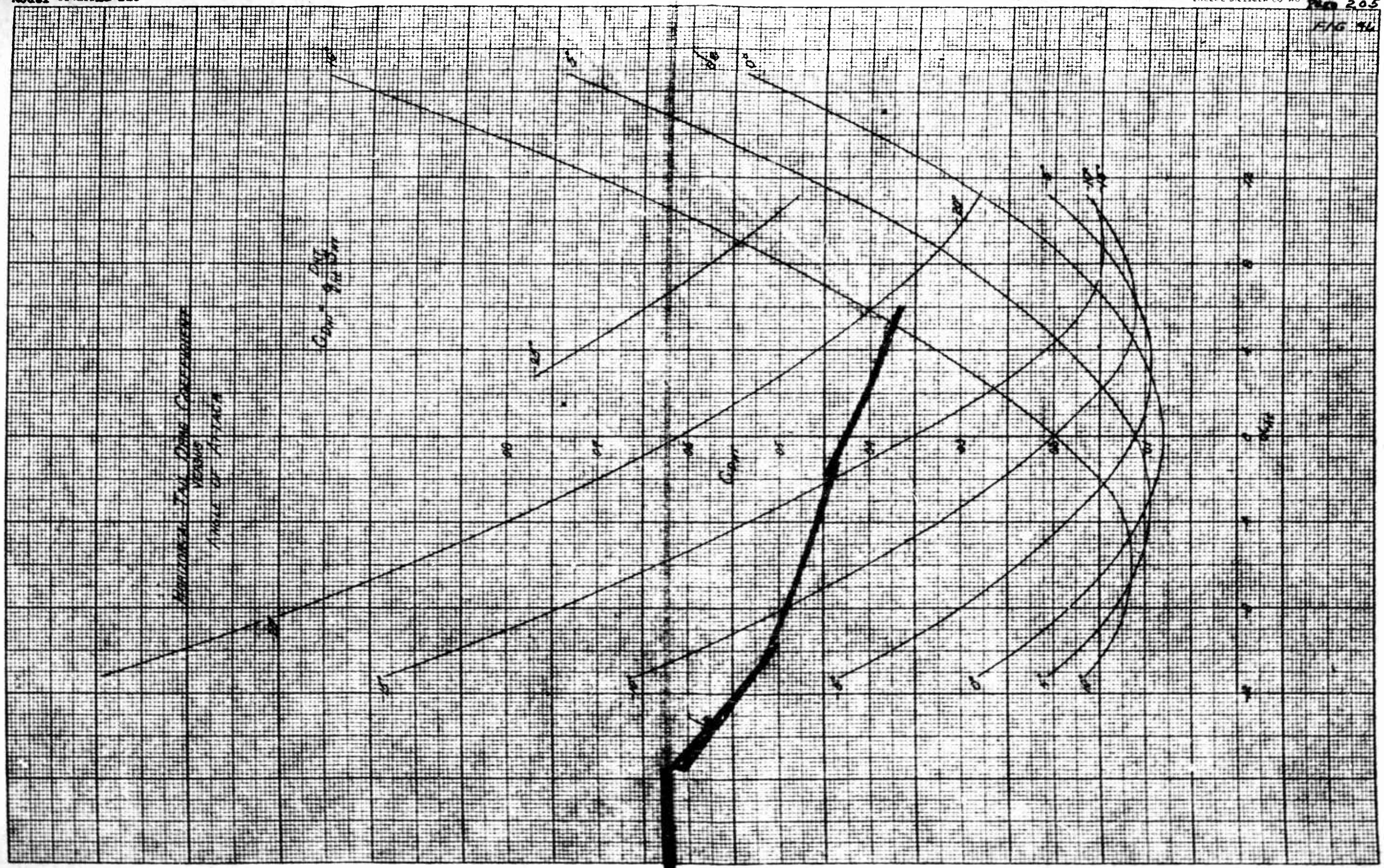

PART II-A-7

d. Polar Diagram

Figure 97 on the following page presents horizontal tail polar diagrams for various elevator deflections.

FIG 33
FIG 97

POLAR DIAGRAM OF HORIZONTAL TAIL

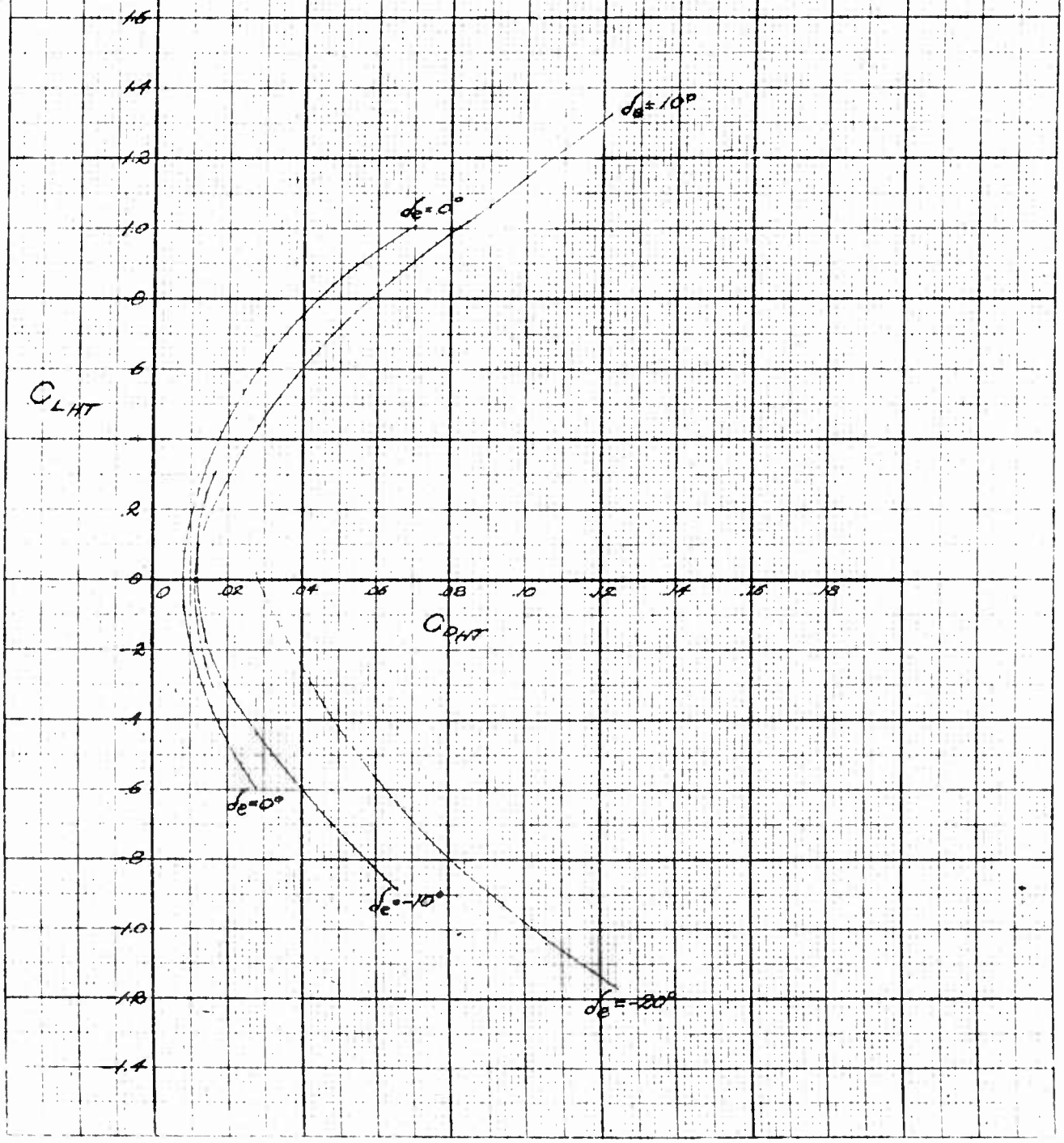

PART II-A-7-e

e. Aerodynamic Force Coefficients

The aerodynamic force coefficients $C_{X_{HT}}$ and $C_{Z_{HT}}$ are assumed to be numerically equal to $C_{D_{HT}}$ and η_{ht} $C_{L_{HT}}$ respectively. This approximation is experimentally justified and considerably reduces the amount of labor required to balance the complete airplane.

PART II-A-7-f

f. Pitching Moment about Aerodynamic Center

From available data the aerodynamic center location of the horizontal tail, flapped or unflapped, is estimated to be located at .25 c_{ht}.

For the flapped section between the fins:

For a symmetrical airfoil the section pitching moment with elevators neutral is zero.

Section pitching moments due to elevator deflection are obtained from figure 1 reference (8) for $\frac{c_e}{c_{ht}} = .325$

$c_{m_{\delta_e}} = -.0031 \quad \alpha_{\delta_e} = +.60 \quad \frac{c_{m_{\delta_e}}}{\alpha_{\delta_e}} = -.0135$

Since $c_{m_{\delta_e}}$ and α_{δ_e} are closely related, the previously determined α_{δ_e} for $\frac{c_e}{c_{e_b}} = .325 \quad \frac{c_{e_b}}{c_e} = .370$ and open gap is used to estimate $c_{m_{\delta_e}}$.

$$c_{m_{ht_{\delta_e}}} = -.0135 \times +.682 = -.0092$$

Correcting to three dimensional data by the method of reference (11) where

$$C_{M_{HT_{\delta_e}}} = I \; c_{m_{ht_{\delta_e}}}$$

$I = .956$ figure 7 reference (11) for $A_{ht_f} = 2.96$

$b_e/b_{ht_f} = .87$

$$C_{M_{HT_{\delta_e}}} = .956 \times -.0092$$

$$C_{M_{HT_{\delta_e}}} = -.0088$$

For the tip section outboard of the fins:

The pitching moment of an unflapped symmetrical airfoil is equal to zero

For the complete horizontal tail:

Taking a weighted average based on areas we obtain

$$C_{M_{HT_{\delta_e}}} = \frac{-.0088 \times 286.2}{346.2} = -.0073$$

Figure 98 presents a plot of $C_{M_{HT}}$ versus α_{ht} for various δ_e.

FIG 34
FIG 98

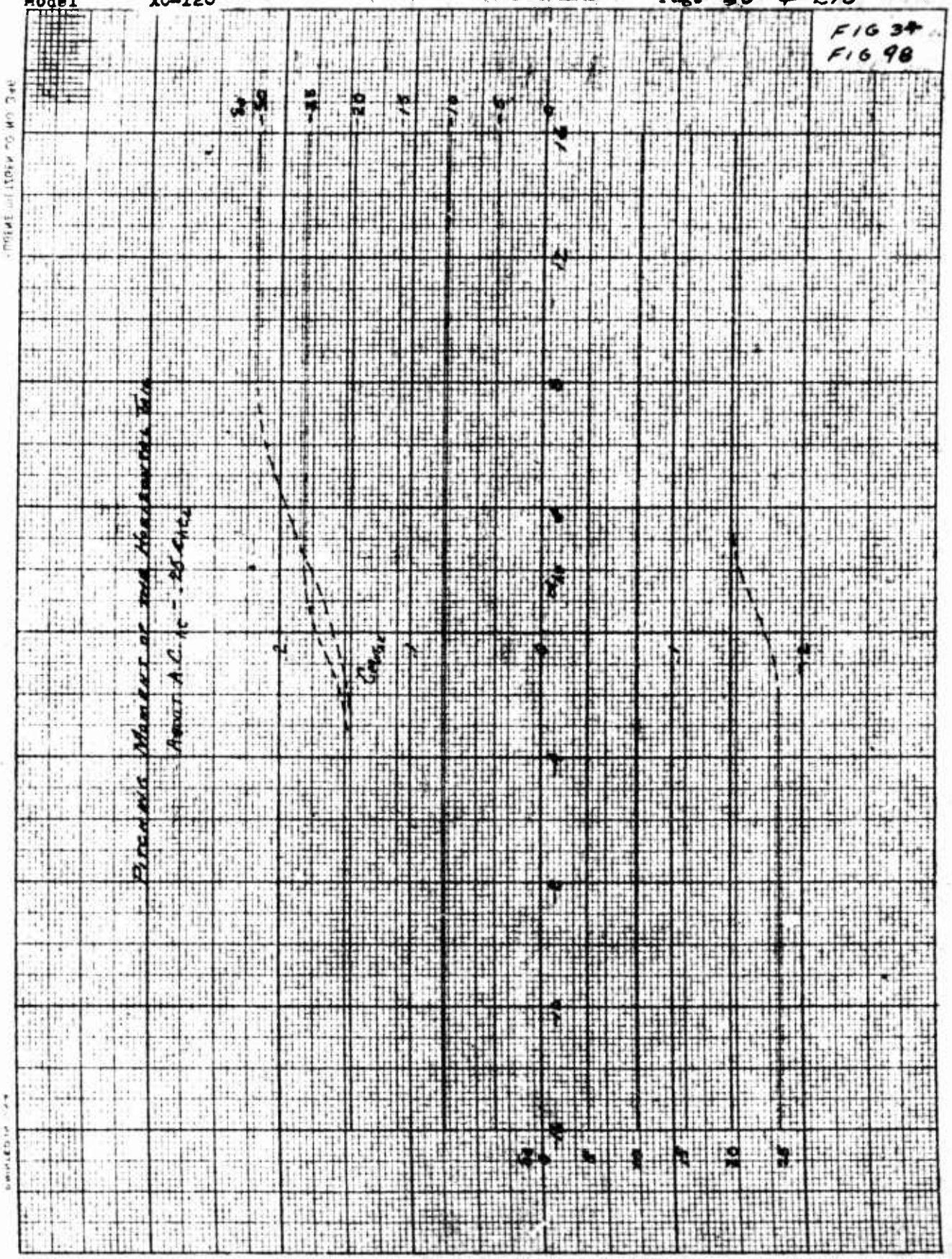
Pressure Measurement on Tail Horizontal Tail
About A.C. - 25 chord

PART II-A-7

g. Yawing Moment

It is assumed that the horizontal tail yawing moment due to yaw is negligible.

PART II-A-7-h

h. Downwash and Dynamic Pressure Ratio

The value of the downwash was calculated in the same manner as in reference (1). The computations are shown in the table immediately following. The geometric relationship of the horizontal tail to the wing is shown in figure 99. The incidence of the horizontal tail to the thrust line is 1.0 degree, so that the angle of attack of the horizontal tail is

$$\alpha_{ht} = \alpha_{TL} + 1.0^\circ - \epsilon_{ave}$$

The upper edge of the wing wake is always below the horizontal tail, so that

$$q_{ht}/q = 1.00$$

at all times, power off.

The variation in angle of attack of the horizontal tail with angle of attack of the thrust line is shown in figures 100 and 101 for flaps retracted and extended, respectively.

COMPUTATION OF POWER-OFF DOWNWASH

	α_{TL}	C_{L_W}	θ	$\sin\theta$	σ_{ht}	$\alpha_{\ell_{eq}}$	$\sin\alpha_{\ell_{eq}}$	d	$\Delta C_{L_{WF}}$	$C_{L_W}+\Delta C_{L_{WF}}$	e	Δe_f
Flaps Up	3.75	1.00	2.83	.0495	.0427	10.75	.1865	-.0418	0	1.00	-.0695	0
	-12.15	0	-13.07	-.2260	-.195	-5.15	-.0899	.0199	.338	-.338	.0285	-.0534
	-7.40	.4	-8.32	-.1447	-.125	-.40	-.0070	.0016	.338	.062	-.0045	-.0534
Flaps Down	-2.65	.8	-3.57	-.0624	-.0539	4.35	.0760	-.0170	.338	.462	-.0322	-.0534
	2.10	1.2	1.18	.0206	.0178	9.10	.1582	-.0354	.338	.862	-.0600	-.0534
	6.85	1.6	5.93	.1032	.0891	13.85	.2395	-.0536	.338	1.262	-.0878	-.0534

α_{TL}	m	ϵ_{ℓ_W}	ϵ_{ℓ_f}	ϵ_ℓ	ϵ_{AVE}
3.75	-.0876	5.2	0	5.2	4.9
-12.15	-.2240	-1.5	3.0	1.5	1.5
-7.40	-.2001	.9	2.1	3.4	3.5
-2.65	-.1755	2.1	2.3	5.4	5.5
2.10	-.1500	4.1	3.5	7.6	7.7
6.85	-.1247	6.2	3.7	9.9	10.1

GEOMETRIC RELATIONSHIP OF HORIZONTAL TAIL TO CENTERLINE OF WAKE

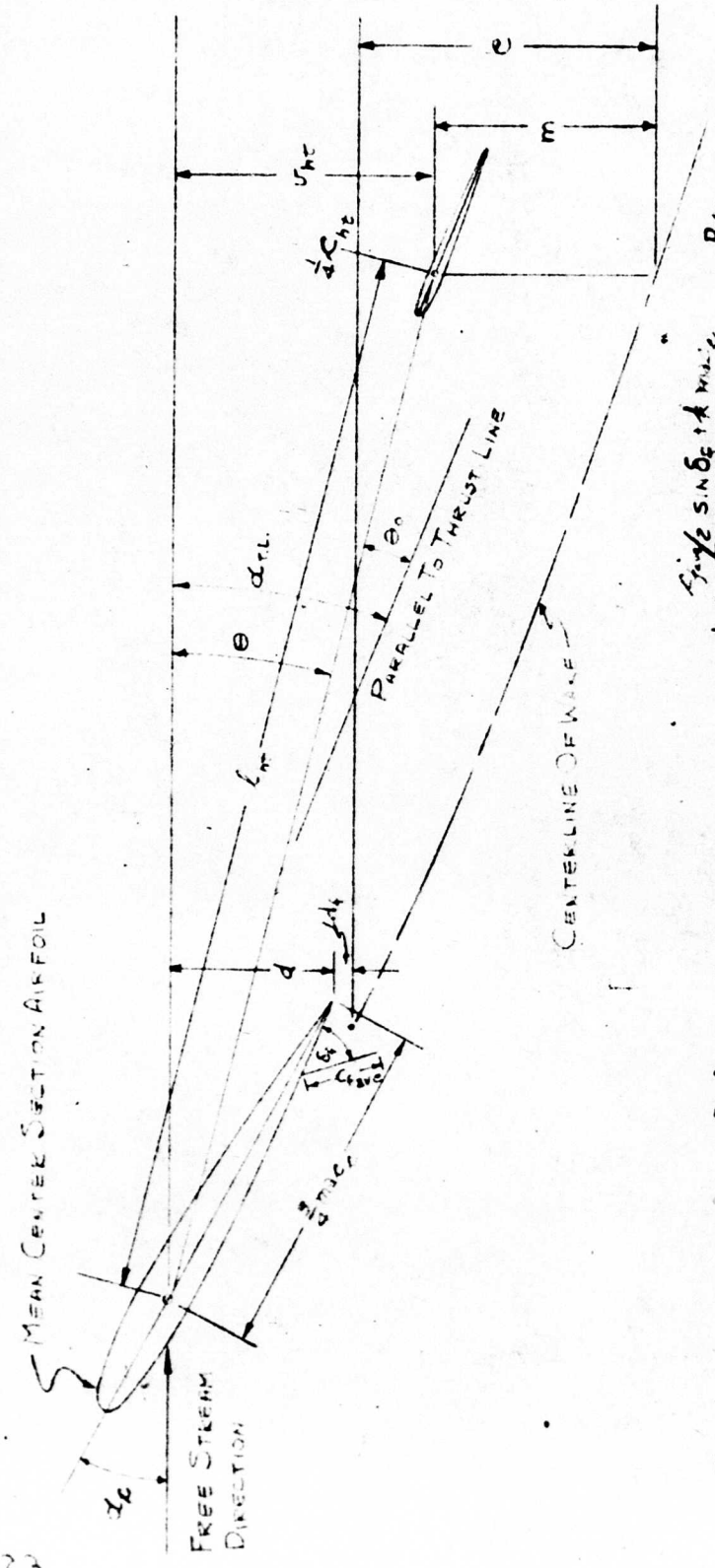

$\Delta d_f = \frac{f_{avg}\frac{1}{2}\sin\delta_f + f_{max}}{B_w/2} = -.02\,\frac{B_w}{2}$

$k = -.018$ FROM FIG. 18 OF REF. 6

$d = -\frac{3}{4}\,m\,\alpha_c$

$u_h = l_{hc} \times \sin\theta$

e FROM CHARTS OF REF 6

$m = d + \Delta d_f + e - u_h$

α_{TL} ~ ANGLE OF ATTACK OF THRUST LINE

$\alpha_c = \alpha_{TL} + 7°$ ~ ANGLE OF ATTACK OF MEAN C.S. CHORD

$\theta_0 = -.92°$

$\theta = \theta_0 + \alpha_{TL}$

B ~ SPAN WING

$l_{hc} = .87\,B_w/2$ ~ HORIZONTAL TAIL LENGTH

$\frac{3}{4}C_{hc} = .23\,B_w/2$

$C_{f\,avg} = .07\,B_w/2$

$\delta_f = 40°$

RESTRICTED

FIG. 35
FIG. 100

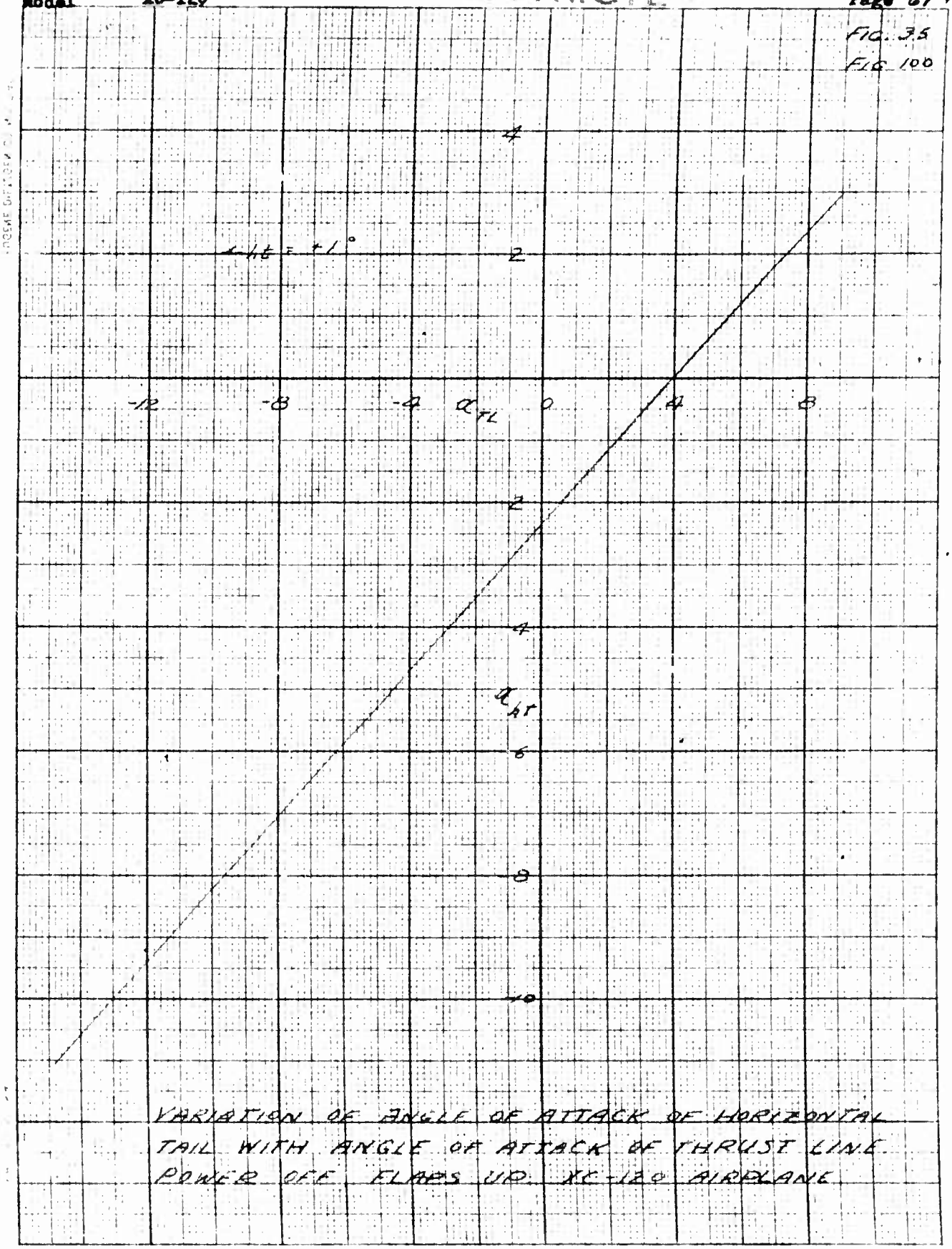

VARIATION OF ANGLE OF ATTACK OF HORIZONTAL TAIL WITH ANGLE OF ATTACK OF THRUST LINE POWER OFF FLAPS UP XC-120 AIRPLANE

FIG. 36
FIG. 101

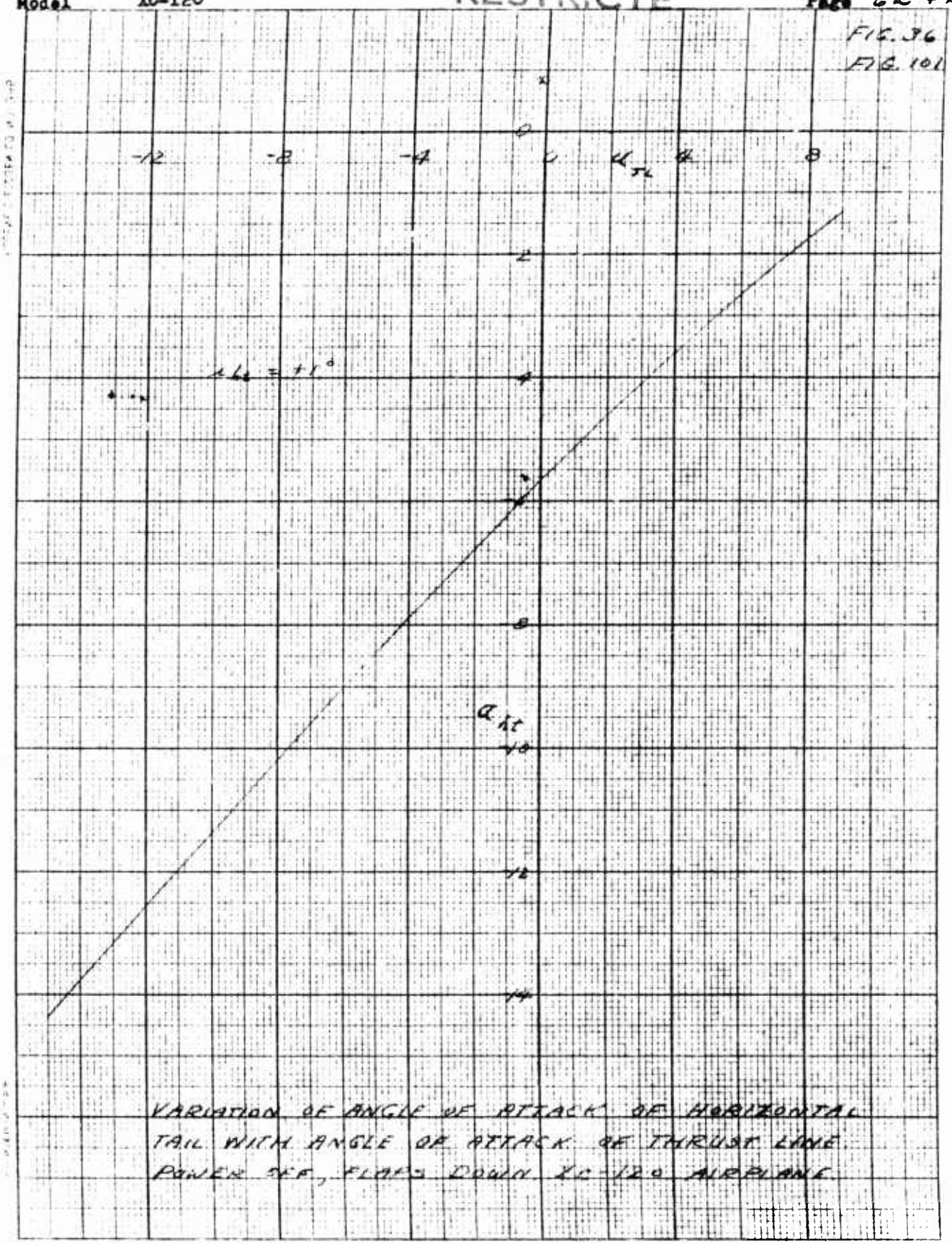

VARIATION OF ANGLE OF ATTACK OF HORIZONTAL TAIL WITH ANGLE OF ATTACK OF THRUST LINE. POWER OFF, FLAPS DOWN XC-120 AIRPLANE

PART II-A-7-1

1. **Elevator Hinge Moments**

In order to check the computed values of the hinge moment parameters, the results of flight tests are analyzed.

These data were obtained from reference (12). The airplane was flown with engines idling ($T_c = 0$), and flaps and gear down.

The wheel force is given by

$$F_w = .359\ \overline{c_e}^2\ b_e\ q_{ht}\ (C_{H_e\delta_e}\delta_e + C_{H_e\alpha_{ht}}\alpha_{ht})$$

where

.359 = elevator movement in radians per foot of wheel movement for C-119A (M-105) airplane.

$\overline{c_e}$ = 38.25 inches, root mean square elevator chord

b_e = 289 inches, elevator span of C-119A airplane

q_{ht} = dynamic pressure at tail, taken to be equal to free stream q.

Let $C_{H_e} = (C_{H_e\delta_e}\delta_e - C_{H_e\alpha_{ht}}\alpha_{ht})$

$$F_w = .359\ \frac{\overline{38.25}^2 \times 289}{1728}\ q_{ht}\ C_{H_e}$$

$$C_{H_e} = .01138\ \frac{F_w}{q_{ht}}$$

$$C_{H_e\alpha_{ht}} = \frac{C_{H_e}}{\alpha_{ht}} - \frac{C_{H_e\delta_e}\delta_e}{\alpha_{ht}}$$

Since C_{H_e} can be defined from the wheel force and the speed, and δ_e is known, it remains only to obtain α_{ht} in order to relate $C_{H_e\delta_e}$ and $C_{H_e\alpha_{ht}}$. There will be one such straight line relationship of the two parameters for each value of force and speed. By plotting several of these relationships, a series of lines will be obtained whose point of intersection determine the absolute values of the parameters.

PART II-A-7-i

The necessary values of α_{ht} for the C-119A airplane are determined from the estimated values of Part II-A-7-h, reference (1).

Two additional check points from reference (13) are also computed.

These were stall tests for which stick force, elevator position, and trim tab setting were observed. The elevator positions were corrected to effective (from the standpoint of hinge moments) elevator positions at zero tab deflection from data on the effectiveness of the tab in reducing stick forces.

The aforementioned data furnished eight lines, each representing the values of $C_{H_e\delta_e}$ and $C_{H_e\alpha_{ht}}$ that would satisfy one of the observed datum. They should all intersect in one point which should then represent the actual values of the hinge moment parameters. These data are plotted in figure 100. Although they do not intersect at a point due to accumulative inaccuracies in measurement, they do define a small area quite well. In particular, those data taken at low speed where the angle of attack of the tail is small define the value of $C_{H_e\delta_e}$ well, while those data taken at the higher speeds with small elevator deflections define $C_{H_e\alpha_{ht}}$ well. The encircled point represents the estimate of the value of $C_{H_e\delta_e}$ and $C_{H_e\alpha_{ht}}$ which is believed to best fit all of the observed data. The other point, enclosed in a triangle, represents the value of the parameters as estimated from section data. It is felt that the flight test data are the more reliable and indicative, so that the values of the hinge moment parameters used in this report are taken to be defined by them.

$$\frac{d\,C_{H_e}}{d\,\delta_e} = -.0015$$

$$\frac{d\,C_{H_e}}{d\,\alpha_{ht}} = -.0007$$

Figure 101 shows the variation of elevator hinge moment coefficient with elevator deflections and with angle of attack of the horizontal tail.

RESTRICTED

Subject:— BASIC AERODYNAMIC DATA

	$V\sqrt{\sigma}$	q	Wheel Force	δ_e	$\delta_{e_{tt}}$	Eff. δ_e	α_{ht}	C_{H_e}	$\frac{C_{H_e}}{\alpha_{ht}}$	$\delta_{e_{Eff.}}/\alpha_{ht}$
Configuration L = 55,000#	131	44.0	0	1.4	0	1.4	-5.55	0	0	-.2520
	120.5	37.1	15	-.7	0	-.7	-4.58	.00460	-.001004	.1527
	110	31.0	24	-2.8	0	-2.8	-3.46	.00882	-.00255	.810
	100	25.6	30	-6.5	0	-6.5	-1.90	.01334	-.00703	3.42
	95	23.1	33	-9.7	0	-9.7	- .94	.01627	-.01730	10.32
	93	22.1	47	-13.1	0	-13.1	- .50	.02420	-.04840	26.20
Configuration L = 49,783#	83	17.63	45	-15.3	-1.0	-16.69	.76	.02910	.0383	-.2197
Configuration L = 49,783#	75	14.40	20	-4.4	-2.5	-7.87	-2.22	.01583	-.00713	3.55

FIG 102

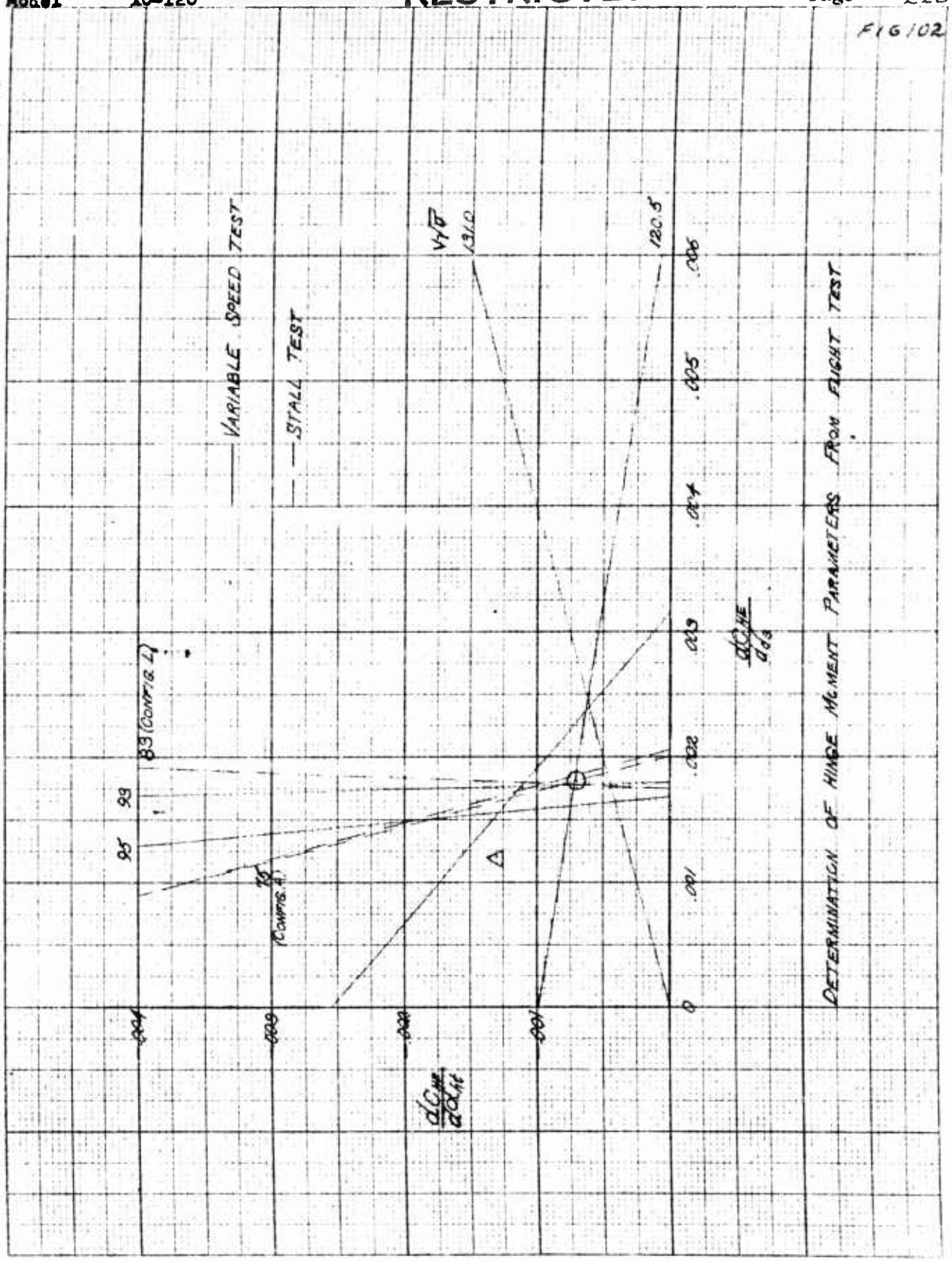

DETERMINATION OF HINGE MOMENT PARAMETERS FROM FLIGHT TEST

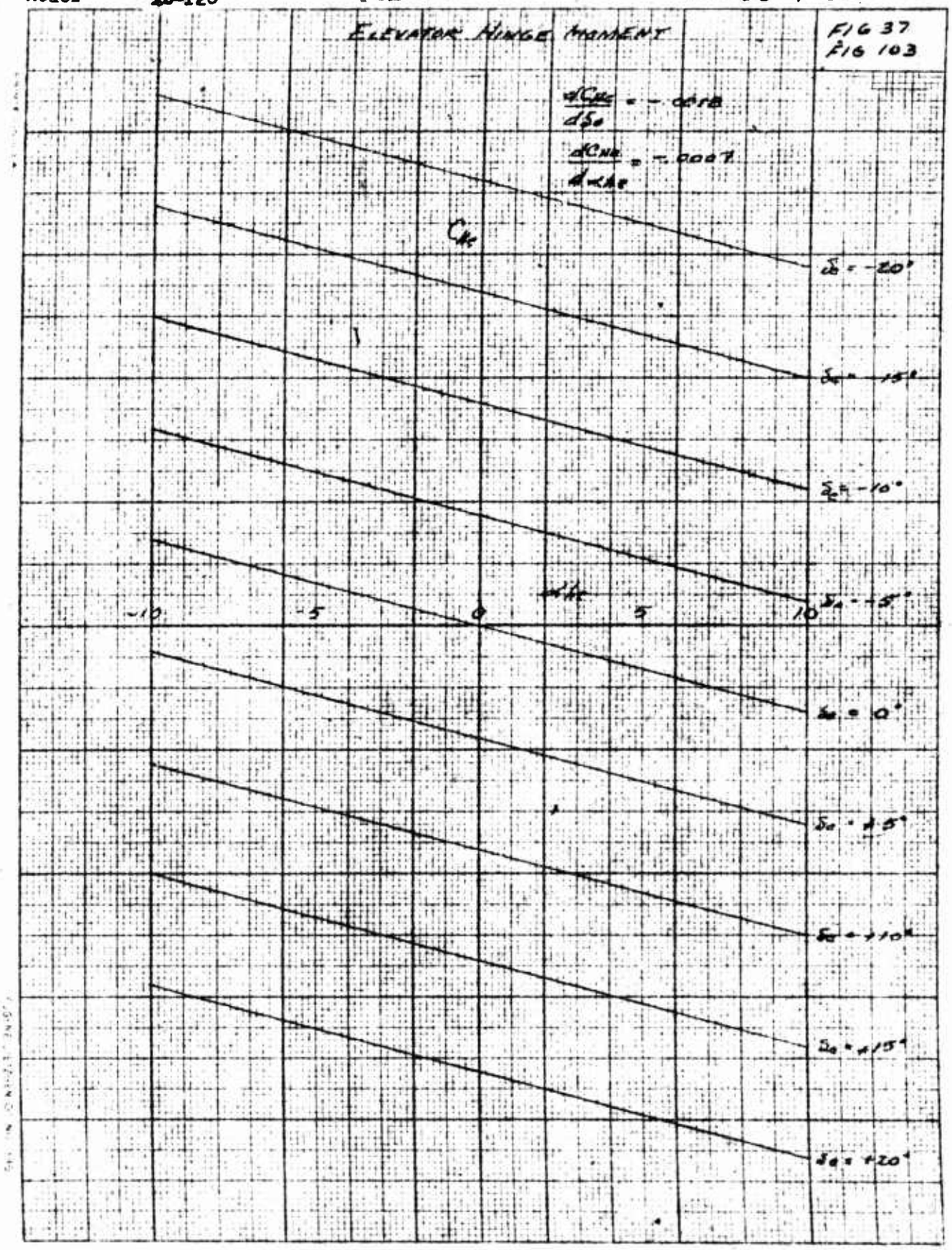
ELEVATOR HINGE MOMENT
FIG 37
FIG 103
dCHe/dδe = -.0418
dCHe/dαHe = -.0007
CHe
δe = -20°
δe = -15°
δe = -10°
δe = -5°
δe = 0°
δe = +5°
δe = +10°
δe = +15°
δe = +20°
αHe
-10
-5
0
5
10

PART II-A-5

8. ELEVATOR TABS

Since the elevator tabs are identical to those on the C-119B airplane, all calculations and figures presented in Part II-A-5, reference (1), apply to the XC-120 airplane.

All aerodynamic coefficients are based on tab area, elevator area or horizontal tail area depending upon the item affected by the tab. For convenience, the important tab characteristics are tabulated below as well as being shown graphically in the summary section.

ELEVATOR TAB AERODYNAMIC CHARACTERISTICS

SYMBOL	ITEM	TRIM TAB	SPRING TAB
$C_{L_{HT}\delta_{e\ tab}}$	$d\,C_{L_{HT}}/d\,\delta_{e\ tab}$	.00235	.00172
$C_{H_{e}\delta_{e\ tab}}$	$d\,C_{H_e}/d\,\delta_{e\ tab}$	-.0034	-.0025
$C_{H_{e\ tab}}/\delta_{e\ tab}$	$d\,C_{H_{e\ tab}}/d\,\delta_{e\ tab}$	-.0060	-.0060
$\alpha_{ht\,\delta_{e\ tab}}$	$d\alpha_{ht}/d\,\delta_{e\ tab}$	-.0385	-.0275

PART II-A-9

9. Vertical Tail

It is the purpose of this section to determine the aerodynamic characteristics of the vertical tail of the Model XC-120 airplane, power-off.

The characteristics as determined herein are the results of calculations and/or wind tunnel data. All coefficients are for one vertical tail and are based on one vertical tail area and/or chord and are presented versus the angle of attack of the vertical tail.

The final vertical tail characteristics may be found in the following figures or sections.

Lift	Figure 105
Drag	Figure 106
Polar Diagram	Figure 107
Force Coefficients	See discussion Section e
Yawing Moments	Figure 108
Dynamic Pressure	See discussion Section g
Sidewash	Figure 109
Rudder Hinge Moments	Figure 43

PART II-A-9

a. Vertical Tail Drawing

Figure 104 presents a drawing of one complete vertical tail less tabs. Pertinent dimensions used in this analysis are shown on the drawing.

FIG. 104

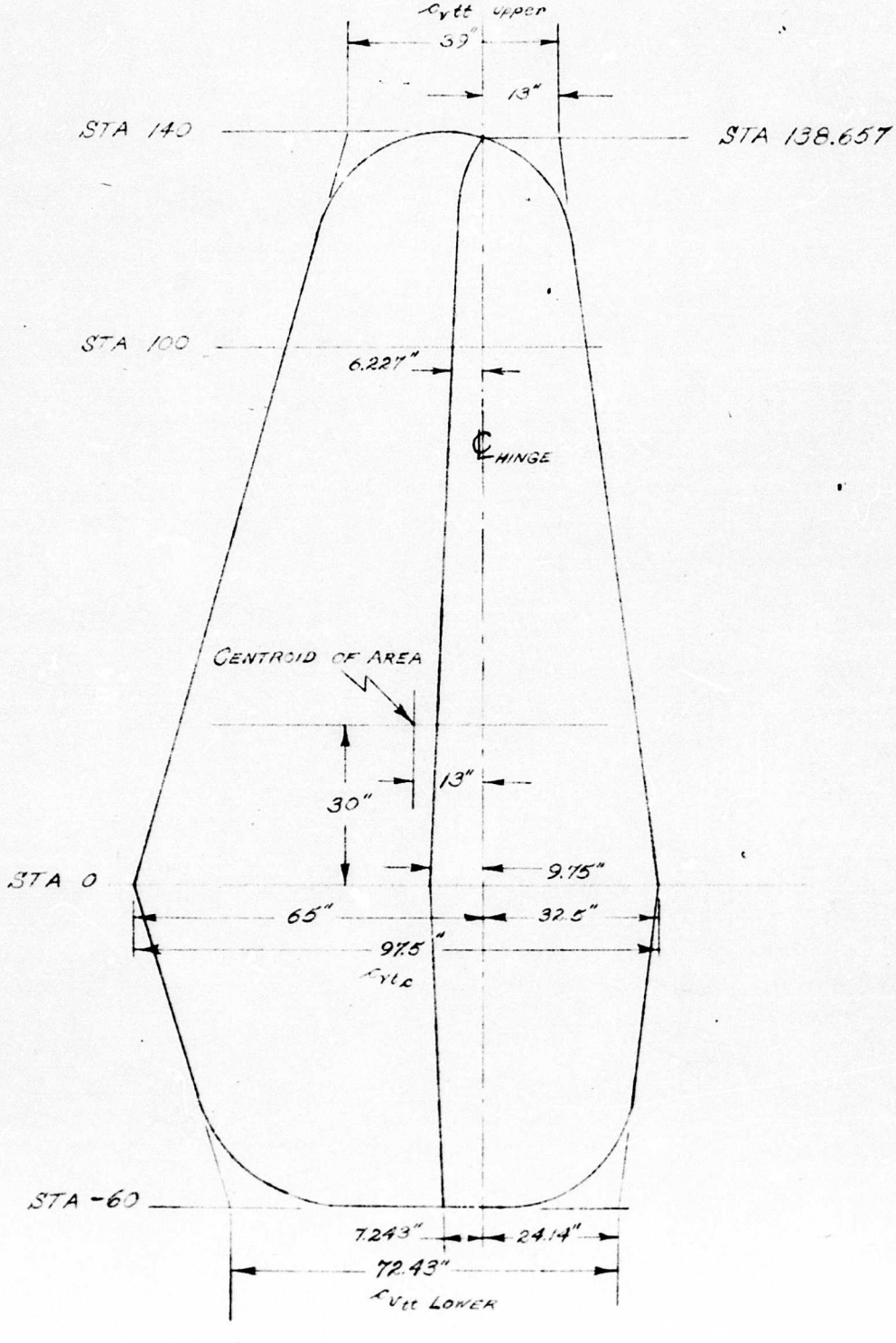
℄ Vtt upper
39"
13"
STA 140
STA 138.657
STA 100
6.227"
℄ HINGE
CENTROID OF AREA
30"
13"
STA 0
9.75"
65"
32.5"
97.5"
℄ Vtl c
STA -60
7.243"
24.14"
72.43"
℄ Vtt LOWER

PART II-A-9

b. Cross Force Analysis

In the determination of the lift force of the vertical tail, the section lift-curve slope was obtained from reference (7) and the three dimensional lift curve slope was obtained from reference (4). The sidewash was estimated by means of refernce (5). The use of the above characteristics in conjunction with the 1/32 scale model tests of the XC-120 airplane at the 5-Foot wind tunnel at Wright Field, reference (2) determined the three dimensional $\Delta\alpha_{vt}/\Delta\delta_r$ and the vertical tail efficiency η_{vt}.

Lift Curve Slope

Section Data

From reference (7) for flapped sections, .005 c_r gap with blunt nose profile rudder

Airfoil	$c_{l\alpha_{vt}}$	c_r/c_{vt}	c_{r_b}/c_{vt}
.0009	.088	.30	.30
.0015	.084	.30	.30
.0012	.086	.333	.30

So:

$$c_{c\alpha_{vt}} = c_{l\alpha_{vt}} = .086$$

Three Dimensional Data

From reference (15)

Effective Aspect Ratio = 1.09 Geometric Aspect Ratio

Geometric Aspect Ratio = $\frac{(200/12)^2}{99.6} = 2.79$

From reference (16) for zero sweep, effective aspect ratio = 3.04 and taper ratio = .4

$$c_{L\alpha_{vt}} = .0560$$

PART II-A-9

The effective lift curve slope of the vertical tail is obtained from wind tunnel data of reference (2) as follows:

$$\left(\frac{d\,C_N}{d\,\psi}\right)_{VT} = \left(\frac{d\,C_L}{d\,\alpha}\right)_{VT} \frac{S_{VT}}{S_W}\,\frac{l_{vt}}{B_W}\,\eta_{vt}\left(1 - \frac{d\sigma}{d\psi}\right)$$

$$\eta_{vt}\left(\frac{dC_L}{d\alpha}\right)_{VT} = \frac{\left(\frac{dC_N}{d\psi}\right)_{VT}\,S_W}{S_{vt}\,\frac{l_{vt}}{B_W}\left(1 - \frac{d\sigma}{d\psi}\right)}$$

S_W = 1447.25 sq. ft.

S_{vt} = 199.2 sq. ft.

$\frac{l_{vt}}{B_W}$ = .468 for 24.7% C.G.

$\left(\frac{d\,C_N}{d\,\psi}\right)_{VT}$ = -.0024 reference (2)

$$\eta_{vt}\left(\frac{d\,C_L}{d\,\alpha}\right)_{VT} = \frac{.0373}{\left(1 - \frac{d\sigma}{d\psi}\right)}$$

Using the estimated value of $\frac{d\sigma}{d\psi}$ from Part II-A-9-g

$\frac{d\sigma}{d\psi}$ = .107 power off, flaps and gear up

Substituting

$$\eta_{vt}\left(\frac{d\,C_L}{d\,\alpha}\right)_{VT} = .042$$

and the efficiency of the vertical tail is then

$$\eta_{vt} = \frac{.042}{.056} = .75$$

PART II-A-9 (Cont.)

Lift Effectiveness Parameter

The section value of α/δ is obtained from figure 49 of reference (4)

$$\alpha'/\delta = -.62 \text{ plain sealed} \quad \text{for } \frac{c_r}{c_{vt}} = .333 \quad \phi = 14.2^\circ$$

Correcting from plain sealed to open gap

$$\frac{k}{k_o} = 1.028 \quad \text{figure 6 reference (9)}$$

where $k_o = \alpha/\delta$ for plain sealed gap.
and the balance factor $K_1 = .0395$

from figure 3 reference (9) for blunt nose control surface

$$\frac{c_{r_b}}{c_r} = .30 \quad \text{and} \quad \frac{t/2}{c_r} = .1248$$

Then

$$\alpha/\delta \text{ open gap} = -1.028 \times .62 = -.637$$

The three dimensional value of the lift effectiveness parameter of the vertical tail is determined from the wind tunnel data of reference (2) in the same manner.

$$\left(\frac{d\,C_N}{d\,\psi}\right)_{VT} = \left(\frac{d\,C_L}{d\,\alpha}\right)_{VT} \frac{S_{vt}\,l_{vt}}{S_w\,B_w}\,\eta_{vt}\left(1 - \frac{d\,\sigma}{d\,\psi}\right)$$

$$\frac{\Delta\alpha_{vt}}{\Delta\delta_r} = -\frac{\frac{d\,C_N}{d\,\delta_r}}{\frac{d\,C_N}{d\,\alpha_{vt}}} \qquad \frac{d\,C_N}{d\,\alpha_{vt}} = \frac{\left(\frac{d\,C_N}{d\,\psi}\right)_{VT}}{\left(1 - \frac{d\,\sigma}{d\,\psi}\right)}$$

so:

$$\frac{\Delta\alpha_{vt}}{\Delta\delta_r} = -\frac{\frac{d\,C_N}{d\,\delta_r}}{\frac{\left(\frac{d\,C_N}{d\,\psi}\right)_{VT}}{\left(1 - \frac{d\,\sigma}{d\,\psi}\right)}}$$

PART II-A-9

or:

$$-\frac{\left(\frac{d\,C_N}{d\,\psi}\right)_{VT}}{\frac{d\,C_N}{d\,\delta_r}} \quad \frac{\Delta\alpha_{vt}}{\Delta\delta_r} = \left(1 - \frac{d\,\sigma}{d\,\psi}\right)$$

$$\frac{d\,C_N}{d\,\delta_r} = -.0013 \qquad \text{reference (2)}$$

Substituting we obtain

$$-\frac{\Delta\alpha_{vt}}{\Delta\delta_r} \times \frac{-.0024}{-.0013} = \left(1 - \frac{d\,\sigma}{d\,\psi}\right)$$

Again using the estimated value of $\frac{d\,\sigma}{d\,\psi} = .107$

for power-off, flaps and gear up

$$\alpha_{vt}\,\delta_r = -.480$$

<u>Summary of Cross Force Analysis</u>

$$C_{C\alpha_{vt}} = .056$$

$$\alpha_{vt}\,\delta_r = -.480$$

$$\eta_{vt} = .75 \text{ for cross forces}$$

$$C_{C_{VT}} = C_{C\alpha_{vt}}\,\alpha_{vt} - C_{C\alpha_{vt}}\,\alpha_{vt}\,\delta_r \quad \delta_r$$

$$C_{C_{VT}} = .056\,\alpha_{vt} + .056 \times .480\,\delta_r$$

$$C_{C_{VT}} = .056\,\alpha_{vt} + .0269\,\delta_r$$

$$\eta_{vt}\,C_{C_{VT}} = .75(.056\,\alpha_{vt} + .0269\,\delta_r)$$

Figure 105 presents a plot of $C_{C_{VT}}$ versus α_{vt} for various rudder deflections.

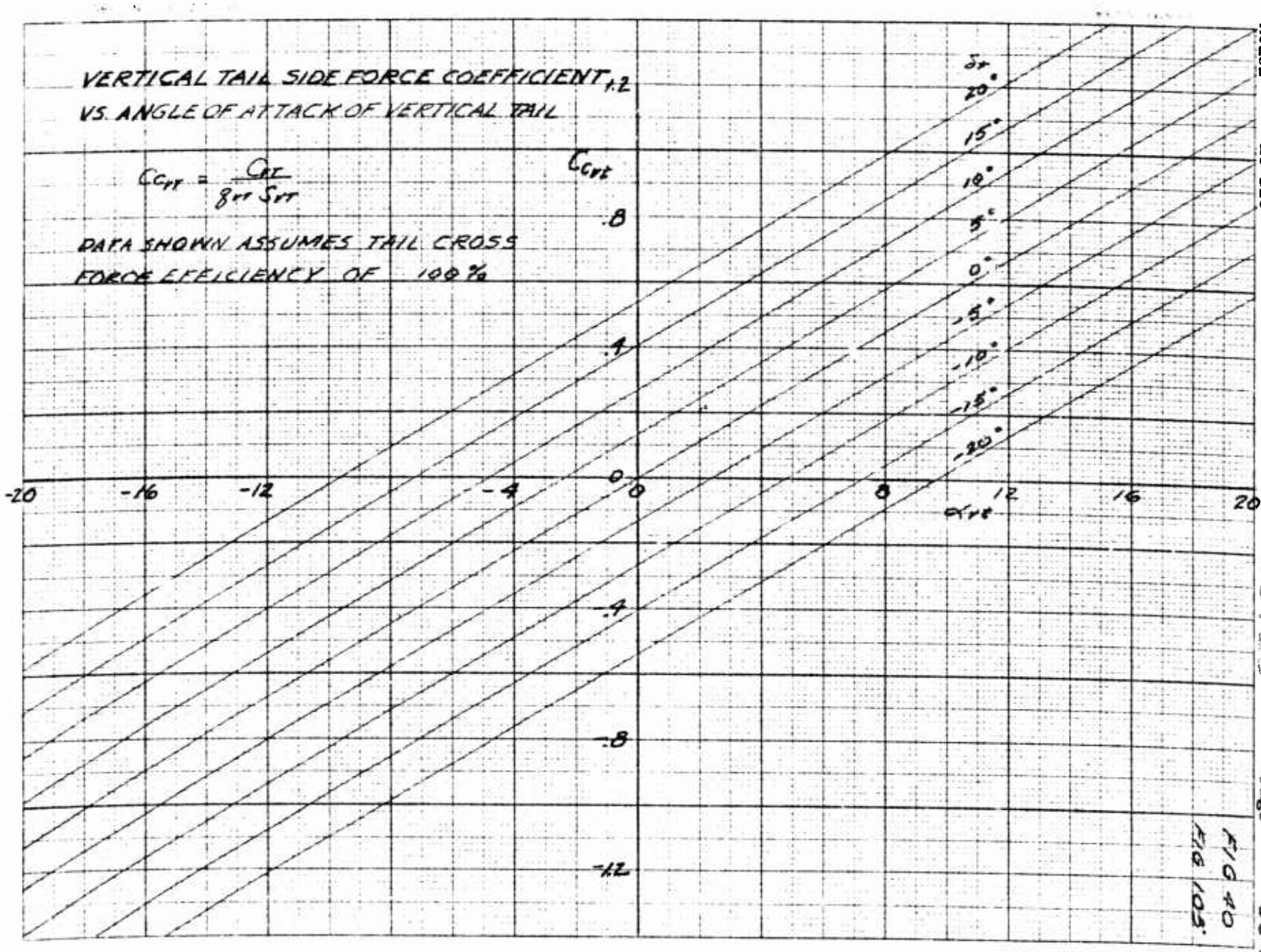

FIG 40
FIG 105.

PART II-A-9

c. Drag Analysis

It is the purpose of this section to determine the drag characteristics of the vertical tail.

In determining the drag, the induced drag is first calculated for various α_{vt}'s and δ_r to obtain total drag.

Induced Drag

From reference (11) the induced drag is

$$C_{D_{I_{VT}}} = \frac{C_{C_{VT}}^2}{\pi A_{VT_{effective}} \mu} + C_{C_{VT}} \Delta c_{c_r} v + \Delta c_{c_r}^2 w$$

where μ, v and w are factors obtained from figure 8 of reference (11)

$$\mu \cong 1.00$$
$$v = 0$$
$$w = 0$$

$$A_{vt\ effective} = 3.04$$

so that

$$C_{D_{I_{VT}}} = \frac{C_{C_{VT}}^2}{3.1416 \times 3.04} = .1046\ (C_{C_{VT}})^2$$

$$C_{C_{VT}} = .056\,\alpha_{vt} + .0269\,\delta_r$$

The calculations for induced drag are presented in the following table.

RESTRICTED

PART II-A-9

CALCULATIONS FOR INDUCED DRAG OF VERTICAL TAIL

(1)	(2)	(3)	(4)	(5)	(6)	(7)
vt	r	.056 x (1)	.0269 x (2)	$C_{C_{VT}}$ = (3) - (4)	$C_{C_{VT}}{}^2$ = (5)^2	$C_{D_{i_{VT}}}$ .1046 (6)
0	0	0	0	0	0	0
	± 5		± .135	± .135	.0182	.0019
	±10		± .269	± .269	.0724	.0076
	±15		± .404	± .404	.1632	.0171
	±20		± .538	± .538	.2894	.0303
3.13	- 20	.175	- .538	-.363	.1318	.0138
	-15		- .404	-.229	.0524	.0055
	-10		- .269	-.094	.0088	.0009
	- 5		- .135	.040	.0016	.0002
	0		0	.175	.0324	.0034
	5		.135	.310	.0961	.0101
	10		.269	.444	.1971	.0206
	15		.404	.579	.3352	.0351
	20		.538	.713	.5084	.0532
5	- 20	.280	- .538	.258	.0666	.0070
	- 15		- .404	.124	.0154	.0016
	- 10		- .269	.011	.0001	0
	- 5		- .135	.145	.0210	.0022
	0		0	.280	.0784	.0082
	5		.135	.415	.1722	.0180
	10		.269	.549	.3014	.0315
	15		.404	.684	.4679	.0489
	20		.538	.818	.6691	.0700
10	- 20	.560	- .538	.022	.0005	.0001
	- 15		- .404	.156	.0243	.0025
	- 10		- .269	.291	.0847	.0089
	- 5		- .135	.425	.1806	.0189
	0		0	.560	.3136	.0328
	5		.135	.695	.4830	.0505
	10		.269	.829	.6872	.0719
	15		.404	.964	.9293	.0972
	20		.538	1.098	1.2056	.1261

PART II-A-9

Profile Drag

The profile drag of the vertical tail has been determined in Part II-A-9-c of reference (1) for various combinations of angle of attack of the vertical tail and rudder deflections.

PART II-A-9

TOTAL VERTICAL TAIL DRAG

(1) α_{VT}	(2) δ_r	(3) $C_{D_{O_{VT}}}$	(4) $C_{D_{L_{VT}}}$	(5) $C_{D_{VT}}$
0	0	.0081	0	.0081
	± 5	.0102	.0019	.0121
	± 10	.0171	.0076	.0247
	± 15	.0286	.0171	.0457
	± 20	.0503	.0303	.0806
3.13	- 20	.0457	.0138	.0595
	- 15	.0216	.0055	.0271
	- 10	.0127	.0009	.0136
	- 5	.0094	.0002	.0096
	0	.0082	.0034	.0116
	5	.0119	.0101	.0220
	10	.0205	.0206	.0411
	15	.0346	.0351	.0697
	20	.0544	.0532	.1076
5	- 20	.0423	.0070	.0493
	- 15	.0177	.0016	.0193
	- 10	.0103	0	.0103
	- 5	.0088	.0022	.0110
	0	.0083	.0082	.0165
	5	.0129	.0180	.0309
	10	.0223	.0315	.0538
	15	.0377	.0489	.0866
	20	.0567	.0700	.1267
10	- 20	.0335	.0001	.0336
	- 15	.0112	.0025	.0137
	- 10	.0085	.0089	.0174
	- 5	.0083	.0189	.0272
	0	.0087	.0328	.0415
	5	.0150	.0505	.0655
	10	.0269	.0719	.0988
	15	.0435	.0972	.1407
	20	.0621	.1261	.1882

RESTRICTED

FIG. 106

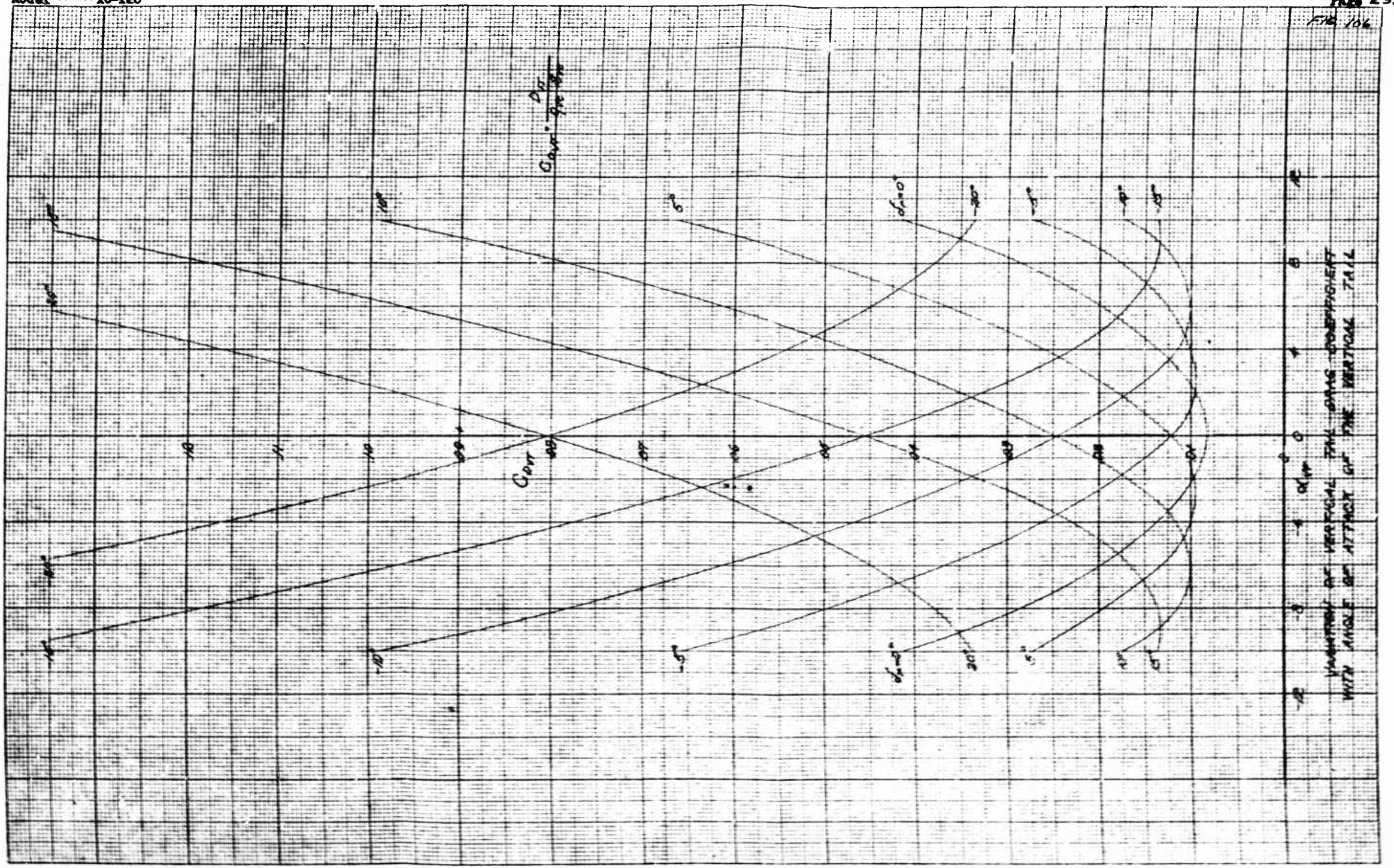

PART II-A-9

d. Polar Diagram of Vertical Tail

Figure 107 presents the vertical tail polar diagram for various rudder deflections.

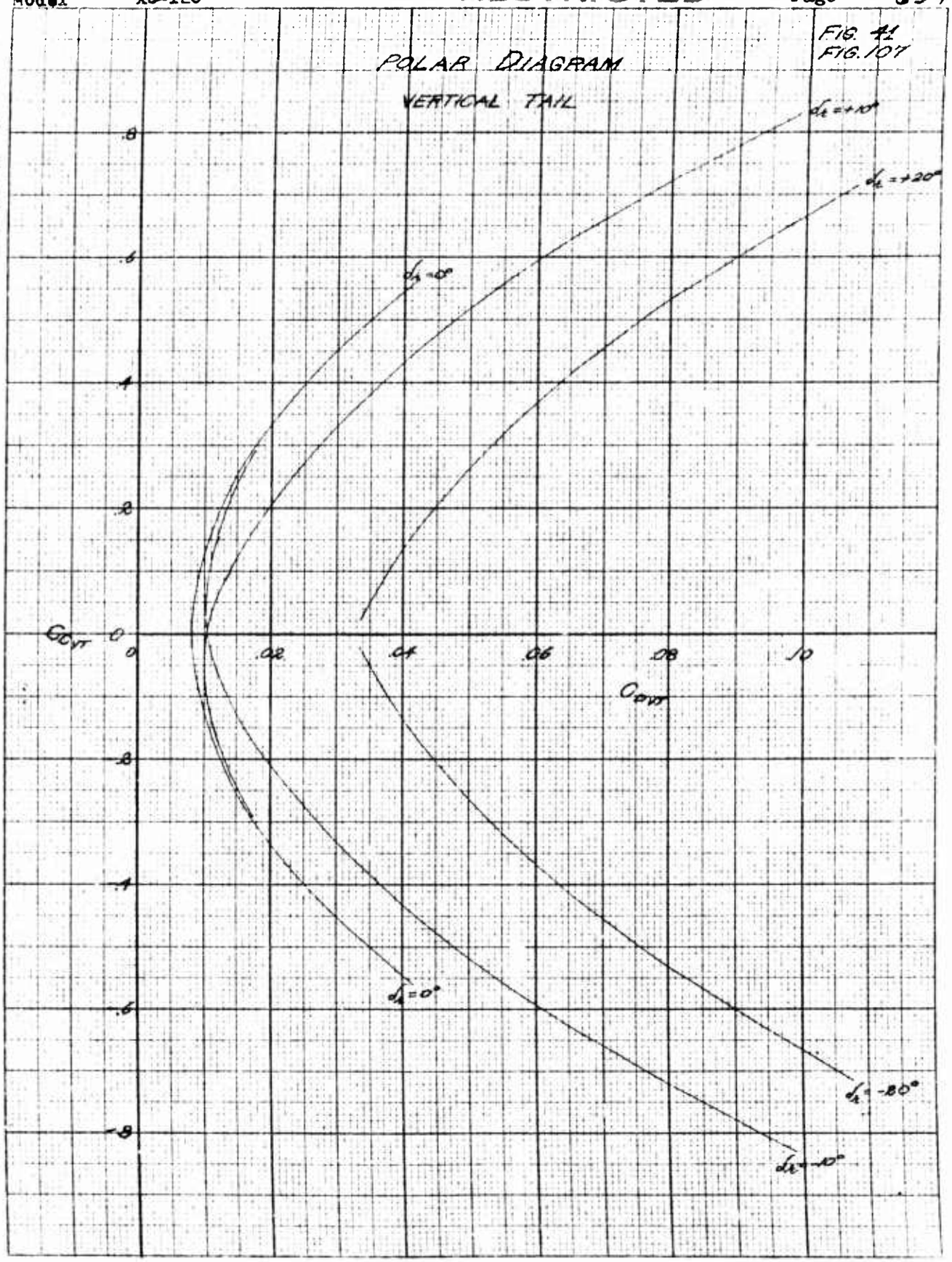
FIG. 41
FIG. 107
POLAR DIAGRAM
VERTICAL TAIL
$\delta_h = +10°$
$\delta_h = +20°$
$\delta_h = 0°$
$\delta_h = 0°$
$\delta_h = -20°$
$\delta_h = -10°$
$C_{D_{VT}}$
$C_{L_{VT}}$
.8
.6
.4
.2
0
-.2
-.4
-.6
-.8
0
.02
.04
.06
.08
.10

PART II-A-9

e. Aerodynamic Force Coefficients

The aerodynamic force coefficients $C_{X_{VT}}$ and $C_{Y_{VT}}$ are assumed to be equal to $C_{D_{VT}}$ and $\eta_{vt}\, C_{C_{VT}}$ respectively. All coefficients are considered to be independent of angle of pitch.

PART II-A-9

f. Yawing Moment About Aerodynamic Center

It is the purpose of this section to determine the yawing moment of the vertical tail about its aerodynamic center.

From figure 1 reference 5

$$\frac{d\,c_m}{d\,\delta_r} = -.0075 \qquad \frac{d\,\alpha}{d\,\delta_r} = -.615$$

$$\frac{c_m\,\delta_r}{-\alpha\,\delta_r} = -.01275 \qquad \text{for } \frac{c_r}{c_{vt}} = .333$$

Using the previously determined section α/δ_r from Part II-A-9-b we have $c_{m_{vt}\,\delta_r} = -.01275 \times .637 = -.00801$ converting the section pitching moment thus obtained to section yawing moment

$$c_{n_{vt}\,\delta_r} = c_{m\delta_r} \times \frac{c_{vt}}{R_{vt}}$$

$$c_{n\,\delta_r} = -.00801 \times \frac{73.23}{200} = -.00293$$

Correcting to three dimensional data by the method of reference (11)

$$C_{N_{VT}\,\delta_r} = I\ c_{n_{vt}\,\delta_r}$$

$I = 1.07$ from figure reference (11)

$$C_{N_{VT}\,\delta_r} = 1.07 \times -.00293 = -.00314$$

Figure 108 presents a plot of $C_{N_{VT}}$ versus δ_r for any α_{vt} as $C_{N_{VT}}$ is constant with α_{vt} for any δ_r, $C_{N_{VT}}$ being taken about the vertical tail aerodynamic center, located at the .25 c_{vt}.

RESTRICTED

FIG. 42
FIG 108

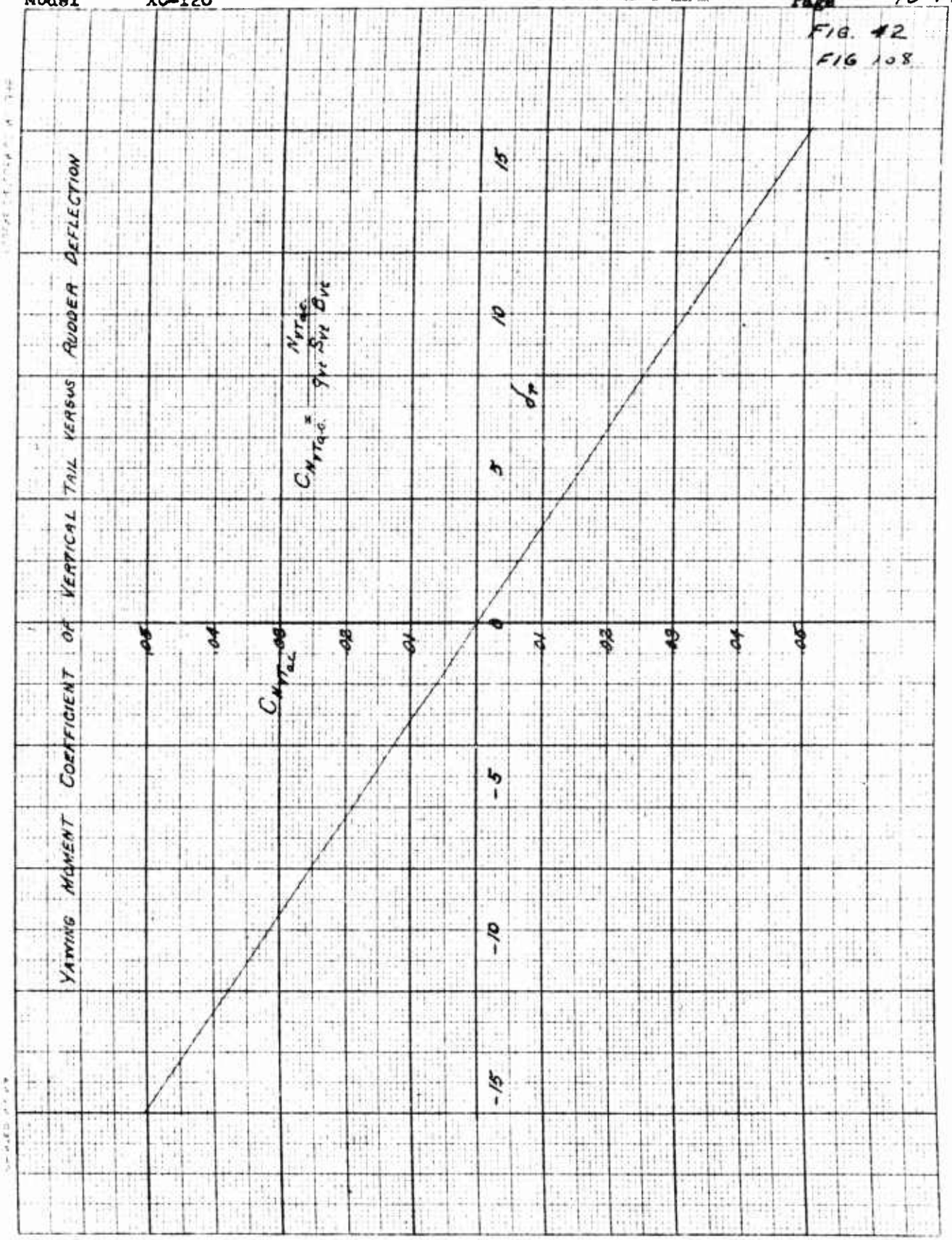

PART II-A-9-g

g. SIDEWASH AND DYNAMIC PRESSURE RATIO

This section contains the estimation of the sidewash at the vertical tails due to the wing. The results are summarized herewith:

Flaps Up $\frac{d\sigma}{d\psi} = .107$

Flaps Down $\frac{d\sigma}{d\psi} = .072$

Figure 105 presents a plot of σ versus ψ.

The value of the dynamic pressure ratio is 1.00 at all times, since the wing wake passes below the vertical tails.

PART II-A-9-g

ESTIMATION OF SIDEWASH

It was established in reference (1) that a reasonable estimation of the value of the sidewash could be obtained from reference (5) providing a factor to account for the difference in tail length and wing aspect ratio was used. This factor was determined to be about 0.66 for the C-82. It will be taken to be the same for the XC-120.

The increased incidence of the wing of the XC-120 over that for the C-82 has the effect of raising the tail relative to the wing at any given value of lift coefficient. This change corresponds very closely to the change from mid-wing to low-wing configuration of reference (5). Therefore, the values of $\frac{d\sigma}{d\psi}$ will be determined from the data for the low-wing configuration of Table VIII of reference (5).

δ_F	Configuration	Dihedral	$\frac{d\sigma}{d\psi}$ (ref. 5)	$\frac{d\sigma}{d\psi}$ (XC-120)
0°	Low-Wing	0°	.09	.059
0°	Low-Wing	5°	.21	.139
0°	Low-Wing	3°		.107

For the flaps down configuration, the data of reference (5) do not appear to be reliable in the low-wing configuration, since they indicate a negative value of $\frac{d\sigma}{d\psi}$. This is possible only if the vertical tail is below the vortex sheet from the wing which is improbable for the low-wing configuration.

Instead of attempting to correct the data for the low-wing, flaps down configuration, the ratio of $\frac{d\sigma}{d\psi}$ flaps down to $\frac{d\sigma}{d\psi}$ flaps up will be determined for the mid-wing and high-wing configurations, and this ratio used to arrive at the value of $\frac{d\sigma}{d\psi}$ flaps down for the XC-120.

PART II-A-9-g (Cont.)

Configuration	Dihedral	$\frac{\sigma_\psi \text{ flaps down}}{\sigma_\psi \text{ flaps up}}$
High - wing	0°	.595
Mid - wing	0°	.577
High - wing	5°	.726
Mid - wing	5°	.757
Low - wing	3°	.67

Applying this ratio, the value of $\frac{d\sigma}{d\psi}$, flaps down, for the XC-120 is

$$\frac{d\sigma}{d\psi} = .107 \times .67 = .072$$

FIG. 43
FIG 109

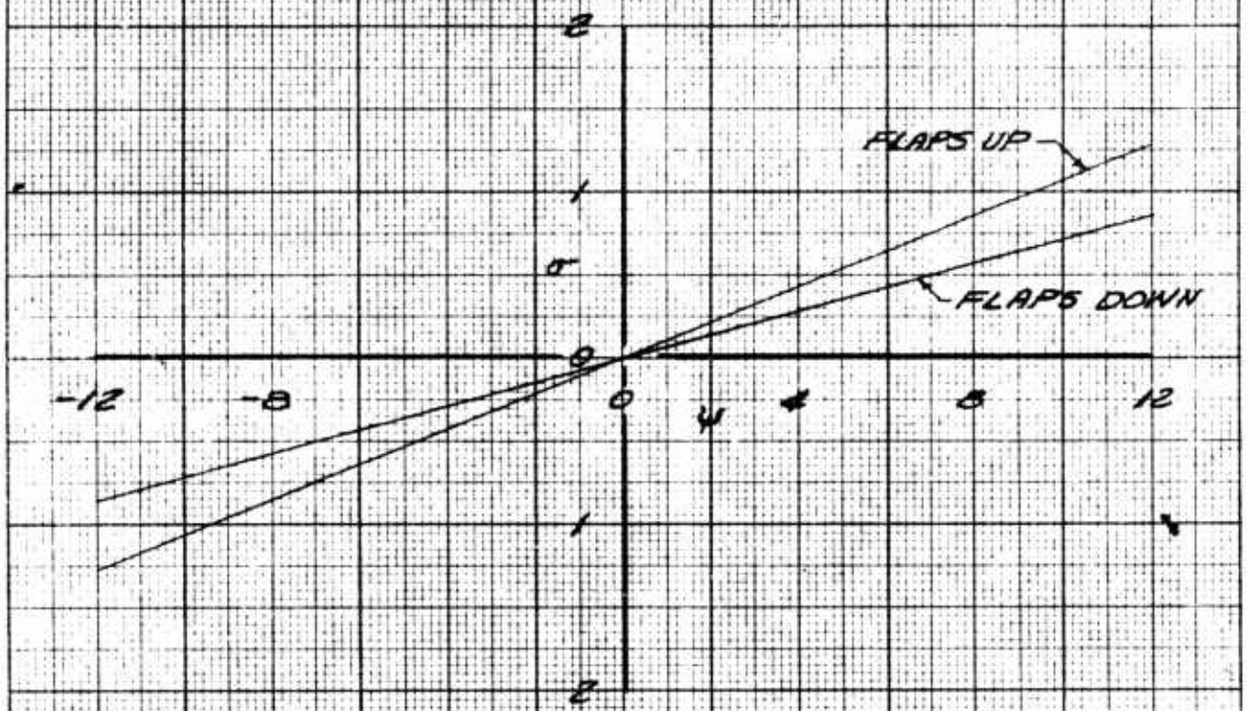

VARIATION OF SIDEWASH ANGLE WITH ANGLE OF YAW, POWER OFF XC-120 AIRPLANE

PART II-A-9

h. Rudder Hinge Moments

The rudder hinge moments have been determined in Part II-A-9-h of reference (1) based on estimates, wind tunnel data and flight test data of the C-82 airplane. For convenience they are also shown in the vertical tail summary section.

PART II-A-10

10. RUDDER TABS

Since the rudder tabs are identical to those on the C-119B airplane, all calculations and figures presented in Part II-A-10, reference (1) apply to the XC-120 airplane.

All aerodynamic coefficients are based on tab area, rudder area or vertical tail area, depending upon the item affected by the tab. For convenience, the important tab characteristics are tabulated below as well as being shown graphically in the summary section.

TAB AERODYNAMIC CHARACTERISTICS

SYMBOL	ITEM	TRIM TAB	SPRING TAB
$C_{C_{VT}\delta_r \text{ tab}}$	$d\,C_{C_{VT}} / d\,\delta_{r\text{ tab}}$	.00277	.00166
$C_{H_r\,\delta_{r\text{ tab}}}$	$d\,C_{H_r} / d\,\delta_{r\text{ tab}}$	-.0034	-.0021
$C_{H_{r\text{tab}}\,\delta_{r\text{ tab}}}$	$d\,C_{H_{r\text{tab}}} / d\,\delta_{r\text{ tab}}$	-.0043	-.0043
$\alpha_{vt\,\delta_{r\text{ tab}}}$	$d\alpha_{vt} / d\,\delta_{r\text{ tab}}$	-.0605	-.0364

PART II-A-11

11. LANDING GEAR

This section presents an analysis of the aerodynamic characteristics of the landing gear of the XC-120 airplane. All the coefficients presented herein are for one main landing gear.

Due to the special configuration of the XC-120 airplane (with removable pack) a quadricycle type landing gear is necessary. Figure 110 presents a view of one main gear.

The final aerodynamic characteristics of the landing gear are presented in figure 112 based on wing area and free stream dynamic pressure.

PART II-A-11-a

a. LANDING GEAR DRAWING

Figure 110 presents a front and side view of one main landing gear. Pertinent dimensions and areas used in the analysis of the aerodynamic characteristics are shown.

REPORT NO. R107-012	FAIRCHILD AIRCRAFT DIVISION OF FAIRCHILD ENGINE & AIRPLANE CORPORATION		PAGES	PAGE 249
MODEL XC-120	PREPARED BY	CHECKED BY	APPROVED BY	
Subject: BASIC AERODYNAMIC DATA			DATE July 9, 1948	
			REVISED	

FIG. 110

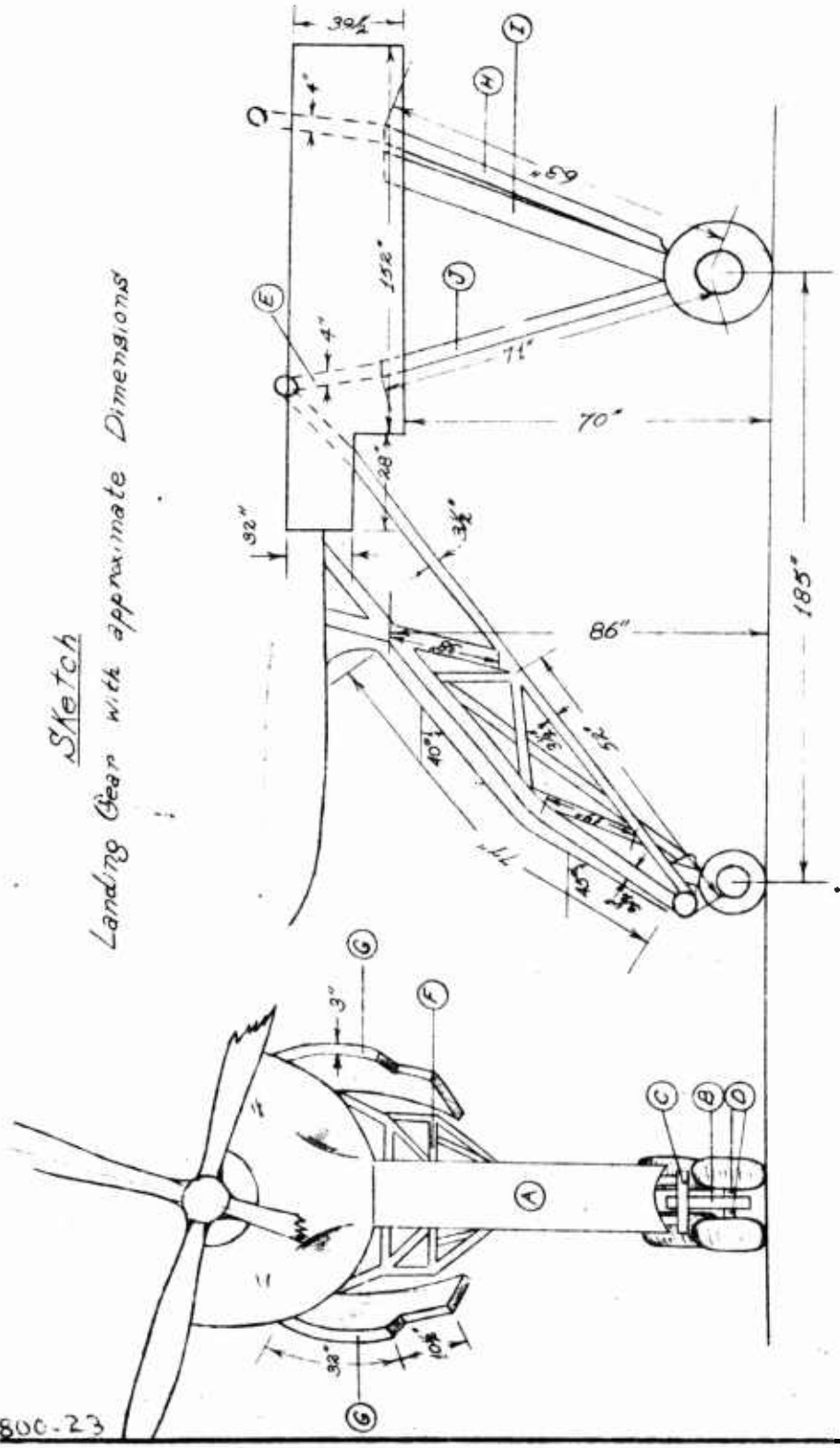

Front Tires 11 x 12 (Low pressure)

Rear Tires 15.50 x 20

Front Wheels		
	Quantity	Dimensions
A	1	20" x 11"
B	1	4½" x 25"
C	1	3" x 18½"
D	1	3½" x 7½"

Rear Wheels		
	Quantity	Dimensions
E	2	4" x 21"
F	1	3" x 40"
G	Doors (2)	3 x 42½"
H	2	4" x 63"
I	1	6" x 72"
J	2	4" x 71

FA-800-23

RESTRICTED

PART II-A-11-b

b. **DRAG ANALYSIS**

Using the pertinent dimensions shown in figure 110, an analysis of the drag is presented below:

ITEM		GENERAL	K_X
Front Leg			
Front Leg Cover Plate			
plate area	sq. ft.	10.7	
angle inclined to thrust line	degrees	42°	
C_{D_o} based on plate area		1.0	
K_X of cover plate	lb./mph^2		.0274
Front Leg Wheel Forks			
frontal area	sq. ft.	1.36	
C_{D_o} based on frontal area		1.0	
K_X of wheel forks	lb./mph^2		.00348
Dual Front Wheels			
type tires		11" x 12" Low Press.	
diameter of wheels		2.83	
frontal area (2 wheels)	sq. ft.	5.0	
D/W one wheel		3.09	
K_X per sq. ft. frontal area	lb./mph^{2}ft^2	.00069	
K_X of dual front wheels	lb./mph^2		.00345
Interference & Roughness			
interference factor	% smooth drag	10	
roughness factor	% smooth drag	10	
K_X due to interference & roughness	lb./mph^2		.0069
TOTAL K_X FRONT LEG	lb./mph^2		.04123
Rear Leg			
4 Inch Struts			
estimated length exposed	ft.	32	
frontal area	sq. ft.	10.6	
C_{D_o} based on frontal area		1.0	
K_X of 4 inch struts	lb./mph^2		.0271

RESTRICTED

PART II-A-11-b

ITEM		GENERAL	K_X
Main Oleo Strut			
length	ft.	6	
diameter	inches	6	
frontal area	sq. ft.	3	
C_{D_o} based on frontal area		1.0	
K_X of main oleo strut	lbs/mph2		.00767
Dual Rear Wheels			
type tires		15.5" x 20"	
diameter of wheels	ft.	4.25	
frontal area	sq. ft.	11	
D/W one wheel		3.29	
K_X per sq. ft. frontal area	lb/mph^2 ft^2	.00071	
K_X of dual rear wheels	lb/mph^2		.0078
Interference & Roughness			
interference factor	% smooth drag	10	
roughness factor	% smooth drag	10	
K_X due to interference & roughness	lb/mph^2		.00852
TOTAL K_X REAR LEG	lb/mph^2		.05109
Open Main Doors			
flat area parallel to air stream	sq. ft.	95.84	
Reynolds Number at 160 mph		22.45 x 10^6	
C_{D_f} based on flat area		.0026	
K_X of open main doors	lb/mph^2		.000637
Interference & Roughness			
interference factor	% smooth drag	100	
roughness factor	% smooth drag	100	.001274
K_X due to interference & roughness	lb/mph^2		
TOTAL K_X OPEN DOORS	lb/mph^2		.001911

PART II-A-11-b

ITEM		GENERAL	K_X
Open Wheel Well			
area of opening	sq. ft.	106.54	
C_{D_0} based on open area		0.1	
K_X due to open well	lb/mph^2		.0272
TOTAL K_X OPEN WELL	lb/mph^2		.0272
Total Gear Drag			
K_X front leg			.04123
K_X rear leg			.05109
K_X open doors			.00191
K_X wheel well			.0272
TOTAL K_X GEAR	lb/mph^2		.12143
TOTAL C_D GEAR			.0328

The location of the drag centroid is shown in figure /// as 78 inches below the thrust line and 206 inches aft of the propeller disc.

RESTRICTED

LANDING GEAR DRAG DISTRIBUTION
GEAR FULL DOWN

FIG 111

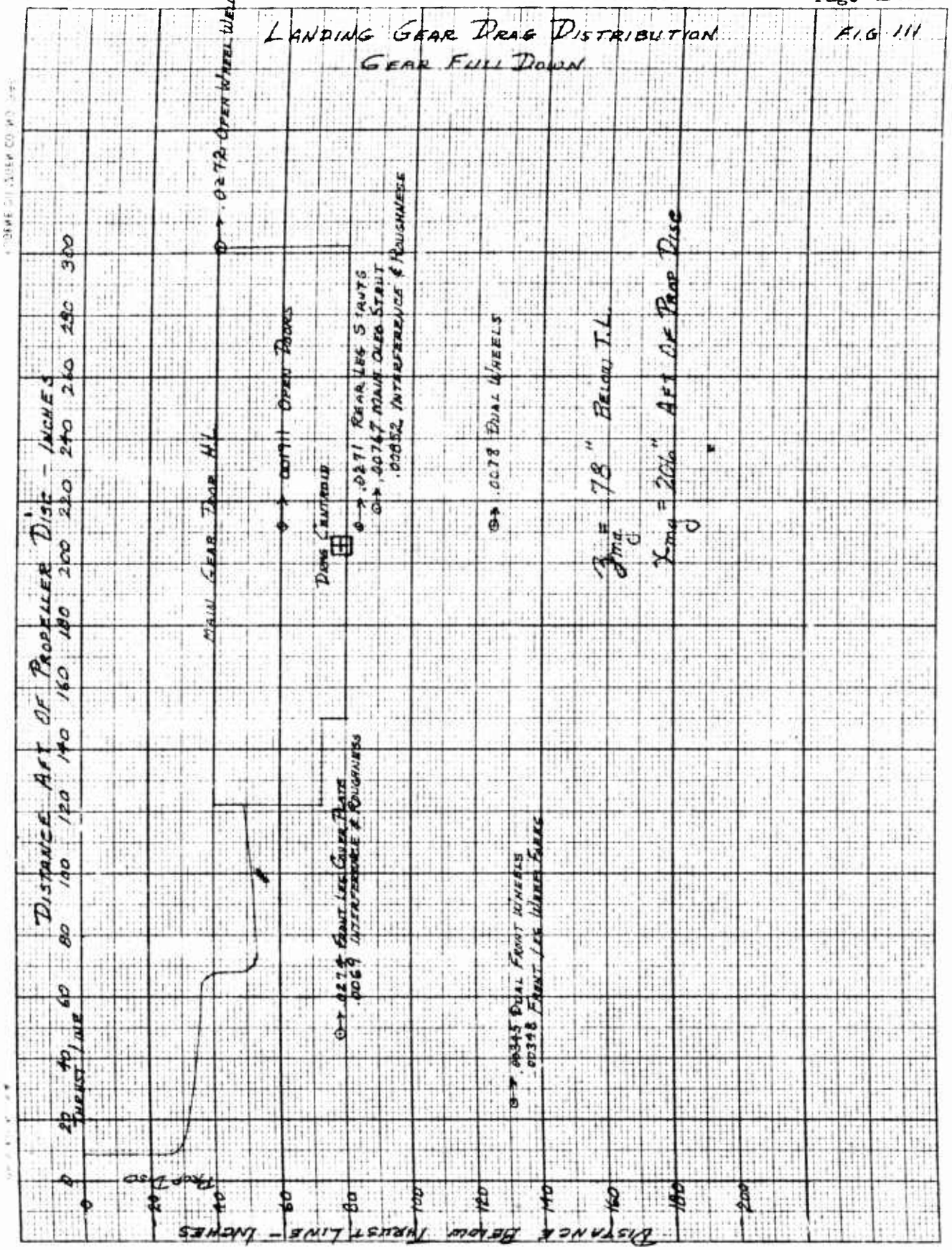

PART II-A-11-c

c. AERODYNAMIC FORCE COEFFICIENTS

The aerodynamic force coefficients for one main gear are determined in the table on the following page.

Figure 112 shows the variation of C_{X_G} and C_{Z_G} with angle of attack of the thrust line for one main landing gear.

LANDING GEAR C_{X_G} & C_{Z_G}

1	2	3	4	5	6
α_{TL}	$\sin \alpha_{TL}$	$\cos \alpha_{TL}$	C_D one gear	C_{Z_G}	C_{X_G}
-12	-.2079	.9781	.0328	-.00681	.0321
-8	-.1392	.9903	.0328	-.00456	.0325
-4	-.0698	.9976	.0328	-.00229	.0327
0	0	1.0000	.0328	0	.0328
+4	.0698	.9976	.0328	.00229	.0327
+8	.1392	.9903	.0328	.00456	.0325

RESTRICTED

FIG 47
FIG 112

LANDING GEAR FORCE COEFFICIENTS
FOR
ONE LANDING GEAR

$$C_{X_G} = \frac{X_G}{q\,S_W}$$

$$C_{Z_G} = \frac{Z_G}{q\,S_W}$$

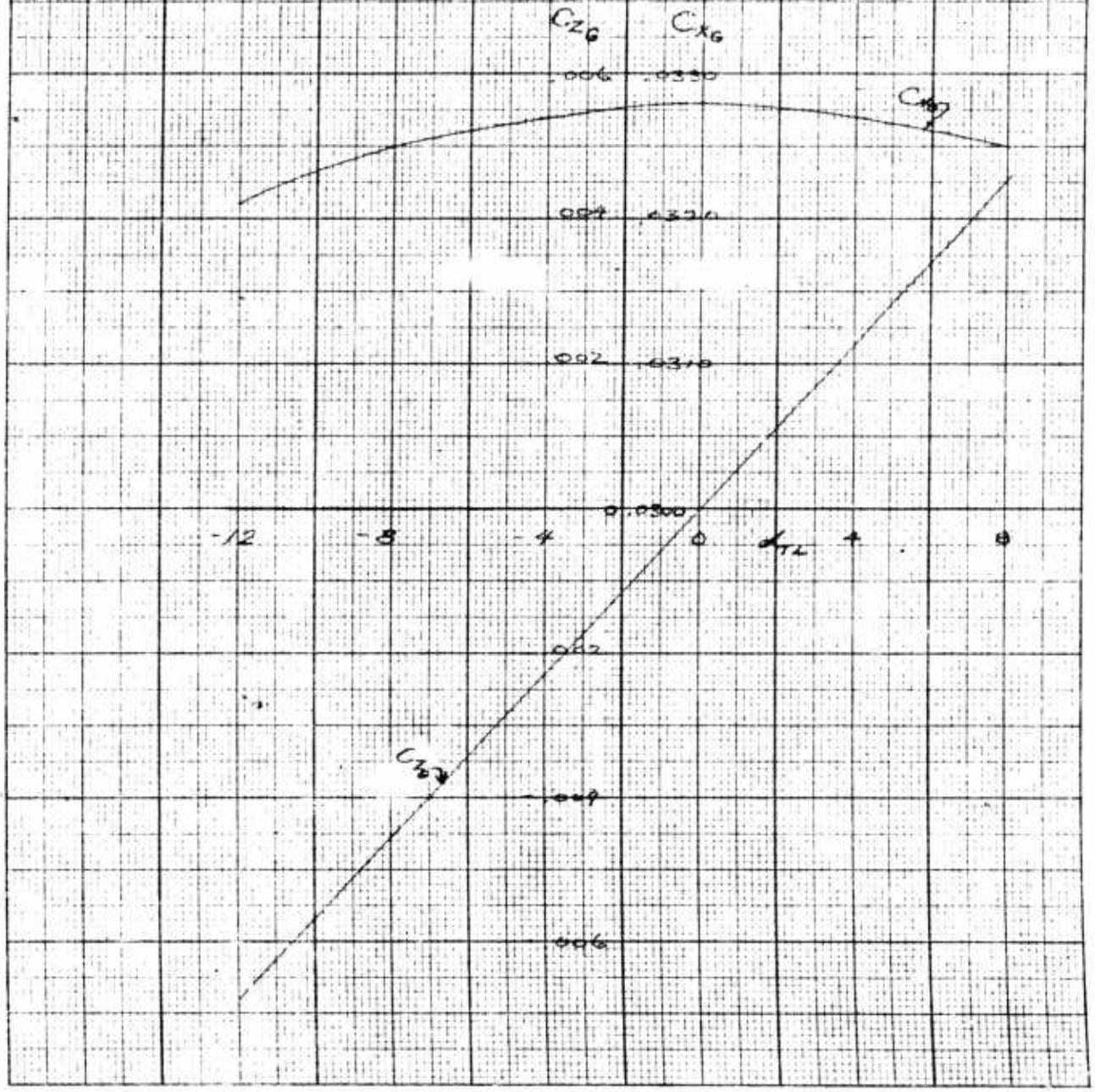

PART II-B

B. POWER-ON

It is the purpose of this portion of the report to evaluate the power effects on the various component parts of the airplane.

PART II-B-1

1. WING UNFLAPPED

This section presents the detailed analysis to determine the effects of power on the aerodynamic characteristics of the unflapped wing.

All characteristics are calculated as incremental effects due to one engine in operation at military power and are all based on total wing area.

PART II-B-1-a

a. SLIPSTREAM EFFECTS ON PITCHING MOMENT

An analysis of the effects of slipstream on the pitching moment of an unflapped wing indicates that, in general, the effects are negligible. Therefore, it is assumed that the pitching moment characteristics of the unflapped wing power-on are the same as for power-off condition.

b. SLIPSTREAM EFFECTS ON LIFT

The increment of wing lift coefficient due to the slipstream is computed in the following tables in the same manner as in reference (1).

The geometric parameters necessary for the calculation have the following values:

h_p = 15.00 feet

v_p = 1.07 feet

$\bar{c}_{wi}$ = 15.43 feet

Figure 113 presents the variation of increment of lift coefficient due to one propeller operation with thrust coefficient for constant values of angle of attack of the thrust line.

FA-800-2

TABLE
COMPUTATION OF INCREMENT OF LIFT COEFFICIENT
DUE TO PROPELLER OPERATION
FLAPS UP
ONE ENGINE

	(1)	(2)	(3)	(4)	(5)	(6)	(7)	(8)	(9)	(10)	(11)	(12)
	α_{TL} Degrees	α_{TL} Radian	$1-\epsilon_p/\alpha_{TL}$	(2)×(3)	h_p×(4)	ν_s	ν_s^2	4×(7)	D_s^2−(8)	b_{wi}	$\frac{b_{wi}c_{wi}}{S_w}$	$C_{L_{i_{AVE}}}$ Power Off
	-15	-.262	.840	-.220	-3.30	-4.37	19.10	76.40	144.42	12.02	.128	-.579
	-9	-.157		-.152	-1.98	-3.05	9.30	37.20	183.68	13.55	.144	-.073
T_c=.05	-3	-.0524		-.044	-.66	-1.73	2.99	11.96	206.86	14.45	.154	.432
	3	.0524		.044	.66	-.41	.17	.68	220.14	14.84	.158	.937
	9	.157		.132	1.98	.91	.83	3.32	217.50	14.75	.157	1.441
	-15	-.262	.804	-.210	-3.15	-4.22	17.83	71.32	144.18	12.01	.128	-.579
	-9	-.157		-.126	-1.89	-2.96	8.76	35.04	180.46	13.44	.143	-.073
T_c=.10	-3	-.0524		-.042	-.63	-1.70	2.89	11.56	203.94	14.29	.152	.432
	3	.0524		.042	.63	-.44	.19	.76	214.74	14.65	.156	.937
	9	.157		.126	1.89	.82	.67	2.68	212.82	14.59	.155	1.441
		(13)	(14)	(15)	(16)	(17)	(18)	(19)	(20)	(21)	(22)	(23)
	α_{TL}	(11)×(12)	S×(13)	$\lambda' a_s$ (11)	ϵ_p×S	(15)×(16)	$\Delta C_{L_{wi}}$	T_c	S	$\frac{1+S/2}{1+S}$	$\sqrt{(21)}$	D_s
	-15	-.074	-.005	.0077	-.149	-.001	-.004	.05	.062	.970	.985	14.86
	-9	-.011	-.001	.0086	-.089	-.001	0					
T_c=.05	-3	.067	.004	.0092	-.030	0	.004					
	3	.148	.009	.0095	.030	0	.009					
	9	.226	.014	.0094	.089	.001	.013					
	-15	-.074	-.009	.0077	-.353	-.003	-.006	.10	.120	.947	.973	14.68
	-9	-.010	-.001	.0086	-.211	-.002	.001					
T_c=.10	-3	.066	.008	.0091	-.071	-.001	.009					
	3	.146	.018	.0094	.071	.001	.017					
	9	.225	.027	.0093	.211	.002	.025					

TABLE (CONTINUED)

	(1)	(2)	(3)	(4)	(5)	(6)	(7)	(8)	(9)	(10)	(11)	(12)
	α_{TL} DEGREES	α_{TL} RADIAN	$1-\epsilon_p/\alpha_{TL}$	(2)×(3)	h_p×(4)	ν_s	ν_s^2	4×(7)	D_s^2-(8)	b_{wi}	$\frac{b_{wi}\bar{c}_{wi}}{S_w}$	$C_{L_{i_{WF}}}$ POWER OFF
	-15	-.262	.742	-.194	-2.91	-3.98	15.84	63.36	143.14	11.97	.127	-.579
	-9	-.157		-.116	-1.74	-2.81	7.90	31.60	174.90	13.22	.141	-.075
T_c=.20	-3	-.0524		-.0388	-.58	-1.65	2.72	10.88	195.62	13.98	.149	.432
	3	.0524		.0388	.58	-.49	.24	.96	205.54	14.34	.153	.937
	9	.157		.116	1.74	.67	.45	1.80	204.70	14.31	.152	1.441
	-15	-.262	.649	-.170	-2.55	-3.62	13.10	52.40	141.64	11.90	.127	-.579
	-9	-.157		-.102	-1.53	-2.60	6.76	27.04	167.00	12.92	.138	-.013
T_c=.40	-3	-.0524		-.0340	-.51	-1.58	2.50	10.00	184.04	13.57	.144	.432
	3	.0524		.0340	.51	-.56	.31	1.24	192.80	13.88	.148	.937
	9	.157		.102	1.53	.46	.21	.84	193.20	13.90	.148	1.441

	(13)	(14)	(15)	(16)	(17)	(18)	(19)	(20)	(21)	(22)	(23)
	α_{TL}	(11)×(12)	S×(13)	$\lambda' a_s$ (11)	ϵ_p×S	(15)×(16)	$\Delta C_{L_{WT}}$	T_c	S	$\frac{1+S/2}{1+S}$	$\sqrt{(21)}$	D_s
	-15	-.073	-.017	.0076	-.883	-.007	-.010	.20	.228	.908	.953	14.37
	-9	-.010	-.002	.0085	-.529	-.004	.002					
T_c=.20	-3	.064	.015	.0089	-.175	-.002	.017					
	3	.143	.033	.0092	.175	.002	.031					
	9	.219	.050	.0091	.529	.005	.045					
	-15	-.073	-.031	.0076	-2.21	-.017	-.014	.40	.420	.853	.924	15.93
	-9	-.010	-.004	.0083	-1.327	-.011	.007					
T_c=.40	-3	.062	.026	.0086	-.441	-.004	.030					
	3	.139	.058	.0089	.441	.004	.054					
	9	.213	.089	.0089	1.327	.012	.077					

RESTRICTED

TABLE (CONCLUDED)

	(1)	(2)	(3)	(4)	(5)	(6)	(7)	(8)	(9)	(10)	(11)	(12)
	α_{TL} Degrees	α_{TL} Radian	$1-\epsilon_p/\alpha_{TL}$	(2)×(3)	h_p×(4)	ν_s	ν_s^2	4×(7)	D_s^2-(8)	b_{w_i}	$\frac{b_{w_i}\bar{c}_{w_i}}{S_w}$	$C_{l_{i_{AVE}}}$ Power Off
T_c=.70	-15	-.262	.559	-.146	-2.19	-3.26	10.62	42.48	139.23	11.80	.126	-.579
	-9	-.157		-.088	-1.32	-2.39	5.71	20.84	160.87	12.68	.135	-.073
	-3	-.0524		-.0292	-.44	-1.51	2.28	9.12	172.59	13.14	.140	.432
	3	.0524		.0292	.44	-.63	.40	1.60	180.11	13.42	.143	.937
	9	.157		.088	1.32	.25	.06	.24	181.47	13.47	.144	1.441
T_c=1.00	-15	-.262	.505	-.132	-1.98	-3.05	9.30	37.20	157.30	11.74	.125	-.579
	-9	-.157		-.079	-1.19	-2.26	5.10	20.40	154.10	12.42	.132	-.073
	-3	-.0524		-.0264	-.40	-1.47	2.16	8.64	165.86	12.88	.137	.432
	3	.0524		.0264	.40	-.67	.45	1.80	172.70	13.14	.140	.937
	9	.157		.079	1.19	.12	.01	.04	174.46	13.21	.141	1.441

	(13)	(14)	(15)	(16)	(17)	(18)	(19)	(20)	(21)	(22)	(23)
	α_{TL}	(11)×(12)	S×(13)	$\lambda' a_s$(11)	ϵ_p×S	(15)×(16)	$\Delta C_{L_{WI}}$	T_c	S	$\frac{1+3/2}{1+S}$	$\sqrt{(21)}$	D_s
T_c=.70	-15	-.073	-.049	.0076	-4.43	-.034	-.015	.70	.669	.800	.894	13.48
	-9	-.010	-.007	.0081	-2.66	-.022	.015					
	-3	.061	.041	.0084	-.89	-.007	.048					
	3	.134	.090	.0086	.89	.008	.082					
	9	.208	.139	.0087	2.66	.023	.116					
T_c=1.00	-15	-.072	-.063	.0075	-6.55	-.049	-.014	1.00	.882	.766	.876	13.21
	-9	-.010	-.009	.0079	-3.92	-.031	.022					
	-3	.059	.052	.0082	-1.32	-.011	.063					
	3	.131	.115	.0084	1.32	.011	.104					
	9	.205	.179	.0085	3.92	.033	.146					

FIG. 113

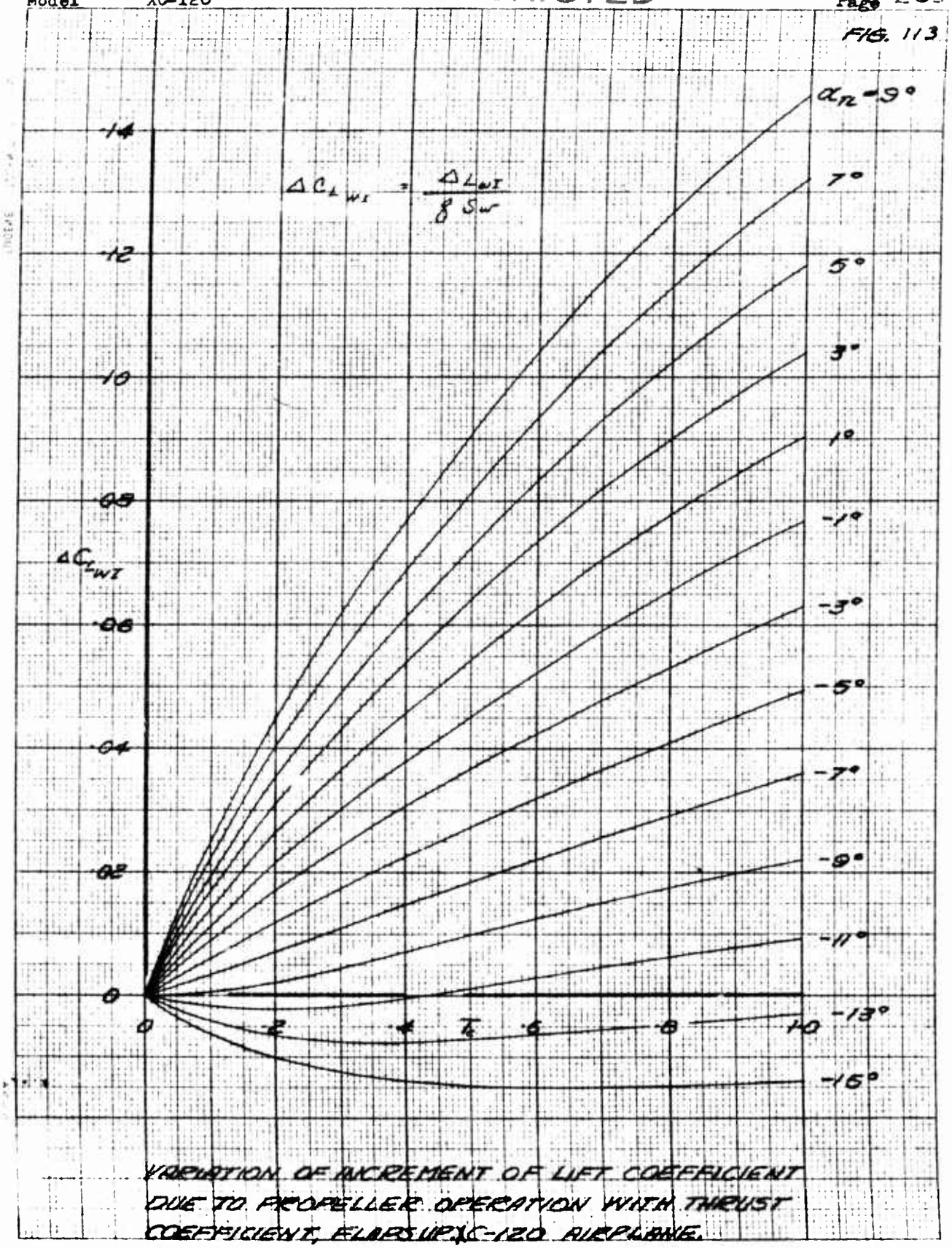

VARIATION OF INCREMENT OF LIFT COEFFICIENT DUE TO PROPELLER OPERATION WITH THRUST COEFFICIENT, FLAPS UP, XC-120 AIRPLANE.

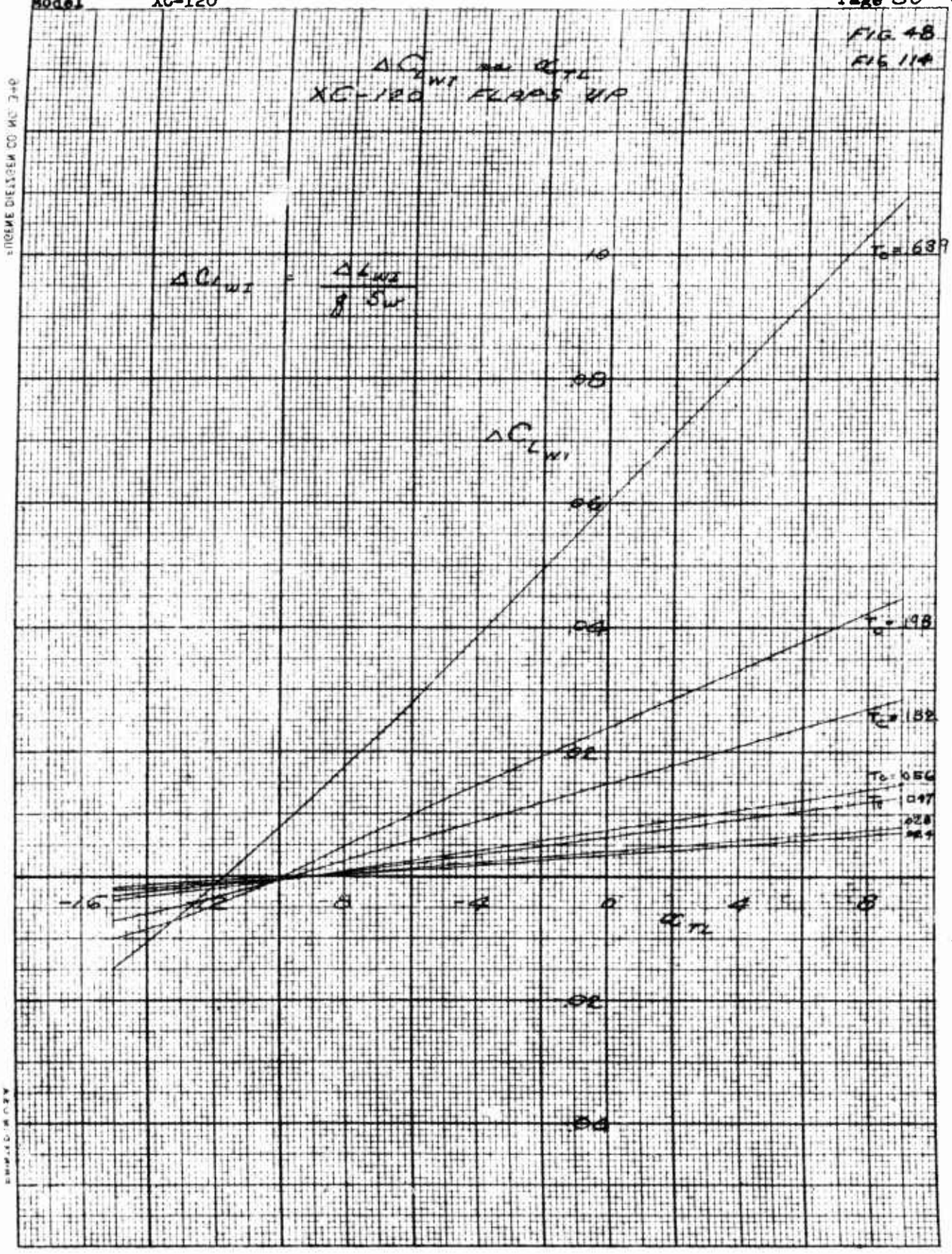
FIG. 48
FIG. 114
XC-120 FLAPS UP
$\Delta C_{L_{WI}}$
$\Delta C_{L_{WI}} = \frac{\Delta L_{WI}}{q\, S_W}$
$T_c = .639$
$T_c = .198$
$T_c = .182$
$T_c = .056$
$T_c = .047$
$T_c = .028$
$T_c = .014$
.10
.08
.06
.04
.02
-.02
-.04
-16
-12
-8
-4
0
4
8
α_{TL}

PART II-B-1-c

c. SLIPSTREAM EFFECTS ON DRAG

The computation of the increments of induced drag coefficient, profile drag coefficient and total drag coefficient due to propeller operation follow the method as outlined in Part II-B-1-c of reference (1).

The results are shown graphically in figure 115 to 117.

RESTRICTED

TABLE
COMPUTATION OF INCREMENT OF INDUCED DRAG
COEFFICIENT DUE TO PROPELLER OPERATION
FLAPS UP ONE ENGINE

	(1)	(2)	(3)	(4)	(5)	(6)	(7)	(8)
	α_{TL}	$\Delta C_{l_{i\,AVE}}$ Due T. Power	$C_{l_{i\,AVE}}$ Power Off	$C_{l_{i\,AVE}}$ Power On	ϵ_p Radian	(4) x (5)	$\frac{b_{wi} \cdot \tau_{wi}}{S_w}$	$\Delta C_{D_{I_{WI}}}$
$T_c = .05$	-15	-.016	-.579	-.595	-.0419	.0249	.128	.0032
	-9	0	-.073	-.073	-.0252	.0018	.144	.0003
	-3	.016	.432	.448	-.0084	-.0038	.154	-.0006
	3	.037	.937	.974	.0084	.0082	.158	.0013
	9	.053	1.441	1.494	.0252	.0377	.157	.0059
$T_c = .10$	-15	-.025	-.579	-.604	-.0514	.0310	.128	.0040
	-9	.004	-.073	-.069	-.0308	.0021	.145	.0003
	-3	.037	.432	.469	-.0105	-.0048	.152	-.0007
	3	.070	.937	1.007	.0105	.0104	.156	.0016
	9	.102	1.441	1.543	.0308	.0475	.155	.0074
$T_c = .20$	-15	-.041	-.579	-.620	-.0676	.0419	.127	.0053
	-9	.008	-.073	-.065	-.0405	.0026	.141	.0004
	-3	.070	.432	.502	-.0135	-.0068	.149	-.0010
	3	.127	.937	1.064	.0135	.0144	.153	.0022
	9	.185	1.441	1.626	.0405	.0659	.152	.0100
$T_c = .40$	-15	-.057	-.579	-.636	-.0920	.0585	.127	.0074
	-9	.029	-.073	-.044	-.0551	.0024	.138	.0003
	-3	.123	.432	.555	-.0184	-.0102	.144	-.0015
	3	.221	.937	1.158	.0184	.0213	.148	.0032
	9	.316	1.441	1.757	.0551	.0969	.148	.0143
$T_c = .70$	-15	-.062	-.579	-.641	-.1157	.0741	.126	.0094
	-9	.062	-.073	-.011	-.0694	.0008	.135	.0001
	-3	.197	.432	.629	-.0231	-.0145	.140	-.0020
	3	.336	.937	1.273	.0231	.0294	.143	.0042
	9	.475	1.441	1.916	.0694	.1330	.144	.0191
$T_c = 1.00$	-15	-.057	-.579	-.636	-.1294	.0825	.125	.0103
	-9	.090	-.073	.017	-.0777	-.0013	.132	-.0002
	-3	.258	.432	.690	-.0259	-.0179	.137	-.0025
	3	.426	.937	1.363	.0259	.0353	.140	.0049
	9	.599	1.441	2.040	.0777	.1583	.141	.0223

FA-800-43

RESTRICTED

FIG. 115

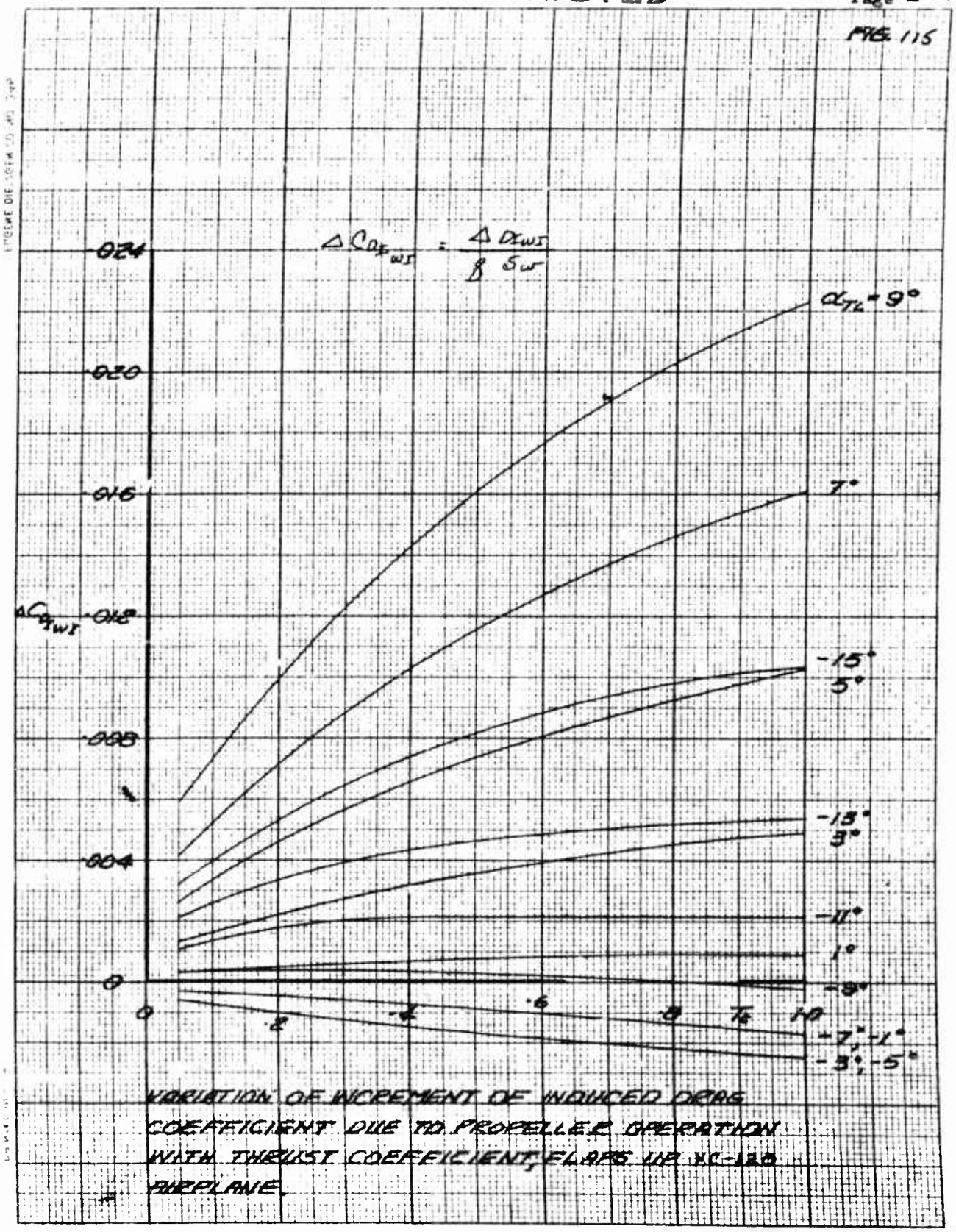

VARIATION OF INCREMENT OF INDUCED DRAG COEFFICIENT DUE TO PROPELLER OPERATION WITH THRUST COEFFICIENT, FLAPS UP XC-120 AIRPLANE

TABLE

COMPUTATION OF INCREMENT OF DRAG COEFFICIENT
DUE TO PROPELLER OPERATION
FLAPS UP ONE ENGINE

	(1)	(2)	(3)	(4)	(5)	(6)	(7)
	α_{TL}	$\frac{8}{\pi} T_c$	$\frac{b_{wi} \times \bar{c}_{wi}}{S_w}$	(2) × (3)	$C_{d_{TWS}}$ Power Off	$\Delta C_{D_{WI}}$	$\Delta C_{D_{WI}}$
	-15	.1273	.128	.0163	.0103	.0002	.0034
	-9		.144	.0183	.0069	.0001	.0004
$T_c = .05$	-3		.154	.0196	.0085	.0002	-.0004
	3		.158	.0201	.0165	.0003	.0016
	9		.157	.0200	.0327	.0007	.0066
	-15	.2545	.128	.0326	.0103	.0005	.0043
	-9		.143	.0364	.0069	.0008	.0005
$T_c = .10$	-3		.152	.0387	.0085	.0005	-.0004
	3		.156	.0397	.0165	.0007	.0022
	9		.155	.0394	.0327	.0013	.0087
	-15	.509	.127	.0646	.0103	.0007	.0060
	-9		.141	.0717	.0069	.0005	.0009
$T_c = .20$	-3		.149	.0758	.0085	.0006	-.0004
	3		.153	.0778	.0165	.0013	.0035
	9		.152	.0773	.0327	.0025	.0125
	-15	1.018	.127	.1295	.0103	.0013	.0087
	-9		.138	.1407	.0069	.0010	.0013
$T_c = .40$	-3		.144	.1467	.0085	.0012	-.0003
	3		.148	.1507	.0165	.0025	.0057
	9		.148	.1507	.0327	.0049	.0192
	-15	1.783	.126	.225	.0103	.0023	.0117
	-9		.135	.241	.0069	.0017	.0018
$T_c = .70$	-3		.140	.250	.0085	.0021	.0001
	3		.143	.255	.0165	.0042	.0084
	9		.144	.257	.0327	.0084	.0275
	-15	2.545	.128	.318	.0103	.0033	.0136
	-9		.132	.336	.0069	.0023	.0021
$T_c = 1.00$	-3		.137	.349	.0085	.0030	.0005
	3		.140	.356	.0165	.0059	.0108
	9		.141	.359	.0327	.0117	.0340

RESTRICTED

FIG 116

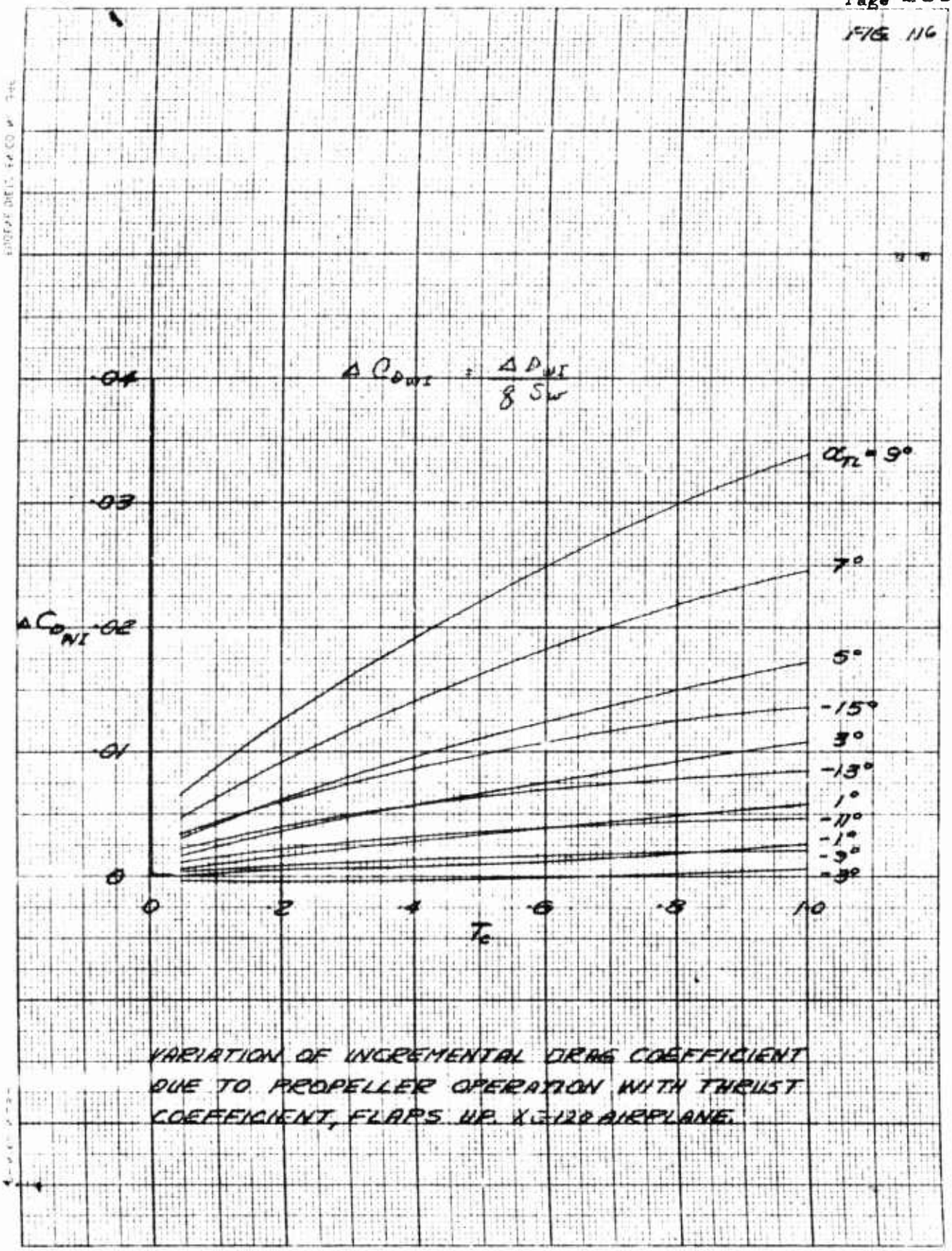

VARIATION OF INCREMENTAL DRAG COEFFICIENT DUE TO PROPELLER OPERATION WITH THRUST COEFFICIENT, FLAPS UP. XC-120 AIRPLANE.

RESTRICTED

F1 . 117

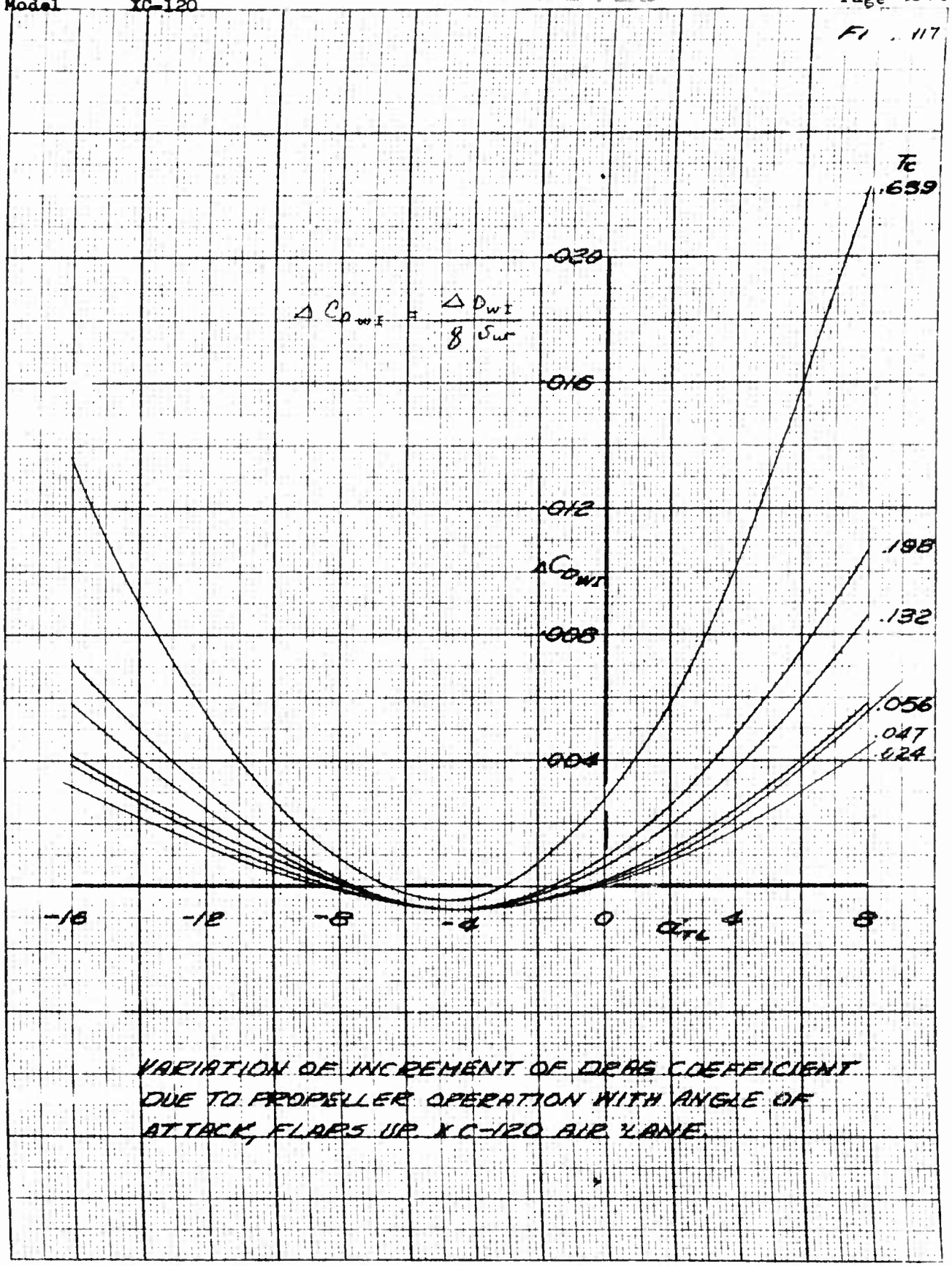

VARIATION OF INCREMENT OF DRAG COEFFICIENT DUE TO PROPELLER OPERATION WITH ANGLE OF ATTACK, FLAPS UP XC-120 AIR PLANE.

PART II-B-1-d

d. POLAR DIAGRAM

Figure 118 presents the variation of incremental lift coefficient versus incremental drag coefficient due to one propeller operation with military power for various thrust coefficients.

RESTRICTED

FIG 49
FIG 118

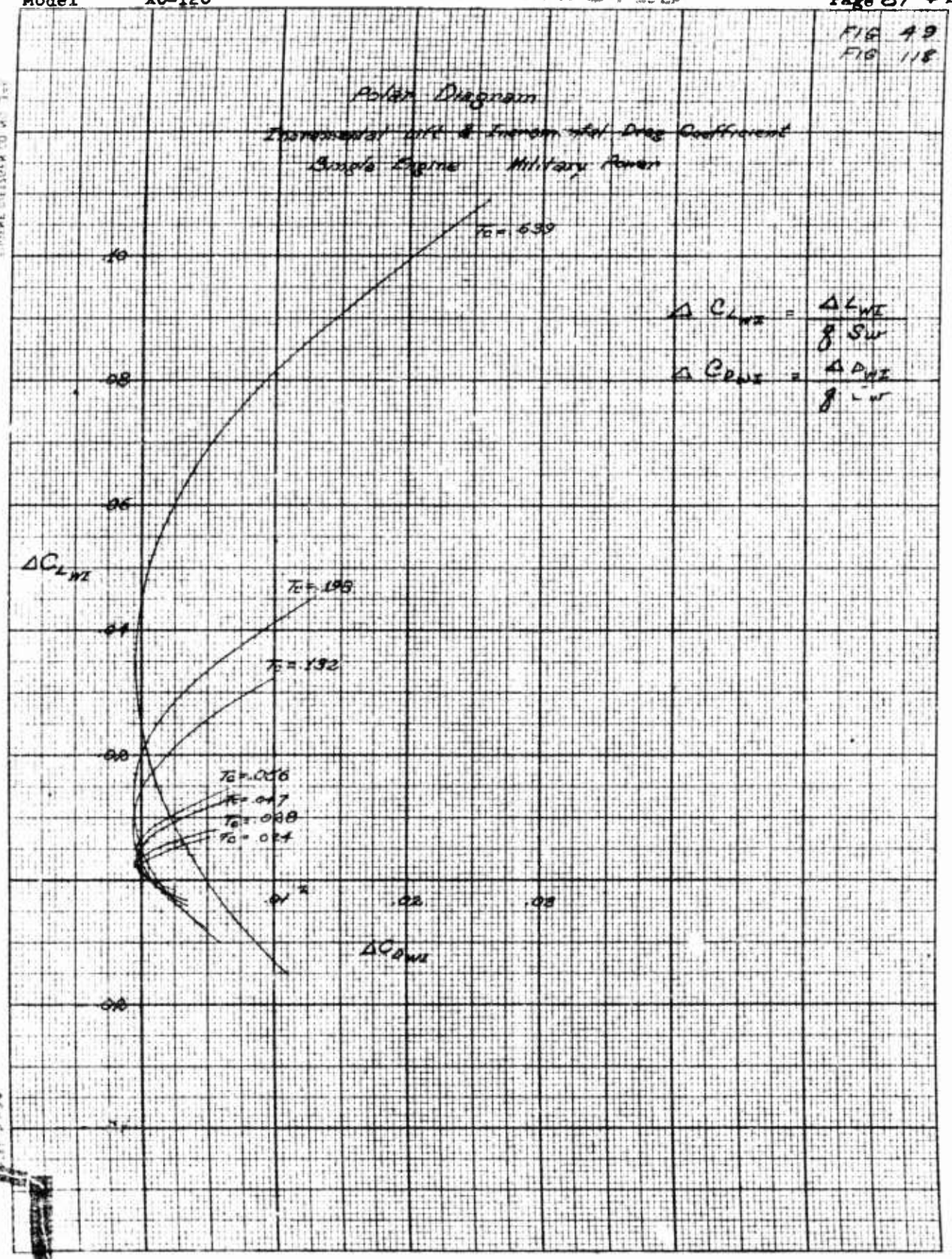

PART II-B-1-e

e. AERODYNAMIC FORCE COEFFICIENTS

The previously determined increments of lift and drag coefficients are resolved into X - and Z - force coefficients in the following table. These data are presented graphically in figures 119 to 122 inclusive.

TABLE

COMPUTATION OF INCREMENTS OF X - AND Z - FORCE COEFFICIENTS DUE TO PROPELLER OPERATION

FLAPS UP ONE ENGINE

	(1)	(2)	(3)	(4)	(5)	(6)	(7)	(8)	(9)	(10)	(11)
	α_n	$\Delta C_{L_{WI}}$	$\Delta C_{D_{WI}}$	$\sin\alpha_n$	$\cos\alpha_n$	(2)×(5)	(3)×(4)	(3)×(5)	(2)×(4)	$\Delta C_{Z_{WI}}$	$\Delta C_{X_{WI}}$
	-15	-.004	.0034	-.2588	.9659	-.0039	-.00088	.00328	.0010	-.0048	.00228
	-9	0	.0004	-.1564	.9877	0	-.00006	.00040	0	0	.00040
T_c=.05	-3	.004	-.0004	-.0523	.9986	.0040	-.00002	-.0040	-.0002	.0040	-.00020
	3	.009	.0016	.0523	.9986	.0090	.00008	.0160	.0005	.0091	.00110
	9	.013	.0066	.1564	.9877	.0157	.00103	.00652	.0020	.0138	.00432
	-15	-.006	.0043	-.2588	.9659	-.0058	-.00111	.00415	.0016	-.0069	.00255
	-9	.001	.0005	-.1564	.9877	.0010	-.00008	.00049	-.0002	.0010	-.00008
T_c=.10	-3	.009	-.0004	-.0523	.9986	.0090	.00002	-.00040	-.0005	.0090	.00010
	3	.017	.0023	.0523	.9986	.0170	.00012	.00230	.0009	.0171	.00140
	9	.025	.0087	.1564	.9877	.0247	.00136	.00859	.0039	.0261	.00469
	-15	-.010	.0060	-.2588	.9659	-.0097	-.00155	.00580	.0026	-.0113	.00320
	-9	.002	.0009	-.1564	.9877	.0020	-.00014	.00089	-.0005	.0019	.00119
T_c=.20	-3	.017	-.0004	-.0523	.9986	.0170	.00002	-.00040	-.0005	.0170	.00050
	3	.031	.0035	.0523	.9986	.0310	.00018	.00350	.0016	.0312	.00190
	9	.045	.0125	.1564	.9877	.0444	.00196	.01235	.0070	.0464	.00555
	-15	-.014	.0087	-.2588	.9659	-.0135	-.00225	.00840	.0036	-.0158	.00480
	-9	.007	.0013	-.1564	.9877	.0069	-.00020	.00128	-.0011	.0067	.00238
T_c=.40	-3	.030	-.0005	-.0523	.9986	.0300	.00002	-.00030	-.0016	.0300	.00130
	3	.054	.0057	.0523	.9986	.0539	.00030	.00569	.0028	.0542	.00289
	9	.077	.0192	.1564	.9877	.0761	.00300	.01896	.0120	.0791	.00636
	-15	-.015	.0117	-.2588	.9659	-.0145	-.00303	.01130	.0039	-.0175	.00740
	-9	.015	.0018	-.1564	.9877	.0148	-.00028	.00178	-.0023	.0143	.00403
T_c=.70	-3	.048	.0001	-.0523	.9986	.0479	-.00001	.00010	-.0025	.0479	.00210
	3	.082	.0084	.0523	.9986	.0819	.00044	.00829	.0043	.0828	.00593
	9	.116	.0275	.1564	.9877	.1146	.00430	.02716	.0181	.1109	.00906
	-15	-.014	.0136	-.2588	.9659	-.0135	-.00352	.01314	.0036	-.0170	.00954
	-9	.022	.0021	-.1564	.9877	.0217	-.00033	.00207	-.0034	.0214	.00547
T_c=1.00	-3	.063	.0005	-.0523	.9986	.0629	-.00003	.00050	-.0033	.0639	.00380
	3	.104	.0108	.0523	.9986	.1039	.0056	.01078	.0054	.1045	.00558
	9	.146	.0340	.1564	.9877	.1442	.00532	.03358	.0228	.1494	.01078

FIG. 119

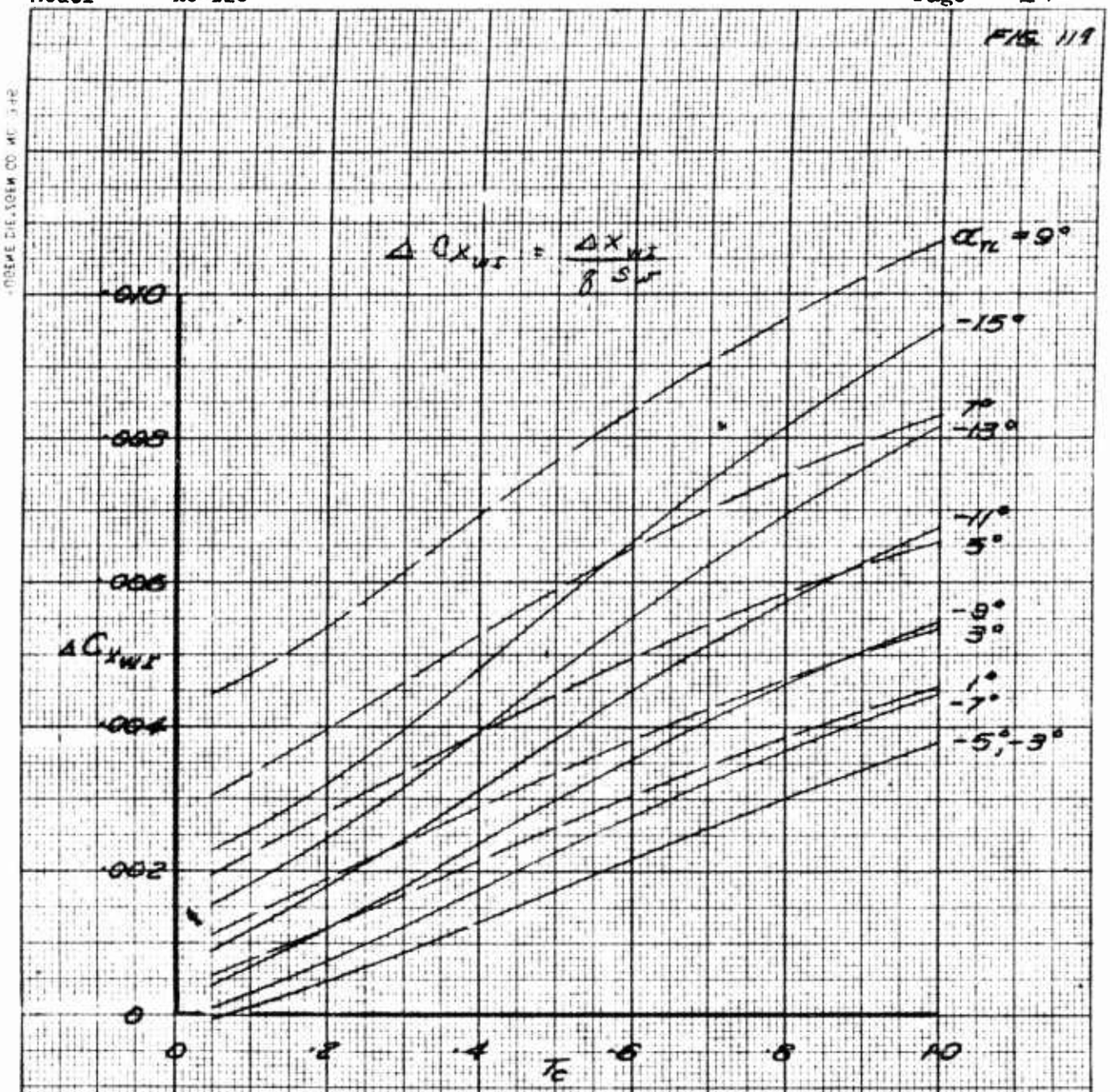

VARIATION OF INCREMENT OF X-FORCE COEFFICIENT DUE TO PROPELLER OPERATION WITH THRUST COEFFICIENT, FLAPS UP XC-120 AIRPLANE.

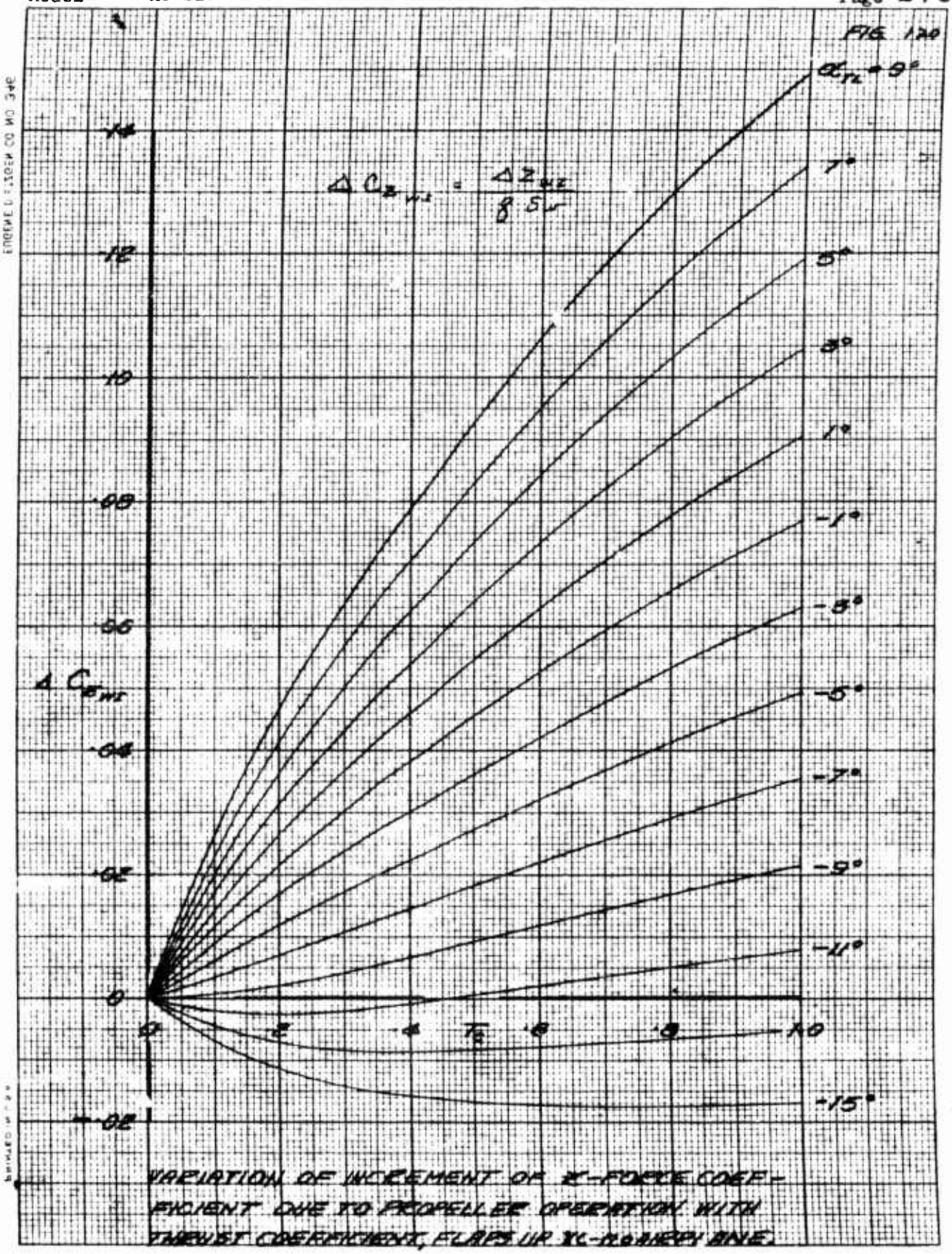

VARIATION OF INCREMENT OF Z-FORCE COEFFICIENT DUE TO PROPELLER OPERATION WITH THRUST COEFFICIENT, FLAPS UP XC-120 WITH ONE

RESTRICTED

FIG 50
FIG 121

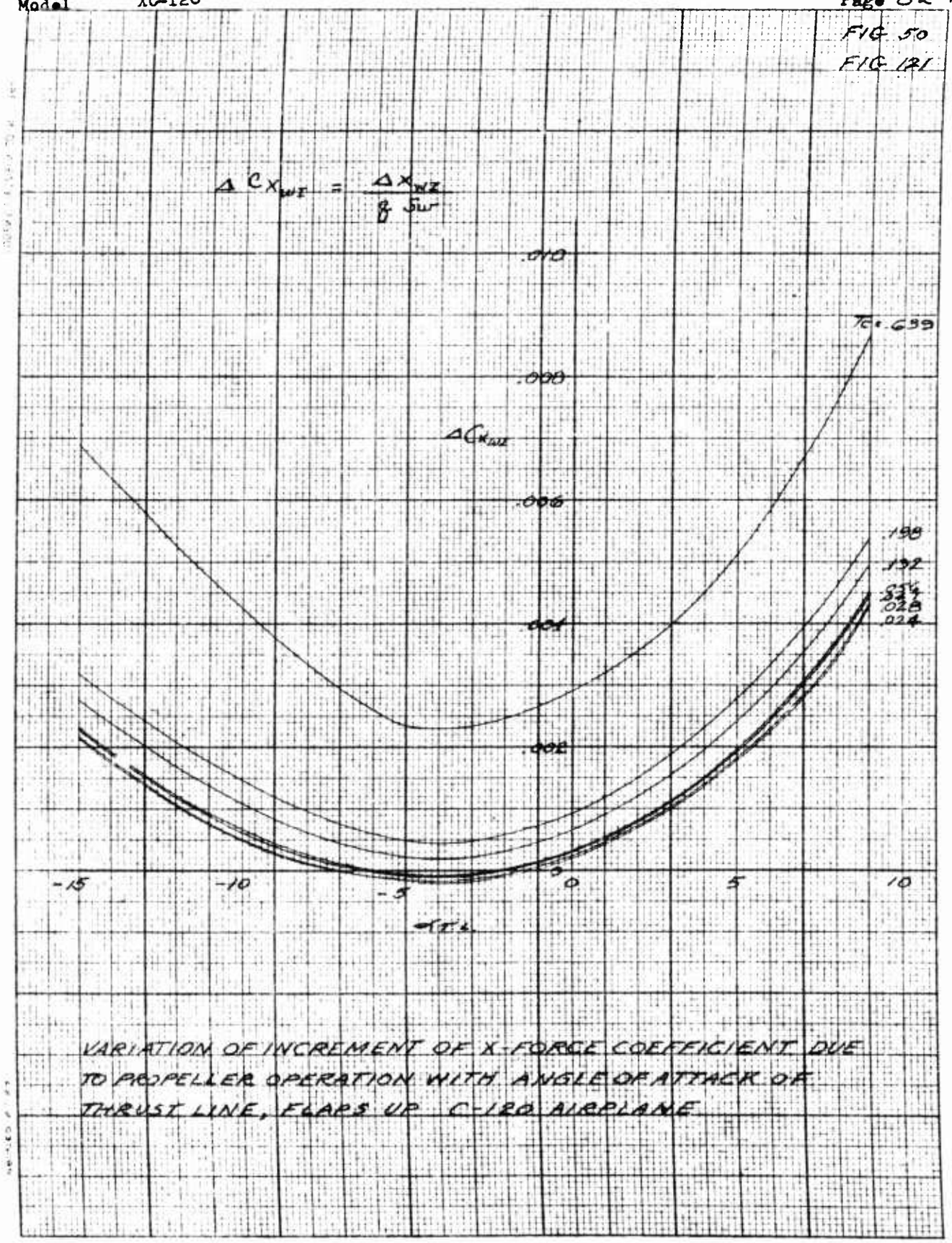

VARIATION OF INCREMENT OF X-FORCE COEFFICIENT DUE TO PROPELLER OPERATION WITH ANGLE OF ATTACK OF THRUST LINE, FLAPS UP C-120 AIRPLANE

RESTRICTED

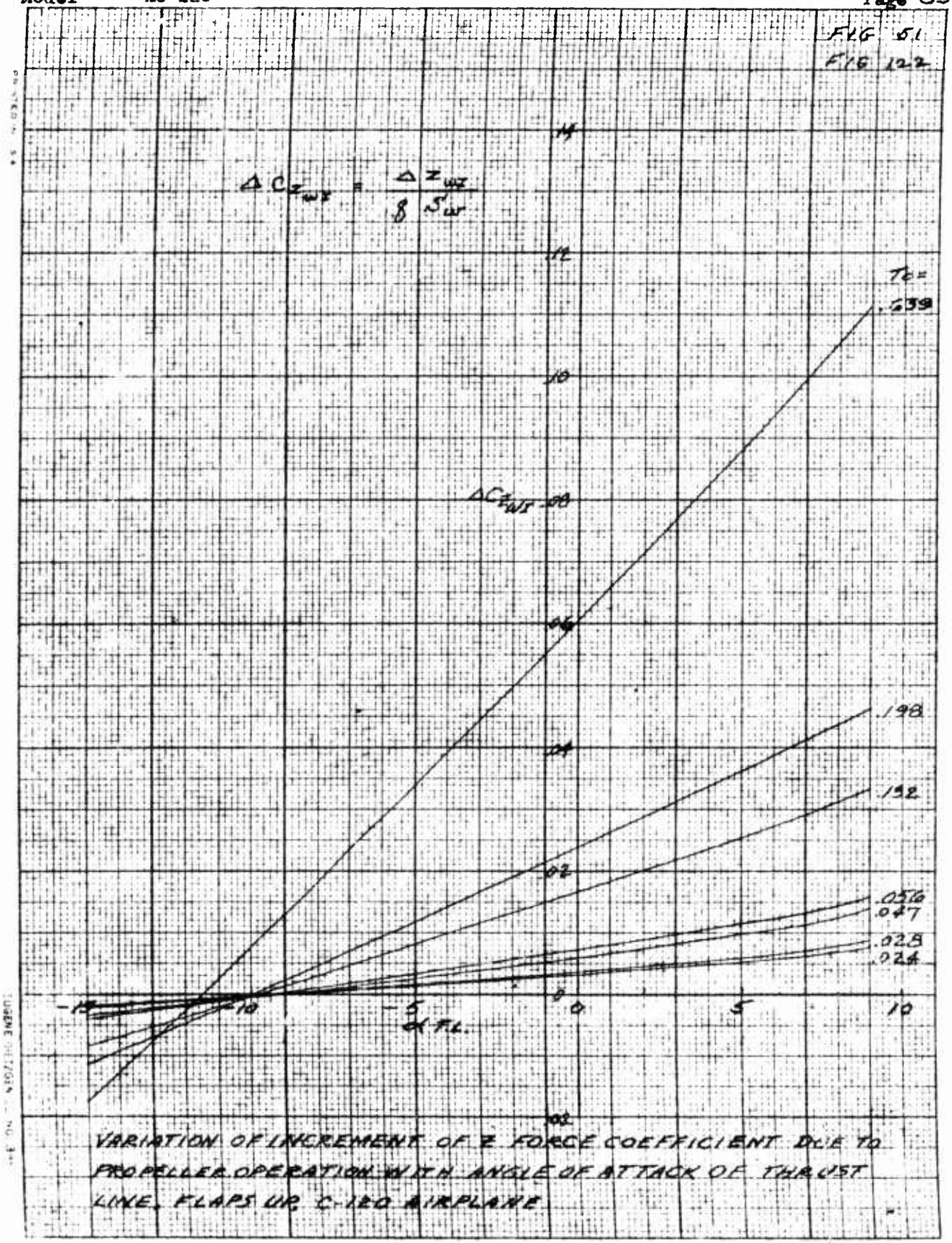

VARIATION OF INCREMENT OF Z FORCE COEFFICIENT DUE TO PROPELLER OPERATION WITH ANGLE OF ATTACK OF THRUST LINE, FLAPS UP, C-120 AIRPLANE

PART II-B-1-f

f. CHARACTERISTICS IN YAW

The characteristics of the unflapped wing with power-on in yaw are considered to be the same as those of the unflapped wing, power-off as presented in Part II-A-1-p taking into consideration the fact that the wing lift coefficient with power-on for the same angle of attack will be different.

PART II-B-2

2. WING FLAPPED

This section presents the detailed analysis to determine the effects of power on the aerodynamic characteristics of the flapped wing.

All characteristics are calculated as incremental effects due to one engine in operation with military power and all coefficients are based on total wing area.

PART II-B-2-a

a. SLIPSTREAM EFFECTS ON PITCHING MOMENT

The methods of reference (1) were used in the computation of the increment of wing pitching moment coefficient due to propeller operation, presented in the following table. Figure 123 presents the results of the computation in graphical form.

RESTRICTED

TABLE
COMPUTATION OF INCREMENT OF PITCHING MOMENT
COEFFICIENT DUE TO PROPELLER OPERATION
FLAPS DOWN ONE ENGINE

	(1)	(2)	(3)	(4)	(5)	(6)
	α_{TL}	b_{wi}	$C_{m_{acwi}} \times b_{wi} \times \bar{c}_{wi}^2$	(3) / $MAC \times S_w$	$\frac{\delta}{\pi} T_c$	$\Delta C_{M_{WFI}}$
	-15	12.02	-1012	-.0499	.1273	-.0064
	-9	13.55	-1140	-.0562		-.0072
$T_c = .05$	-3	14.45	-1217	-.0600		-.0076
	3	14.84	-1250	-.0616		-.0079
	9	14.75	-1241	-.0611		-.0078
	-15	12.01	-1011	-.0499	.2545	-.0127
	-9	13.44	-1132	-.0559		-.0142
$T_c = .10$	-3	14.29	-1202	-.0593		-.0151
	3	14.65	-1233	-.0609		-.0155
	9	14.59	-1228	-.0605		-.0154
	-15	11.97	-1008	-.0496	.509	-.0252
	-9	13.22	-1113	-.0549		-.0279
$T_c = .20$	-3	13.98	-1177	-.0580		-.0295
	3	14.34	-1208	-.0595		-.0303
	9	14.31	-1205	-.0594		-.0302
	-15	11.90	-1002	-.0494	1.018	-.0503
	-9	12.92	-1088	-.0536		-.0546
$T_c = .40$	-3	13.57	-1142	-.0564		-.0574
	3	13.88	-1169	-.0576		-.0587
	9	13.90	-1170	-.0576		-.0587
	-15	11.80	-994	-.0490	1.783	-.0873
	-9	12.68	-1068	-.0526		-.0939
$T_c = .70$	-3	13.14	-1107	-.0545		-.0971
	3	13.42	-1130	-.0556		-.0991
	9	13.47	-1133	-.0558		-.0994
	-15	11.74	-989	-.0487	2.545	-.1240
	-9	12.42	-1046	-.0515		-.1311
$T_c = 1.00$	-3	12.88	-1084	-.0535		-.1362
	3	13.14	-1107	-.0545		-.1388
	9	13.21	-1112	-.0548		-.1396

FIG 123

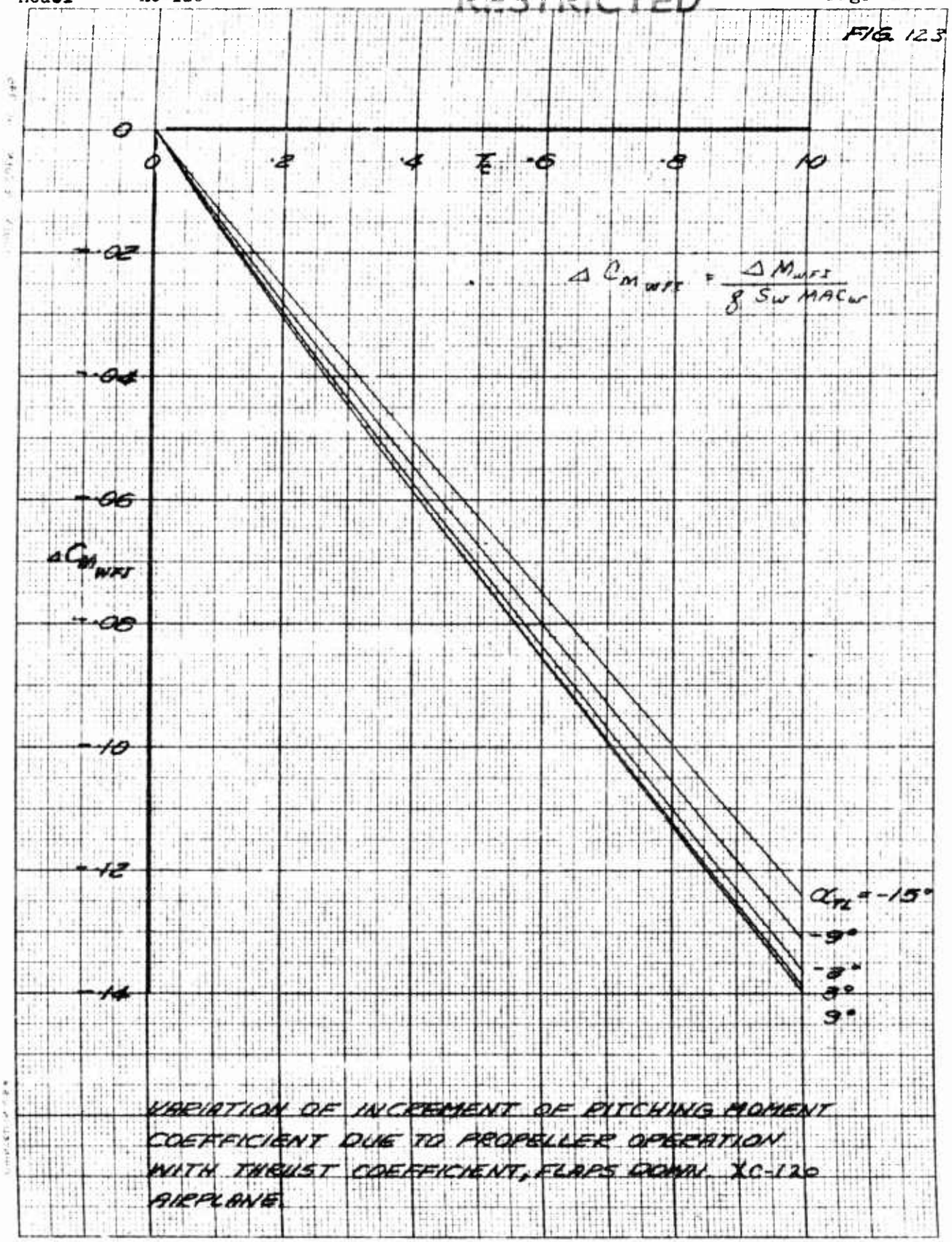

VARIATION OF INCREMENT OF PITCHING MOMENT COEFFICIENT DUE TO PROPELLER OPERATION WITH THRUST COEFFICIENT, FLAPS DOWN. XC-120 AIRPLANE.

FIG 52
FIG 124

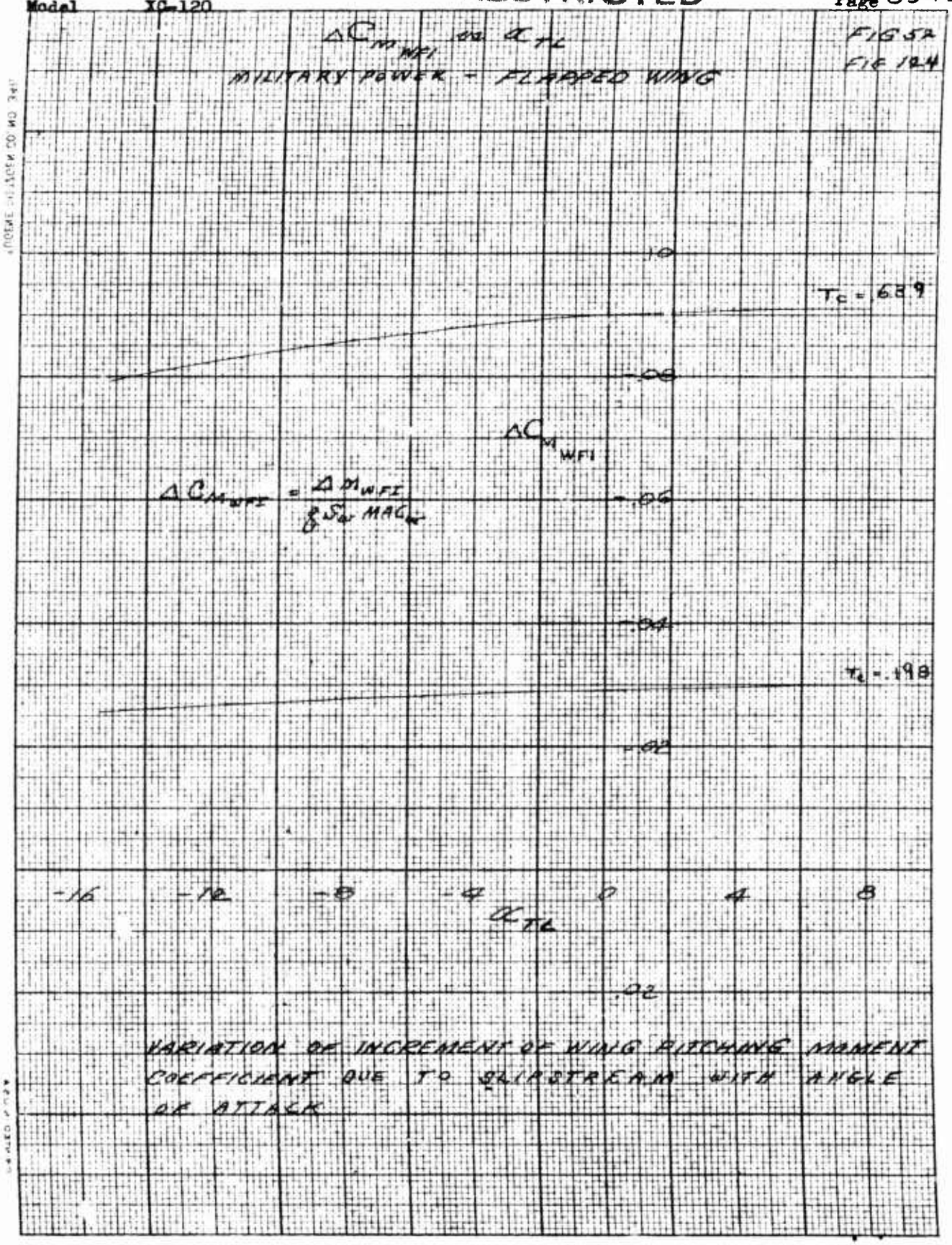

VARIATION OF INCREMENT OF WING PITCHING MOMENT COEFFICIENT DUE TO SLIPSTREAM WITH ANGLE OF ATTACK

PART II-B-2-b

b. SLIPSTREAM EFFECTS ON LIFT

The increment of wing lift coefficient due to propeller operation is computed in the manner outlined in reference (1). Calculations are presented in the following table and shown graphically in figure 125 .

TABLE

COMPUTATION OF INCREMENT OF LIFT COEFFICIENT
DUE TO PROPELLER OPERATION
FLAPS DOWN ONE ENGINE

	(1)	(2)	(3)	(4)	(5)	(6)	(7)	(8)	(9)	(10)	(11)
	α_{TL}	b_{wi}	$\frac{b_{wi}\bar{c}_{wi}}{S_w}$	$C_{L_{i_{BASIC}}}$ Power Off	(3)×(4)	5×(5)	1.6×(6)	$\lambda' a_s$ (3)	ϵ_p×5	(8)×(9)	$\Delta C_{L_{WFI}}$
	-15	12.02	.128	-.040	-.005	0	0	.0077	-.149	-.001	.001
	-9	13.55	.144	.465	.067	.004	.006	.0086	-.089	-.001	.007
T_c=.05	-3	14.45	.154	.970	.149	.009	.014	.0092	-.030	0	.014
	3	14.84	.158	1.475	.233	.014	.022	.0095	.030	0	.022
	9	14.75	.157	1.980	.311	.019	.030	.0094	.089	.001	.029
	-15	12.01	.128	-.040	-.005	-.001	-.002	.0077	-.353	-.003	.001
	-9	13.44	.143	.465	.067	.008	.013	.0086	-.211	-.002	.015
T_c=.10	-3	14.29	.152	.970	.147	.018	.029	.0091	-.071	-.001	.030
	3	14.65	.156	1.475	.230	.028	.045	.0094	.071	.001	.044
	9	14.59	.155	1.980	.307	.037	.059	.0093	.211	.002	.057
	-15	11.97	.127	-.040	-.005	-.001	-.002	.0076	-.883	-.007	.005
	-9	13.22	.141	.465	.066	.015	.024	.0085	-.529	-.004	.028
T_c=.20	-3	13.98	.149	.970	.145	.033	.053	.0089	-.175	-.002	.055
	3	14.34	.153	1.475	.225	.051	.082	.0092	.175	.002	.080
	9	14.31	.152	1.980	.301	.069	.109	.0091	.529	.008	.104
	-15	11.90	.127	-.040	-.005	-.002	-.003	.0076	-2.21	-.017	.014
	-9	12.92	.138	.465	.064	.027	.043	.0083	-1.327	-.011	.054
T_c=.40	-3	13.57	.144	.970	.140	.059	.094	.0086	-.441	-.004	.098
	3	13.88	.148	1.475	.218	.092	.147	.0089	.441	.004	.143
	9	13.90	.148	1.980	.293	.123	.197	.0089	1.327	.012	.185
	-15	11.80	.126	-.040	-.005	-.003	-.005	.0076	-4.43	-.034	.029
	-9	12.68	.135	.465	.063	.042	.067	.0081	-2.66	-.022	.089
T_c=.70	-3	13.14	.140	.970	.136	.091	.146	.0084	-.89	-.007	.153
	3	13.42	.143	1.475	.211	.141	.226	.0086	.89	.007	.219
	9	13.47	.144	1.980	.285	.191	.306	.0087	2.66	.023	.283
	-15	11.74	.125	-.040	-.005	-.004	-.006	.0075	-6.55	-.049	.043
	-9	12.42	.132	.465	.061	.054	.086	.0079	-3.92	-.031	.117
T_c=1.00	-3	12.88	.137	.970	.133	.117	.187	.0082	-1.32	-.011	.198
	3	13.14	.140	1.475	.206	.182	.291	.0084	1.32	.011	.280
	9	13.21	.141	1.980	.279	.246	.394	.0085	3.92	.033	.361

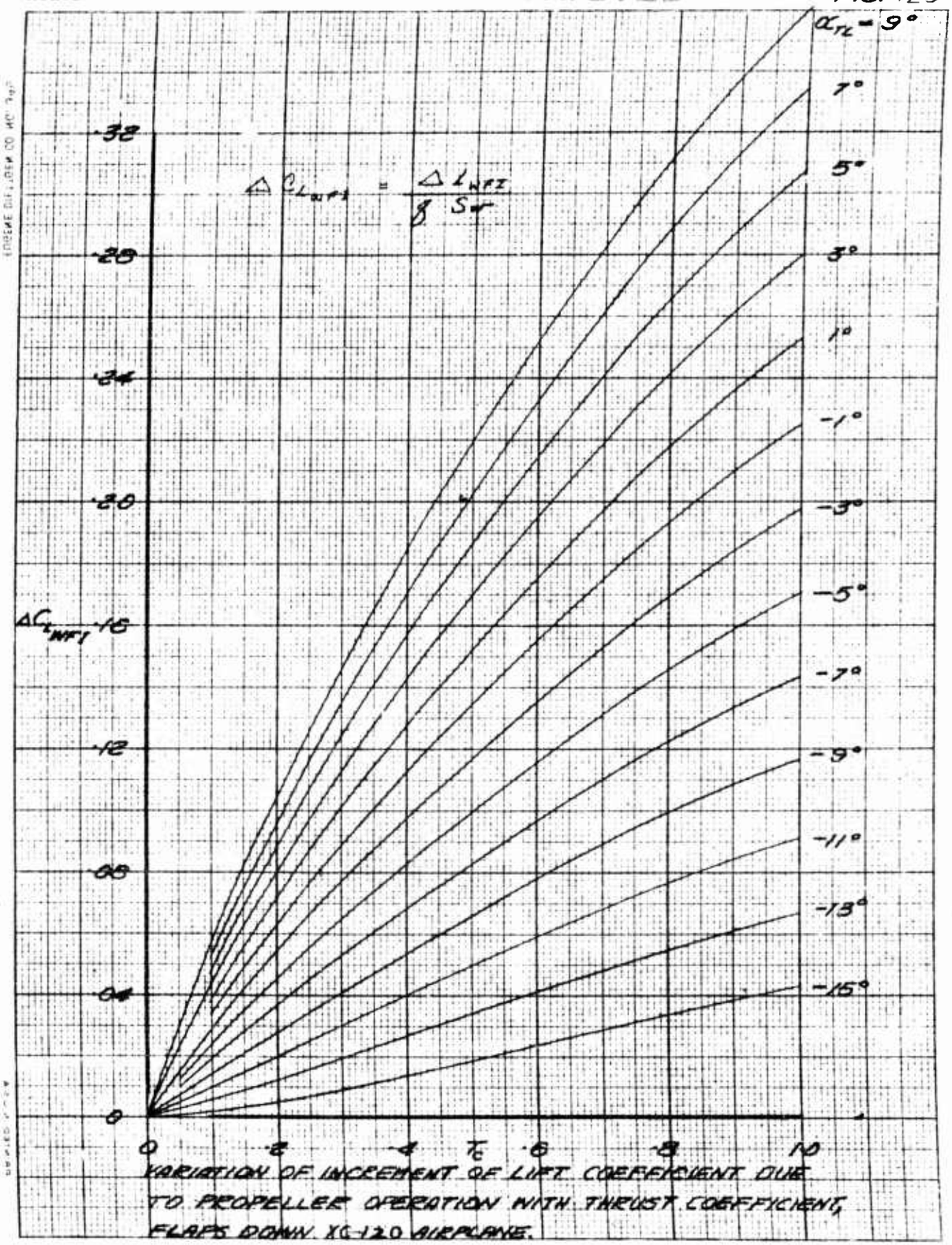

VARIATION OF INCREMENT OF LIFT COEFFICIENT DUE TO PROPELLER OPERATION WITH THRUST COEFFICIENT, FLAPS DOWN. XC-120 AIRPLANE.

RESTRICTED

FIG 53
FIG 126

$\Delta C_{L_{WF1}}$ vs α_{TL}

MILITARY POWER — FLAPPED WING

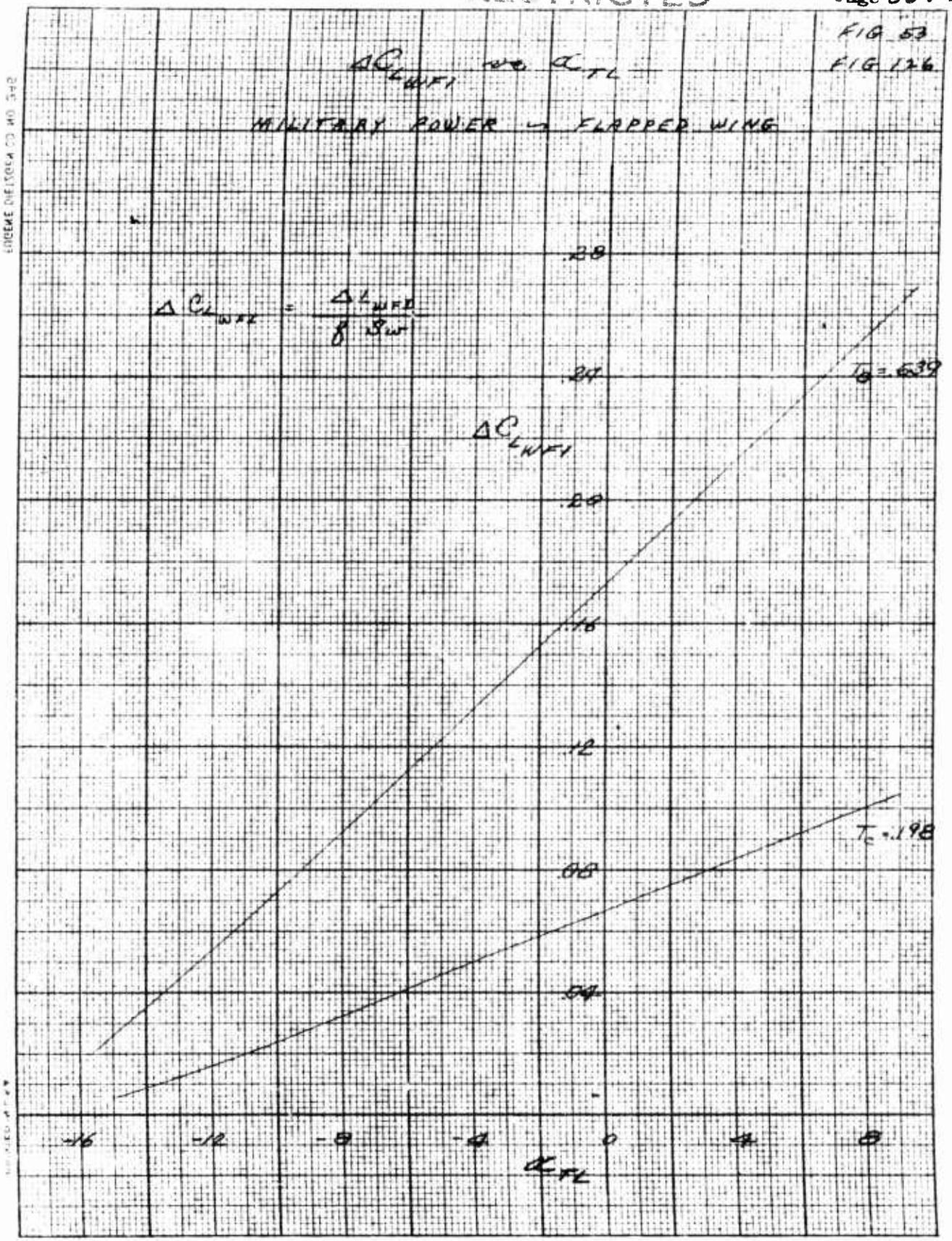

PART II-B-2-c

c. SLIPSTREAM EFFECTS ON DRAG

The computation of the increments of induced drag coefficient, profile drag coefficient and total drag coefficient due to propeller operation follow the method outlined in Part II-B-2-c of reference (1).

The results are shown graphically in figures 127, 128 & 129

RESTRICTED

TABLE
COMPUTATION OF INCREMENT OF INDUCED DRAG
COEFFICIENT DUE TO PROPELLER OPERATION
FLAPS DOWN - ONE ENGINE

	(1)	(2)	(3)	(4)	(5)	(6)	(7)	(8)	(9)	(10)	(11)	(12)
	α_{TL}	$\Delta C_{L_{i_{AVE}}}$ Opr to Power	$C_{L_{WF}}$	$w \times (2)(3)$	$w \times (2)^2$	$C_{L_{i_{AVE}}}$ Power Off	$C_{L_{i_{AVE}}}$ Power On	ϵ_p Radian	(7) × (8)	$\frac{b_{w_i} z_{w_i}}{S_w}$	(9) × (10)	$\Delta C_{D_{i_{WFI}}}$
	-15	.004	-.240	0	0	-.040	-.036	-.0419	.0015	.128	.0002	.0002
	-9	.029	.265	0	0	.465	.494	-.0252	-.0124	.144	-.0018	-.0018
$T_c = .05$	-3	.057	.770	0	0	.970	1.027	-.0084	-.0086	.154	-.0013	-.0013
	3	.090	1.275	-.0001	0	1.475	1.565	.0084	.0131	.158	.0021	.0020
	9	.119	1.780	-.0003	.0001	1.980	2.099	.0252	.0529	.157	.0083	.0081
	-15	.004	-.240	0	0	-.040	-.056	-.0514	.0019	.128	.0002	.0002
	-9	.062	.265	0	0	.465	.527	-.0308	-.0162	.145	-.0023	-.0023
$T_c = .10$	-3	.123	.770	-.0001	.0001	.970	1.093	-.0103	-.0113	.152	-.0017	-.0017
	3	.180	1.275	-.0003	.0001	1.475	1.655	.0103	.0171	.156	.0027	.0025
	9	.234	1.780	-.0005	.0002	1.980	2.214	.0308	.0681	.155	.0106	.0103
	-15	.021	-.240	0	0	-.040	-.019	-.0676	.0013	.127	.0002	.0002
	-9	.115	.265	0	.0001	.465	.580	-.0405	-.0235	.141	-.0033	-.0032
$T_c = .20$	-3	.226	.770	-.0002	.0002	.970	1.196	-.0135	-.0161	.149	-.0024	-.0024
	3	.328	1.275	-.0005	.0005	1.475	1.803	.0135	.0244	.153	.0037	.0037
	9	.427	1.780	-.0009	.0008	1.980	2.407	.0405	.0976	.152	.0148	.0147
	-15	.057	-.240	0	0	-.040	.017	-.0920	-.0016	.127	-.0002	-.0002
	-9	.221	.265	-.0001	.0002	.465	.686	-.0551	-.0379	.138	-.0052	-.0051
$T_c = .40$	-3	.402	.770	-.0004	.0007	.970	1.372	-.0184	-.0252	.144	-.0036	-.0035
	3	.586	1.275	-.0009	.0015	1.475	2.061	.0184	.0379	.148	.0056	.0062
	9	.758	1.780	-.0016	.0026	1.980	2.738	.0551	.1510	.148	.0224	.0234
	-15	.119	-.240	0	.0001	-.040	.079	-.1157	-.0091	.126	-.0011	-.0010
	-9	.365	.265	-.0001	.0006	.465	.830	-.0694	-.0576	.135	-.0078	-.0075
$T_c = .70$	-3	.627	.770	-.0006	.0018	.970	1.597	-.0231	-.0369	.140	-.0052	-.0040
	3	.898	1.275	-.0014	.0036	1.475	2.373	.0231	.0549	.143	.0079	.0101
	9	1.160	1.780	-.0025	.0061	1.980	3.140	.0694	.2180	.144	.0314	.0350
	-15	.176	-.240	.0001	.0001	-.040	.136	-.1294	-.0176	.125	-.0022	-.0020
	-9	.480	.265	-.0002	.0010	.465	.945	-.0777	-.0734	.132	-.0097	-.0089
$T_c = 1.00$	-3	.811	.770	-.0008	.0030	.970	1.781	-.0259	-.0461	.137	-.0063	-.0041
	3	1.148	1.275	-.0018	.0059	1.475	2.623	.0259	.0680	.140	.0095	.0136
	9	1.480	1.780	-.0032	.0098	1.980	3.460	.0777	.2690	.141	.0379	.0445

RESTRICTED

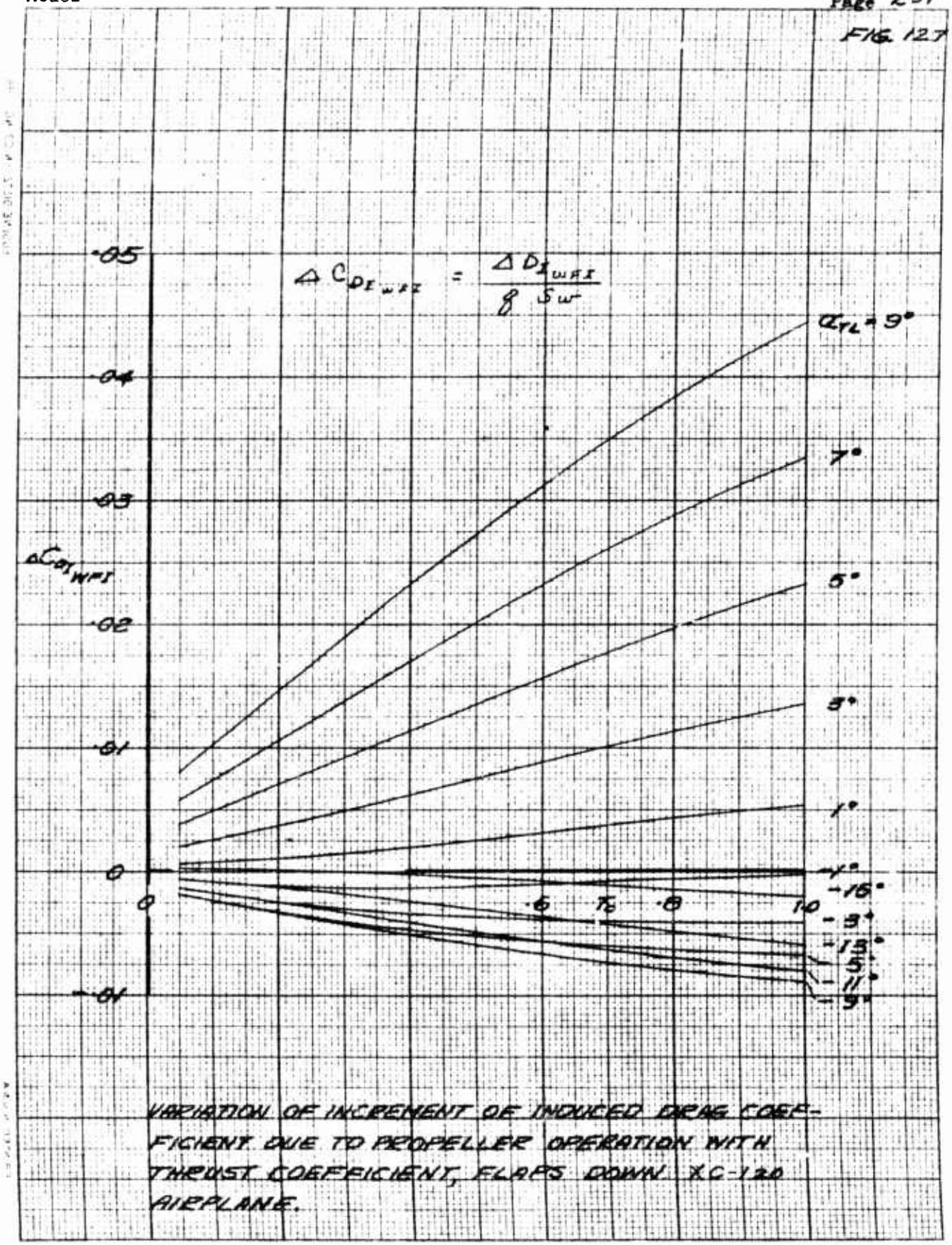

VARIATION OF INCREMENT OF INDUCED DRAG COEFFICIENT DUE TO PROPELLER OPERATION WITH THRUST COEFFICIENT, FLAPS DOWN XC-120 AIRPLANE.

TABLE
COMPUTATION OF INCREMENT OF DRAG COEFFICIENT
DUE TO PROPELLER OPERATION
FLAPS DOWN - ONE ENGINE

	(1)	(2)	(3)	(4)	(5)	(6)	(7)
	α_{TL}	$\frac{8}{\pi} T_c$	$\frac{b_{wi} \times \bar{c}_{wi}}{S_w}$	(2)×(3)	$C_{d_{2\,AVE}}$ Power Off	$\Delta C_{D_{0_{WFI}}}$	$\Delta C_{D_{WFI}}$
	-15	.1273	.128	.0163	.0220	.0004	.0006
	-9		.144	.0183	.0207	.0004	-.0014
T_c=.05	-3		.154	.0196	.0253	.0005	-.0008
	3		.158	.0201	.0341	.0007	.0027
	9		.157	.0200	.0581	.0012	.0093
	-15	.2545	.128	.0326	.0220	.0007	.0009
	-9		.143	.0364	.0207	.0008	-.0015
T_c=.10	-3		.152	.0387	.0253	.0010	-.0007
	3		.156	.0397	.0341	.0013	.0038
	9		.155	.0394	.0281	.0023	.0126
	-15	.509	.127	.0646	.0220	.0014	.0016
	-9		.141	.0717	.0207	.0015	-.0017
T_c=.20	-3		.149	.0758	.0253	.0019	-.0005
	3		.153	.0778	.0341	.0027	.0064
	9		.152	.0773	.0581	.0045	.0192
	-15	1.018	.127	.1293	.0220	.0028	.0026
	-9		.138	.1407	.0207	.0029	-.0022
T_c=.40	-3		.144	.1467	.0253	.0037	.0004
	3		.148	.1507	.0341	.0051	.0113
	9		.148	.1507	.0581	.0088	.0322
	-15	1.783	.126	.225	.0220	.0050	.0040
	-9		.135	.241	.0207	.0050	-.0023
T_c=.70	-3		.140	.250	.0253	.0063	.0023
	3		.143	.255	.0341	.0087	.0188
	9		.144	.257	.0581	.0149	.0499
	-15	2.545	.125	.318	.0220	.0070	.0050
	-9		.132	.336	.0207	.0070	-.0019
T_c=1.00	-3		.137	.349	.0253	.0088	.0047
	3		.140	.356	.0341	.0121	.0257
	9		.141	.359	.0581	.0209	.0654

FIG. 128

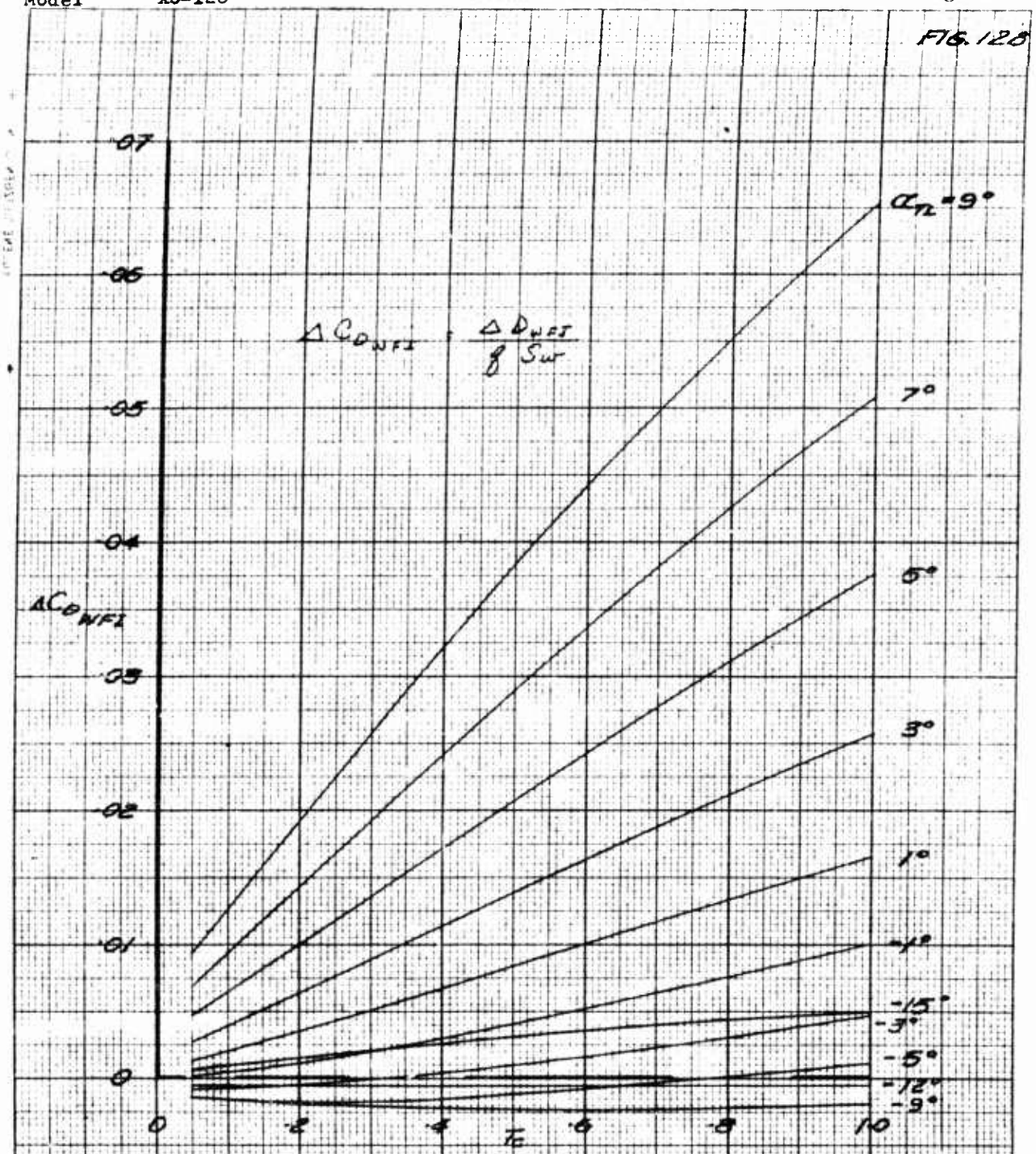

VARIATION OF INCREMENT OF DRAG COEFFICIENT DUE TO PROPELLER OPERATION WITH THRUST COEFFICIENT, FLAPS DOWN. XC-120 AIRPLANE.

FIG 129

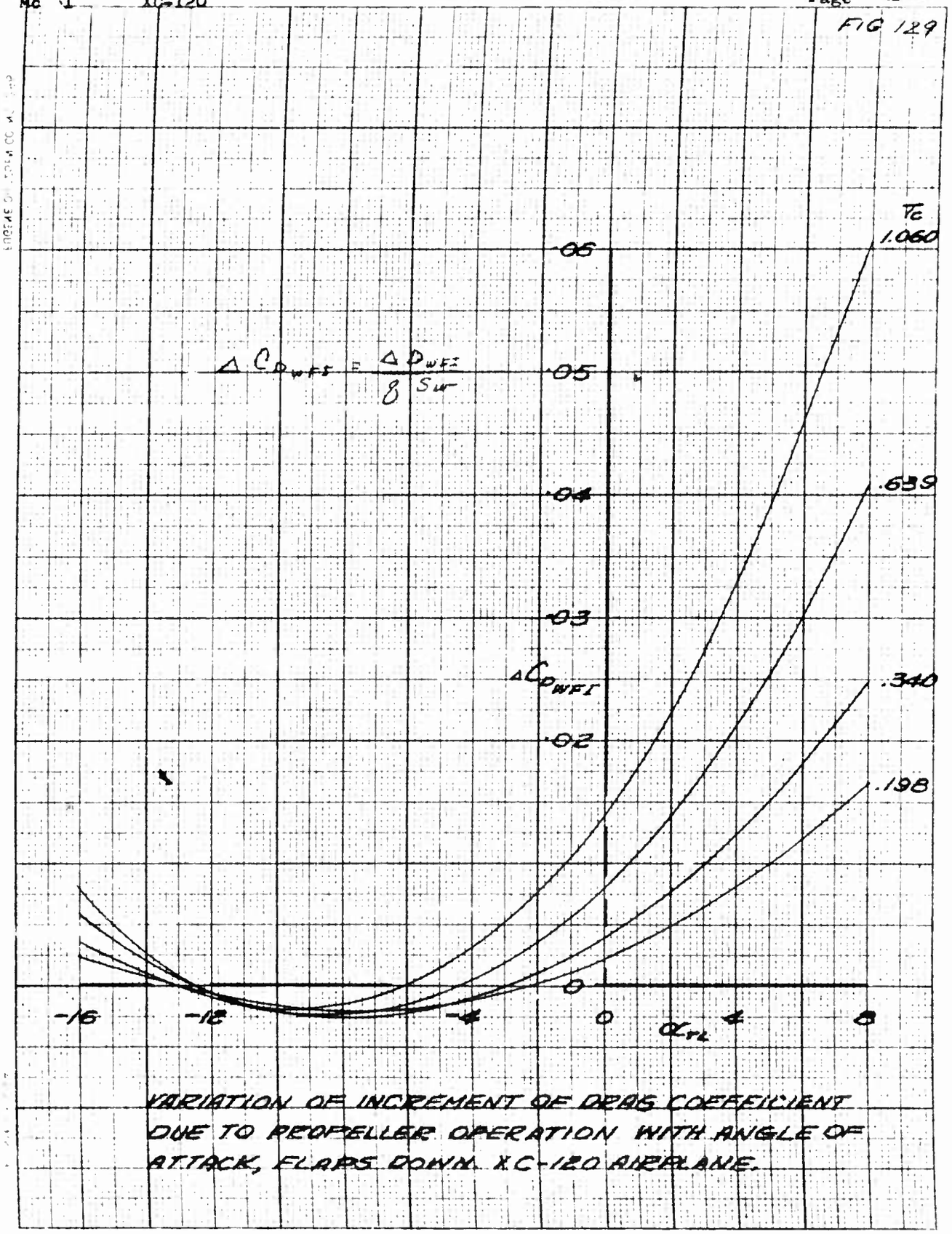

VARIATION OF INCREMENT OF DRAG COEFFICIENT DUE TO PROPELLER OPERATION WITH ANGLE OF ATTACK, FLAPS DOWN. XC-120 AIRPLANE.

PART II-B-2-d

d. POLAR DIAGRAM

Figure 130 presents the variation of incremental lift coefficient versus incremental drag coefficient due to one propeller operation with military power for various thrust coefficients.

Pg 58
Fig 130

POLAR DIAGRAM
INCREMENTAL LIFT vs INCREMENTAL DRAG

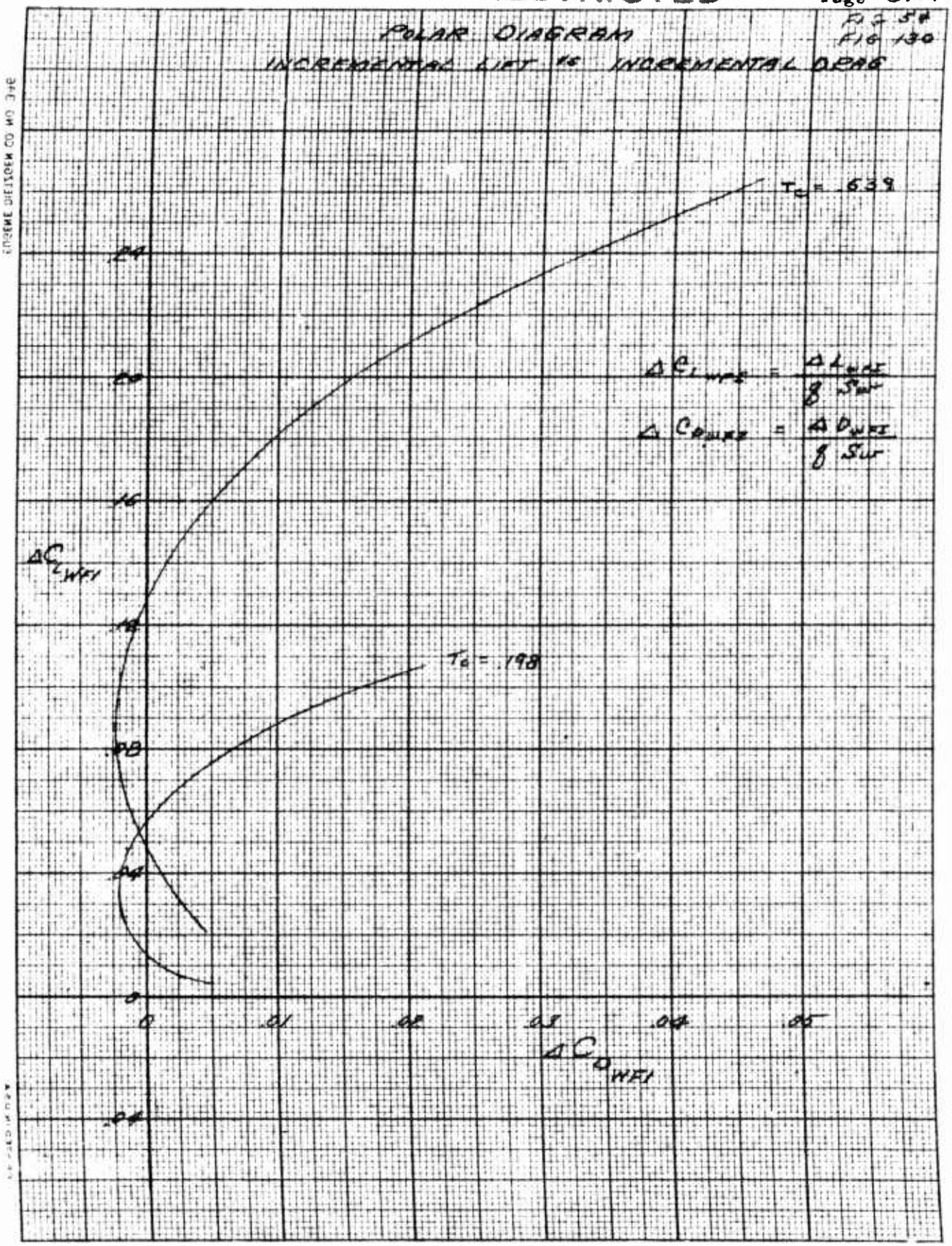

PART II-B-2-e

e. AERODYNAMIC FORCE COEFFICIENTS

The previously determined increments of lift and drag coefficients are resolved into X - and Z - force coefficients in the following table. The variation of these coefficients with thrust coefficient is shown in figures 131 to 133 inclusive.

TABLE
COMPUTATION OF INCREMENT OF X - AND Z - FORCE
COEFFICIENTS DUE TO PROPELLER OPERATION - FLAPS
DOWN - ONE ENGINE

	(1)	(2)	(3)	(4)	(5)	(6)	(7)	(8)	(9)	(10)	(11)
	α_{TL}	$\Delta C_{L_{WPS}}$	$\Delta C_{D_{WPS}}$	$\sin\alpha_{TL}$	$\cos\alpha_{TL}$	(2)×(5)	(3)×(4)	(3)×(5)	(2)×(4)	$\Delta C_{Z_{WPS}}$	$\Delta C_{X_{WPS}}$
	-15	.001	.0006	-.2588	.9659	.0010	-.00016	.00058	-.0003	.0008	.00088
	-9	.007	-.0014	-.1564	.9877	.0069	.00022	-.00138	-.0011	.0071	-.00028
T_c = .05	-3	.014	-.0008	-.0523	.9986	.0140	.00004	-.00080	-.0007	.0140	-.00010
	3	.022	.0027	.0523	.9986	.0220	.00014	.00270	.0012	.0231	.00150
	9	.029	.0093	.1564	.9877	.0286	.00145	.00919	.0045	.0300	.00469
	-15	.001	.0009	-.2588	.9659	.0010	-.00023	.00087	-.0008	.0008	.00117
	-9	.015	-.0015	-.1564	.9877	.0148	.00023	-.00148	-.0023	.0150	.00082
T_c = .10	-3	.030	-.0007	-.0523	.9986	.0300	.00004	-.00070	-.0016	.0300	.00090
	3	.044	.0058	.0523	.9986	.0439	.00320	.00579	.0023	.0441	.00149
	9	.057	.0126	.1564	.9877	.0568	.00197	.01245	.0089	.0583	.00355
	-15	.005	.0016	-.2588	.9659	.0048	-.00041	.00155	-.0013	.0044	.00285
	-9	.022	-.0017	-.1564	.9877	.0217	.00027	-.00168	-.0044	.0280	.00272
T_c = .20	-3	.043	-.0005	-.0523	.9986	.0549	.00003	-.00050	-.0029	.0549	.00240
	3	.080	.0064	.0523	.9986	.0799	.00033	.00639	.0042	.0802	.00219
	9	.104	.0192	.1564	.9877	.1027	.00300	.01896	.0163	.1057	.00266
	-15	.014	.0026	-.2588	.9659	.0135	-.00067	.00251	-.0036	.0128	.00611
	-9	.054	-.0022	-.1564	.9877	.0535	.00034	-.00217	-.0034	.0536	.00623
T_c = .40	-3	.098	.0004	-.0523	.9986	.0979	-.00002	.00040	-.0031	.0979	.00550
	3	.145	.0113	.0523	.9986	.1428	.00059	.01128	.0075	.1434	.00578
	9	.185	.0327	.1564	.9877	.1827	.00504	.03180	.0289	.1877	.00290
	-15	.029	.0040	-.2588	.9659	.0279	.00103	.00386	-.0075	.0270	.01136
	-9	.089	-.0029	-.1564	.9877	.0879	.00046	-.00287	-.0139	.0875	.01163
T_c = .70	-3	.153	.0023	-.0523	.9986	.1528	-.00012	.00230	-.0080	.1527	.01030
	3	.219	.0188	.0523	.9986	.2187	.00098	.01877	.0115	.2197	.00727
	9	.283	.0499	.1564	.9877	.2795	.00780	.04929	.0443	.2873	.00499
	-15	.042	.0050	-.2588	.9659	.0415	-.00129	.00483	-.0111	.0402	.01993
	-9	.117	-.0019	-.1564	.9877	.1156	.00020	-.00188	-.0183	.1150	.01648
T_c = 1.00	-3	.198	.0047	-.0523	.9986	.1977	-.00025	.00466	-.0104	.1974	.01509
	3	.280	.0257	.0523	.9986	.2796	.00134	.02568	.0146	.2809	.01106
	9	.361	.0654	.1564	.9877	.3566	.01023	.06460	.0565	.3668	.00810

RESTRICTED

FIG. 131

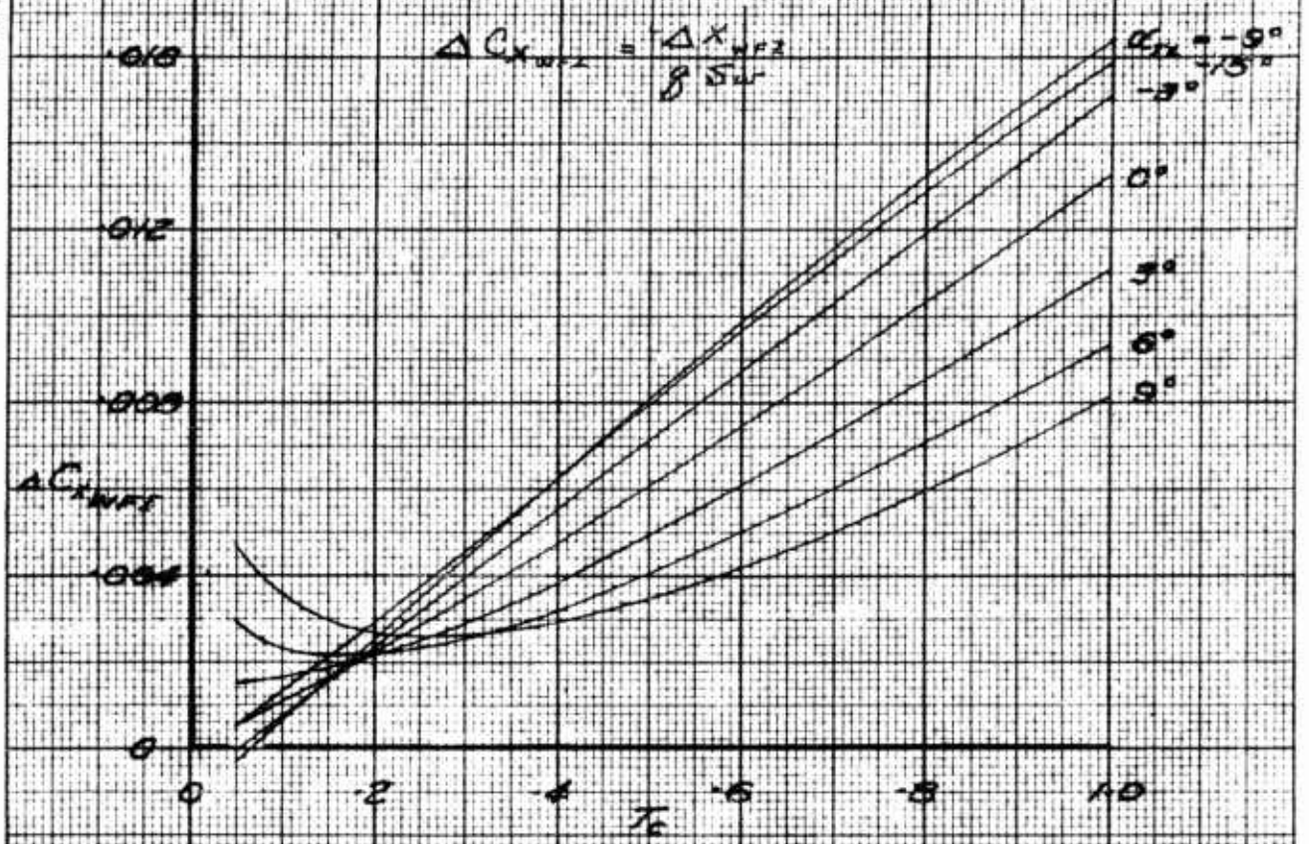

VARIATION OF INCREMENT OF X-FORCE COEFFICIENT DUE TO PROPELLER OPERATION WITH THRUST COEFFICIENT, FLAPS DOWN. XC-120 AIRPLANE.

RESTRICTED

FIG 85
FIG 188

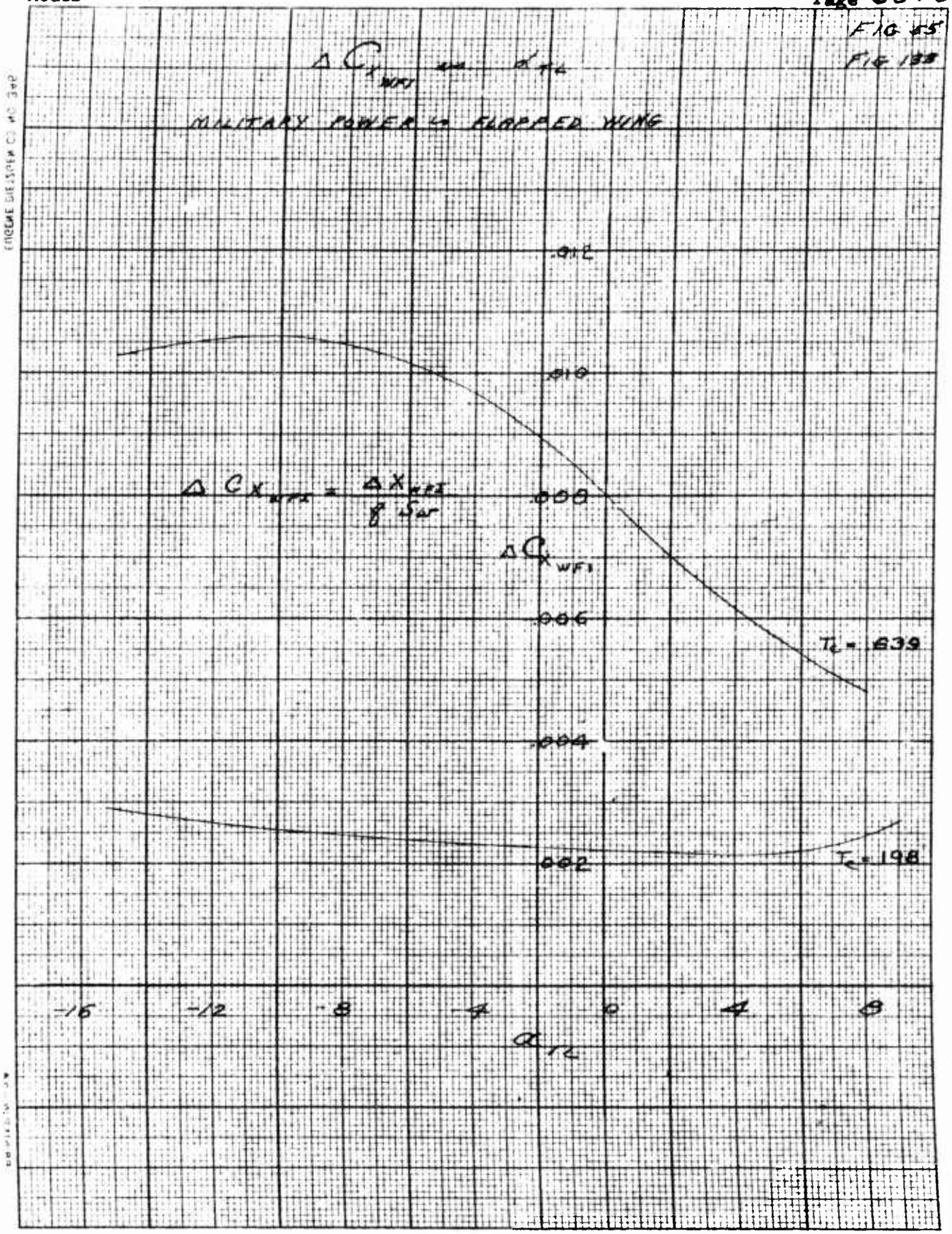

FIG. 133

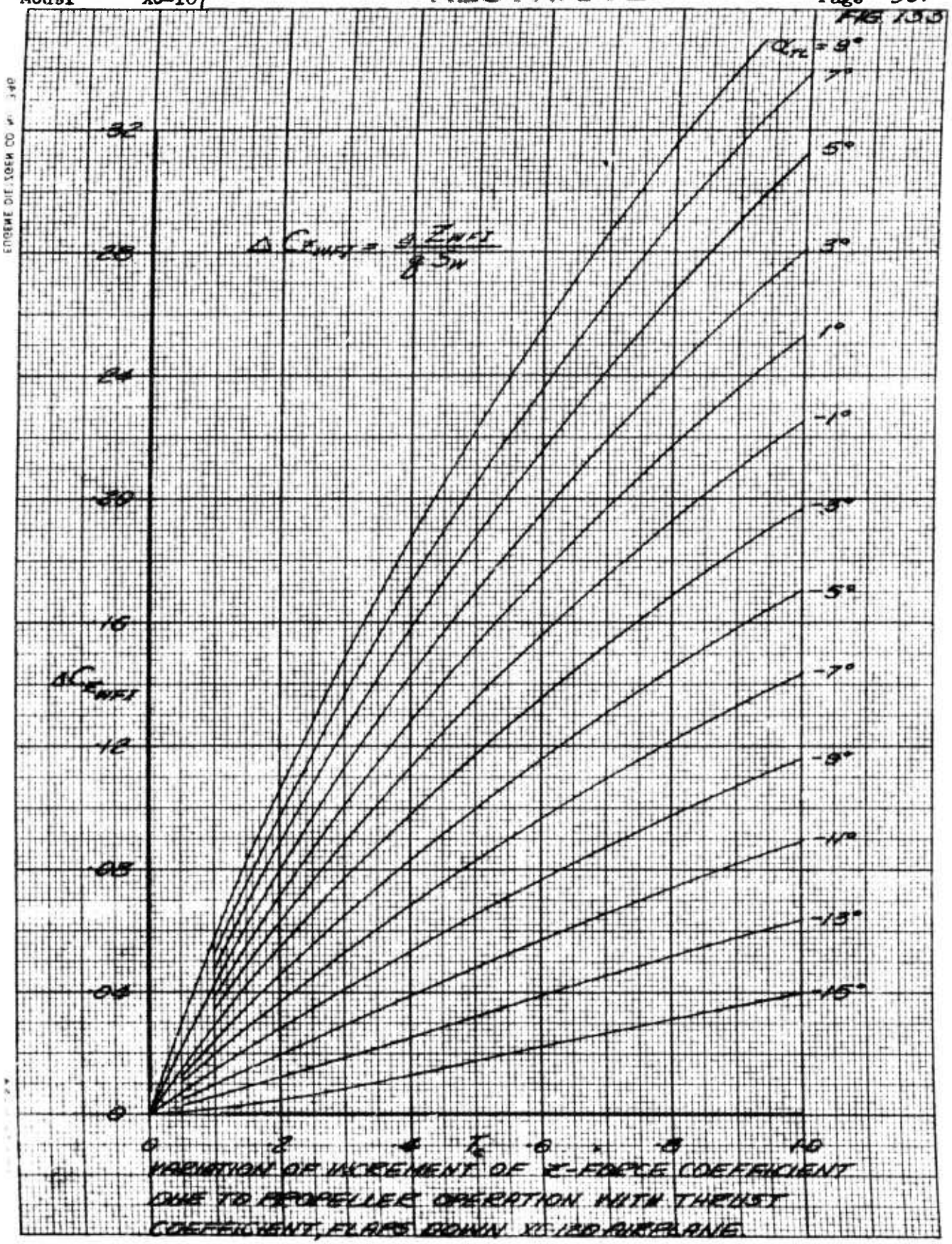

VARIATION OF INCREMENT OF Z-FORCE COEFFICIENT DUE TO PROPELLER OPERATION WITH THRUST COEFFICIENT, FLAPS DOWN XC-120 AIRPLANE

RESTRICTED

FIG 56
FIG 134

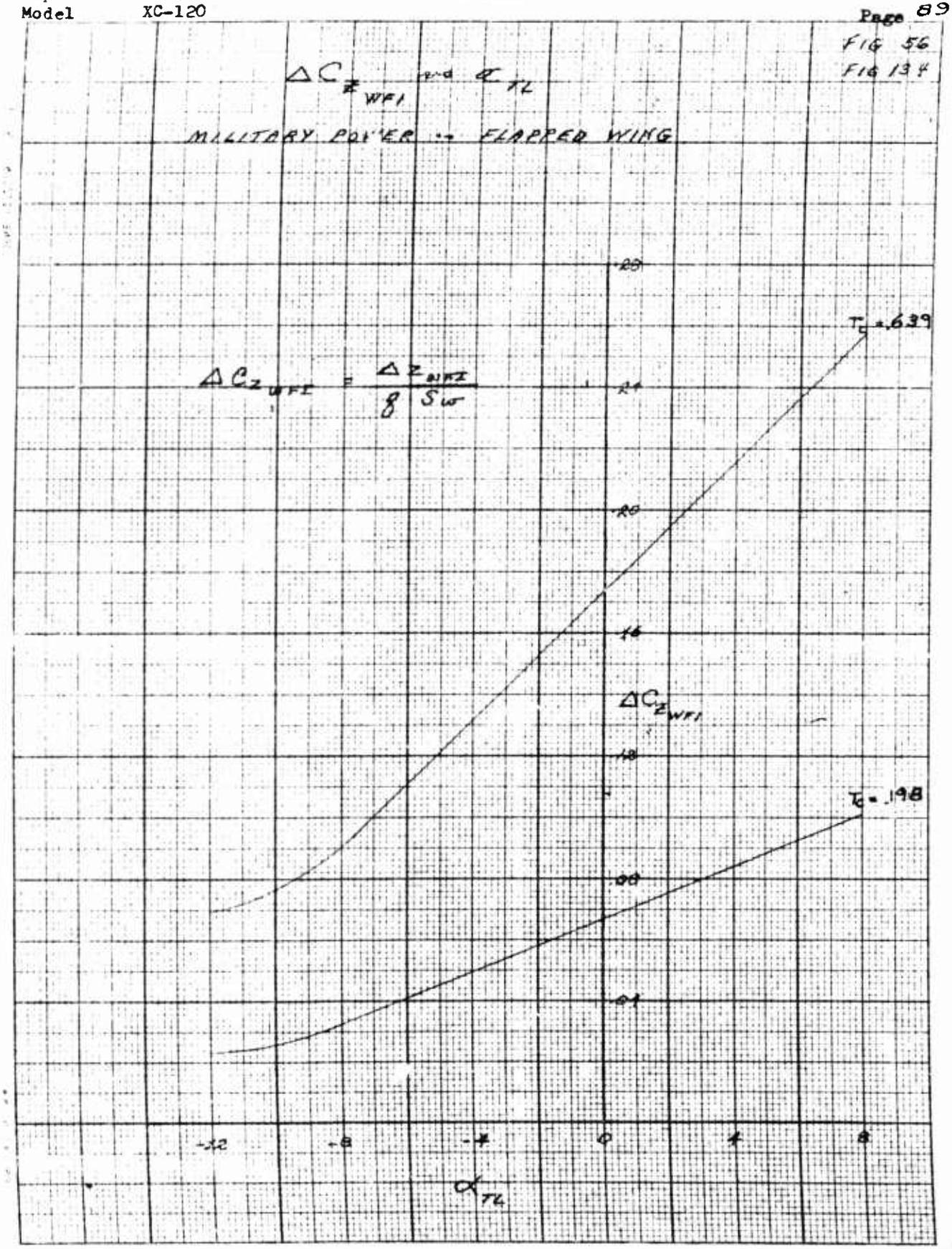

PART II-B-2-f

f. CHARACTERISTICS IN YAW

The characteristics of the flapped wing with power on in yaw are considered to be the same as those of the unflapped wing as presented in Part II-A-1-p, taking into consideration the fact that the wing lift coefficient with power on for the same angle of attack will be different.

PART II-B-3

3. AILERONS

The aerodynamic characteristics of the ailerons with power on are considered to be the same as with power off as determined in Part II-A-3.

PART II-B-4

AILERON TABS

The aerodynamic characteristics of the aileron trim tab and balance tabs are considered to be the same with power-on as with power-off as determined in Part II-A-4.

PART II-B-5

FUSELAGE

The aerodynamic characteristics of the fuselage with power-on are considered to be the same as with power-off and have been determined in Part II-A-5.

PART II-B-5A

Crew Nacelle

The aerodynamic characteristics of the crew nacelle with power on are considered to be the same as with power off and have been presented in Part II-A-5A.

PART II-B-6

BOOMS

The aerodynamic characteristics of the booms with power-on are considered to be the same as with power-off and have been determined in Part II-A-6.

PART II-B-7

7. POWER PLANT

The power plant installation for the XC-120 airplane is the same as that of the C-119B airplane and consists of two Pratt and Whitney R-4360-20 engines.

All power plant data shown in Part II-B-7 of reference (1) for the C-119B airplane therefore applies to the XC-120 airplane.

The cooling drag of the power plant is included in the drag of the booms.

For convenience the variation of normal rated and military rated brake horsepower with altitude is shown in the power on summary section.

PART II-B-8

8. PROPELLER

The propeller engine combination on the XC-120 airplane is the same as that of the C-119B airplane. Therefore, all propeller aerodynamic characteristics will be the same as those shown in Part II-B-8 of reference (1).

It is to be noted that all coefficients are based on the frontal area of one propeller.

For convenience, the aerodynamic characteristics are shown graphically in the power on summary section.

PART II-B-9

9. HORIZONTAL TAIL

This section covers the determination of the effects of power on the aerodynamic characteristics of the horizontal tail and the change in aerodynamic conditions at the horizontal tail with power on.

PART II-B-9-a

a. AERODYNAMIC CHARACTERISTICS

It is assumed that the effects of power on the characteristics of the horizontal tail can be represented by an effective dynamic pressure ratio and change in angle of attack. The basic aerodynamic characteristics of the horizontal tail are therefore taken to be the same as for power off, as determined in Part II-A-9.

b. DOWNWASH AND DYNAMIC PRESSURE RATIO

The computation of the downwash and dynamic pressure ratio at the horizontal tail due to propeller operation for flaps retracted is carried out in the following table in the same menner as in reference (1).

The geometric parameters necessary for the computation have the following values:

h_p = 15.00 feet

l_{ht} = 47.1 feet

v_t = 2.53 feet

The results of the computation for flaps retracted are presented in figures 136 to 139 inclusive.

RESTRICTED

MODEL XC-120 PREPARED BY CHECKED BY APPROVED BY

DATE July 9, 1948

Subject: BASIC AERODYNAMIC DATA

REVISED

FIG. 135

Part II-B-9-b

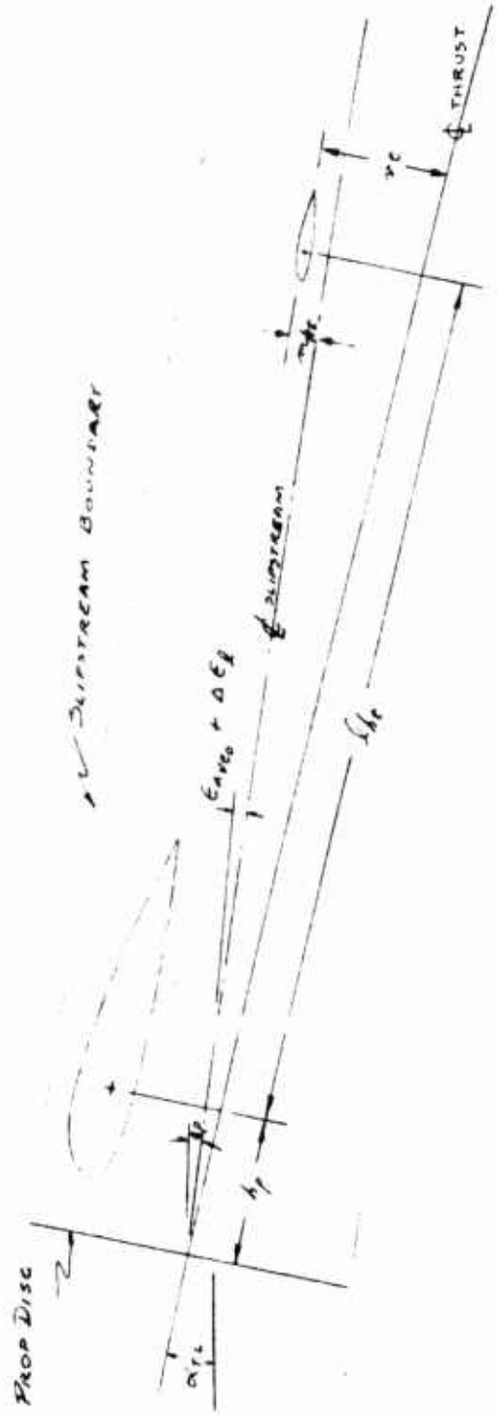

GEOMETRIC RELATIONSHIP OF HORIZONTAL TAIL WITH CENTERLINE OF THRUST

RESTRICTED

TABLE
COMPUTATION OF DOWNWASH AND DYNAMIC PRESSURE RATIO AT HORIZONTAL TAIL DUE TO PROPELLER OPERATION
FLAPS UP - TWO ENGINES

	(1)	(2)	(3)	(4)	(5)	(6)	(7)	(8)	(9)	(10)	(11)	(12)
	α_{TL}	$\Delta C_{L_{WI}}$	$\Delta \epsilon_1$	ϵ_p	(3)+(4)	$\frac{(1)-(4)}{57.3}$	$(1)-(5)-\epsilon_{AVE_0}$	$\frac{(7)}{57.3}$	$l_{ht}\times(8)$	m_{ht}	$(10)^2$	$R_i^2-(11)$
	-15	-.004	-.02	-2.40	-2.42	-3.30	-9.79	-.171	-5.06	-13.89	193.0	(-)
	-9	0	0	-1.44	-1.44	-1.98	-7.20	-.125	-5.89	-10.40	108.2	(-)
T_c=.05	-3	.004	.02	-.48	-.46	-.66	-4.66	-.0815	-3.84	-7.05	49.4	7.5
	3	.009	.06	.48	.54	.66	-2.13	-.0372	-1.75	-3.62	13.1	43.8
	9	.018	.08	1.44	1.52	1.98	.42	.0073	.34	-.22	.05	56.85
	-15	-.006	-.04	-2.94	-2.98	-3.16	-9.28	-.161	-7.59	-15.28	176.3	(-)
	-9	.001	.01	-1.76	-1.75	-1.90	-6.89	-.120	-5.65	-10.08	101.6	(-)
T_c=.10	-3	.009	.06	-.29	-.53	-.65	-4.59	-.0801	-3.78	-6.96	48.5	8.4
	3	.017	.10	.59	.69	.65	-2.28	-.0398	-1.88	-3.76	14.1	42.8
	9	.025	.15	1.76	1.91	1.90	.03	.0005	.02	-.61	.37	56.53

	(13)	(14)	(15)	(16)	(17)	(18)	(19)	(20)	(21)	(22)
	α_{TL}	$b_{ht_{fi}}$	b_{ht_i}	$\frac{b_{ht_i} \bar{c}_{ht_i}}{S_{ht}}$	$\frac{b_{ht_i}}{c_{ht_i}}$	λ_t	S	q_{ht}/q	$\Delta\epsilon_{AVE}$	ϵ_{AVE_p}	α_{ht}
	-15	0	0	0	0		.062	0	0	-2.79	-11.21
	-9	0	0	0	0			0	0	-.36	-7.64
T_c=.05	-3	2.74	5.48	.155	.559	1.110		1.021	-.07	1.98	-3.99
	3	6.61	10.78	.305	1.098	1.291		1.049	.16	4.51	-.91
	9	7.53	11.70	.331	1.192	1.316		1.054	.50	8.06	1.94
	-15	0	0	0	0		.120	0	0	-2.79	-11.21
	-9	0	0	0	0			0	0	-.36	-2.64
T_c=.10	-3	2.89	5.78	.168	.589	1.129		1.044	-.09	1.94	-3.94
	3	6.54	10.71	.303	1.092	1.289		1.094	.21	5.01	-1.01
	9	7.51	11.68	.330	1.190	1.316		1.104	.63	8.92	1.68

RESTRICTED

A-800-25

TABLE
(Continued)

	(1)	(2)	(3)	(4)	(5)	(6)	(7)	(8)	(9)	(10)	(11)	(12)
	α_{TL}	$\Delta C_{L_{WT}}$	$\Delta \epsilon_1$	ϵ_p	(3)+(4)	$\frac{(1)(4)}{57.5}$	(1)-(5) $-\epsilon_{AVE_a}$	$\frac{(7)}{57.5}$	$l_{ht} \times$ (8)	m_{ht}	(10)^2	R_p^2 - (11)
	-15	-.010	-.06	-5.87	-5.93	-2.92	-8.28	-.144	-6.79	-12.14	147.6	(-)
	-9	.002	.01	-2.32	-2.31	-1.75	-6.33	-.110	-5.19	-9.47	89.6	(-)
T_c=.20	-3	.017	.10	-.77	-.67	-.58	-4.54	-.0792	-3.73	-6.84	46.8	10.1
	3	.051	.19	.77	.96	.58	-2.55	-.0445	-2.10	-4.05	16.4	40.5
	9	.045	.28	2.32	2.60	1.75	-.66	-.0115	-.54	-1.32	1.74	55.16
	-15	-.014	-.09	-5.26	-5.35	-2.55	-6.86	-.120	-5.66	-10.74	115.4	(-)
	-9	.007	.04	-3.16	-3.12	-1.53	-5.52	-.0964	-4.54	-8.60	74.0	(-)
T_c=.40	-3	.030	.18	-1.05	-.87	-.51	-4.25	-.0742	-3.50	-6.54	42.7	14.2
	3	.054	.33	1.05	1.38	.51	-2.97	-.0519	-2.44	-4.46	19.9	37.0
	9	.077	.47	3.16	3.63	1.53	-1.63	-.0285	-1.34	-2.34	5.5	51.4

	(13)	(14)	(15)	(16)	(17)	(18)	(19)	(20)	(21)	(22)
	α_{TL}	$b_{ht_{fi}}$	b_{ht_i}	$\frac{b_{ht_i}\bar{c}_{ht_i}}{S_{ht}}$	$\frac{b_{ht_i}}{c_{ht_i}}$	λ_t	S	q_{ht}/q	$\Delta\epsilon_{AVE}$	ϵ_{AVE_p}	α_{ht}
	-15	0	0	0	0		.228	0	0	-2.79	-11.21
	-9	0	0	0	0			0	0	-.36	-7.64
T_c=.20	-3	3.18	6.36	.180	.630	1.146		1.094	-.12	1.88	-3.87
	3	6.36	10.53	.298	1.074	1.285		1.175	.29	5.17	-1.77
	9	7.44	11.61	.328	1.174	1.313		1.197	.85	8.76	1.24
	-15	0	0	0	0		.420	0	0	-2.79	-11.21
	-9	0	0	0	0			0	0	-.36	-7.64
T_c=.40	-3	3.78	7.56	.214	.771	1.181		1.230	-.19	1.74	-3.74
	3	6.08	10.25	.290	1.045	1.275		1.310	.40	5.39	-1.39
	9	7.16	11.33	.320	1.156	1.309		1.552	1.16	9.38	.62

RESTRICTED

FA-800-23

TABLE
(Concluded)

	(1)	(2)	(3)	(4)	(5)	(6)	(7)	(8)	(9)	(10)	(11)	(12)
	α_{TL}	$\Delta C_{L_{WI}}$	$\Delta \epsilon_1$	ϵ_p	(3)+(4)	$\frac{h_t (1)(4)}{57.3}$	(1)-(5) $-e_{AVE_0}$	$\frac{*(7)}{57.3}$	l_{ht}*(8)	m_{ht}	(10)^2	R_p^2-(11)
T_c=.70	-15	-.015	-.09	-6.63	-6.72	-2.19	-5.49	-.0958	-4.51	-9.23	85.2	(-)
	-9	.015	.09	-3.98	-3.89	-1.32	-4.75	-.0829	-3.90	-7.75	60.0	(-)
	-3	.048	.30	-1.33	-1.03	-.44	-4.09	-.0714	-3.36	-6.55	40.0	16.9
	3	.082	.51	1.33	1.84	.44	-3.43	-.0599	-2.82	-4.91	24.2	32.7
	9	.116	.72	3.98	4.70	1.32	-2.76	-.0481	-2.27	-3.48	12.1	44.8
T_c=1.00	-15	-.014	-.09	-7.43	-7.52	-1.98	-4.69	-.0818	-3.85	-8.36	70.0	(-)
	-9	.022	.14	-4.45	-4.31	-1.19	-4.33	-.0755	-3.56	-7.28	53.0	3.9
	-3	.065	.39	-1.48	-1.09	-.40	-4.03	-.0703	-3.31	-6.24	38.9	18.0
	3	.104	.64	1.48	2.12	.40	-3.71	-.0647	-3.05	-5.18	26.8	30.1
	9	.146	.90	4.45	5.35	1.19	-3.41	-.0595	-2.80	-4.14	17.1	39.8

	(13)	(14)	(15)	(16)	(17)	(18)	(19)	(20)	(21)	(22)
α_{TL}	$b_{ht_{fi}}$	b_{ht_i}	$\frac{b_{ht_i} \bar{c}_{ht_i}}{S_{ht}}$	$\frac{b_{ht_i}}{c_{ht_i}}$	λ_t	S	q_{ht}/q	$\Delta\epsilon_{AVE}$	ϵ_{AVE_p}	α_{ht}
T_c=.70 -15	0	0	0	0		.669	0	0	-2.79	-11.21
-9	0	0	0	0			0	0	-.36	-7.64
-3	4.10	8.20	.252	.835	1.201		1.373	-.24	1.64	-3.64
3	5.71	9.88	.279	1.007	1.264		1.471	.51	5.61	-1.61
9	6.70	10.87	.307	1.108	1.295		1.531	1.44	9.94	.06
T_c=1.00 -15	0	0	0	0		.882	0	0	-2.79	-11.21
-9	1.38	3.96	.112	.404	1.084		1.214	-.48	-1.32	-6.68
-3	4.24	8.41	.238	.858	1.211		1.509	-.26	1.60	-3.60
3	5.48	9.65	.273	.984	1.254		1.604	.58	5.75	-1.25
9	6.50	10.47	.296	1.067	1.282		1.669	1.58	10.22	-.22

RESTRICTED

FIG. 136

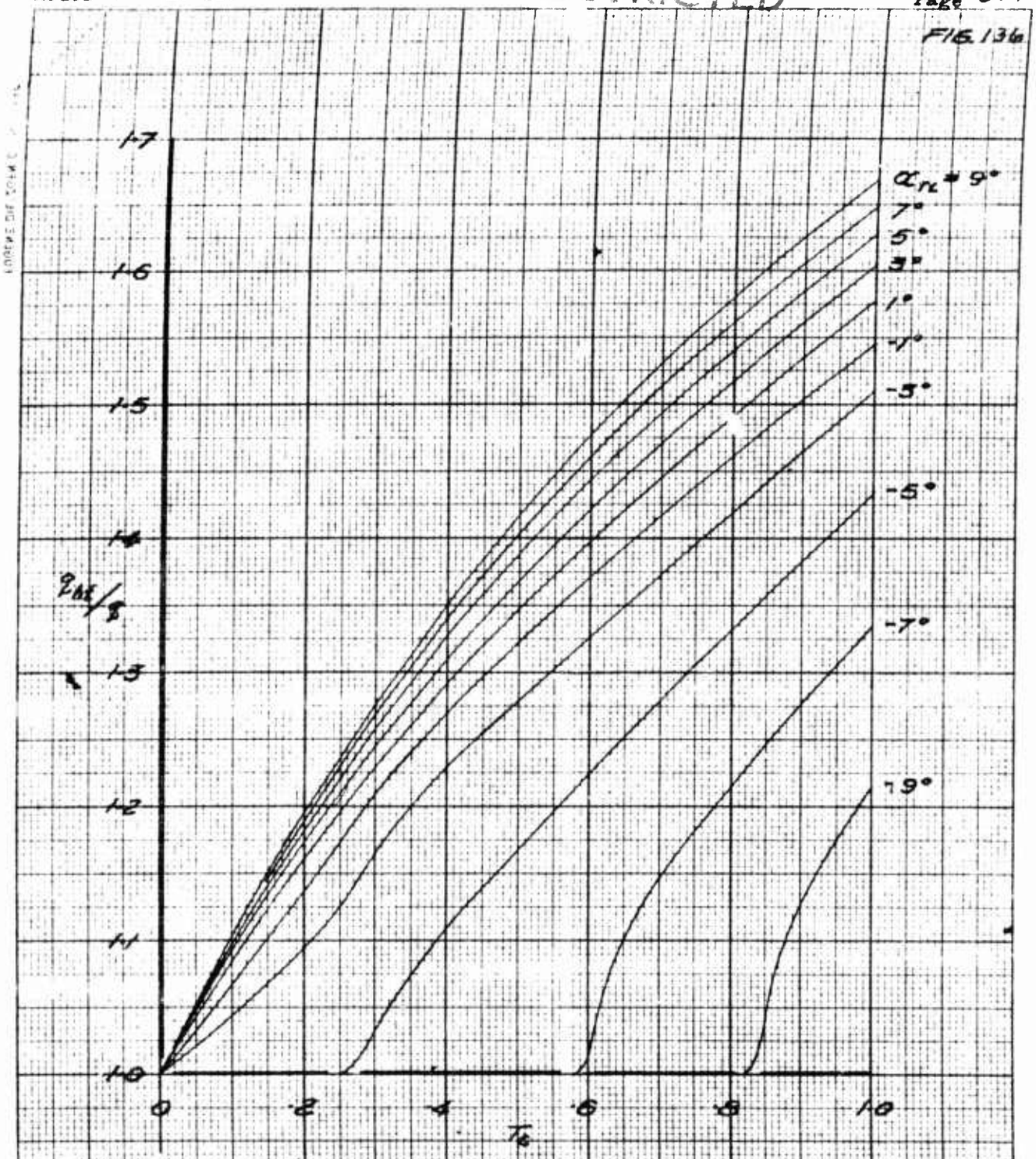

VARIATION OF DYNAMIC PRESSURE RATIO AT THE HORIZONTAL TAIL WITH THRUST COEFFICIENT, FLAPS UP. MILITARY POWER TO TWO ENGINES. XC-120 AIRPLANE.

RESTRICTED

FIG 62
FIG 137

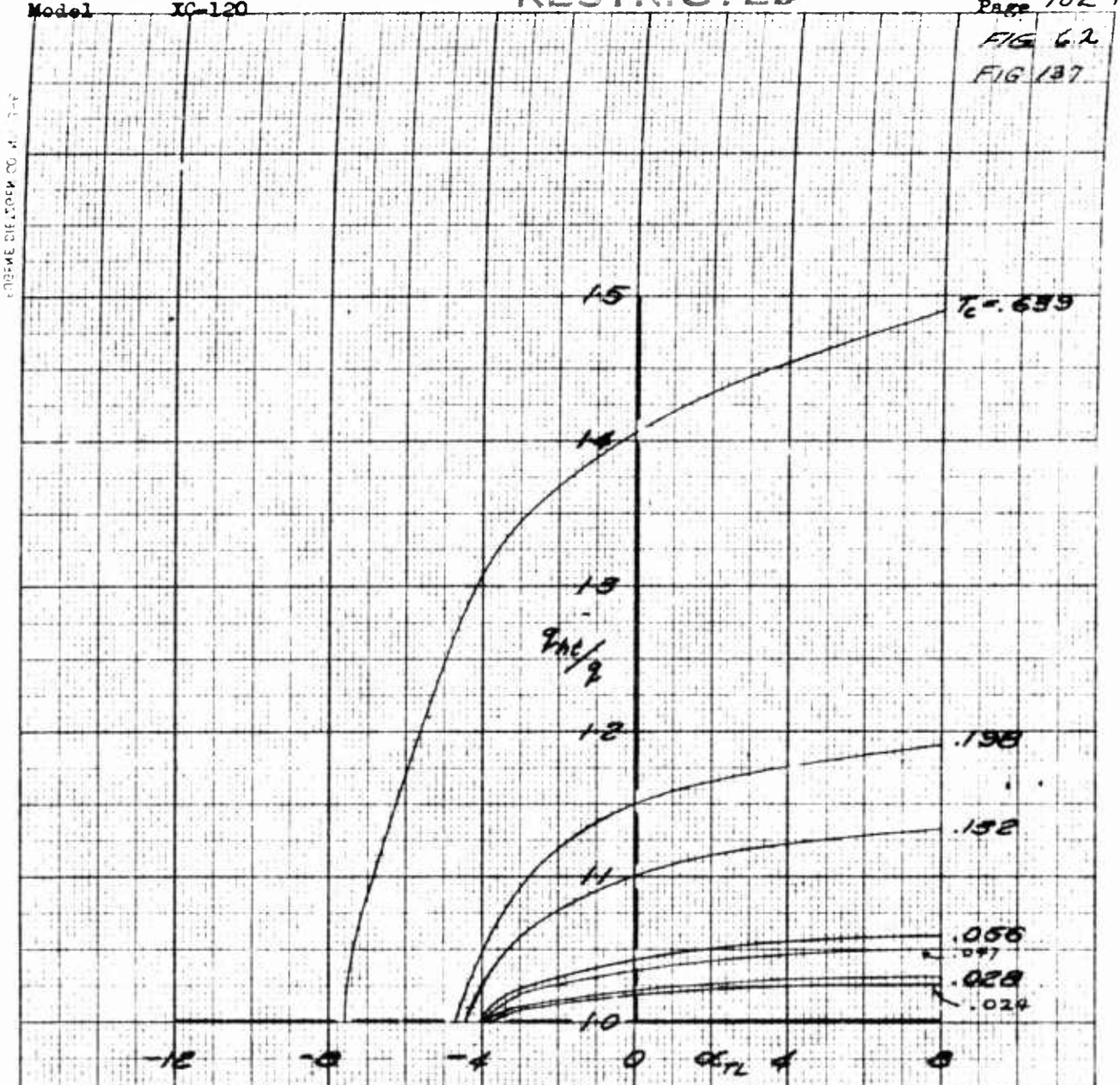

VARIATION OF DYNAMIC PRESSURE RATIO AT HORIZONTAL TAIL WITH ANGLE OF ATTACK OF THRUST LINE, FLAPS UP, MILITARY POWER TO TWO ENGINES. XC-120 AIRPLANE.

FIG 138

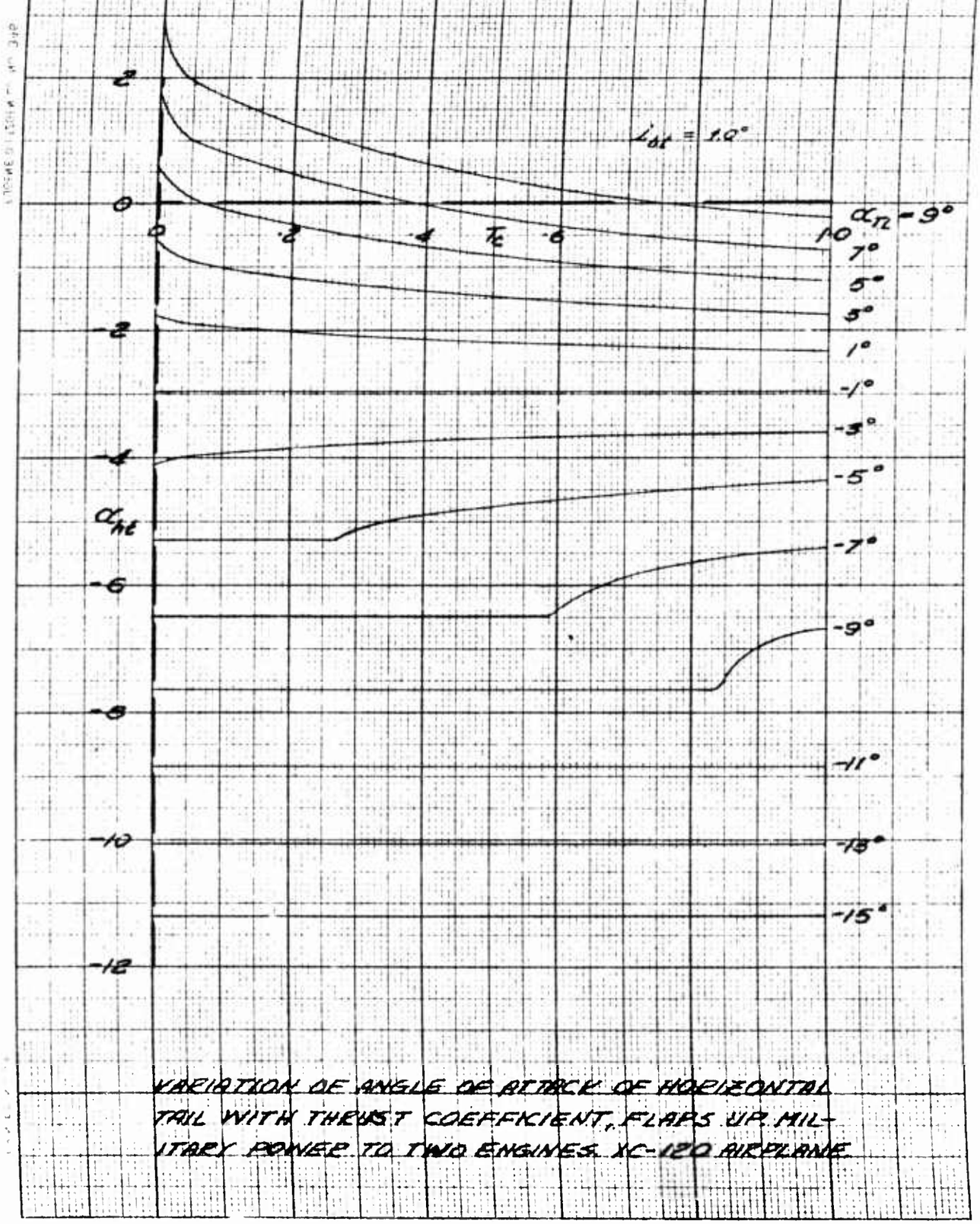

VARIATION OF ANGLE OF ATTACK OF HORIZONTAL TAIL WITH THRUST COEFFICIENT, FLAPS UP, MILITARY POWER TO TWO ENGINES, XC-120 AIRPLANE

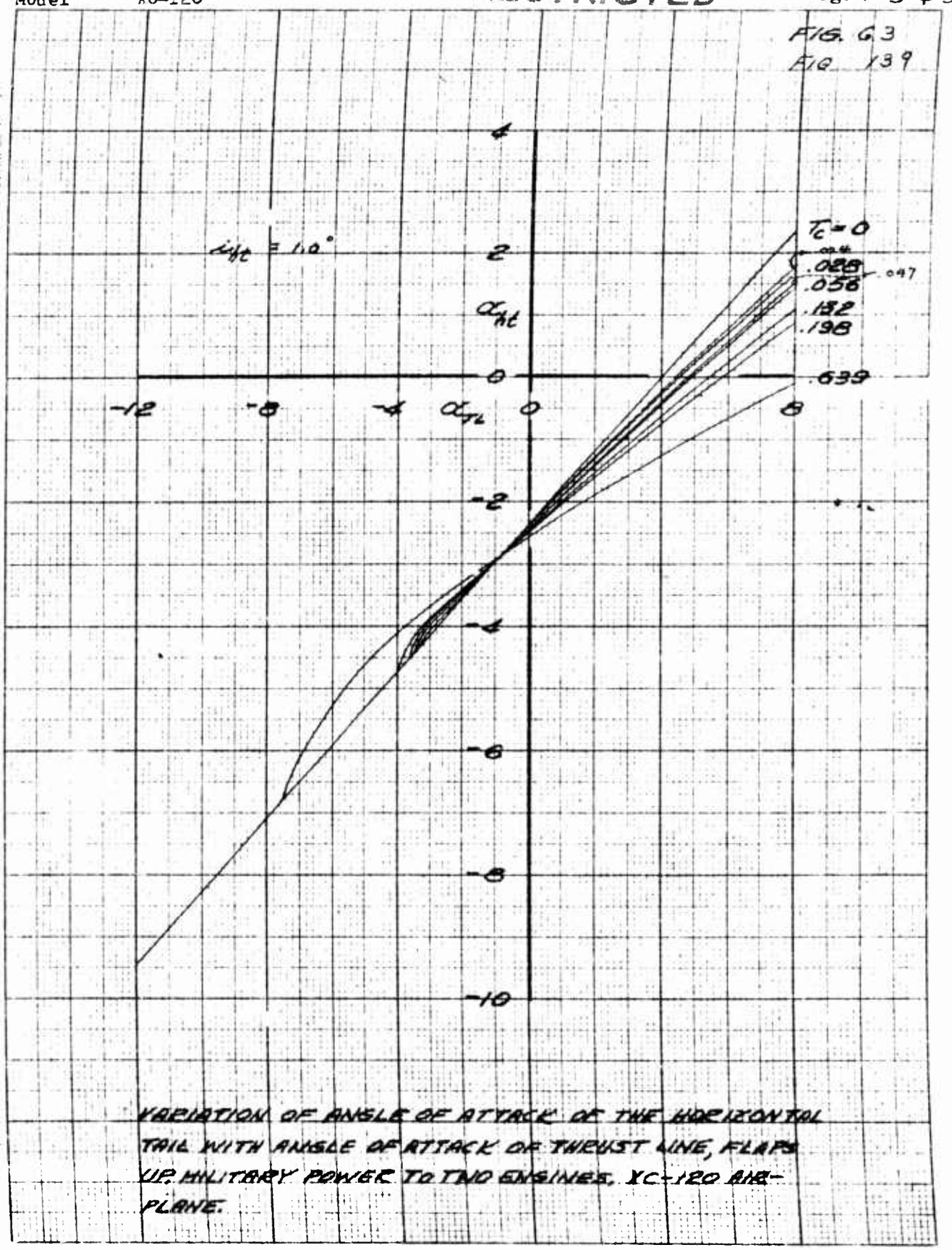

VARIATION OF ANGLE OF ATTACK OF THE HORIZONTAL TAIL WITH ANGLE OF ATTACK OF THRUST LINE, FLAPS UP, MILITARY POWER TO TWO ENGINES, XC-120 AIRPLANE.

PART II-B-9-b (Cont.)

With flaps extended the slipstream falls below the horizontal tail, so that the dynamic pressure ratio has the constant value of 1.00. The increment of downwash is rather indeterminate, but is taken to be one half the value of downwash due to the incremental wing lift due to propeller operation. The following table presents the computation of the downwash, flaps extended, and figures 140 and 141 show the results of the computations.

TABLE
COMPUTATION OF DOWNWASH AT HORIZONTAL TAIL
DUE TO PROPELLER OPERATION
FLAPS DOWN - TWO ENGINES

	α_{TL}	$\Delta C_{L_{WFI}}$	$\Delta\epsilon_i$	ϵ_{AVG_P}	α_{ht}
	-15	.001	.01	.34	-14.34
	-9	.007	.04	2.84	-10.84
T_c=.05	-3	.014	.09	5.45	-7.45
	3	.022	.14	8.25	-4.35
	9	.029	.18	11.52	-1.52
	-15	.001	.01	.34	-14.34
	-9	.015	.09	2.89	-10.89
T_c=.10	-3	.030	.19	5.55	-7.55
	3	.044	.27	8.38	-4.38
	9	.057	.35	11.69	-1.69
	-15	.005	.03	.36	-14.36
	-9	.028	.17	2.97	-10.97
T_c=.20	-3	.055	.34	5.70	-7.70
	3	.080	.49	8.60	-4.60
	9	.104	.64	11.98	-1.98
	-15	.014	.08	.42	-14.42
	-9	.054	.33	3.13	-11.13
T_c=.40	-3	.098	.60	5.96	-7.96
	3	.145	.88	8.99	-4.99
	9	.189	1.14	12.48	-2.48
	-15	.029	.18	.51	-14.51
	-9	.089	.55	3.35	-11.35
T_c=.70	-3	.155	.94	6.30	-8.30
	3	.219	1.35	9.46	-5.46
	9	.283	1.75	13.09	-3.09
	-15	.045	.27	.60	-14.60
	-9	.117	.72	3.52	-11.52
T_c=1.00	-3	.198	1.22	6.58	-5.58
	3	.280	1.73	9.84	-5.84
	9	.361	2.23	13.57	-3.57

Subject: BASIC AERODYNAMIC DATA

MODEL XO-120 | PREPARED BY | CHECKED BY | APPROVED BY

DATE July 9, 1948

REVISED

REPORT NO. R107-012 FAIRCHILD AIRCRAFT DIVISION OF FAIRCHILD ENGINE & AIRPLANE CORPORATION

PAGES | PAGE 322

RESTRICTED

FIG. 140

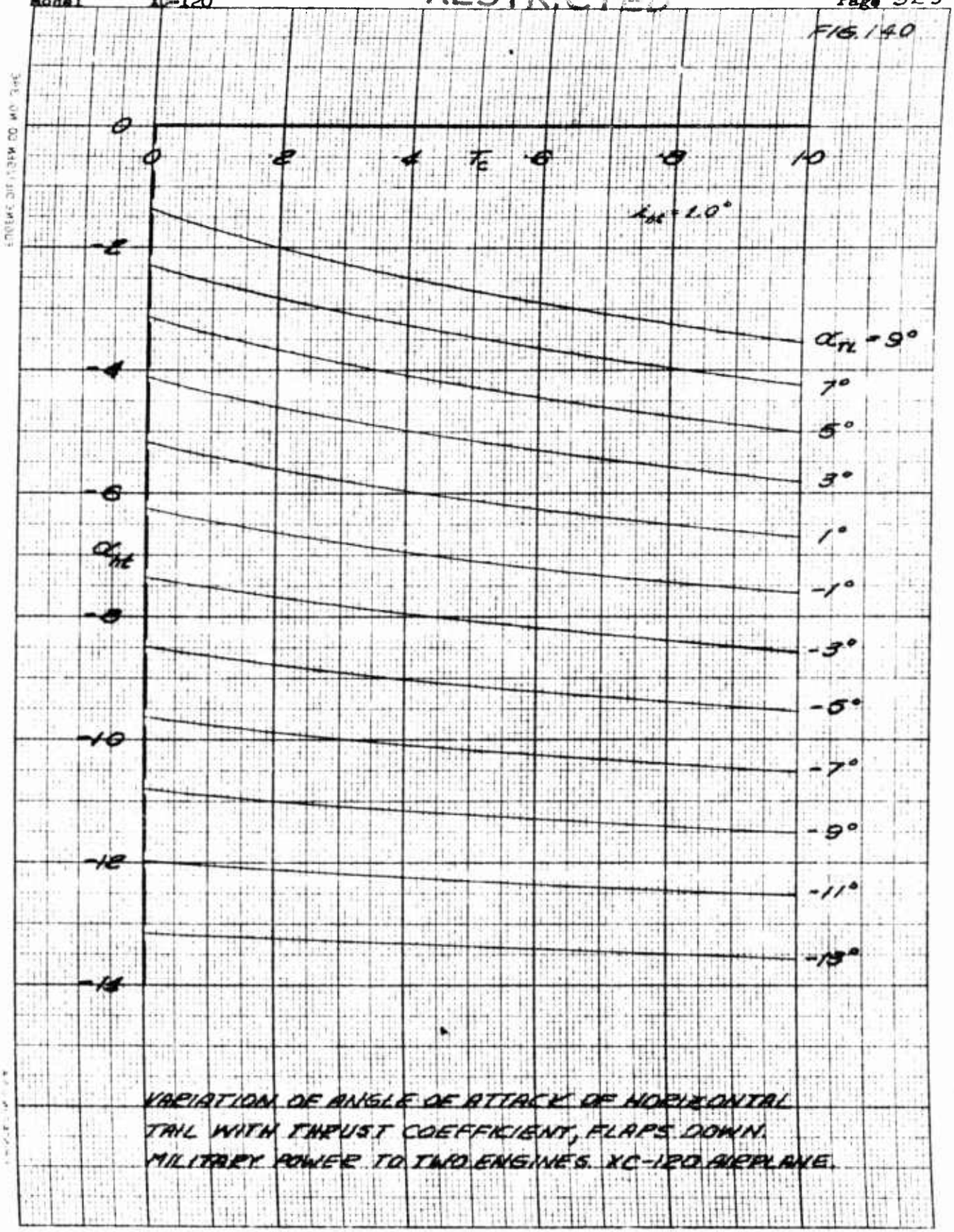

VARIATION OF ANGLE OF ATTACK OF HORIZONTAL TAIL WITH THRUST COEFFICIENT, FLAPS DOWN. MILITARY POWER TO TWO ENGINES. XC-120 AIRPLANE.

RESTRICTED

PAGE 104 + 324
FIG. 64
FIG. 141

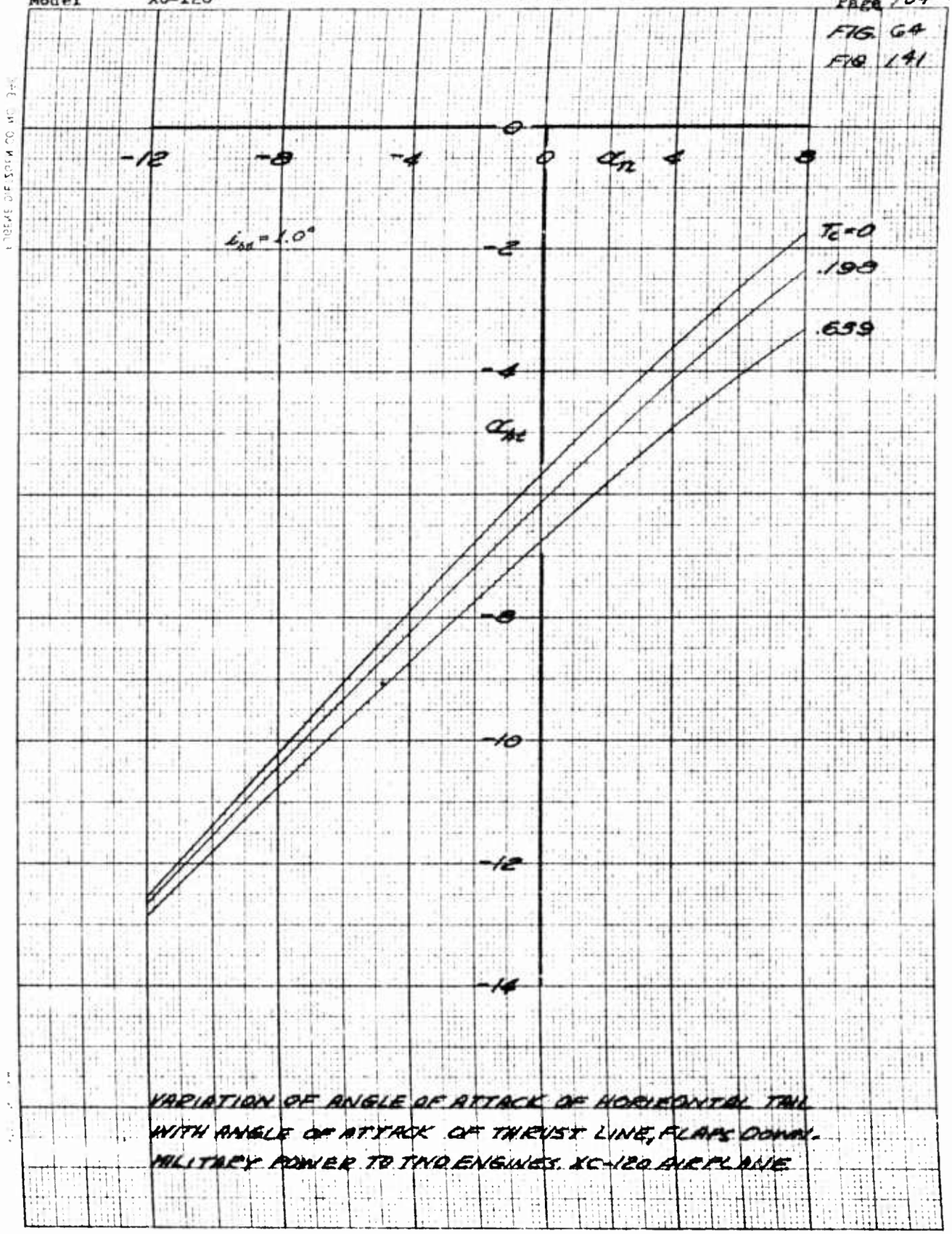

VARIATION OF ANGLE OF ATTACK OF HORIZONTAL TAIL WITH ANGLE OF ATTACK OF THRUST LINE, FLAPS DOWN. MILITARY POWER TO TWO ENGINES. XC-120 AIRPLANE

PART II-B-10

10. ELEVATOR TABS

The aerodynamic characteristics of the elevator trim and spring tabs are considered to be the same with power-on as with power-off as determined in Part II-A-10. However, the variation of dynamic pressure at the horizontal tail (q_{ht}) with power as shown in Part II-B-9 must be taken into account when calculating forces and moments due to the trim tab and spring tab.

The dynamic pressure ratio with power on is the same as shown in Part II-B-9 for the horizontal tail.

PART II-B-11

11. VERTICAL TAIL

This section covers the determination of the effects of power on the aerodynamic characteristics of the vertical tail and the change in aerodynamic conditions at the vertical tail with power on.

RESTRICTED

PART II-B-11

a. AERODYNAMIC CHARACTERISTICS

The effects of power on the aerodynamic characteristics of the vertical tail are assumed to be represented by an effective dynamic pressure ratio and change in angle of attack. Therefore, the basic aerodynamic characteristics are taken to be the same as with power off as determined in Part II-A-11.

b. SIDEWASH AND DYNAMIC PRESSURE RATIO

The effect of propeller operation on the sidewash and dynamic pressure ratio at the vertical tail is determined in the same manner as in Part II-B-11 reference (1).

These computations are carried out in the following table for the case of zero yaw with one engine inoperative and the other developing take-off power for a number of angles of attack of the thrust line. These data are presented in figure 142 as a function of true indicated airspeed. It should be noted that, since rotation in the slipstream has been neglected, there is no sidewash since the angle of yaw is zero.

PART II-B-11 (Cont.)

SIDEWASH AND DYNAMIC PRESSURE RATIO (Cont.)

The sidewash and dynamic pressure ratio is computed for various angles of yaw for a gross weight of 64,000 pounds with take-off power to both engines at a true indicated airspeed of 100 miles per hour. Similar computations have been done for a gross weight of 52,425 pounds with military power to both engines at a true indicated airspeed of 90 miles per hour.

The results of the computations are presented graphically in figures 129 and 130 .

Subject: BASIC AERODYNAMIC DATA

FA-800-12

TABLE

COMPUTATION OF DYNAMIC PRESSURE RATIO AT VERTICAL TAIL DUE TO PROPELLER OPERATION

ONE ENGINE ; TAKE-OFF POWER, $\psi = 0°$

	(1) α_{TL}	(2) T_c	(3) m_{ht}	(4) $m_{ht}+b_{vt}$	(5) $R_p \div$ (4)	(6) $2R_p \div$ (5)	(7) $\frac{b_{vt_i}+z_{vt_i}}{S_{vt}}$	(8) $\frac{b_{vt_i}}{z_{vt_i}}$	(9) λ_t	(10) S	(11) q_{vt}/q_o	(12) $V\sqrt{\sigma}$
	-1	.328	-5.90	-.90	8.40	6.60	.464	.943	1.239	.409	1.236	123.8
	1	.352	-5.27	-.27	7.77	7.28	.518	1.033	1.277	.533	1.320	108.5
FLAPS UP	3	.690	-4.90	.10	7.40	7.60	.534	1.086	1.289	.663	1.456	96.8
55,904 LBS	5	.847	-4.67	.33	7.17	7.83	.550	1.118	1.297	.777	1.554	88.2
	7	1.012	-4.53	.47	7.03	7.97	.560	1.138	1.303	.892	1.651	81.4
	9	1.186	-4.40	.60	6.90	8.10	.569	1.157	1.310	1.003	1.748	75.6
	-3	.377	-9.52	-4.52	12.02	2.98	.209	.426	1.090	.572	1.130	104.5
	-1	.734	-9.22	-4.22	11.72	3.28	.231	.469	1.100	.710	1.180	95.1
	1	.936	-9.10	-4.10	11.60	3.40	.239	.486	1.103	.840	1.222	84.6
FLAPS DOWN	3	1.126	-9.16	-4.16	11.66	3.36	.236	.480	1.102	.965	1.251	77.8
55,904 LBS	5	1.316	-9.37	-4.37	11.87	3.13	.220	.447	1.095	1.084	1.262	72.3
	7	1.327	-9.75	-4.75	12.25	2.75	.193	.393	1.082	1.205	1.252	67.5
	9	1.733	-10.17	-5.17	12.67	2.53	.164	.353	1.068	1.337	1.234	63.2
	-1	.328	-5.90	-.90	8.40	6.60	.464	.943	1.239	.354	1.204	131.8
	1	.456	-5.22	-.22	7.72	7.28	.511	1.040	1.274	.470	1.306	115.6
FLAPS UP	3	.594	-4.77	.23	7.27	7.73	.543	1.103	1.292	[illegible]	1.411	103.3
49,451 LBS	5	.733	-4.50	.50	7.00	8.00	.562	1.143	1.304	.694	1.510	94.2
	7	.877	-4.34	.66	6.84	8.16	.574	1.166	1.311	.797	1.599	86.9
	9	1.025	-4.17	.83	6.67	8.33	.585	1.190	1.316	.899	1.691	80.8
	-3	.423	-9.53	-4.53	12.03	2.97	.209	.424	1.090	.502	1.114	111.9
	-1	.644	-9.13	-4.13	11.63	3.37	.237	.481	1.102	.626	1.163	99.8
	1	.803	-8.97	-3.97	11.47	3.53	.248	.504	1.107	.746	1.205	90.7
FLAPS DOWN	3	.967	-8.93	-3.93	11.43	3.57	.251	.510	1.108	.861	1.240	83.4
49,451 LBS	5	1.155	-9.10	-4.10	11.60	3.40	.239	.486	1.103	.972	1.256	77.6
	7	1.313	-9.40	-4.40	11.90	3.10	.218	.442	1.094	1.082	1.252	72.5
	9	1.504	-9.77	-4.77	12.27	2.73	.192	.390	1.082	1.194	1.248	68.0

FIG 65
FIG 142

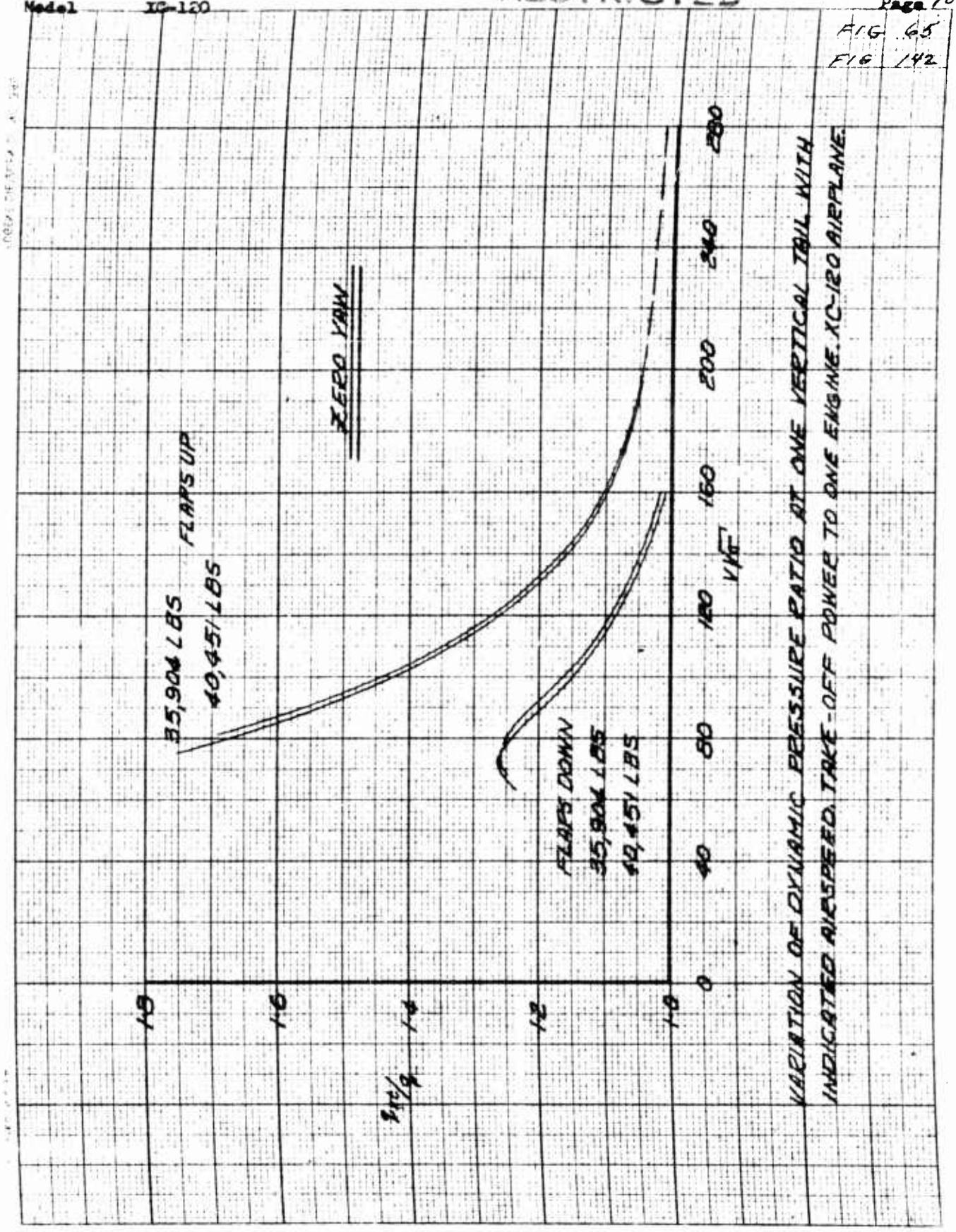

VARIATION OF DYNAMIC PRESSURE RATIO AT ONE VERTICAL TAIL WITH INDICATED AIRSPEED. TAKE-OFF POWER TO ONE ENGINE. XC-120 AIRPLANE.

RESTRICTED

TABLE
COMPUTATION OF SIDEWASH AND DYNAMIC PRESSURE
RATIO AT VERTICAL TAIL DUE TO PROPELLER OPERATION
TWO ENGINES; TAKE-OFF POWER; $V\sqrt{\sigma}$ = 100 MPH
64,000 LBS.

	(1)	(2)	(3)	(4)	(5)	(6)	(7)	(8)	(9)	(10)	(11)
	ψ	$1-\frac{\sigma_p}{\psi}$	$\psi-\sigma_p$	$61.1\times\frac{(3)}{57.5}$	(4)^2	$R_p^2-m_{vt}^2$	$\sqrt{(6)}$	2×(7)	$b_{vt_i}+m_{ht}$	(7)-(9)	(8)-(10)
FLAPS UP $\alpha_{TL}=8.7°$	0	.573	0	0	0	56.25	7.50	15.00	1.61	5.89	9.11
	3		1.72	1.84	3.39	52.86	7.27	14.54		5.66	8.88
	6		3.44	3.67	13.47	42.78	6.54	13.08		4.93	8.15
	9		5.16	5.51	30.4	25.85	5.09	10.18		3.48	6.70
	12		6.88	7.34	53.9	2.35	1.53	3.06		(-)	3.06
	15		8.60	9.18	84.3	—	—	—		—	—
FLAPS DOWN $\alpha_{TL}=3.14°$	0	.573	0	0	0	56.25	7.50	15.00	-3.55	10.85	4.15
	3		1.72	1.84	3.39	52.86	7.27	14.54		10.62	3.92
	6		3.44	3.67	13.47	42.78	6.54	13.08		9.89	3.19
	9		5.16	5.51	30.4	25.85	5.09	10.18		8.44	1.74
	12		6.88	7.34	53.9	2.55	1.53	3.06		4.88	—
	15		8.60	9.18	84.3	—	—	—		—	—

	(12)	(13)	(14)	(15)	(16)	(17)	(18)
ψ	$\frac{b_{vt_i}\bar{c}_{vt_i}}{S_{vt}}$	$\frac{b_{vt_i}}{\bar{c}_{vt_i}}$	λ_t	s	q_{vt}/q_{p_0}	σ_p	$\sigma_{p_{N/B}}$
0	.641	1.302	1.346	.622	1.536	0	0
3	.624	1.268	1.337		1.519	1.28	.80
6	.573	1.164	1.308		1.466	2.56	1.47
9	.471	.957	1.246		1.365	3.84	1.81
12	.215	.437	1.093		1.146	5.12	1.10
15	0	0	—		1.000	6.40	0
0	.292	.593	1.130	.622	1.206	0	0
3	.276	.560	1.121		1.193	1.28	.35
5	.224	.456	1.096		1.153	2.56	.57
9	.122	.248	1.050		1.080	3.84	.47
12	0	0	—		1.000	5.12	0
15	0	0	—		1.000	6.40	0

FIG. 66
FIG. 143

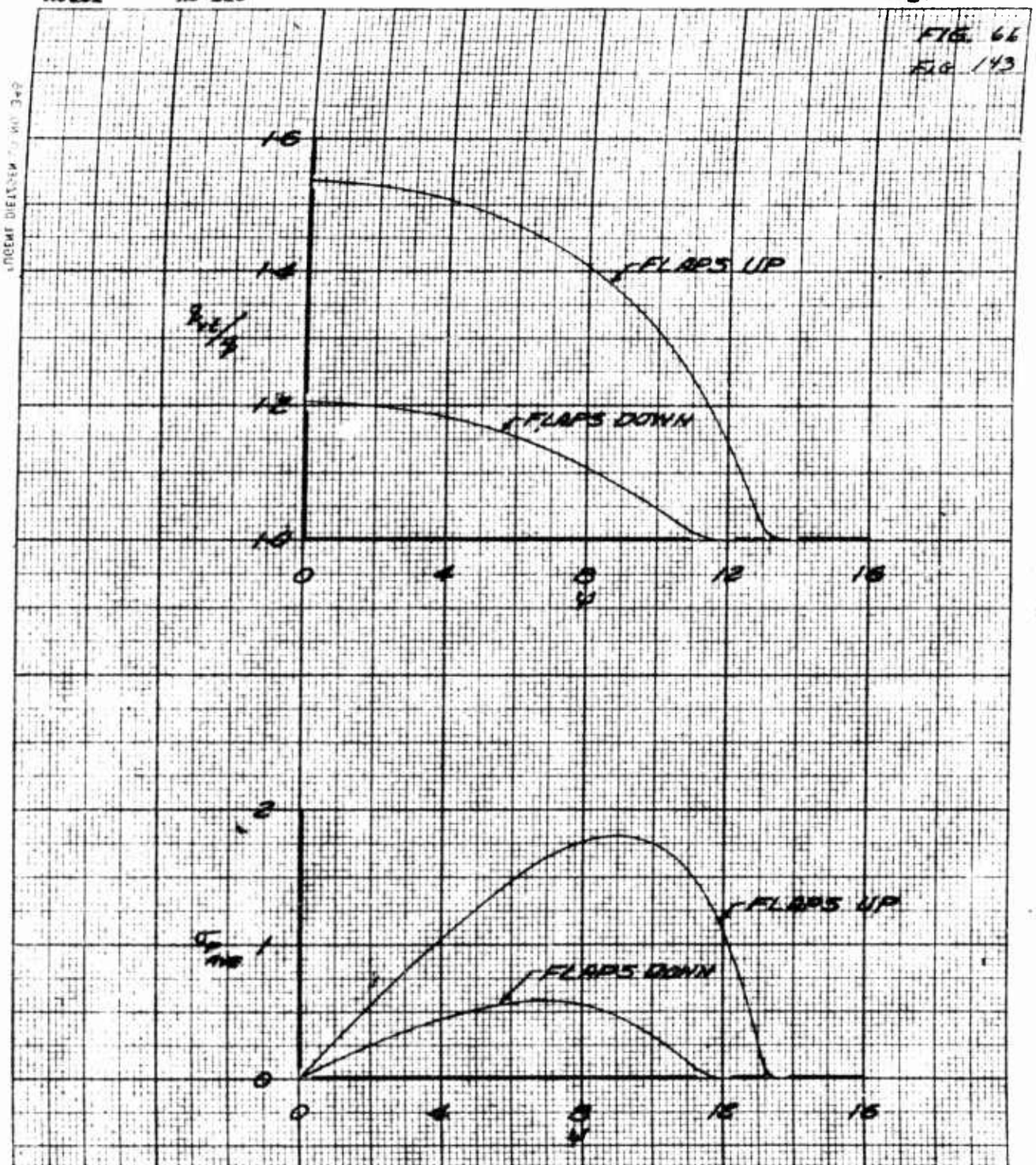

VARIATION WITH ANGLE OF YAW OF DYNAMIC PRESSURE RATIO AND SIDEWASH ANGLE DUE TO PROPELLER AT THE VERTICAL TAILS. TAKE-OFF POWER AT 100 MPH INDICATED AIRSPEED. 64,000 LBS. XC-120 AIRPLANE.

RESTRICTED

TABLE

COMPUTATION OF SIDEWASH AND DYNAMIC PRESSURE RATIO AT VERTICAL TAILS DUE TO PROPELLER OPERATION

TWO ENGINES; TAKE-OFF POWER; $V/\sqrt{\sigma}$ = 90 MPH

52,425 LBS.

	(1)	(2)	(3)	(4)	(5)	(6)	(7)	(8)	(9)	(10)	(11)
	ψ	$1-\frac{\sigma_p}{\psi}$	$\psi-\sigma_p$	$61.1\times\frac{(3)}{57.3}$	(4)^2	$R_p^2-m_{vt}^2$	$\sqrt{(6)}$	$2\times(7)$	$b_{vt_2}+m_{ht}$	(7)-(9)	(8)-(10)
	0	.532	0	0	0	56.25	7.50	15.00	1.08	6.42	8.58
	3		1.60	1.71	2.92	53.33	7.30	14.60		6.22	8.38
Flaps Up α_{TL} = 8.41°	6		3.19	3.40	11.56	44.69	6.69	13.38		5.61	7.77
	9		4.79	5.11	26.15	30.10	5.49	10.98		4.41	6.57
	12		6.38	6.81	46.4	9.85	3.14	6.28		2.06	4.22
	15		7.98	8.52	72.5	—	—	—		—	—
	0	.532	0	0	0	56.25	7.50	15.00	-3.75	11.25	3.75
	3		1.60	1.71	2.92	53.33	7.30	14.60		11.05	3.55
Flaps Down α_{TL} = 2.62°	6		3.19	3.40	11.56	44.69	6.69	13.38		10.44	2.94
	9		4.79	5.11	26.15	30.10	5.49	10.98		9.24	1.74
	12		6.38	6.81	46.4	9.85	3.14	6.28		6.89	—
	15		7.98	8.52	72.5	—	—	—		—	—

	(12)	(13)	(14)	(15)	(16)	(17)	(18)
ψ	$\frac{b_{vt_i}\bar{c}_{vt_i}}{S_{vt}}$	$\frac{b_{vt_i}}{\bar{c}_{vt_i}}$	λ_t	s	q_{vt}/q_0	σ_p	$\sigma_{p_{AVE}}$
0	.603	1.225	1.527	.754	1.603	0	0
3	.589	1.197	1.518		1.585	1.40	.83
6	.546	1.110	1.292		1.531	2.81	1.55
9	.461	.939	1.288		1.430	4.21	1.94
12	.297	.603	1.131		1.253	5.62	1.67
15	0	0	—		1.000	7.02	0
0	.263	.535	1.116	.754	1.221	0	0
3	.249	.507	1.107		1.208	1.40	.35
6	.206	.420	1.087		1.169	2.81	.58
9	.122	.240	1.048		1.096	4.21	.51
12	0	0	—		1.000	5.62	0
15	0	0	—		1.000	7.02	0

FA-806-20

FIG. 67
FIG. 144

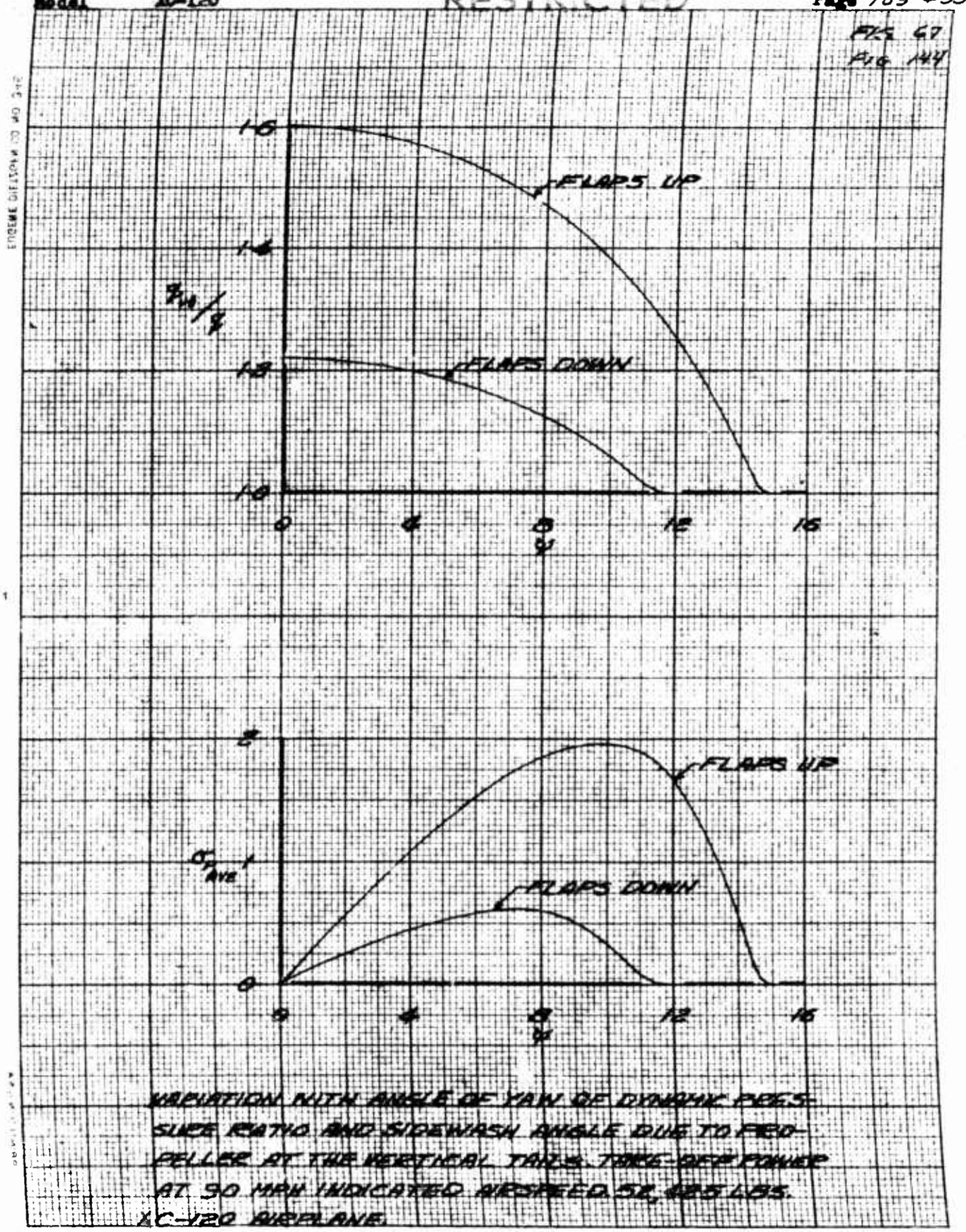

VARIATION WITH ANGLE OF YAW OF DYNAMIC PRESSURE RATIO AND SIDEWASH ANGLE DUE TO PROPELLER AT THE VERTICAL TAILS. TAKE-OFF POWER AT 90 MPH INDICATED AIRSPEED. S.L. 425 LBS.
XC-120 AIRPLANE.

PART II-B-11

Calculations are also shown for sidewash and dynamic pressure ratio at the vertical tail for 5° yaw at V_D for the airplane with pack on and with pack off.

Configuration	V_D	τ_c
Pack on	313 mph	.028
Pack Off	331.3 mph	.024

RESTRICTED

FA-800-23

CALCULATION OF DYNAMIC PRESSURE RATIO AND SIDEWASH ANGLE AT THE VERTICAL TAIL FOR 5° YAW AT V_D

	(1)	(2)	(3)	(4)	(5)	(6)	(7)	(8)	(9)	(10)	(11)	(12)
	ψ	$\frac{dC_{L_p}}{d\alpha_{TL}}$	$\frac{K_p}{(V/nD_p)^2}$	$\frac{\sigma_p}{\alpha_{TL}}$	s	$\frac{1+s/2}{1+s}$	$\sqrt{(6)}$	D_s^2	$1-\frac{\sigma_p}{\psi}$	$\psi-\sigma_p$ deg.	$\psi-\sigma_p$ Rad.	m_{vt}
Pack On $T_c=.028$ $V\sqrt{\sigma}=313$ mph $\alpha_{TL}\cong 6.0°$	5	.00538	.121	.165	.035	.983	.991	223	.835	4.18	.0730	4.54
Pack Off $T_c=.024$ $V\sqrt{\sigma}=321.3$ $\alpha_{TL}\cong 6.2°$	5	.00557	.125	.170	.030	.994	.994	225	.830	4.15	.0724	4.49

	(13)	(14)	(15)	(16)	(17)	(18)	(19)	(20)	(21)	(22)	(23)	(24)
	m_{vt}^2	$R_p^2-m_{vt}^2$	$\sqrt{(14)}$	$2\times(15)$	$b_{vtl}+m_{ht}$	b_{vti}	$\frac{b_{vti}\bar{c}_{vti}}{S_{vt}}$	$\frac{b_{vti}}{\bar{c}_{vti}}$	λ_t	q_{vt}/q	σ_p	$\sigma_{p_{avg}}$
Pack On	20.60	35.65	5.98	11.96	-3.7	2.28	.160	.326	1.12	1.0063	.82	.131
Pack Off	20.15	36.10	6.01	12.02	-3.7	2.31	.162	.330	1.12	1.0055	.85	.1376

PART II-B-12

12. RUDDER TABS

The aerodynamic characteristics of the rudder trim and spring tabs are considered to be the same with power-on as with power-off as determined in Part II-A-12. However, the variation of dynamic pressure at the vertical tail (q_{vt}) with power as shown in Part II-B-11 must be taken into account when calculating forces and moments due to the trim tab and spring tab.

The dynamic pressure ratio with power on is the same as shown in Part II-B-11 for the vertical tail.

PART II-B-13

LANDING GEAR

The aerodynamic characteristics of the landing gear are considered to be the same with power on as with power off and have been determined in Part II-A-13.

REFERENCES

1. Fairchild Engineering Report R110-007, "Basic Aerodynamic Data", dated 22 March 1948.

2. Wind Tunnel Tests of 1/32 Scale Model of XC-120 Airplane. Wright Field 5' Wind Tunnel.

3. Fairchild Engineering Report R107-014, "Basic Flight Criteria", dated 18 February 1949.

4. NACA Technical Note 1291, "Collection and Analysis of Wind Tunnel Data on the Characteristics Isolated Tail Surfaces with and without End Plates", by Bates, dated May 1947.

5. NACA Technical Note 775, "Analysis of Wind Tunnel Data on Directional Stability and Control", Pass, dated 1940.

6. NACA Technical Report 643, "Design Charts for Predicting Downwash Angles and Wake Characteristics behind Plain and Flapped Wings", by Silverstein and Katzoff, dated July 1938.

7. NACA Confidential Bulletin 5B05 (WR A-11), "Computation of Hinge Moment Characteristics of Horizontal Tails from Section Data", by Crane, dated April 1945.

8. NACA Technical Note 796, "Determination of Control Surface Characteristics from NACA Plain Flap and Tab Data", by Ames and Sears, dated February 1941.

9. NACA Advance Confidential Report L4H13, "Analysis of Available Data on Control Surfaces having Plain - Overhang and Frise Balances", by Purser and Toll, dated May 1944

10. NACA Technical Report 267, "Drag of Wings with End Plates", by Hemke, dated 1927.

11. NACA Technical Report 665, "Calculation of the Aerodynamic Characteristics of Tapered Wings with Partial Span Flaps", by Pearson and Anderson, dated 1939.

REFERENCES (CONT.)

12. Fairchild Flight Test Report FT105-5, dated March 1948.

13. Fairchild Flight Test Report FT105-6, dated March 1948.

14. Fairchild Engineering Report R107-017, "Analysis of Wind Tunnel Data on XO-120", dated 31 March 1949.

15. Royal Aeronautical Society Data Sheets 01.01.02, "Slope of Lift Curve for Twin Fins and Rudders", dated May 1946.

16. NACA Technical Note 1491, "Theoretical Additional Span Loading Characteristics of Wings with Arbitrary Sweep, Aspect Ratio, and Taper Ratio", by DeYoung, dated December 1947.

CLASSIFICATION CHANGED TO UNCLASSIFIED

BY AUTHORITY OF ASTIA [illegible]ion cancelled in accordance with [illegible] Order 10501 issued 5 November 1953

R to U Ex Ord

Date 21 February 1957 Signed Richard E. Reedy

OFFICE SECURITY ADVISOR

A.T.I 99299

Reproduced by

DOCUMENT SERVICE CENTER

ARMED SERVICES TECHNICAL INFORMATION AGENCY

KNOTT BUILDING, DAYTON, 2, OHIO

"NOTICE: When Government or other drawings, specifications or other data are used for any purpose other than in connection with a definitely related Government procurement operation, the U.S. Government thereby incurs no responsibility, nor any obligation whatsoever; and the fact that the Government may have formulated, furnished, or in any way supplied the said drawings, specifications or other data is not to be regarded by implication or otherwise as in any manner licensing the holder or any other person or corporation, or conveying any rights or permission to manufacture, use or sell any patented invention that may in any way be related thereto."

UNCLASSIFIED

Filmed

(UNPUBLISHED CARD)

ATI 99 299

AD-B803 042

U

FAIRCHILD ENGINE AND AIRPLANE CORP., FAIRCHILD AIRCRAFT DIV., HAGERSTOWN, MD. (ENGINEERING REPORT NO. R107-012)

BASIC AERODYNAMIC DATA - MODEL XC-120

J.E. EVANS; G.T. GALOW; A. ATHANASIAN AND OTHERS 9 JULY '48 - REVISED 28 FEB '49 346PP GRAPHS, DRWGS

AERODYNAMICS (2)
PERFORMANCE (2)

AIRPLANES - AERODYNAMICS
AIRPLANES, CARGO
C-120 Aircraft

p1/3.5

RESTRICTED

EO 10501 dd 5 NOV 1953

& Transport Aircraft

Aerodynamics